# Integrated Predictive Model for Healing and Fatigue Endurance Limit for Asphalt Concrete

by

Mena Souliman

A Dissertation Presented in Partial Fulfillment
of the Requirements for the Degree
Doctor of Philosophy

Approved April 2012 by the
Graduate Supervisory Committee:

Michael Mamlouk, Co-Chair
Matthew Witczak, Co-Chair
Kamil Kaloush

ARIZONA STATE UNIVERSITY

May 2012

ABSTRACT

One of the main requirements of designing perpetual pavements is to determine the endurance limit of Hot Mix Asphalt (HMA). The purpose of this study was to validate the endurance limit for HMA using laboratory beam fatigue tests. A mathematical procedure was developed to determine the endurance limit of HMA due to healing that occurs during the rest periods between loading cycles. Relating healing to endurance limit makes this procedure unique compared to previous research projects that investigated these concepts separately. An extensive laboratory testing program, including 468 beam tests, was conducted according to AASHTO T321-03 test procedure. Six factors that affect the fatigue response of HMA were evaluated: binder type, binder content, air voids, test temperature, rest period and applied strain. The endurance limit was determined when no accumulated damage occurred indicating complete healing. Based on the test results, a first generation predictive model was developed to relate stiffness ratio to material properties.

A second generation stiffness ratio model was also developed by replacing four factors (binder type, binder content, air voids, and temperature) with the initial stiffness of the mixture, which is a basic material property. The model also accounts for the nonlinear effects of the rest period and the applied strain on the healing and endurance limit.

A third generation model was then developed by incorporation the number of loading cycles at different locations along the fatigue degradation curve for each test in order to account for the nonlinearity between stiffness ratio and loading

cycles. In addition to predicting endurance limit, the model has the ability to predict the number of cycles to failure at any rest period and stiffness combination. The model was used to predict fatigue relationship curves for tests with rest period and determining the $K_1$, $K_2$, and $K_3$ fatigue cracking coefficients. The three generation models predicted close endurance limit values ranging from 22 to 204 micro strains. After developing the third generation stiffness ratio model, the predicted endurance limit values were integrated in the strain-$N_f$ fatigue relationships as a step toward incorporating the endurance limit in the MEPDG software. The results of this study can be used to design perpetual pavements that can sustain a large number of loads if traffic volumes and vehicle weights are controlled.

# DEDICATION

This dissertation is dedicated to my father Mr. Ibrahim Souliman, my mother Mrs. Mervat Shalabi, and my brothers Shenoda and Beshoy for their prayers, love, and support.

ACKNOWLEDGMENTS

First of all, I would like to express my sincere thanks and gratitude to my advisor Dr. Michael Mamlouk who has always been there and helped me during all the time. Without his support and guidance from the first day of my arrival to ASU until now, none of this would have happened.

I shall be failing in my duties if I don't forward my heartfelt thanks to my advising co-chair Dr. Matthew Witczak for his perennial source of help and cooperation in the successful pursuit of this knowledge. Dr. Witczak was the P.I. of the NCHRP 9-44A, under which this study was performed and financially supported. Thanks also go to Dr. Kamil Kaloush for his endless encouragement, help and support.

I would like to express my appreciation to the School of Sustainable Engineering and the Built Environment at ASU and National Cooperative Highway Research Program for their financial support. I would like to acknowledge the effort of Mr. Kenneth Witczak in preparing the beam specimens and Mr. Waleed Zeiada for his advise during the study. I am also grateful to all my friends and colleagues of the Advanced Pavement Group at ASU.

Last but not the least; I owe a great debt of gratitude towards my parents, Mr. Ibrahim Souliman and Mrs. Mervat Shalabi for their perseverance, forbearance and endurance during my absence from home for the acquisition of this knowledge.

TABLE OF CONTENTS

Page

CHAPTER Page

CHAPTER Page

CHAPTER Page

CHAPTER Page

CHAPTER Page

LIST OF TABLES

Table Page

Table Page

Table Page

LIST OF FIGURES

Figure Page

Figure Page

Figure Page

Figure Page

Figure Page

Figure Page

# Chapter 1 INTRODUCTION

## 1.1 Background of Fatigue Cracking

Load associated fatigue cracking is one of the major distress types occurring in flexible pavements. Fatigue cracks are a series of longitudinal and/or interconnected cracks caused by the repeated application of wheel loads that results in fatigue failure of the hot mix asphalt (HMA) surface and/or base courses. This type of cracking generally starts as short longitudinal cracks in the wheel path and progresses to an alligator cracking pattern (interconnected cracks).

The action of repeated loading is caused by traffic induced tensile and shear stresses in the bound layers, which eventually leads to the loss of the structural integrity of the stabilized layer material. Fatigue initiated cracks start at points where maximum tensile strains and stresses exist. Once the crack initiates at the critical location, the action of traffic eventually causes the crack to propagate through the entire bound layer.

Over the last 3 to 4 decades of pavement research, it has been common to assume that fatigue cracking normally initiates at the bottom of the asphalt layer and propagates to the surface (bottom-up cracking). This is due to the bending action of the pavement layer that results in flexural stresses to develop at the bottom of the bound layer. However, numerous recent worldwide studies have also clearly demonstrated that fatigue cracking may also be initiated from the top of the bound layer and propagates down (top-down cracking). This type of fatigue cracking is not well defined from a mechanistic viewpoint as the more classical “bottom-up” fatigue. In general, it is hypothesized that critical tensile

and/or shear stresses develop at the surface at the tire edge-pavement interface, which is coupled with highly aged (stiff) thin surface layer , causing surface cracks to develop.

In order to characterize fatigue in asphalt layers, several model forms can be found in the literature. The most common model form used to predict the number of load repetitions to fatigue cracking is a function of the tensile strain and mix stiffness (modulus) (1).

**1.2 Background of HMA Endurance Limit**

The HMA Endurance Limit, (HMA-EL) is the repeated HMA flexural strain level below which HMA damage is not cumulative. Thus, an HMA layer experiencing strain levels less than the HMA-EL should not fail due to fatigue.

It has long been postulated by Monismith that there appeared to be a strain below which there is no fatigue damage to the HMA (2). This has been investigated by Carpenter (3) starting in 2000, and recently by NCAT by conducting lengthy tests at low strain levels (4). These studies suggested that there is a definite point at which each mixture's traditional strain-$N_f$ curve deviates from the typical log-log straight line relationship and assumes a relatively flat slope.

Depending on different mixture and testing factors, this extended plateau value of curve can be reached at significantly different strain values. Strains below the HMA-EL will begin to show extraordinarily long fatigue lives as compared to those that would be predicted by the traditional phenomenological fatigue model shown in Equation 1. The difficulty in differentiating the mixture

variables and their impact on the HMA-EL derives from the use of this simplified relationship for strain and loads to failure. Since this relationship is not fundamental, it cannot adequately describe the mixture performance under very low strains.

The HMA-EL represents the balance point between damage and healing in the HMA. For strain levels above the HMA-EL, the damage done is considerably greater than the healing potential for the HMA (4). When strains are below the HMA-EL value, the damage is equal to or less than the healing potential and the damage is small enough that it is potentially completely repaired during the load pulse in the field or the load cycle in the lab.

Previous HMA-EL studies (5) indicated that a 70 micro-strain level is a conservative value that guarantees a structural design will perform in the region of extended fatigue life, providing a "no damage" performance. A design incorporating this 70 micro-strain level under the most extreme conditions can be considered a perpetual pavement. If the strain remains around 70 - 100 micro-strains during the pavement life, there is no accumulation of HMA fatigue damage.

Different mixtures produce different HMA-EL values. While this can be mostly attributed to binder differences, the lack of related binder data available to date only allows a comparison with modulus, which for a specific aggregate gradation will be controlled primarily by the binder type, binder content and air voids (5). These data clearly indicate that for mixtures of similar design, alteration of the modulus, essentially through binder differences, produces a

strong relationship between modulus and the HMA-EL. What is important for these mixtures is that there is a strong indication that as the modulus increases, the HMA-EL decreases asymptotically (5).

Some previous studies showed that the relationship between the HMA-EL and the flexural modulus also clearly indicates that there is a lower limit to the HMA-EL that appears to be well above the 70 micro strain level. Further, because healing potential increases as temperature increases, it can be expected that the HMA-EL will change with temperature, which may be indirectly indicated by this modulus relationship (5).

Utilizing HMA-EL concepts with a traditional fatigue curve is not consistent as one incorporates healing while the other ignores it even though it is present. Load damage levels change with the volume and speed of traffic which can be presented as the rest period between each cyclic loading in the beam fatigue testing. The HMA-EL also changes with temperature and binder type. Unless these factors are accounted for, the fatigue pavement design would not provide a consistent relationship between load levels, damage, and load repetitions to failure.

Because the HMA-EL is tied closely to the healing potential of the binder, at higher temperatures healing occurs more rapidly and the strain level that can be tolerated with no damage accumulation is increased (6). To be correctly included in the pavement design the HMA-EL must vary with season, just as the modulus and the resulting strain vary with season. If the variation in HMA-EL is included, the impact of healing in the HMA between load pulses must be considered. Rest

periods heal the damage caused by load applications, and are a major factor in the lab to field shift values of 40 to 400 that have been applied to make existing lab fatigue models applicable to field conditions (5).

Current design methods of flexible pavement assume that a cumulative damage occurs where each load cycle uses up a portion of the finite fatigue life of the HMA. Recent studies, however, show that HMA may exhibit an endurance limit, where properly constructed, thick HMA pavements can be exposed to a very large number of loading cycles without exhibiting fatigue (5, 7, 4).

In NCHRP Project 9-38 (7) beam fatigue was studied to determine the HMA fatigue life. By applying a small strain level to the beam, a fatigue life in excess of 50 million cycles was achieved. The NCHRP Project 9-44 (4) developed a detailed plan to validate the endurance limit concept for HMA pavements and to incorporate it into a mechanistic-empirical algorithm for bottom initiated fatigue cracking in flexible pavements. The current NCHRP 9-44A project implements the concept suggested by the previous NCHRP 9-44 project. Also, the project validates the endurance limit concept, and devises effective methods for incorporating it in mechanistic-empirical pavement design methods. These are the major goals of the current dissertation under the NCHRP 9-44A project.

### 1.3 Problem Definition

The endurance limit, as applied to HMA and flexible pavement design, is the strain level below which the HMA would endure indefinite fatigue loads and the pavement will not experience bottom-up fatigue cracking. Current mechanistic-

empirical fatigue criteria for HMA, including the field calibrated criterion in the Mechanistic-Empirical Pavement Design Guide (MEPDG), assume the fatigue life of HMA to be a power function of the tensile strain at the bottom of the asphalt layer. These criteria do not include the provision for an endurance limit. A concentrated research effort is needed to validate the endurance limit concept, and to devise effective methods for incorporating it in mechanistic-empirical pavement design methods.

### 1.4 Research Objectives

The major objectives of this research project were as follows:

1. Verify the concept of endurance limit of HMA by carrying out laboratory experiments to identify the mixture and pavement layer design features related to endurance limit for bottom-initiated fatigue cracking of HMA, and
2. Develop an integrated predictive model for healing and endurance limit for flexible pavements.
3. Develop a methodology to incorporate the endurance limit into the MEPDG simulation process.

### 1.5 Scope of Research

The scope of this research includes:

- **Conduct Literature Review Search**

  The goal of the literature review was to document previous HMA endurance limit studies needed to accomplish the objectives of this study. Literature review included the concept of fatigue healing, endurance limit,

and the effect of introducing a rest period after loading on the fatigue life. Completion of the literature review was done to ensure that all the essential information needed to accomplish the objectives of this study was obtained.

- **Test Program and Plan**

  A comprehensive test plan was developed to include testing typical mixtures and testing factors that might affect the endurance limit of HMA. Six main factors were selected to be evaluated in this study: binder type, binder content, air voids in the mix, testing temperature), amount of rest period applied between each loading cycle, and number of cycles till failure for the test without rest period ($N_f$).

- **Materials and HMA Mix Design**

  The three binder types that were used in this study were characterized by performing conventional binder tests followed by superpave binder tests. Aggregate gradation determination and Superpave mix design was completed by MACTEC for the 3 mixes used.

- **Specimen Preparation and Beam Fatigue Machine Calibration**

  Specimen preparation and machine calibration procedures are presented.

- **Preliminary Quality Assurance /Quality Control Studies**

  Several small QA/QC studies were performed to insure obtaining comparable results from both beam fatigue machines and to verify the testing conditions.

- **Stiffness Ratio Model Development and Endurance Limit Determination**

  An integrated stiffness ratio (SR) model of all three mixtures was developed in order to calculate the amount of HMA healing. The HMA healing was then coupled with damage produced during loading to estimate HMA-EL under different conditions.

- **Final Report**

  A final report was prepared to document the work completed. The report included the conclusions and recommendations for further research.

### 1.6 Report Organization

The contents of this report are organized into eleven chapters. The descriptions of these chapters are as follows:

1. Introduction and Research Objectives
2. Literature Review
3. Design of Experiment
4. Materials and HMA Mix Design
5. Specimen Preparation and Beam Fatigue Machine Calibration
6. Preliminary QA/QC Studies
7. Healing Index and Endurance Limit Determination
8. Incorporating Endurance Limit in the MEPDG
9. Conclusions and Recommendations for Further Research

Chapter 1 is intended to outline the research background, problem definition, objectives and scope of the research. Chapter 2 provides a literature review and theoretical background of HMA fatigue cracking phenomenon, HMA healing, and HMA endurance limit. Chapter 3 contains the experimental design of the test program. Chapter 4 contains the binder testing characterization, aggregate properties, and the Superpave mix design results. Chapter 5 includes specimen preparation and the machines calibration check procedure. Chapter 6 includes the results of the QA/QC studies conducted before the main experiment in order to evaluate the compliance of measurement equality among beam fatigue testing machines and refining test conditions. Chapter 7 contains the laboratory test results, healing analysis, development of the integrated predictive stiffness ratio model for healing and endurance limits under different conditions. Chapter 8 presents a methodology to incorporate the endurance limit into the MEPDG. Chapter 9 presents the conclusions of the study and the recommendations for future research.

All the supporting test data and additional graphical plots are included in the Appendices.

# Chapter 2 LITERATURE REVIEW

## 2.1 Fatigue Cracking Mechanisms

Fatigue cracking is a long-term distress mode as considered by most design/evaluation procedures. Fatigue cracks are a series of longitudinal and/or interconnected cracks caused by the repeated applications of wheel loads that result in fatigue failure of the HMA surface and/or base mixtures. Fatigue cracks occur in both wheel paths but usually initiate in the outer wheel path for relatively thin HMA surfaced pavements and in the inner wheel path for thick HMA surfaces (8).

There are predominantly two types of fatigue cracks that occur in flexible pavements that are defined based on the direction of crack propagation: bottom-up and top-down. It is difficult to identify where the fatigue cracks initiate without taking cores or excavating test pits to visually observe the direction of crack propagation. Bottom-up fatigue cracking is more common than top-down cracking. However, top-down cracking is more visible and allows water and air to readily infiltrate deeper into the HMA mixture. Conversely, fatigue cracks that initiate at the bottom of the HMA layer must propagate to the surface before they become visible and allow water infiltration.

Fatigue cracks that initiate at the bottom of the HMA layer and propagate to the surface are the more classical defined alligator area cracks, as defined by the LTPP Distress Identification Manual (9). This type of fatigue cracking first shows up as short longitudinal cracks in the wheel path that quickly spread and

become interconnected to form a cracking pattern generally defined as alligator cracks.

Fatigue cracks that initiate at or near the surface of the HMA layer and propagate downward through the HMA layers are less common and generally occur in thick HMA pavements. This type of fatigue cracking first shows up as relatively long longitudinal cracks adjacent to the tires. This type of cracking is characteristic of longitudinal cracks in the wheel path that are not interconnected (8).

### *2.1.1 "Bottom-Up" Fatigue Cracking – Alligator Cracking*

This type of fatigue cracking (alligator cracking) is a result of the repeated bending of the asphalt layer under traffic. Basically, the pavement deflects under wheel loads producing tensile strains and stresses at the bottom of the asphalt layer. With the continued bending, the tensile stresses and strains cause cracks to initiate at the bottom of the layer that eventually propagate to the surface.

The more bending and/or the higher deflections, the greater the tensile strains and stresses and the fewer the number of repeated wheel loads to cause the cracks to initiate at the bottom of the layer and propagate to the surface. The following briefly lists some of the reasons for higher tensile strains and stresses to occur at the bottom of the HMA layer (8).

- Relatively thin or weak HMA layers for the magnitude of the wheel loads.
- High wheel loads and tire pressures.
- Soft spots or areas in unbound aggregate base materials or in the subgrade soil.

- Weak aggregate base/subbase layers caused by an increase in moisture content.

### *2.1.2 "Top-Down" Fatigue Cracking – Longitudinal Cracks in Wheel Path*

For thick HMA layers, load-related cracks may initiate at the surface and propagate downward. There are several opinions on the mechanisms that cause this type of cracks, but there are no conclusive data to suggest that one is more applicable than the other. Some of the suggested mechanisms are (8):

- Tearing of the HMA surface mixture from radial tires with high contact pressures near the edge of the tire, causing the cracks to initiate and propagate both in shear and tension.
- Severe aging of the HMA mixture near the surface resulting in high stiffness and when combined with high contact pressures, adjacent to the tire loads, cause the cracks to initiate and propagate in shear.
- Superposition or combination of wheel load induced tensile stresses and strains with the thermal stresses and strains that occur at the surface when the temperature decreases causing the cracks to initiate and propagate in tension. Aging of the HMA surface mixture accelerates this crack initiation-propagation process.

The stiffer or more brittle the surface in combination with the higher tire pressures and greater temperature changes, the larger the tensile and shear stresses and strains and the fewer the number of wheel loads to cause the cracks to initiate at the top of the layer.

## 2.2 Fatigue Life Models and Relationships

### *2.2.1 General Fatigue Model*

In order to characterize the fatigue in asphalt layer, numerous model forms can be found in the literature. The commonly used mathematical relationship used for fatigue characterization is of the following form (10):

$$N_f = A_f K_1 \left(\frac{1}{\varepsilon_t}\right)^{k_2} \left(\frac{1}{E}\right)^{k_3} = A_f K_1 (\varepsilon_t)^{-k_2} (E)^{-k_3} \quad (1)$$

where:

$N_f$ = number of repetitions to fatigue cracking

$\varepsilon_t$ = tensile strain at the critical location

E = stiffness of the material

$k_1$, $k_2$, $k_3$ = laboratory calibration parameters

$A_f$ = laboratory to field adjustment factor

### *2.2.2 Fatigue Life Relationships*

It has been accepted for many years that the fatigue behavior of the asphalt-aggregate mixes can be characterized by a relationship of the form:

$$N_f = a(1/\varepsilon_t)^b \quad (2)$$

where,

$\varepsilon_t$ = Initial tensile strain

a, b = Experimentally determined coefficients

The above relationship is applicable to a given asphalt mix. Figure 1 shows a general plot of the fatigue relationships for AC mixes. Some researchers (1) have suggested that a relationship which is more applicable to asphalt-aggregate mixes in general is the following.

$$N_f = a\left(1/\varepsilon_o\right)^b \left(1/E_0\right)^c \qquad (3)$$

where,

$E_o$= Initial mix stiffness, and

a, b, c = Experimentally determined coefficients

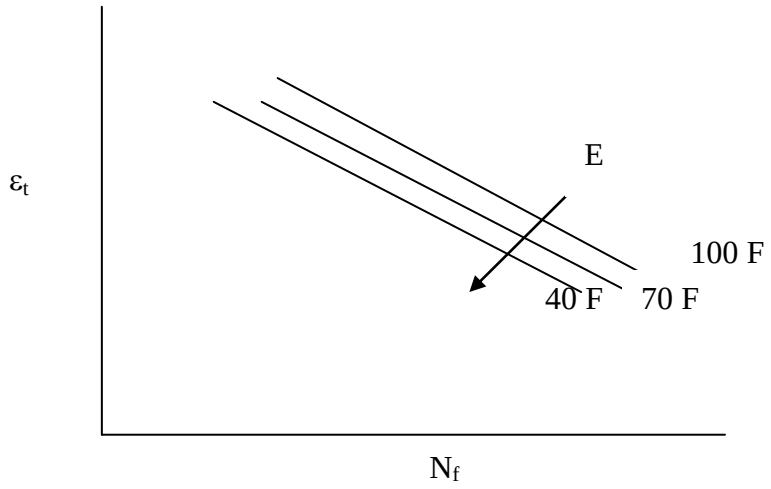


**Figure 1. General fatigue relationship for asphalt mixture under controlled strain at different temperatures (logarithmic scale).**

Based on the laboratory test data presented in the form of the Equation 4, several strain based models have been proposed to predict pavement fatigue life (11, 12, 13).

Other researchers (14, 15, 16, 17, 18) have used an energy approach for describing the fatigue behavior and have shown that the total, or cumulative, dissipated energy to failure is related to fatigue life as follows:

$$W_N = A(N_f)^z \quad (4)$$

where,

$W_N$= Cumulative dissipated energy to failure

A, z = Experimentally determined coefficients

In Equations 3 and 4, fatigue life is related to the initial test conditions namely, the initial strain and initial mix stiffness. In Equation 5, fatigue life is related to terminal test condition, namely the cumulative dissipated energy to failure. Neither approach directly recognizes how damage to the mix actually develops as loading proceeds from the beginning to the end. The cumulative dissipated energy to failure, $W_N$, is related to the energy dissipated during the *i*th load cycle, $w_i$, as follows:

$$W_N = \sum_{i}^{N_f} w_i \quad (5)$$

For a sinusoidal loading condition.

$$w_i = \pi \varepsilon_i^2 S_i Sin\phi_i \quad (6)$$

where,

$w_i$= Dissipated energy at load cycle i,

$\varepsilon_i$ = Strain amplitude at load cycle i,

$S_i$ = Mix stiffness at load cycle i,

$\phi_i$ = Phase shift between stress and strain at load cycle i, and

## 2.3 Fatigue Cracking Prediction Equation Approaches

There are three methodologies or types of models that have been used to predict fatigue cracking as listed below.

1. Basic pavement response; tensile strain, stress, deflection – the methodology commonly used by most of the design procedures in existence to-date. .
2. Fracture mechanics – the methodology commonly used for predicting thermal cracks.
3. Energy or dissipated energy – the least used methodology, but believed to have good potential for accuracy.

Several models have been developed in the last few decades based on the first approach including the Shell model (12), the Asphalt Institute model (13), the University of California at Berkeley model (10, 18, 19), and the MEPDG model (20).

## 2.4 Laboratory Fatigue Tests

Fatigue of the asphalt concrete mixture is the accumulation of damage under the effect of repeated loading.

Asphalt concrete fatigue properties are obtained by laboratory repeated-loading testing using repeated beam bending mode. In general two modes of loading are used in beam fatigue testing: controlled stress and controlled strain.

Results from laboratory fatigue tests are usually reported as the number of load cycles to failure as a function of the initial tensile strain, normally referred to as fatigue curves. In either controlled stress or controlled strain testing mode, different mixture responses have been related to the number of cycles to failure. These responses have included the initial tensile strain, initial tensile stress, and center-beam deflection. The initial tensile strain is the one more commonly used.

Several mathematical equations have been used to describe the results from fatigue tests – relating the mixture response to the number of loading cycles to failure. Most of the mathematical models for the fatigue curves take the following generalized form of Equation 1 (1).The material properties $k_1$, $k_2$, and $k_3$ are obtained through fatigue beam testing in the laboratory.

### *2.4.1 Adjustment to Lab Fatigue Curves*

All laboratory measured fatigue curves must be adjusted or shifted to account for the inaccuracies in simulating field conditions and crack propagation through the HMA layer. The shifting of laboratory measured fatigue curves is defined as the shift factor and is dependent on the extent and severity level of fatigue cracking that are used to define failure along the roadway, as well as the type of fatigue cracks (top-down versus bottom-up fatigue cracks). The shift factors that have been reported in the literature vary widely from 3 to over 100 depending upon the thickness of the asphalt layer, the mix properties, traffic volume and composition, environmental conditions, fatigue failure criterion, and type of fatigue test (8). Shift factors have not been developed separately for the two categories of fatigue cracks (bottom-up and top-down). The lower values of the shift factors maybe

more applicable to top-down cracking, while the larger values maybe more applicable to bottom-up cracking (8).

Fatigue cracking initiates at critical points within the HMA layers where the largest tensile strains occur under repeated traffic loading. Continued traffic loading eventually causes these cracks to propagate through the entire HMA layer thickness. The number of load repetitions to failure, defined on the roadway as a specific area and severity of cracking, is related to the material properties of the HMA mix and the tensile strains at the critical pavement location. The laboratory relationship (Equation 7) is commonly adjusted or shifted to account for this crack propagation and extent.

$$N_{f(fatigue)} = \beta_{f(fatigue)}\left(N_{f(Lab)}\right) \quad (7)$$

where:

$N_{f(fatigue)}$ = Number of load repetitions to a specific area and severity of fatigue cracking

$\beta_{f(fatigue)}$ = Field calibration function (or shift factor) for fatigue cracking relating the laboratory fatigue curve to the area or extent and severity of cracking along the roadway

### *2.4.3 Fatigue Failure Criteria*

Several methods are currently available to define failure in the flexure fatigue test for HMA. These methods may not produce the same results and they may vary depending on their method of detecting the failure point. It is important to select an accurate, standardized, and consistent method to be used in the main

experiment of the study in order to maintain the integrity of the test results and provide a consistent basis for any implementation scheme.

Failure in any mode of loading is the point at which the specimen can no longer sustain a stable resistance to the damage being done by the loading sequence. When the specimen starts to fail, the damage done per load cycle should increase dramatically, regardless of the load sequence.

For controlled-stress tests, failure can be more easily defined, simply when the beam fractures (21, 22, 23). Van Dijk defined failure when the initial strain had doubled (15). Other researchers have defined failure under constant stress as 90 percent reduction in the initial stiffness (24). For controlled-strain tests, failure is more arbitrary and is usually defined at a point during the test with a specific reduction of the original mixture modulus. The more common failure definition used is when 50 percent of the original modulus (23, 17, 19) is reached or as 50 percent reduction in the initial stress or initial force is obtained (10, 16). In either testing mode, different mixture responses have been related to the number of cycles to failure. These responses have included the initial tensile strain, initial tensile stress, and center-beam deflection. The initial tensile strain is more commonly used.

One of the main concepts that are used to define fatigue failure is dissipated energy approach which is defined as the damping energy or the energy loss per load cycle in any repeated or dynamic test as illustrated in Figure 2.

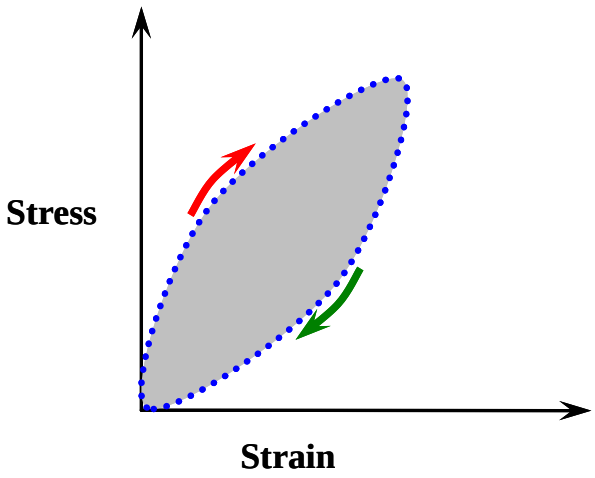


**Figure 2. Dissipated energy approach.**

To determine the fatigue life from dissipated energy, fatigue tests are conducted where the phase angle, mixture modulus, and dissipated energy are measured during the repeated loadings. Several mechanistic parameters are then calculated and used to relate fatigue life to dissipated energy by the following equation (25):

$$N_f = \left(\frac{W}{A}\right)^{-Z} \quad (8)$$

where:

W = Total dissipated energy.

A, Z = Mixture characteristic constants.

Flexure center and third-point beam fatigue tests are normally used when applying such a method with either controlled stress or controlled strain mode of loading. The dissipated energy per cycle for a beam specimen is computed as the

area within the stress -strain hysteresis loop (Figure 3). The dissipated energy is given by the following equation:

$$\omega_i = \pi \sigma_i \varepsilon_i \sin \phi_i \tag{9}$$

where,

$\omega_i$ = Dissipated Energy at load cycle i

$\sigma_i$ = Stress at the load cycle i

$\varepsilon_i$ = Strain at the load cycle i

$\phi_i$ = Phase angle between stress and strain at load cycle i

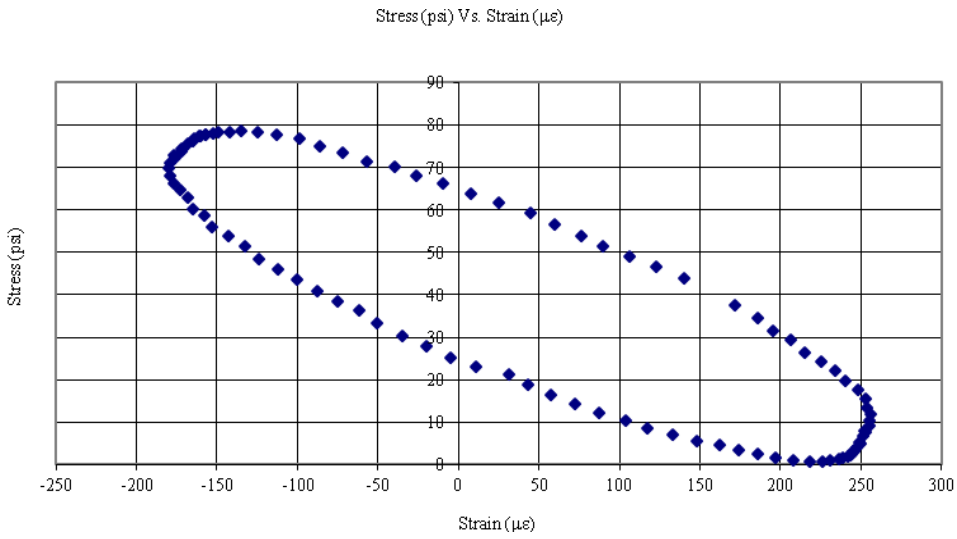


**Figure 3. Stress-strain hysteresis loop for controlled-stain test (8).**

This energy is then summed over load cycle increments where the lag between stress and strain response cycles is constant.

$$W_{total} = \sum_{i=1}^{n} w_i \quad (10)$$

where:

$W_{total}$ = Total dissipated energy

$w_i$ = Dissipated energy in the $i^{th}$ load cycle

While this method provides sound mechanistic relationships between stress, strain, energy, and fatigue life, and can be applied under a wide variety of environmental factors, reliable prediction of fatigue life cannot be predicted without extensive fatigue testing.

The use of dissipated energy for fatigue life prediction has been investigated over the last three decades (5, 6, 26).

A more recent fatigue failure criterion was developed at Arizona State University (ASU) based on the Rowe and Bouldin's failure definition (8). A new stiffness ratio is developed as (Ni*Si/So), where Ni is the cycle number, Si is the stiffness at cycle i, and So is the initial stiffness taken at cycle number 50. By plotting the stiffness degradation ratio value (Ni*Si/So) versus the load cycles a peak value can be obtained. Failure is then defined as the number of load repetitions at the peak value of that curve for both controlled strain and controlled stress modes as shown in the example in Figure 4. The results also show that there is no significant difference between the two curves for controlled stress and controlled strain. It was noted that the curves from constant strain testing and constant stress testing have almost the same trend. Using the ASU method, the final damage ratio was around 0.5 of the initial stiffness. The results of that study

verified the 50 percent of the initial stiffness as the best value for the failure fatigue criterion to be used in this project.

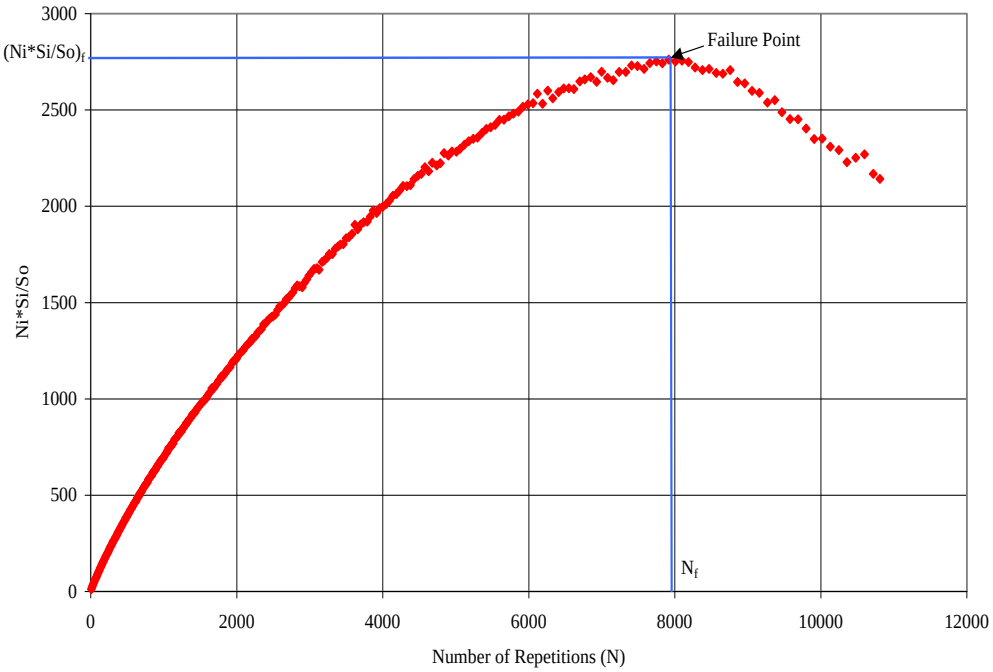


**Figure 4. Example of flexural stiffness degradation ratio Ni Si/So versus number of load repetitions using ASU method (8).**

### *2.4.11 Selection of the failure criterion*

A pilot study (27) was completed under the NCHRP 9-44A project to select the appropriate methodology for detecting fatigue cracking cycles to failure to be used in the current study. Beam fatigue test results conducted at ASU (8) were analyzed using different methods. The study incorporated a total of 62 beam specimens that used three binders (58-22, 64-22 and 76-16) and tested at three temperatures ($40^0$F, $70^0$F, and $100^0$F). The study used a total of seven different methodologies to find the number of cycles till failure: Pronk's Method (26), Pronk and Hopman's Method (17), Rowe's Method (24), ASU Method (8),

Carpenter's Method (3, 5, 6), 3-Stage Weibull Distribution (28, 29, 30), and Francken Models that were developed at ASU (31).

The number of cycles to failure was determined using the seven methods listed above. The results were compared and statistically analyzed. According to the ANOVA statistical analysis, the ASU, Pronk, Hopman, and Rowe methods were statistically the same when considering both the means and variances of the normalized $N_f$ and the stiffness ratio at failure.

Finally, the ease of use to the user of each method was presented. The ease of use was based on the applicability and easiness of the calculation of the results and the implementation in a routine testing program. The ease of use comparison concluded that ASU and Rowe methods are the easiest methods to use (27).

Another factor that was looked at was that the methods that are based on dissipated energy would not be applicable for testing conducted using rest periods since the HMA material relaxes during the rest period and stress and strain will be almost in-phase at the beginning of each cycle. Therefore, the dissipated energy calculated for the test with rest period is expected to be less accurate than the case without rest period. In case of testing with rest periods the stiffness-based methods were more applicable such as the ASU method (27).

For the current study, Pronk's method and the ASU method were recommended, where failure is defined as 50 percent of the initial stiffness.

## 2.5 Factors Affecting Fatigue Cracking Response

The most important factors that affect fatigue response of asphalt mixtures in the laboratory are:

1. Mix variables such as asphalt type and source; aggregate gradation, type and source; air voids content; asphalt content; etc.
2. Environmental variables such as temperature, temperature gradient, moisture, etc.
3. Loading magnitude, type (strain or stress control), frequency, and existence of rest period.
4. Specimen fabrication and preparation procedure and compaction method.
5. Test conditions such as specimen shape, size, loading configuration, etc.
6. Aging of asphalt binder.

The following section discusses these factors.

### *2.5.1 Effect of Asphalt Content and Air Void*

Results from the SHRP A-003A project indicated that lower asphalt contents and lower air voids led to higher stiffness, while higher asphalt contents and lower air voids led to higher fatigue lives (10). Harvey and Tsai (32) produced similar results for a typical California mix. To simulate the effect of air void and asphalt content on several example overlays, the elastic layer theory was used. By using the models for stiffness and fatigue lives obtained from laboratory test results, the simulation indicated that an increase in pavement predicted fatigue life was found for higher asphalt contents and lower air voids.

Tayebali et al. (33) found that air voids have a large effect on fatigue life. As air voids increased, fatigue life decreased for both control strain and control stress. It was found that the observed asphalt content effects on stiffness and fatigue life were small and inconsistent. It was concluded that stiffer mixes would perform better for thick pavements, while low stiffness mixes would perform better for thin pavements.

### *2.5.2 Effect of Aggregate Gradation*

A study conducted by Sousa et al. (34) investigated to what extent gradation has an effect on fatigue performance of asphalt aggregate mixes. The study concluded that fine gradations (passing through or above the restricted zone) appeared to have better fatigue performance than gradations passing below the restricted zone because of their ability to accommodate higher binder contents. Also, the use of a stiff binder may result in good fatigue performance of relatively thick pavements. The SHELL fatigue predictive equation (12) based on percent of binder volume, strain level and moduli was able to predict relatively well the actual laboratory fatigue performance of the mixes. No shift factor was needed between laboratory results and predicted values using the SHELL fatigue equation (34).

### *2.5.3 Effect of Mode of Loading*

The constant stress type of loading is applicable to thick pavement layers usually more the 8 inches (8). For this type of structure, the thick asphalt layer is the main load-carrying component and the strain increases as the material gets weaker under repeated loading. However, with the reduction in the stiffness, because of

the thickness, changes in the stress are not significant and this fact leads to a constant stress situation.

In the controlled stress mode of loading, the stress amplitude is maintained at the same level as the initial force. Because of repetitive application of this stress, the strain amplitude increases until it reaches twice the initial amplitude, when the flexural stiffness is reduced to half the initial flexural stiffness, which constitutes failure according to Button et al. (35). On the other hand, the constant strain type of loading is applicable to thin pavement layers since the pavement layer is not the main load-carrying component (8). The strain in the asphalt layer is governed by the underlying layers and is not affected by the decrease in the asphalt layer stiffness. This situation is conceptually more related to the category of constant strain. However, for intermediate thickness layers, fatigue life is generally governed by a situation that is a combination of constant stress and constant strain.

In the controlled strain test, the strain amplitude is maintained constant and the force required maintaining the initial strain level decreases gradually after crack initiation, as the flexural stiffness of the mix is effectively decreased. The failure, or termination point, is arbitrarily selected as a certain reduction in the initial stiffness from that at the commencement of the test, generally 50-percent, as there is no well-defined fracture of the specimen. In addition, the controlled strain mode of loading simulates conditions in thin asphalt pavement layers usually less than 2 inches. The pavement layer is not the main load carrying component. The strain in the asphalt layer is governed by the underlying layers

and is not greatly affected by the change in the asphalt layer stiffness. This situation is conceptually more related to the category of constant strain. Also, the strain mode of loading accounts for both crack initiation and propagation while the stress strain mode of loading does not account for both crack initiation and propagation, because the number of cycles to crack propagation is small compared to the number of cycles to failure which is defined by the fracture of the sample (36). Therefore, fatigue life is usually greater in control strain than control stress (in general approximately 2.4 times greater) (33).

Mixes of higher stiffness, due to temperature and asphalt type, tend to perform better under controlled stress than controlled strain. Stiffer mixes generally have higher fatigue life under controlled stress, whereas stiffer mixes have lower fatigue life under controlled strain. It was recommended that stiffer layers are preferred for thick pavements and less stiff layers are preferred for thin pavements. It was concluded that controlled stress and controlled strain testing might yield similar mix ranking when test results are interpreted in terms of performance expected of the pavements in which they are placed (33, 10).

The mode of loading analysis was evaluated with a least square calibration of models of the following type (10).

$$N_f = a \exp^{b*MF} \exp^{c*Vo} (\varepsilon_o \text{ or } \sigma_o)^d (S_0)^e \qquad (11)$$

where,

MF = Mode factor assuming a value of 1 for controlled strain and -1 for controlled stress, a, b, c, d, e = Regression constants

The controlled-strain and controlled-stress combined model was as follows:

$$N_f = 0.9500 \exp^{0.4472\,MF} \exp^{-0.2566Vo} (\varepsilon_o)^{-3.3669} (S_0)^{-1.1633} \quad (12)$$

It was suggested in the SHRP Project A-003A that the evaluation of mix performance might well be independent of laboratory mode of loading. Controlled stress and controlled strain testing may yield a similar mix ranking. The effect of mix stiffness on fatigue life is generally reversed for the two modes of loading (10).

As a conclusion, Table 1 shows the difference between controlled stress and controlled strain fatigue testing and their influence on the measured characteristics of HMA specimens.

**Table 1. Difference between Controlled Stress and Controlled Strain Fatigue Testing (37).**

| Variables | Stress Controlled | Strain Controlled |
|---|---|---|
| Thickness of asphalt layer | Comparatively thick asphalt bound layers | Thin asphalt-bound layer; < 3 inches |
| Definition of failure, number of cycles | Well-defined since specimen fractures | Arbitrary in the sense that the test is discontinued when the load level has been reduced to some proportion of its initial value; for example, to 50 percent of the initial level |
| Scatter in fatigue test data | lass scatter | More scatter |
| Required number of specimens | Smaller | Larger |
| Simulation of long term influences | Long-term influences such as ageing lead to increased stiffness and presumably increased fatigue life | Long-term influences leading to stiffness increase will lead to reduced fatigue life |
| magnitude of fatigue life, N | Generally shorter life | Generally longer life |
| Effect of mixture variables | More sensitive | Less sensitive |
| Rate of energy dissipation | Faster | Slower |
| Rate of crack propagation | Faster than occurs in-situe | More representative of in-situe conditions |
| Beneficial effects of rest periods | Greater beneficial effects | Lesser beneficial effect |

### *2.5.4 Effect of Rest Period*

It is known that asphalt mixes recover to some extent after a loading cycle as the result of asphalt relaxation. In practice, intermittent loading has a less damaging effect than continuous loading because of the healing process for asphalt. The effect of discontinuous loading on fatigue properties have been investigated in several studies. Van Dijk and Visser (16) investigated the effect of rest period on the fatigue life of a rolled asphalt base course mix. It was found that increased rest periods can increase fatigue life by a factor of 1 to 10 times.

Over the last 4 decades, several researchers have studied the significance of rest periods between load applications during the fatigue testing of HMA. Different findings have been presented in literature showing diverse opinion on the effect of rest period. Some researchers think that rest period only leads to a temporary modulus recovery without actually extending the fatigue life, while others found that the modulus recovery did extend fatigue life by a certain amount. These different conclusions were mainly based on a large variety of tested mixtures, laboratory testing setup and research approaches.

Depending on the way the material is allowed to rest, there are two different ways of introducing rest periods into fatigue testing:

- With rest intervals: it is a classic fatigue test with continuous loading cycles where rest intervals (storage periods) are introduced after a certain number of continuous loading cycles. At the end of each rest interval, the test is continued until the next rest interval.
- With intermittent loads: Each loading cycle is followed by a rest period.

It sounds as if the second method with intermittent loading resembles more closely the sequence of traffic pulses in the field than the first method, although both testing methods have been applied by researchers for studying the effect of rest period and healing in HMA fatigue behavior.

Monismith, et al. (38) assessed the effect of rest period by conducting repeated flexure tests on beam specimens supported by a spring base. The loading cycles consisted of 1 sec. of load and 1 sec., 3 sec., or 19 sec. of rest period. The tests were performed at a 77ºF temperature and three frequencies of 3, 15, and 30 load applications per minute. It was indicated from the test results that increasing the rest period from 1 to 19 seconds had no effect on fatigue performance. This conclusion is different from many other later research results that showed an enhancement of the fatigue life due to rest periods.

Raithby and Sterling, (39) performed uniaxial tensile cyclic tests on beam samples sawed from a rolled carpet of asphalt concrete to have dimensions of 75mm× 75mm× 225mm. The tests were conducted under controlled stress mode at two loading frequencies (2.5Hz and 25Hz) and two temperatures (10ºC and 25ºC), with sinusoidal load pulse, which has equal tensile and compressive stresses in each cycle. Pulsed loading without and with rest periods varying from 40μs to 800μs was applied until failure occurred. In the tests when rest periods were introduced, the specimens were rested at zero stress. It was observed that the strain recovery during the rest periods resulted in a longer fatigue life by a factor of five or more than the fatigue life under continuous loading.

McElvane and Pell (40) performed a rotating bending fatigue tests on a typical English base course mix at 10ºC using a 16.7 Hz frequency. The specimens were subjected to multi-level loading with random duration of rest periods. It was concluded that rest periods have a beneficial effect on the fatigue life depending on the damage accumulated during loading periods. No evidence was found for a limiting value of the fatigue life extension.

Verstraeten et al. (41) performed dynamic two-point bending beam tests in a constant-stress mode (frequency of 54 Hz, temperatures of -5ºC and 15ºC). The loading conditions were maintained either until failure or 80 % of stiffness reduction. The specimens were then stored for periods varying from 3 to 21 hours at temperatures from -5ºC to 35ºC. The authors concluded that the longer the storage periods and the higher the temperatures, the greater the beneficial effect, although their effects on the susceptibility of mixtures to fatigue couldn't be quantified.

Franken, (42) carried out experiments on a typical Belgian mix using two-point bending beam apparatus. The test was run under a constant stress mode of loading at 55.6 Hz frequency. The test results showed an increase in service life when rest periods were incorporated in the fatigue tests. From the test results, an empirical relation that accounts for the effect of rest period was derived. It is a relation between the cumulative cycle damage ratio in Miner's law (Ni/Nc) and the loading ration (nr/nl):

$$\frac{N_i}{N_c} = 1 + 2.8\left(\frac{n_r}{n_1}\right)^{0.44} \qquad (13)$$

where,

$n_r$ = number of rest periods

$n_l$ = number of loading cycles

Hsu and Tseng, (43) conducted a repeated load fatigue test on beam specimens using haversine wave with a loading duration of 0.1 sec. To study the effect of the rest period on the fatigue response of asphalt concrete mixtures, 1, 4 and 8 loading ratios which represent the ratio of the duration of the rest period to that of loading were applied (or 0.1, 0.4, and 0.8 sec.). During the test, approximately 10% of the applied load was pulled upward on the specimen for each loading to simulate the rebound of the pavement for each passing of the vehicles. The test results of controlled stress test showed that asphalt concrete mixtures with higher loading ratios and asphalt content 0.5% more than optimum exhibited longer fatigue life.

Breysse, et al. (44) performed the two-point pending fatigue test on trapezoidal specimens, clamped at the lower base and submitted to a cyclic loading at its free end, to study the balance between damage and recovering in HMA. A controlled-displacement test was performed at a 20 C temperature and a 40 Hz loading frequency. In that study, specimens were continuously loaded until the overall stiffness reduction reached a given ratio of α% then the test was stopped. The stiffness recovery during the rest periods was then monitored by applying a low magnitude loading (supposed not to create any damage) until the response was stabilized. This process was repeated iteratively as many times as wanted, for the same α% ratio. The tests were driven for various α values (10 –

50%) to study the effect of low and severe damage histories on the stiffness recovery values. The obtained results showed the maximum magnitude of recovery depends on the number of applied fatigue cycles that have been applied before. It was noticed that part of the recovery observed due to the interrupted loading sequence is a temporary stiffness recovery rather than a true healing. This is why material will return to its original status (damaged status) very quickly after reloaded.

Castro, et al. (45) had conducted flexural beam fatigue tests with and without rest periods. As a consequence, a constant rest period of 1 second following every 0.1 second loading was applied to the test. The fatigue curves were evaluated by means of discriminate analysis so as to rigorously confirm that they were different. It was concluded that the rest period could increase the fatigue life of an AC specimen up to 10 times, compared to tests without rest periods.

Previous studies showed that introducing a rest period in the loading wave increases fatigue life. Also, increasing the duration of the rest period increases fatigue life up to a certain value, above which the increase in fatigue life is minimal. Since increasing the duration of the rest period increases the testing time, it is important to determine the "optimum" value of the rest period such that its increase would not cause a significant increase in fatigue life and avoid an excessive duration of the test.

In an attempt to investigate a rational value of the optimum rest period, Raithby and Sterling (46) applied a range of rest periods between null and 25

times the loading time (i.e., 0.1 sec. loading time and 2.5 sec. rest period) on a rolled asphalt base course using a dynamic push-pull test. A constant stress mode producing different waveforms (sine, triangle, and square) was used. It was found that fatigue life does not increase significantly for rest periods greater than ten times the loading time (or 1 sec. rest period) and waveform influence was less important than the duration of rest periods.

Van Dijk and Visser (16) had tested a rolled asphalt base course mixture in a three-point bending beam apparatus in a constant strain mode (frequency 40 Hz, temperature 20 ºC) with loading ratios varying from 1 to 25 (0.025 sec. loading time and up to 0.625 sec. rest period). The results showed an increasing fatigue life with increasing rest periods. The maximum beneficial effect of rest period on the fatigue life (life ratio of about 10) was determined by means of extrapolation to be achieved at a loading ratio of about 50.

Bonnaure, et al. (47) conducted a three point bending beam fatigue test on rectangular beams with dimensions of 230mm× 30mm× 20mm in order to study the effect of rest periods. An intermittent loading with various rest periods 0, 3, 5, 10, and 25 times the length of the loading cycle (0, 0.075, 0.125, 0.25 and 0.625 sec.) was applied. The tests were done under both constant stress and constant strain modes of loading at three temperatures (5ºC, 20ºC, and 25ºC) and a 40Hz frequency. The authors concluded that:

1. Increasing the rest period between the loading cycles increases fatigue life. The maximum beneficial effect of rest periods on the

fatigue life was at a rest period equal to 25 times the loading cycle (0.625 sec.).

2. Higher fatigue life occurs at higher temperatures.
3. Softer binders increase fatigue life.

The authors also concluded that the stress and strain levels seemed to have no effect on the increase of the fatigue life due to rest periods. In addition, the constant-stress mode results in a greater increase in fatigue life as compared to the constant-strain mode.

It was also concluded that the optimum rest period would be different according to mixture properties (aggregate gradation, binder content, binder grade, mixture volumetric), test type (flexure beam fatigue, direct tension, tension-compression, etc.) and test conditions including mode of loading, temperature, frequency, stress or strain levels, etc.

**2.6 Fatigue Test Types**

Since the 1960s, many beam fatigue tests have been conducted in the pavement community and have been reported in the literature. A great deal of fatigue testing of asphalt mixture has been conducted at the University of California at Berkeley as well as the University of Nottingham, England. The prediction quality of the fatigue life using any of these test methods depends on how accurate is that method to simulate, as closely as possible, the condition of loading, support, stress state and environment which the material is subjected in the pavement. Moreover, selecting any of these test methods can depend on the simplicity and the feasibility of the method.

Brief description along with the advantages, disadvantages and limitations of selected test methodologies can be found in the SHRP's "Summary Report on Fatigue Response of Asphalt mixes (25). Following is a summary of the most popular fatigue test types.

### *2.6.1 Flexure Beam Test*

One of the principal research tasks of the Strategic Highway Research Program Project A-003A (48) was to develop a proposed test method and associated equipments for testing and evaluation of fatigue properties of asphalt mixes using repetitive flexural bending of beam specimens (10).

One of the principal products of SHRP A-003A project was the development of surrogate fatigue equations to model the behavior of asphalt mixtures under controlled stress and controlled strain conditions. Flexural beam tests were used as a means of accelerated testing of asphalt concrete mixture for both fatigue life and flexural stiffness under controlled conditions and the aid of the computerized control and data acquisition. A comprehensive methodology to predict asphalt pavement fatigue life was formulated in this project. Using the third-point bending beam apparatus for this test, a load is applied, under either controlled strain or controlled stress loading, on the beam specimen until failure. The beam test specimen generally have a rectangular cross section of standard dimension of 2.5 in. (63.5 mm) wide, 2.0 in. (50.8 mm) high, and 15 in. (381 mm) long. Failure is arbitrarily defined by a certain percent reduction in the initial stiffness. In general, a 50 percent of the initial stiffness under controlled strain or complete fracture of the beam specimen (under controlled stress) is used.

Two major improvements were made during the SHRP A-003A project, (18), in order to minimize the setup and testing time and to improve reliability for the test results. The target was to increase the ease, simplicity, and reliability for the beam fatigue test. The improvements are:

1. Increasing the size of beam test specimen from 1.5 in. (38.1 mm) wide, 1.5 in. (38.1 mm) high, and 15 in. (381 mm) long to 2.5 in. (63.5 mm) wide, 2.0 in. (50.8 mm) high, and 15 in. (381 mm) long.
2. Building and designing a new beam fatigue module as a stand-alone device. Software has been developed to automatically perform the SHRP Designation M009 test. The latest software allows for both controlled strain and controlled stress loadings.

### *2.6.2 Cantilever Beam Rotating Test*

At the University of Nottingham, U. K. Pell and Hanson (49) used a rotating cantilever machine where specimen is mounted vertically on a rotating cantilever shaft. A load is applied at the top of the specimen to induce a bending stress of constant amplitude through the specimen. The tests were usually conducted at a temperature of 10 °C and a speed of 1,000 rpm. The dynamic stiffness was measured by applying constant sinusoidal amplitude deformations.

Another way to carry out this test was done also by Pell using a controlled-strain torsional fatigue machine where the sample is clamped vertically on a shaft. The bottom of the sample is clamped to the bottom of the machine and the loading arrangement gives a sinusoidal varying shear strain of constant amplitude into the specimen.

### *2.6.3 Trapezoidal Cantilever Beam Test*

The trapezoidal cantilever beam test has been popular in Europe. Tests on trapezoidal specimens have been conducted by the Shell researchers (15) and LCPC (50). The larger dimension of the trapezoidal specimen is fixed and the smaller end is subjected to either a sinusoidal applied strain or stress. The trapezoid shape of the specimens can promise to have failure at about mid height where the bending stress is largest rather than at the base where boundary conditions might adversely affect interpretation of test results. As an example, specimens tested by van Dijk (15) had a base cross section of 2.2 in by 0.8 in (55 mm by 20 mm), a top cross section of 0.8 in by 0.8 in (20 mm by 20 mm), and a height of 10 in (250 mm).

### *2.6.4 Supported Flexure Test*

Supported flexure test was used to better simulate stress state and mode-of-loading as in field conditions. Several researchers have used this test with mainly two different specimen shapes; circular slab and beam. Majidzadeh (51) and others used circular samples supported on a rubber mat and subjected to a circular shaped repeated load applied to the center of the slab resulting in a stress state in the slab which is very similar to that occurring in the pavement structure. Barksdale (52) used asphalt concrete beams placed upon 4 inch thickness of rubber mate supporting the beam subjected to a haversine load pulse of 0.06 second duration and 45 cpm frequency. The fatigue specimen and rubber support were enclosed in a temperature control chamber maintained at 80°F (27°C).

This test method can reduce the scatter of test results by duplication of field conditions in a better way. On the other hand, high cost, time consuming, sample size and the need for more complicated test machines are the main serious concerns.

### *2.6.5 Triaxial Test*

Several agencies such as the University of Nottingham (22) and the University of California, Berkeley (53) developed this type of device to best represent the state of stress in situ. Pell and Cooper used a setup where they tested cylindrical specimens with a diameter of 4 in (100 mm) and a height of 8 in (200 mm). The specimen was bonded to end caps with epoxy resin and was mounted on the rig. Specimens enclosed in a Perspex triaxial cell were subjected to a sinusoidally varying axial stress inside. The only concern about this kind of test is that the shear strains must be well controlled; otherwise the predicted fatigue lives could be considerably different than the field results.

Sousa (53) developed equipment which is capable of applying shear strains by torsion (repeated or constant) together with radial tensile stress using specimens fabricated as hollow cylinders. To date, only shear fatigue (torsional) tests have been conducted. This equipment can be further developed to apply repeated radial tensile stresses through the pulsating fluid within the hollow cylinder, thus simulating the necessary conditions including shear stresses (through torsion) and vertical stresses.

Triaxial tests simulate the field loading condition in which compression is followed by tension and the results can be used for mixture design and, with field

correlation factors, for structural design. This type of test is costly, requires specialized equipment, and is time consuming.

### *2.6.6 Direct Tension Test*

The Transport and Road Research Laboratory (TRRL) of the United Kingdom (54) has performed uniaxial tensile tests without stress reversal using a loading frequency of 25 Hz; duration of 40 milliseconds; and rest periods varying from 0 to 1 sec. These tests were conducted in the controlled-stress mode. Later on, direct tension tests have been performed in the Netherlands (55) at frequencies of 1 and 0.1 Hz using haversine loading in the controlled-strain mode. More recently, this test have been used in the U.S. by Texas A &M and North Carolina State University to characterize microdamage healing in asphalt and asphalt concrete using viscoelastic continuum damage, fracture micromechanics and dissipated energy approaches.

One advantage of the direct tension test is the test specimen may be circular as well as rectangular in cross section. In addition, the direct tension test is less costly as testing time is shorter because fewer loading cycles can be sustained before failure. The primary disadvantages of this test are that loading condition does not necessarily represent field conditions and the fact that the test requires extensive preparation.

### *2.6.7 Tension/Compression Test*

The tension/Compression fatigue test was developed at the Transport and Road Research Laboratory (TRRL) (54). Axial tensile and compressive loading was applied using in a servo-controlled electro-hydraulic machine. Specimens were

prismoidal, with 3 in (75 mm) square cross sections and 9 in (225 mm) lengths. Loading frequencies were 16.7 and 25 Hz, and the effects of rest periods, shape of wave form, and the sequence of load application (compression/tension, tension/compression, compression only, and tension only) were evaluated.

Except for the ability to simulate the loading pulse observed in the field, this test does not well represent field conditions, requires long time, is costly and requires specialized equipment.

### *2.6.8 Diametral Test*

The diametral fatigue test is an indirect tensile test (ITT) conducted by repetitively loading a cylindrical specimen with a compressive load which acts parallel to and along the vertical diametral plane. This loading configuration develops a reasonably uniform tensile stress in the specimen perpendicular to the direction of the applied load. Test specimens are usually 4 or 6 inches in diameter and 2.5 to 3.0 in high. Load is transmitted to the sides of the cylinder through a 0.5 in wide loading strip. Usually a haversine/sine load pulse can be applied. The load frequency most commonly used is 20 to 120 cycles per minute.

Most of the repeated-load indirect tensile tests have been conducted at the Center for Highway Research at the University of Texas at Austin (57, 57, 58, 59). The diametral test offers a biaxial state of stress, which is possibly of a type that better represents field conditions. A key problem with this method is that it will significantly underestimate fatigue life if the principal tensile stress is used as the damage determinant.

### *2.6.9 Wheel-Track Test*

In order to better simulate the effects of a rolling wheel on the pavement and to better understand the pattern of crack initiation and propagation, a wheel-track test has been developed to study fatigue characteristics of asphalt pavements. The Wheel-track test can be conducted in laboratory and in full scale pavement section.

For laboratory wheel-track test, Van Dijk (15) has developed a loaded wheel with a pneumatic tire that rolled back and forth over a slab of asphalt concrete. The wheel has a diameter of 0.25 m and its path is 0.60 m long with a width in the range of 0.05 to 0.07 m. The slab is supported by a rubber mat. Strains at the bottom of slabs, and the detection of crack initiation and propagation were measured. Results can be expressed in terms of three fatigue stages associated with the development of hairline cracks, real cracks, and failure of the slab. Based on the test results, Van Dijk suggested that controlled-strain data may be more appropriate to define pavement cracking than controlled-stress data.

The main limitation of laboratory wheel-track test is the speed of the rolling wheel. In addition, the test is time consuming and does not measure a fundamental mixture property. Moreover, for mixes of low stiffness, rutting becomes significant and may affect fatigue measurements.

Full-scale testing facilities have been built in several countries around the world. Well-known examples include the circular tracks located at Nantes in France, at Pullman, near the Washington State University campus, the Federal

Highway Administration's ALF (Accelerated Loading Facility), in Australia (ARRB), New Zealand (Canterbury), Denmark, and in United Kingdom (TRRL). The tracks are often divided into sections, each with a different pavement structure, and loads are applied by several sets of dual truck tires.

With full-scale testing facilities, it is possible to examine the effect of changes in the pavement structural section on pavement performance and other forms of pavement distress in addition to fatigue can be studied as well. High initial investment cost and annual operation and maintenance costs are the main disadvantages. Also, a parallel, supplementary laboratory testing program is still needed, since the field track tests do not directly measure fundamental mixture properties.

## 2.7 Healing of HMA

### *2.7.1 Healing Mechanism*

Healing phenomena have been investigated in literatures for many years. Healing is generally considered as the capability of a material to self-recover its mechanical properties (stiffness or strength) to some extent upon resting due to the closure of cracks. In fact, various engineering materials are found to have this ability whether they are metallic or non-metallic.

For metallic materials such as steel, aluminum, etc., Suresh, (60) categorized the various mechanisms of fatigue crack closure or healing that are induced by a variety of mechanical, microstructural and environmental factors based on his own results and of the work of other researchers. These mechanisms of crack closure include the followings:

1. Residual plastic stretch at crack wake (plasticity-induced crack closure),
2. Corrosion layers formed within a fatigue crack (oxide-induced crack closure),
3. Microscopic roughness of the fatigue fracture surfaces (roughness-induced crack closure),
4. Viscous fluids penetrated inside the crack (viscous fluid-induced crack closure), and
5. Stress- or strain- induced phase transformations at the crack tip (transformation-induced crack closure).

For non-metallic materials and composites such as glass, polymers, Portland cement concrete, and asphalt concrete mixtures, there are several mechanisms which hinder the growth of fatigue cracks and induce crack healing, which can be summarized as follow (60):

1. Crack deflection;
2. Crack-bridging or trapping; and
3. Crack-shielding due to microcracking, phase transformations or dislocations.

### *2.7.2 Effect of Healing on Fatigue Life*

A significant amount of work has documented the effect of rest periods on the fatigue life of asphalt mixtures, but little research has focused on the mechanism of healing.

Phillips (61) proposed that the healing of asphalt binders is a three-step process consisting of:

1. The closure of microcracks due to wetting (adhesion of two crack surfaces together driven by surface energy);
2. The closure of macrocracks due to consolidating stresses and binder flow; and
3. The complete recovery of mechanical properties due to diffusion of asphaltene structures.

Step 1 is supposed to be the fastest, resulting only in the recovery of stiffness, while steps 2 and 3 are thought to occur much slower but improve both the stiffness and strength of the material similar to the virgin material.

Jacobs, (62) studied the fatigue properties of asphalt mixes under sinusoidal loading, and found that the introduction of rest periods has a beneficial effect on the fatigue resistance of the mixes. He proposed that this healing effect is caused by diffusion of maltenes (low molecular weight bitumen component) through the microcracks, re-establishing the bonds in the cracked area. The maltenes are involved, as they are the most mobile components of the bitumen, although higher molecular weight molecules could also diffuse during longer rest periods, resulting in completely restored material properties.

Lytton (63) used the "dissipated pseudo strain energy concept" to explain the fracture and healing process. The fracture or healing of an asphalt mixture is related to two mechanisms: the surface energy storage or the surface energy release. Which one dominates is related to polar or non-polar characteristic of the binder. The energy stored on or near the newly created crack faces governs the energy available to make the crack grow. This surface energy depends mainly on

the chemical composition of the binder. The micro-fracture and healing of the asphalt-aggregate mixture is governed by the energy balance per unit of crack area between the “dissipated pseudo-strain energy” released and the energy that is stored on the surface of the crack.

Even when considering healing, people disagree whether it happens only during rest periods, during all the loading and unloading periods, or just under certain conditions such as certain temperature and material damage level. These different conclusions are mainly based on a large variety of laboratory testing setup and research approaches.

Although healing has received little attention by pavement engineers, it is a well-known subject in polymer engineering. A considerable volume of work has been done in studying on the healing phenomenon of polymeric materials. Prager and Tirrell (64) described the healing phenomenon:

"When two pieces of the same amorphous polymeric material are brought into contact at a temperature above the glass transition, the junction surface gradually develops increasing mechanical strength until, at long enough contact times, the full fracture strength of the virgin material is reached. At this point the junction surface has in all respects become indistinguishable from any other surface that might be located within the bulk material: we say the junction has healed."

In asphalt concrete pavements, healing is the process of structural changes that occurs during rest periods, and leads to a structural regain, enhancement, or beneficiation. According to Peterson (65), the association force (secondary bond)

is the main factor controlling the physical properties of asphalt cement. That is, the higher the polarity, the stronger the association force, and the more viscous the fraction even if molecular weights are relatively low. Ensley et al. (66) subscribe to the view that asphalt cement consists of aggregations of micelles. These micelles consists of two or more molecules of asphaltenes and associated (if present) peptizing materials of lower molecular weight. The interactions of these micelles among themselves and with aggregates largely determine cohesion and bond strengths, respectively.

A significant breakthrough in understanding the effect of asphalt composition on the healing of asphalt cement was made by Kim et al. (67). They observed that healing was directly proportional to the amounts of longer-chained aliphatic molecules in the saturates and long-chained aliphatic side chains in the napthene aromatics, polar aromatics and asphaltenes generic fractions. They proposed methylene to methyl ratio (MMHC) as a quantifier of the nature of the long-chained aliphatic molecules and side chains. The MMHC is defined as the ratio of the number of methyl and methylene carbon atoms in independent aliphatic molecules or aliphatic chains attached to cyc10alkanes or aromatic centers. While the effects of rest periods on the fatigue life of asphalt mixes have been intensely studied, only limited research in the area of asphalt concrete healing has been reported (68, 69, 70, 71). In recent years, a mechanical approach in identifying the healing potential of asphalt concrete was made by Kim and Little (69). They performed cyclic loading tests with varying rest periods on notched beam specimens of sand asphalt. They obtained a consensus that the rest

periods enhance the fatigue life through healing and relaxation mechanisms. They proposed a concept called the healing index and found it to be highly sensitive to the binder used in the tests. Schapery's elastic-viscoelastic correspondence principle (72) was applied in their study to separate viscoelastic relaxation from chemical healing. After separating the relaxation from the healing, the magnitudes of pseudo energy density before and after rest periods were used to calculate the healing index.

Schapery (73) proposed the mechanics of quasi-static crack closing and bonding of the same or different linear viscoelastic materials. He developed equations for predicting crack length or contact size as a function of time for relatively general geometries using continuum mechanics. Atomic and molecular processes associated with the healing or bonding process are taken into account using a crack tip idealization. Using his correspondence principle, an expression was derived for the rate of the edge of the bonded area that is a function of a pseudo stress intensity factor. He found that both the bonding-zone length and speed increase with decreasing this pseudo stress intensity factor.

### *2.7.3 Field Tests*

A field study on fatigue damage growth and microdamage healing during rest periods was performed by Kim and Kim (71). The stress wave test technique and dispersion analysis method based on Short Kernel Method employed in their study effectively assessed the changes in elastic modulus due to fatigue damage growth and microdamage healing in asphalt surface layer. It was found that the elastic modulus decreases following a characteristic S-shape curve when plotted

against number of loading cycles. The major reduction in the elastic modulus occurred during early stage of fatigue life when there were no visible cracks on the pavement surface. This reduction was concluded to be related to microcrack initiation, propagation and densification. Introduction of rest between loading cycles shifts the curve upward, resulting in a longer fatigue life.

## 2.8 HMA Endurance Limit

### *2.8.1 Historical Background*

Pavements have been primarily designed to resist rutting of the subgrade and bottom-up fatigue cracking. In classical pavement design, as design load applications increase, pavement thickness must also increase. There is a growing belief that for thick pavements bottom up fatigue cracking does not occur. The concept of an endurance limit has been developed. This concept assumes that there is a strain level below which no fatigue damage occurs. This strain level is referred to as the endurance limit. Therefore, additional pavement thickness, greater than that required to keep strains below the endurance limit, would not provide additional life. This concept has significant design and economic implications.

The fatigue endurance limit concept was first proposed by Wöhler (74) for metallic materials. The classical Wöhler S/N curve was found to approximate a hyperbola (75), as shown in Figure 5. The asymptote of this line parallels to the time (load cycle) axis indicating there is a load level below which the number of cycles to failure does not proportionally increase with decreasing load thus the

material tends to have unlimited fatigue life. This asymptote represents the fatigue endurance limit (FEL).

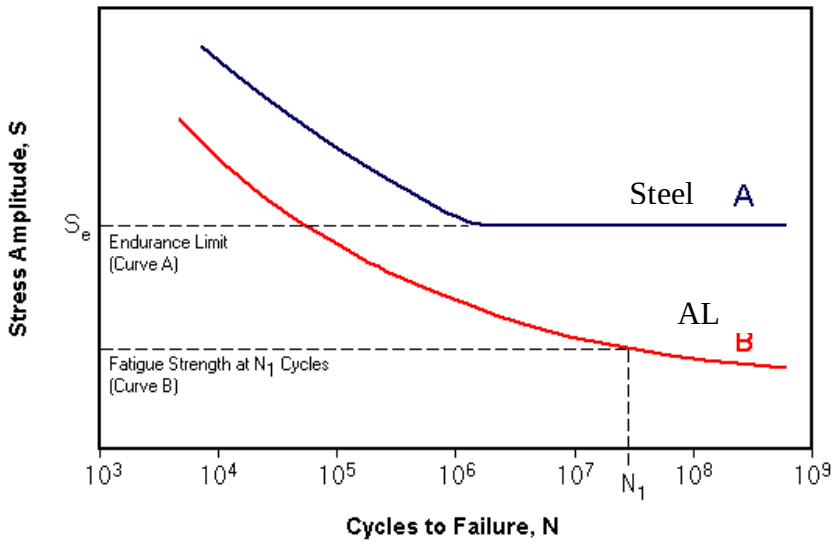


**Figure 5. Fatigue Endurance Limit concept (from Wöhler curve).**

Wöhler's fatigue endurance limit concept was later applied to adhesive joints by Lagace and Allen et al. (76), and explained as: "If a stress exists below which the life of a joint is not dependent upon the loading but only on the ability of the adhesive to resist oxidation or other environmental degradation, then joints could be designed to have a safe working life determined only by the chemical stability of the adhesive." Although the "endurance limit" concept has been widely studied and defined in metal and other materials, relatively less work was done for viscoelastic HMA materials.

### *2.8.2 Endurance Limit Studies*

Monismith and McLean (77) first proposed an endurance limit of 70 micro-strains for asphalt pavements. It was observed that the log-log relationship between

strain and bending cycles converged at approximately 70 micro strains at approximately 5 million cycles. Maupin and Freeman (78) noted a similar convergence.

In the field, Nunn (79) in the United Kingdom (UK) and Nishizawa et al (6) in Japan proposed concepts for long-life pavements for which classical bottom-up fatigue cracking would not occur. Nunn (79) defines long-life pavements as those that last at least 40 years without structural strengthening. The UK's pavement design system was based on experimental roads which had carried up to 20 million 18-Kips standard axles. When this study was conducted, these relationships were being extrapolated to more than 200 million standard axles. Nunn (79) evaluated the most heavily traveled pavements in the UK, most of which had carried in excess of 100 million standard axles to evaluate the then current design system. Nunn (79) concluded:

- For pavements in excess of 180 mm thick, rutting tended to occur in the HMA layers, not in the underlying structure.
- Surface initiated cracking was common in high traffic pavements, but there was little evidence of bottom-up fatigue. Surface initiated cracks tended to stop at a depth of 100 mm.
- It was observed that the stiffness of thick pavements increased with time, most likely due to binder aging. This would not tend to occur if the pavement was weakening due to accumulated damage.
- A minimum thickness for a long-life pavement was recommended as 7.9 inches with a maximum thickness of 15.4 inches. The range

is based on a variety of factors such as binder stiffness.

Nishizawa (80) reported an endurance limit of 200 micro-strains based on the analysis of in-service pavements in Japan. Similarly, strain levels at the bottom of the asphalt layer of between 96 and 158 micro-strains were calculated based on back-calculated stiffness data from the falling-weight deflectometer for a long-life pavement in Kansas (81). Other studies (82, 83) report similar findings, particularly the absence of bottom-up fatigue cracking in thick pavements and the common occurrence of top-down cracking.

Monismith et al. (38) found that when performing laboratory testing, if the bending deformations were very low (of the order of 100 micro strains) the beams were able to carry a large number of repetitions (approximately 106 load repetitions) without fracture. He and other researchers (84, 85) further proposed that limiting tensile strain at the bottom of the asphalt layers no greater than 70 micro strains can extensively increase pavement fatigue life. A similar convergence was noted by Maupin and Freeman (78).

Another study that was performed by Von Quintus (86, 87) suggested that the endurance limit design premise has some validity. He believed that the endurance limit is a valid design premise and is a HMA mixture property and then he concluded that as the modulus decreases, the endurance limit increases.

Carpenter supported the idea of the existence of a fatigue endurance limit (88). He concluded that the endurance limit is most dependent on binder type and is not readily connected with mix composition. The magnitude of an endurance limit for all mixtures is never lower than 70 micro-strains, and for some mixtures

it goes up to 100 micro-strains, with polymer modified mixtures showing HMA-EL values approaching 300 micro-strains. This provides a valid design concept for extended life hot mix asphalt pavements.

Only limited HMA fatigue research was conducted at low strain levels until recently when the Asphalt Pavement Alliance began promoting the concept of perpetual pavement design (89). A perpetual pavement is an asphalt pavement that provides a very long life without structural failure and only requires periodic replacement of the surface. A key element of perpetual pavement design is to eliminate fatigue cracking that initiates at the bottom of the HMA base due to repeated flexure under traffic loading and to confine distresses to the surface of the pavement, which can easily be renewed by milling and resurfacing.

In response to increasing interest in perpetual pavements, a substantial amount of laboratory fatigue testing has recently been performed in the United States in an effort to demonstrate that HMA does exhibit an endurance limit. Most of this work has been performed at the University of Illinois (3, 5) and the National Center for Asphalt Technology (NCAT) (7). These studies provide clear evidence that the fatigue behavior of HMA is much different in low strain level tests compared to normal strain level tests. Figure 6 shows a consolidated plot of the University of Illinois fatigue data including low and normal strain level test data. Below approximately 100 micro strains, the fatigue life is significantly longer than estimated from extrapolation of normal strain level test data. Healing of micro damage has been proposed as the primary reason for the increased fatigue life at low strain levels (90, 6, 91). For cyclic tests at low strain levels, it

appears that the damage that is caused by loading is offset by healing that occurs during unloading resulting in essentially infinite fatigue life.

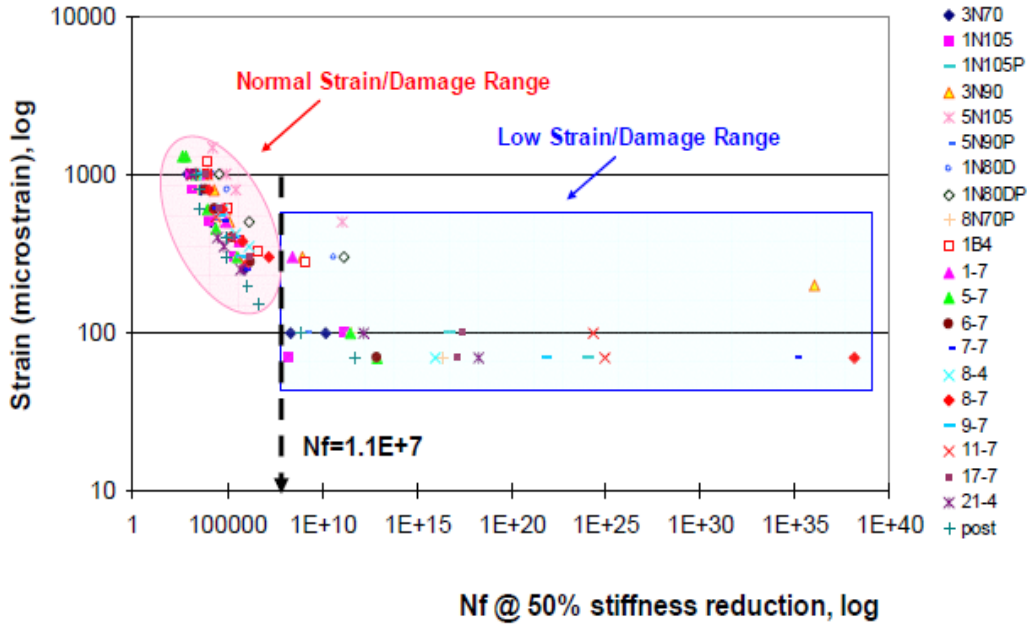


**Figure 6. Results of flexural fatigue tests by Carpenter et al. (3) including extrapolated results at low strain levels.**

Kansas Department of Transportation, KDOT, conducted a field trial to investigate the suitability of the perpetual pavement concept for Kansas highway pavements (92). The experiment involved the construction of four thick flexible pavement structures on a new alignment on US-75 near Sabetha, Kansas. The four pavements were instrumented with gauges for measuring the strains at the bottom of the asphalt base layers. Seven sessions of pavement response measurements under known vehicle load, consisting of multiple runs of a single-axle dump truck at three speeds, were performed between, before and after the pavement sections were opened to traffic. The analysis of the measured strain data recorded led to the following major conclusions:

- With few exceptions, the longitudinal and transverse strains were lower than 70 micro strains which is matching the endurance strain limit recommended in the literature for asphalt–concrete.
- The pavement response was affected significantly by the temperature in the asphalt layers and by the speed of the loading vehicle. The strains recorded for a truck speed of 20 mph were almost double the strains recorded for a speed of 60 mph.

Bhattacharjee et al (93) presented an improved method to determine the fatigue endurance limit of asphalt concrete without the need for long-term fatigue tests. The recommended approach employs the elastic–viscoelastic correspondence principle and identifies the strain level at which hysteresis loops form in a stress-pseudo strain relationship, indicating that damage is occurring. The approach requires the linear viscoelastic characterization of the mixture through dynamic modulus testing. This was followed by an increasing amplitude fatigue test to determine the strain level above which damage occurs in the mix. This method was recommended as an alternative method of determining the fatigue endurance limit of HMA. The endurance limit values obtained through uniaxial testing ranged from 115 to 250 micro strains which showed comparable magnitudes as those obtained from beam fatigue tests (93).

Detailed investigation of four heavily trafficked pavements in the United Kingdom support the perpetual pavement concept and the likelihood of an endurance limit for HMA. This comprehensive study found no evidence of fatigue damage at the bottom of properly constructed thick flexible pavements

with total HMA thickness ranging from 230 to 350 mm (94). Cracks in these pavements were found to have initiated at the surface and deflections monitored over a number of years generally showed steady or decreasing deflection with increasing cumulative traffic, indicating that fatigue damage to the bottom of the HMA was not occurring. Similar conclusions concerning the absence of cracking at the bottom of thick HMA pavements have been reported by others (95, 81, 96). In summary, there is mounting evidence that an endurance limit for HMA does exist. It has been observed in laboratory studies of fatigue at low strain levels, and several documented case studies indicate that bottom initiated fatigue cracking is almost non-existent in properly constructed, thick HMA pavements. The HMA endurance limit, however, does not reflect an absence of load induced damage in the HMA. It is the result of a balance of damage caused by loading and healing or damage recovery that occurs during rest periods (5). The endurance limit for HMA is, therefore, not a single value, but will change depending on the loading and environmental conditions applied to the HMA. Considering an endurance limit in flexible pavement design requires the consideration of the effects of loading, environment and material properties on both damage accumulation and healing. These findings concerning the endurance limit for HMA served as the research hypothesis upon which the HMA Endurance Limit Validation Study Research Plan (4) was formulated. In conclusion, the literature provides ELs at certain conditions but there is no general model is currently available to estimate EL values under different conditions

# Chapter 3 STATISTICAL DESIGN OF EXPERIMENT

## 3.1 Background

The main objective of this chapter is to present the proposed statistical experimental plan, originally developed in a previous study (NCHRP 9-44) and the final recommendations developed by the ASU NHCRP 9-44A project team. The NCHRP 9-44 plan was a provisional design of experiment that was used by the ASU team to provide a general work plan for the current NCHRP 9-44A project as required by the NCHRP project panel. As such, the ASU research team has carefully analyzed the initial NCHRP 9-44 plan and developed a more enhanced, thorough and detailed experimental plan for the NCHRP 9-44A study.

## 3.2 NCHRP 9-44 Proposed Design

The work plan proposed by the NCHRP Project 9-44 (4) consisted of 5 separate experiments as summarized in Table 2. The plan shows that 10 factors can possibly influence the fatigue endurance limit. Using a full factorial design would lead to an enormous amount of testing to evaluate their effects.

It was clear that some type of reduced statistical plan is needed to address all variables and. Therefore, the NCHRP 9-44 proposal breaks down the study into 5 (sequential) study experiments, each of which is based upon the results of the succeeding experiment and 2 to 3 more variables are to be evaluated in the following experiment. For example, Experiment 1 was intended to identify mixture compositional factors that affect healing. Experiments 2-5 use the significant factors identified in Experiment 1 and determine the effects of other

factors separately. Although this approach reduces the required number of tests, it might not produce accurate and meaningful results as discussed below.

**Table 2. Summary of Laboratory Experiments Proposed by the NCHRP 9-44 Project (4).**

| Experiment | Topic | Factors |
|---|---|---|
| 1 | Mixture Compositional factors affecting healing in HMA | • Binder type<br>• Binder age<br>• Effective binder conent<br>• Air voids<br>• Design compaction<br>• Gradation<br>• Filler content |
| 2 | Efect of Applied strain on healing | • Strain level<br>• Healing from experiment 1 |
| 3 | Effect of temperature and rest perod duration on healing | • Temperature<br>• Rest period from experiment 1 |
| 4 | Development of testing and analysis procedures to determine allowable strain levels | • Healing rate from experiment 1<br>• Mixtures from NCHRP 9-38 |
| 5 | Estimation of allowable strain levels from mixture composition | • Mix compositional factors affecting damage accummulation<br>• Significant factors from experiment 1<br>• Temperature<br>• Rest period duration |

In Experiment 1, a fractional factorial experiment has been proposed using 7 factors and 2 levels for each factor. However, all tests are performed at 20$^{o}$C, resulting in 16 tests. This experimental design has some shortcomings that may produce inaccurate results. For example, different temperatures may produce different results. Factors that are not significant at 20$^{o}$C might be significant at lower or higher temperatures. Also, the proposed plan uses the Plackett-Burman

design approach (97), which considers the main effects of the different factors involved, but assumes that there is no interaction among the different factors. For example, the interaction between binder type, binder content and strain level could have a significant effect on healing, while individual factors such as the strain level only might not be significant. Another well-established interaction in fatigue practice is that the $N_f$ (failure repetitions) of any specimen has been conclusively shown to interact with the $V_{fb}$, $V_{beff}$ and AV%.

Another limitation of the proposed NCHRP 9-44 plan was the lack of importance of the correct number of replicates to be used. The NCHRP 9-44 plan recommended to use two replicates for each testing condition, which represents the lowest number required to compute the standard deviation of any variable. One should recognize that fatigue is indeed a highly variable phenomenon, and the variance of any computed healing index value would be the sum of the variances associated with the stiffness with and without rest period. In other words, one should logically expect that the variance of the Healing Index (HI) parameter may be very large. This leads to the possible unfortunate consequence that the ANOVA assessment of the significance of the variance components would be hard to prove since the statistical F-ratios of the variances would be large.

A third limitation of the proposed NCHRP 9-44 plan was related to the spreading the variables among 5 experiments rather than considering all variables in one experiment. The following sections discuss some of the factors proposed in the NCHRP 9-44 plan and their limitations as related to the ASU used plan.

*AC Binder Type*

For all practical purposes, the proposed NCHRP 9-44 plan simply eliminates properties of the AC Binder as a primary variable. This experimental design cannot produce global conclusions related to the effect of the AC Binder type. What is missing in the plan is to assess if there are any, quantifiable differences between the PG grades (Shear Stiffness) in healing between different PG's neat asphalt binders. In this initial quantitative study, it is imperative to assess what properties of a given grade (as well as perhaps any interactions of this property with other variables) may be present to alter the Healing Index and Fatigue Endurance Limit of the mix.

*Binder Ageing*

The proposed NCHRP 9-44 plan called for the analysis of 2 levels of aging to be employed in the experiment. While it is not denied that aging is not a factor in fatigue endurance, it appears that the first order effect of aging can be viewed as an increase in stiffness of the binder. As such, the importance of a wider range of AC Performance Grades should allow a first order assessment of the influence of aging by varying this as a consequence of increased binder stiffness.

*Compaction Level*

The use of the design compaction level controlled by the number of compaction gyrations is a major variable in the NCHRP 9-44 project plan. The design level of gyrations directly impacts the actual target air voids and design asphalt content. Therefore, it is better to use the $V_{beff}$%, volume of effective bitumen percent, to quantify the amount of asphalt in a given mix. If the AV% and $V_{beff}$% are used as

two prime mix volumetric variables that are included in the main experiment, the impact of mix volumetrics should already be included in any mathematical algorithm used in the overall study. Thus, the use of Design Compaction would actually serve as a redundant variable.

*Gradation / Filler Content*

In the NCHRP 9-44 project plan, gradation and filler content are treated as main factors. Again, these variables must be viewed as factors that possibly may have a potential impact upon the fatigue endurance limit. However, AC base gradation specifications will not vary significantly between DOT agencies. The research team felt that highway agencies typically use standard base gradations and filler contents based on their previous experience. These standard gradations and filler contents have been selected to optimize the properties of their mixes and any changes in these factors might result in poor performance. Thus, the selection of a typical gradation for the mixtures used in this experiment should suffice until more results are finalized from this and other studies.

In summary, this discussion states that major concerns and subsequent changes to the original NCHRP 9-44 Work Plan have occurred from the ASU team. In retrospect, changes have been made by the ASU team to alter and enhance the probability of success of the NCHRP 9-44A project. However, the excellent work accomplished by the NCHRP 9-44 team is certainly acknowledged. Section 3.3 below details the specific experimental plan recommendations that are used in the current study.

### 3.3 Design of Experiment Used In the Current Study (NCHRP 9-44A Design)

Because of the noted enhancements to the initial NCHRP 9-44 approach, the ASU research team proposed a revised experimental design approach that produces a more comprehensive solution to mathematically define the fatigue endurance algorithm. The design approach is based on studying all major factors and levels together in one main experiment rather than dealing with incomplete, separate sequential experiments. The experiment considers more important factors than those proposed in the NCHRP 9-44 study and ignores a few unimportant factors, as perceived from the experience of the Senior ASU team members. This main experiment was considered by the team, as a dynamic and flexible undertaking. As results on main portions of the experimental plan are accomplished; necessary changes and modifications to the initial plan were made in the project to ensure that the latest experimental results were constantly used to increase the efficiency of the remaining portions of the study plan. The ASU proposal results in many more tests than those proposed by the original NCHRP 9-44 study.

This study considers the following factors.

1. Binder type (3 levels: PG 58-28, PG 64-22, PG 76-16)
2. Binder content (2 levels: optimum ± 0.5 %)
3. Air voids (2 levels: 4.5, 9.5 %)
4. $N_f$ as controlled by the strain level (2 levels: L, H)
5. Temperature (3 levels: 40, 70, 100 $^{\circ}$F)
6. Rest period (2 levels: 0, 5 sec.)

It was initially planned to start the experiment using three replicates for each factor combination. As results were obtained and evaluated; an analysis was conducted to re-evaluate the efficiency and accuracy of the use of three replicate specimens and to find ways to reduce the number of tests instead of using a full factorial design.

Two possible factorial design approaches were evaluated by the ASU team to study the effect of the 6 main factors. The 6-factor design approach considers all 6 factors together in one experiment. The 5-factor design approach uses the first 5 factors stated above for each rest period separately. In other words, the effect of the first 5 factors will be evaluated without a rest period and with a 5-second rest period separately. The two design approaches are discussed below.

### *3.3.1 Six-Factor Design*

In this design, all 6 factors stated above will be evaluated. From the fatigue test results, the stiffness ratio (SR) will be obtained. Using a statistical program (98), a model will be developed to estimate the SR as a function of all 6 factors as shown in the following equation.

$$SR = f(BT, AC, V_a, SL, T, RP) \quad (14)$$

Where BT is the binder type, AC is the binder content, AV is the air voids, SL is the strain level, T is the temperature, and RP is the rest period. Substituting values of 0 and 5 seconds in the model produces the corresponding stiffness values at failure. Figure 7 shows stiffness ratio versus number of loading cycles for the cases with and without rest period. Healing Index (HI) can be defined as the difference between the stiffness ratios for the tests with and without rest

period at $N_f$ w/o RP (number of cycles to failure for the test without rest period) as shown in Figure 7.

$$HI = [SR_{w/\ RP} - SR_{w/o\ RP}]_{at\ Nf\ w/o\ RP} \quad (15)$$

where,

$SR_{w/\ RP}$ = Stiffness ratio with rest period

$SR_{w/o\ RP}$ = Stiffness ratio without rest period

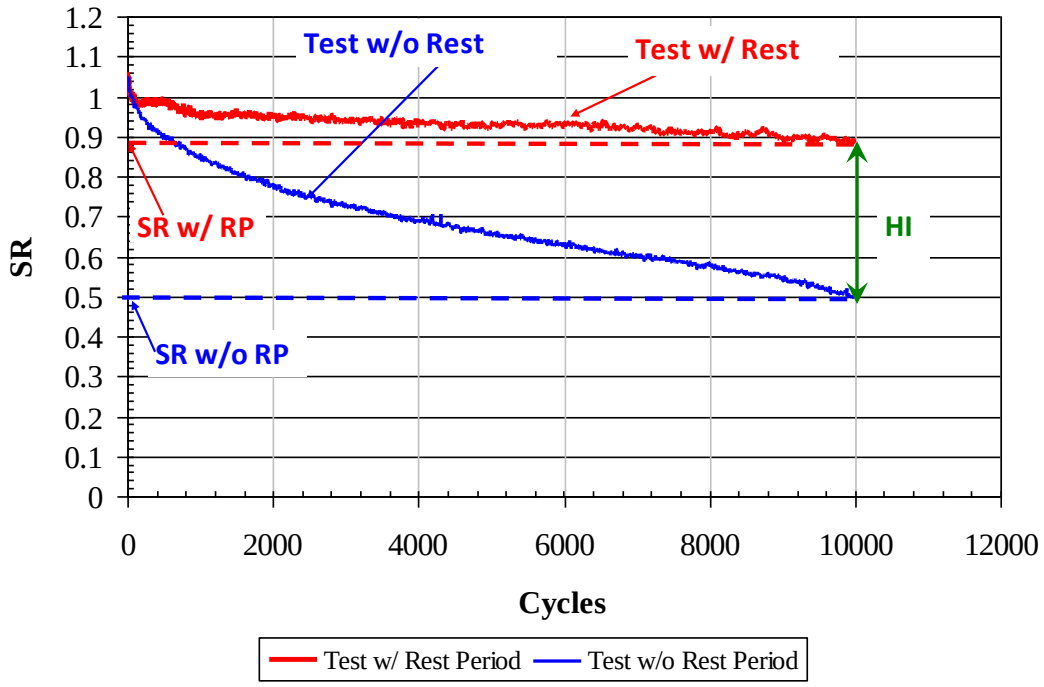


**Figure 7. Example of stiffness versus number of loading cycles with and without rest period.**

According to this HI definition, SR needs to be recorded for both tests with and without rest period at $N_f$ w/o RP as shown in Figure 7. Also, extrapolation was used to predict the SR for the test with rest period at $N_f$ w/o RP since it was decided to run all tests with rest period up to 20,000 cycles only. Figure 8 shows the extrapolation process to determine SR for the tests with rest-period at $N_f$ w/o RP.

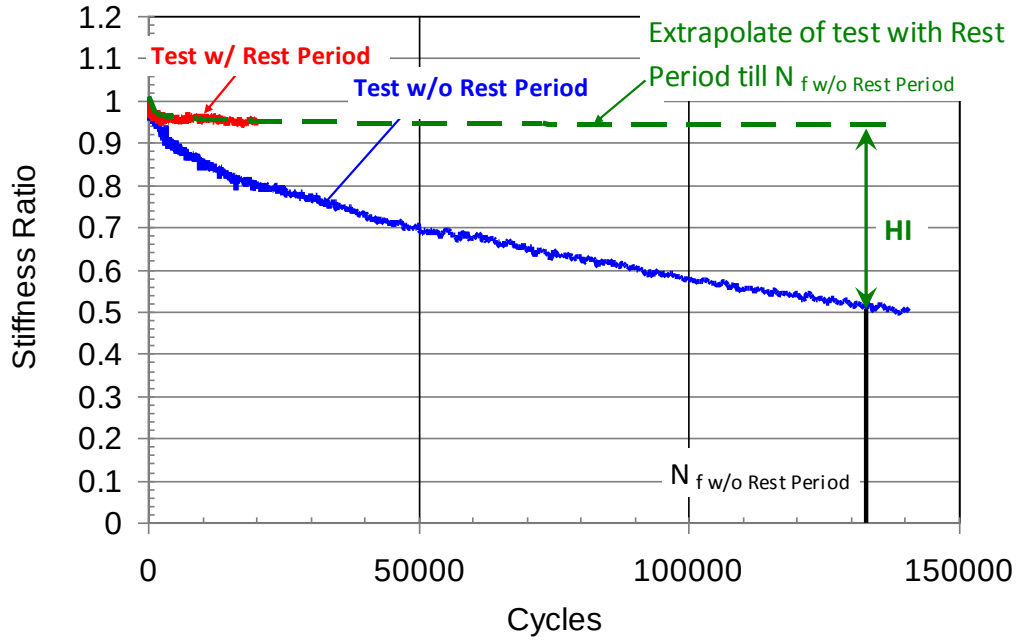


**Figure 8. Extrapolation process to estimate SR (with rest-period) at $N_{f\ w/o\ RP}$ (PG 64-22, 40F, 4.2 AC%, 4.5 $V_a$%, 200 micro strains).**

*Six-Factor Full Factorial Design*

Table 3 shows the full factorial design in which all factor combinations are tested. The full factorial design will require 3 x 2 x 2 x 2 x 3 x 2 x 3 replicates = 432 tests. This full factorial design would allow a full analysis of all possible interactions of all main variables.

**Table 3. Six-Factor Full Factorial Design.**

| Binder Type | | | PG 76-16 | | | | PG 64-22 | | | | PG 58-28 | | | |
|---|---|---|---|---|---|---|---|---|---|---|---|---|---|---|
| Binder Content | | | 4.2 | | 5.2 | | 4.2 | | 5.2 | | 4.2 | | 5.2 | |
| Air Voids (%) | | | 4.5 | 9.5 | 4.5 | 9.5 | 4.5 | 9.5 | 4.5 | 9.5 | 4.5 | 9.5 | 4.5 | 9.5 |
| Temp | $N_f$ w/o RP | Rest Period (sec) | | | | | | | | | | | | |
| L | L | 0 | | | | | | | | | | | | |
| | | 5 | | | | | | | | | | | | |
| | H | 0 | | | | | | | | | | | | |
| | | 5 | | | | | | | | | | | | |
| M | L | 0 | | | | | | | | | | | | |
| | | 5 | | | | | | | | | | | | |
| | H | 0 | | | | | | | | | | | | |
| | | 5 | | | | | | | | | | | | |
| H | L | 0 | | | | | | | | | | | | |
| | | 5 | | | | | | | | | | | | |
| | H | 0 | | | | | | | | | | | | |
| | | 5 | | | | | | | | | | | | |

In an effort to reduce the number of tests and still produce accurate results, a fractional factorial design approach was then considered. The fractional factorial approach has been designed in such a way as to produce the main effects, as well as all salient 2-factor and 3-factor interactions (99). The only drawback of the fractional factorial design is that all 4-factor and higher interactions would be ignored. This however, is not considered a quantitative limitation at all. From a practical viewpoint, 4-factor and higher interactions are of little to no consequence to the final accuracy of the experiment. Two fractional factorial designs were studied further. One was considered a complete randomization and the other viewed as a partial randomization. These are discussed in the following paragraphs.

*Six-Factor Fractional Factorial Design with Complete Randomization*

This statistical fractional factorial design considers all 6 factors with all levels previously listed. There are many design optimality criteria and the most popular

criterion is called D-optimality (99). The D-optimality design minimizes the volume of the joint confidence region on the vector of regression coefficient. A computer generated design is used to reduce the number of runs using the JMP software (98). Table 4 shows the factor combinations at which the test would be performed. The table shows that 96 combinations would be tested with 3 replicates for each combination. This design would require a total of 288 tests instead of the 432 tests required for the 6-factor full factorial design. This would save 144 tests as compared to the full factorial design.

**Table 4. Factor Combinations at Which the Test Will be Performed for the 6-Factor Fractional Factorial Completely Randomized Design.**

| Binder Type | | | PG 76-16 | | | | PG 64-22 | | | | PG 58-28 | | | |
|---|---|---|---|---|---|---|---|---|---|---|---|---|---|---|
| Binder Content | | | 4.2 | | 5.2 | | 4.2 | | 5.2 | | 4.2 | | 5.2 | |
| Air Voids (%) | | | 4.5 | 9.5 | 4.5 | 9.5 | 4.5 | 9.5 | 4.5 | 9.5 | 4.5 | 9.5 | 4.5 | 9.5 |
| Temp | $N_f$ w/o RP | Rest Period (sec) | | | | | | | | | | | | |
| L | L | 0 | ■ | | | ■ | | ■ | ■ | | ■ | ■ | ■ | ■ |
| | | 5 | | ■ | ■ | | ■ | | | ■ | ■ | ■ | ■ | ■ |
| | H | 0 | | ■ | ■ | | ■ | ■ | | ■ | ■ | ■ | ■ | ■ |
| | | 5 | ■ | | | ■ | | ■ | ■ | | ■ | ■ | | ■ |
| M | L | 0 | | ■ | ■ | | ■ | ■ | ■ | ■ | ■ | | | ■ |
| | | 5 | ■ | | | ■ | ■ | ■ | ■ | ■ | | ■ | ■ | |
| | H | 0 | ■ | | | ■ | ■ | ■ | ■ | ■ | | ■ | ■ | |
| | | 5 | | ■ | ■ | | ■ | ■ | ■ | ■ | ■ | | | ■ |
| H | L | 0 | ■ | ■ | ■ | ■ | ■ | | | ■ | | ■ | ■ | |
| | | 5 | ■ | ■ | ■ | ■ | | ■ | ■ | | ■ | | | ■ |
| | H | 0 | ■ | ■ | ■ | ■ | | ■ | ■ | | ■ | | | ■ |
| | | 5 | ■ | ■ | ■ | ■ | ■ | | | ■ | | ■ | ■ | |

Table 5 shows the lists of the main and two and three-factor interaction terms that can be estimated from this experimental design. It is obvious that all of the major three factor interactions are accounted for in the fractional design and a model with up to 41 variable parameters can be developed.

**Table 5. Factors and Factor Interactions Estimated from the Experiment.**

| All main effect | Two-factor interactions | Three-factor interactions |
|---|---|---|
| Binder Content | Binder Content*Air Voids | Binder Content*Air Voids* Damage Level |
| Air Voids | Binder Content* Damage Level | Binder Content*Air Voids*Rest Period |
| Damage Level | Binder Content*Rest Period | Binder Content*Air Voids*Temperature |
| Rest Period | Binder Content*Temperature | Binder Content* Damage Level*Rest Period |
| Temperature | Air Voids* Damage Level | Binder Content* Damage Level*Temperature |
| | Air Voids*Rest Period | Binder Content* Rest Period*Temperature |
| | Air Voids*Temperature | Air Voids* Damage Level*Rest Period |
| | Damage Level*Rest Period | Air Voids* Damage Level*Temperature |
| | Damage Level*Temperature | Air Voids*Rest Period*Temperature |
| | Rest Period*Temperature | Damage Level*Rest Period*Temperature |

*Six-Factor Fractional Factorial Design with Partial Randomization*

It is important to randomize the tests in the lab in order to reduce the effect of errors. For example, if a machine error occurs on a certain day, randomization would distribute the error among different factor combinations instead of concentrating the error on a few factor combinations. However, complete randomization may not be practical in some cases. For example, complete randomization would require testing a specimen with a certain factor combination followed by a specimen with a completely different factor combination, etc. This would reduce the efficiency of the specimen preparation and testing program.

In the experiment involving Partial Randomization; a split-plot design is used in which the factors are divided into two groups: whole plot and subplot

(99). The whole plot includes factors whose levels are hard to randomize, while the subplot includes factors whose levels are easy to randomize. In this experiment, the whole plot will be the binder type, while the subplot includes the rest of the factors. This means that all tests of the first binder will be completed first followed by the second binder tests and then the third binder tests. Within each binder, all other factors will be randomized. This order of testing is more practical than completely randomizing all tests. The results will be analyzed according to the split-plot design procedure (98). This statistical design method does not affect the required number of tests for the fractional factorial design.

This approach, in reality, is a practical necessity in the lab as specimen preparation can be easily accomplished for each specific binder type used in the study. Use of a completely randomized design would probably induce potential lab chaos during the production process by requiring random use of the various binder types to be used during the beam specimen manufacturing process.

Table 6 shows the factor combinations at which the tests will be performed. The table shows that 96 combinations will be tested with 3 replicates for each combination with a total of 288 tests. Similar to the completely randomized experiment, all main and two and three-factor interaction terms will be estimated as shown in Table 4.

**Table 6. Factor Combinations at Which the Test Will Be Performed For the 6-Factor Fractional Factorial Split-Plot Design.**

| Binder Type | | | PG 76-16 | | | | PG 64-22 | | | | PG 58-28 | | | |
|---|---|---|---|---|---|---|---|---|---|---|---|---|---|---|
| Binder Content | | | 4.2 | | 5.2 | | 4.2 | | 5.2 | | 4.2 | | 5.2 | |
| Air Voids (%) | | | 4.5 | 9.5 | 4.5 | 9.5 | 4.5 | 9.5 | 4.5 | 9.5 | 4.5 | 9.5 | 4.5 | 9.5 |
| Temp | $N_f$ w/o RP | Rest Period (sec) | | | | | | | | | | | | |
| L | L | 0 | | ■ | ■ | | ■ | ■ | | ■ | ■ | | | ■ |
| | | 5 | ■ | | | ■ | ■ | | ■ | ■ | | ■ | ■ | ■ |
| | H | 0 | ■ | | | ■ | ■ | | ■ | ■ | | ■ | ■ | |
| | | 5 | ■ | ■ | ■ | | | ■ | ■ | ■ | ■ | | | ■ |
| M | L | 0 | | ■ | ■ | | | ■ | ■ | | ■ | | | ■ |
| | | 5 | ■ | | ■ | ■ | ■ | ■ | | ■ | | ■ | ■ | ■ |
| | H | 0 | ■ | | ■ | ■ | ■ | ■ | | ■ | | ■ | ■ | ■ |
| | | 5 | | ■ | ■ | | ■ | | ■ | ■ | ■ | ■ | ■ | |
| H | L | 0 | ■ | | | ■ | ■ | | | ■ | | ■ | ■ | |
| | | 5 | ■ | ■ | ■ | ■ | | ■ | ■ | | ■ | | ■ | ■ |
| | H | 0 | | ■ | ■ | ■ | | ■ | ■ | | ■ | | ■ | ■ |
| | | 5 | ■ | ■ | ■ | ■ | ■ | ■ | | ■ | ■ | ■ | ■ | ■ |

### *3.3.2 Five Factor Design*

Since the healing index requires testing with and without rest period, another possible experimental design would be to remove the factor of rest period from the statistical model and use the remaining 5 factors only. This method would require developing two 5-factor models, with and without rest period. The number of cycles to failure will be compared the same way as the case of the 6-factor design to determine the healing index.

From the fatigue test results, the Stiffness Ratio (SR) will be obtained. Using the statistical program (98), a model will be developed to estimate SR as a function of all 5 factors for each case of rest period as shown in Equation 16.

$$SR = f(BT, AC, AV, SL, T) \quad (16)$$

Comparing the SR for the case without rest period with the number of cycles for a 5-second rest period, the healing potential of the material can be estimated by determining the Healing Index (HI) as shown in Equation 15.

*Five-Factor Full Factorial Design*

Table 7 shows the full factorial design in which all factor combinations are tested. The full factorial design would require 3 x 2 x 2 x 2 x 3 x 3 = 216 tests. If two rest periods are used (0 and 5 seconds), the total number of tests would be 216 x 2 = 432 tests.

**Table 7. Five-Factor Full Factorial Design For Each Rest Period.**

| Binder Type | | PG 76-16 | | | | PG 64-22 | | | | PG 58-28 | | | |
|---|---|---|---|---|---|---|---|---|---|---|---|---|---|
| Binder Content | | 4.2 | | 5.2 | | 4.2 | | 5.2 | | 4.2 | | 5.2 | |
| Air Voids (%) | | 4.5 | 9.5 | 4.5 | 9.5 | 4.5 | 9.5 | 4.5 | 9.5 | 4.5 | 9.5 | 4.5 | 9.5 |
| Temp | $N_f$ w/o RP | | | | | | | | | | | | |
| L | L | | | | | | | | | | | | |
| | H | | | | | | | | | | | | |
| M | L | | | | | | | | | | | | |
| | H | | | | | | | | | | | | |
| H | L | | | | | | | | | | | | |
| | H | | | | | | | | | | | | |

*Five-Factor Fractional Factorial Design with Complete Randomization*

Using the D-optimality design previously mentioned, Table 8 shows the factor combinations at which the fractional factorial test will be performed. This design would require a total of 156 tests for each case of rest period, or 312 tests for the two cases.

**Table 8. Factor Combinations at Which the Test Will Be Performed For the 5-Factor Fractional Factorial Completely Randomized Design For Each Case of Rest Period.**

| Binder Type | | PG 76-16 | | | | PG 64-22 | | | | PG 58-28 | | | |
|---|---|---|---|---|---|---|---|---|---|---|---|---|---|
| Binder Content | | 4.2 | | 5.2 | | 4.2 | | 5.2 | | 4.2 | | 5.2 | |
| Air Voids (%) | | 4.5 | 9.5 | 4.5 | 9.5 | 4.5 | 9.5 | 4.5 | 9.5 | 4.5 | 9.5 | 4.5 | 9.5 |
| Temp | $N_f$ w/o RP | | | | | | | | | | | | |
| L | L | | | | | | | | | | | | |
| | H | | | | | | | | | | | | |
| M | L | | | | | | | | | | | | |
| | H | | | | | | | | | | | | |
| H | L | | | | | | | | | | | | |
| | H | | | | | | | | | | | | |

*Five-Factor Fractional Factorial Design with Partial Randomization*

Using the split-plot design mentioned above, Table 9 shows the factor combinations at which the test will be performed. This design would require a total of 156 tests for each case of rest period, or 312 tests for the two cases.

**Table 9. Factor Combinations at Which The Test Will Be Performed For The 5-Factor Fractional Factorial Split-Plot Design For Each Case of Rest Period.**

| Binder Type | | PG 76-16 | | | | PG 64-22 | | | | PG 58-28 | | | |
|---|---|---|---|---|---|---|---|---|---|---|---|---|---|
| Binder Content | | 4.2 | | 5.2 | | 4.2 | | 5.2 | | 4.2 | | 5.2 | |
| Air Voids (%) | | 4.5 | 9.5 | 4.5 | 9.5 | 4.5 | 9.5 | 4.5 | 9.5 | 4.5 | 9.5 | 4.5 | 9.5 |
| Temp | $N_f$ w/o RP | | | | | | | | | | | | |
| L | L | | | | | | | | | | | | |
| | H | | | | | | | | | | | | |
| M | L | | | | | | | | | | | | |
| | H | | | | | | | | | | | | |
| H | L | | | | | | | | | | | | |
| | H | | | | | | | | | | | | |

The order of test runs for each rest period will be as shown below. Note that there are 52 runs, where each run consists of 3 replicates to be performed together without randomization.

### *3.3.3 Comparison between 6-Factor and 5-Factor Factorial Designs*

Considering all six experimental designs discussed above, the 6-factor design is preferred over the 5-factor design because it would provide better results and requires less number of tests. The 6-factor design is developed to capture and evaluate the significance of the rest period factor on the fatigue results (see Equation 41), whereas the 5-factor design does not consider this factor effect (see Equation 43). If the results show that the rest period and its interaction terms are significant, they will be added to the general model of estimating the fatigue. Thus, the model produced by the 6-factor design allows the user to input different values of rest period (such as 1 or 3 seconds) and estimate the fatigue results. In the other hand, the results of the 5-factor design rely on only the calculation of 0 and 5 second rest periods. That is, it cannot estimate the fatigue results of the other rest periods.

Comparing all three possible 6-factor designs, the 6-factor fractional factorial design with partial randomization is recommended in this study. The complete randomization condition cannot be satisfied in this experiment due to the constraints of the production process and testing. Thus, it is more appropriate to do the experiment by using partial randomization in order to accommodate the study constraints. It also reduces the number of tests from 432 (full factorial design) to 288 (fractional factorial design with partial randomization).

### *3.3.4 Other Detailed Experiments*

Based in the outcomes of the previous study, other detailed experiments will be performed to study certain factors in more details. For example, other rest periods

and strain levels might be tested with a smaller number of other factors. The details of these experiments will be discussed in other sections of the report.

### 3.4 Final Design

The final design approach is based on studying all factors together in one main experiment rather than dealing with incomplete, separate experiments. The study considers the factors of binder type, binder content, air voids, $N_f$ level, temperature and rest period.

It was decided to use the 6-factor fractional factorial design with partial randomization since it would provide better results and requires less number of tests. A total of 288 tests are required as shown in Table 9 with 3 replicates for each factor combinations.

# Chapter 4 MATERIALS AND MIX DESIGN

## 4.1 Background

This chapter reports and discusses the MACTEC in Phoenix, Arizona, and ASU test results and the asphalt binder characterization test results. MACTEC undertook 1) the determination of the range of compaction and mixing temperatures, 2) asphalt binder characterization using the Superpave binder tests including the Dynamic Shear Rheometer (DSR) and the Bending Beam Rheometer (BBR), and 3) the mixture design. The ASU conducted a comprehensive characterization study of the rheological properties of asphalt binder, using one Superpave test (Brookfield viscometer) and two conventional binder tests (Penetration and Softening point) at a wide range of temperatures.

## 4.2 Materials

Three types of AC binders were provided by Holly Asphalt Company in Phoenix, Arizona, and used by both MACTEC and ASU, in order to conduct the mix design and binder characterization tests. They are all unmodified and classified as PG 58-28, PG 64-22, and PG 76-16. Mineral aggregates were supplied by the CEMEX plant #1386 in Phoenix, Arizona, and were used by MACTEC for the mix design.

## 4.3 Binder Aging Methods

For the binder characterization tests (MACTEC and ASU), samples of the three asphalt binder types were aged for the short-term (RTFO) and long-term (PAV) conditioning. The RTFO and PAV aging were conducted in accordance with AASHTO T240 and AASHTO R28, respectively.

For the RTFO test (Figure 9), unaged asphalt binder is placed in a cylindrical jar, which is then placed in a carousel inside a specially designed oven. The oven is heated to 325°F (163°C) and the carrousel is rotated at 15 RPM for 85 minutes. The carousel rotation continuously exposes new asphalt binder to the heat and air flow and slowly mixes each sample.


**Figure 9. RTFO test setup.**

In the PAV test, the RTFO aged asphalt binder is placed in an unpressurized PAV preheated to the test temperature. When the PAV reaches the test temperature it is pressurized to 300 psi (2.07 MPa). After 20 hours of treatment the samples are removed, degassed and stored for future testing. Figure 10 shows the major PAV equipment.


**Figure 10. PAV apparatus.**

## 4.4 MACTEC Asphalt Binder Test Results

### *4.4.1 Viscosity Binder Temperature Curves*

The laboratory mixing and compaction temperatures for the mix design were determined using the viscosity – temperature relationship. The temperatures were selected corresponding with binder viscosity values of 0.17±0.02 Pa·s for mixing and 0.28±0.03 Pa.s for compaction. Viscosity values were determined using a Brookfield Rheometer (ASTM D 4402). To develop the viscosity binder temperature curves, three viscosity values were measured at temperatures of 275, 311, and 347°F (135, 155, and 175°C) for the PG 58-28 and PG 64-22 binders,

while two viscosity values were measured at temperatures of 275 and 347°F (135 and 175°C) for the PG 76-16 binder. Table 10 summarizes the lab mixing and compaction temperatures determined.

**Table 10. Summary of Laboratory Mixing and Compaction Temperatures for Mix Design, °F (°C) Provided by MACTEC.**

| | Temperature, °F (°C) | Binder Type | | |
|---|---|---|---|---|
| | | PG 58-28 | PG 64-22 | PG 76-16 |
| Mixing | Min | 295 (146) | 308 (153) | 329 (165) |
| | Max | 305 (152) | 320 (160) | 340 (171) |
| Compaction | Min | 275 (135) | 287 (142) | 310 (154) |
| | Max | 284 (140) | 296 (147) | 318 (159) |

### *4.4.2 Superpave Binder Characterization Tests*

The Dynamic Shear Rheometer (DSR) and Bending Beam Rheometer (BBR) tests were performed to characterize the three asphalt binders used for the mix design and to confirm that the binders meets the specifications.

For the characterization of binder at intermediate and high temperatures, the DSR test was conducted at 15, 30, 45, 70, 95, and 115°C. The complex shear modulus (G*) and phase angle was measured at a constant frequency (10 rad /sec). For the low temperature binder response, the BBR test was conducted and the flexural creep stiffness (S) at 60s at a specified temperature and slope (m-value) were measured. The temperatures used to measure the flexural creep stiffness were -18, -12, and -6°C for PG 58-28, PG 64-22, and PG 76-16, respectively. Table 11 summarizes the test methods and their properties and test conditions. It should be noted that the DSR test was separately conducted with

each aging condition: Neat or Tank, RTFO, RTFO+PAV, while the BBR test was conducted only with the PAV condition.

**Table 11. Summary of Superpave Binder Characterization Tests Provided by MACTEC.**

| Test | Property | Method | Conditions |
|---|---|---|---|
| Dynamic Shear Rheometer | Complex Shear Modulus (G*) and Phase Angle (δ) | AASHTO T315 | 10 rad/sec 59, 86, 113, 158, 203, and 239°F (15, 30, 45, 70, 95, and 115°C) |
| Bending Beam Rheometer | Creep Stiffness (S) and Slope (m-value) | AASHTO T313 | 60 sec -0.4, 10.4, and 21.2 °F, (-18, -12, and -6°C) |

A viscosity – temperature relationship was developed using the DSR test results (e.g., G* and phase angle) at three aging conditions. It is obvious that, from the plots, the binder becomes more viscous as the binder is aged. Note that the viscosity values in each plot were obtained from the G* and phase angle values at the specified test temperatures by converting them into viscosity by the Cox-Merz equation.

$$\eta = \frac{G^*}{10}\left(\frac{1}{\sin\delta}\right)^{4.8628} \times 1000 \qquad (17)$$

where,

$\eta$ = viscosity, cP

G* = complex shear modulus, Pa

$\delta$ = phase angle, degree

The creep stiffness results from the BBR test were found satisfactory with the Superpave specifications. Table 12 shows the test results for each binder type indicating that they met the specifications.

**Table 12. Summary of BBR Test Results (S and m-Value).**

| Property | Binder Type | | | Specification Limits |
|---|---|---|---|---|
| | PG 58-28 | PG 64-22 | PG 76-16 | |
| Creep Stiffness, S (MPa) | 232 | 191 | 138 | 300 max |
| Slope, m-value (unitless) | 0.323 | 0.316 | 0.337 | 0.300 min |

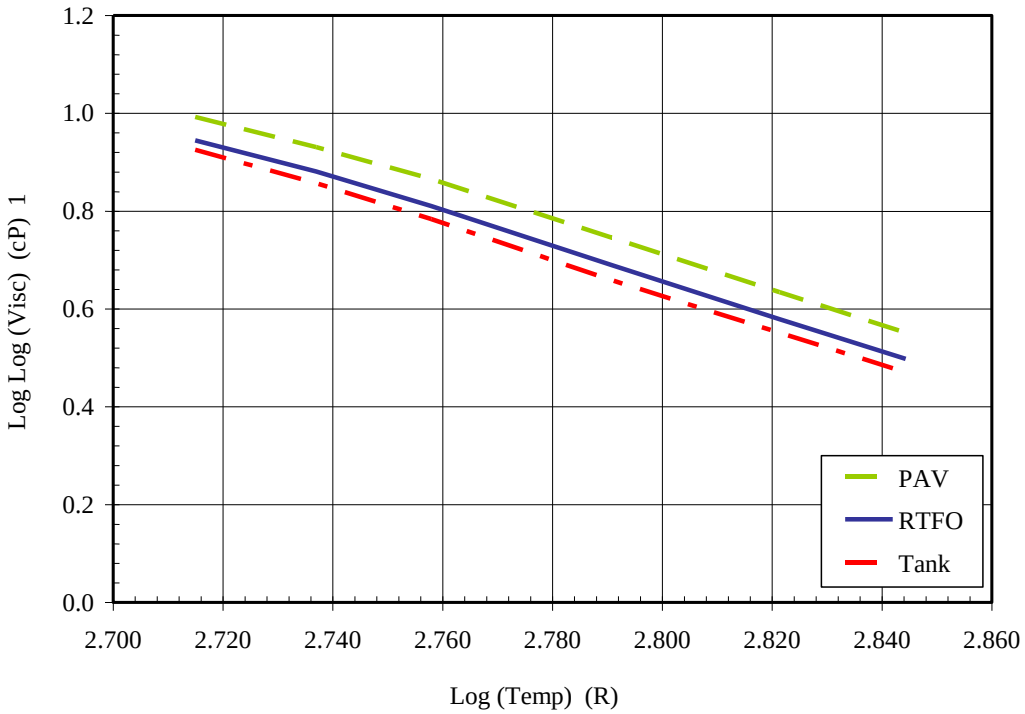


**Figure 11. Temperature - viscosity relationship from DSR results, (PG 58-28).**

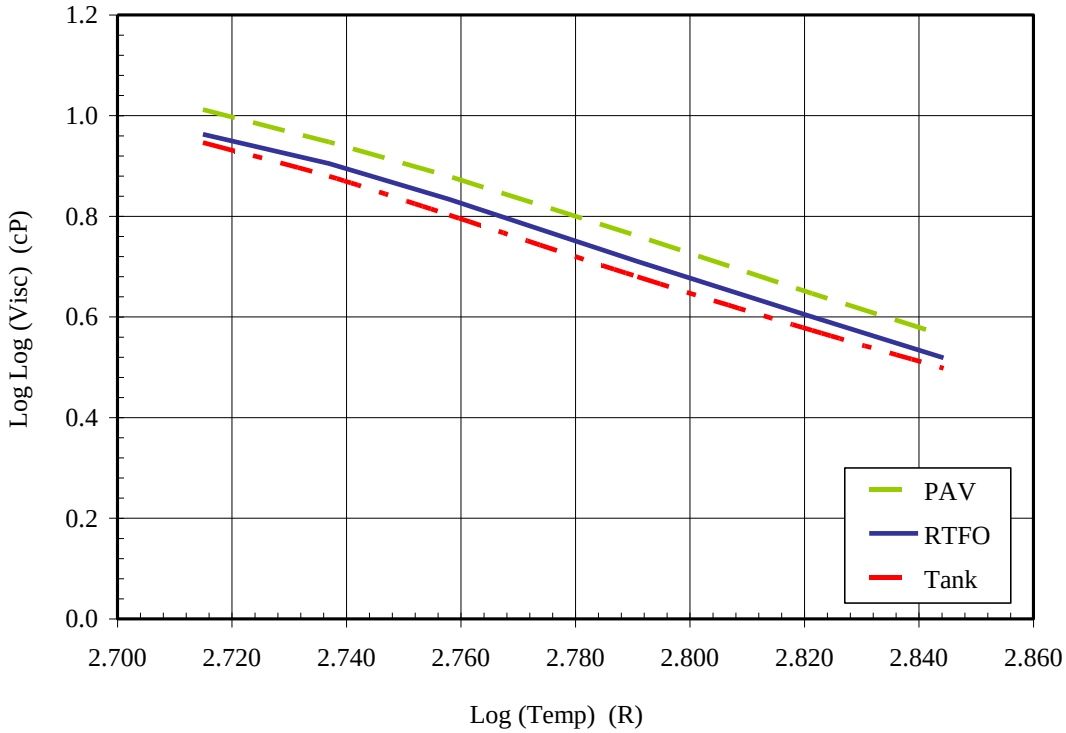


**Figure 12. Temperature - viscosity relationship from DSR results, (PG 64-22).**

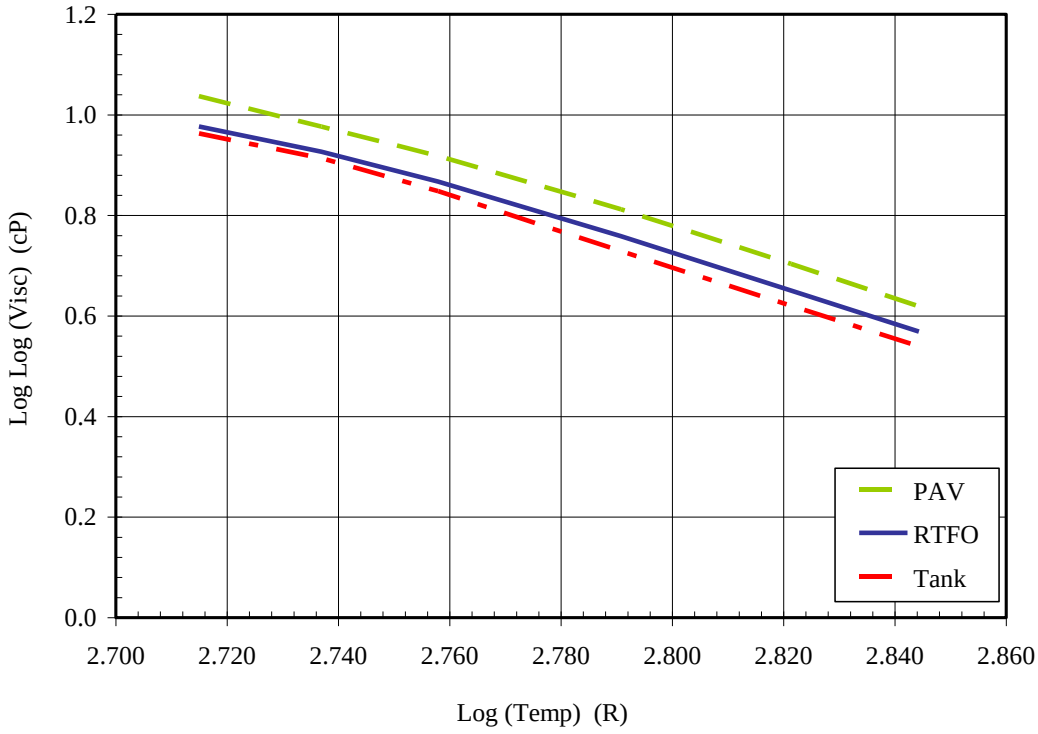


**Figure 13. Temperature - viscosity relationship from DSR results, (PG 76-16).**

### 4.5 ASU Asphalt Binder Characterization

A comprehensive characterization study of the rheological properties of the three binder types (PG 58-28, PG 64-22, and PG 76-16) was conducted by ASU (27), using one Superpave test and two conventional binder tests. The objective of this work was to characterize the asphalt binder used in this project over the wide range of temperatures and subsequently to develop a linear relationship (e.g., Ai-VTSi relationship) between temperature and viscosity. All binder tests were performed for three aging conditions: Neat (Tank) or Original, Short-Term Aged (RTFO), and Long-Term Aged (RTFO + PAV). The conventional binder tests used in this study include Penetration test and Softening Point (Ring and Ball test). The Superpave binder test includes Rotational Viscometer (Brookfield test). While binder testing was conducted by laboratory technicians, the author documented the results since it will be used to differentiate between different binder grades during developing Endurance Limit model in Chapter 7.

Note that each of the three binder types was obtained from two sample cans (Sample 1 and 2) and each can was duplicated (Replicates A and B). This scheme applies to each aging condition. Thus, for one PG binder at a certain aging condition, four specimens (2 cans * 2 duplicates) were tested for the three binder types. These four specimens were called a set and a unique number was assigned for each set as a set number. Table 13 shows an example of this set numbering scheme.

**Table 13. Example of Binder Sample Preparation Scheme.**

| Binder Type | Aging Condition | Sample Can | Replicate | Set Number |
|---|---|---|---|---|
| PG 58-28 | Tank Condition | 1 | A | 10 |
| | | | B | 12 |
| | | 2 | A | 11 |
| | | | B | 13 |

Table 14 summarizes the properties measured, the test standard, and the test condition for each test.

**Table 14. Summary of Conventional and Superpave Binder Characterization Tests.**

| | Property | Method | Conditions |
|---|---|---|---|
| Conventional Test | Penetration | AASHTO T49 | 100 g, 5 sec, 40, 55, 77, and 90°F (4, 12.8, 25, and 32°C) |
| | Softening Point | AASHTO T53 | Measured Temperature |
| Superpave Test | Brookfield Viscosity | AASHTO T316 | 200, 250, 300, 350°F (93, 121, 149, 177°C) |

### *4.5.2 Data Analysis*

A combination of nine viscosity–temperature data points (four penetration values, one softening point value, and four Brookfield values) are plotted together in a viscosity–temperature graph, in order to characterize the viscosity-temperature susceptibility relation over a wide range of temperatures. The linear relationship can be established based upon the following equation:

$$\log\log\eta = A + VTS\log T_R \qquad (18)$$

where,

$\eta$ = viscosity, cP

$T_R$ = temperature, Rankine

A = regression intercept

VTS = regression slope of viscosity temperature susceptibility

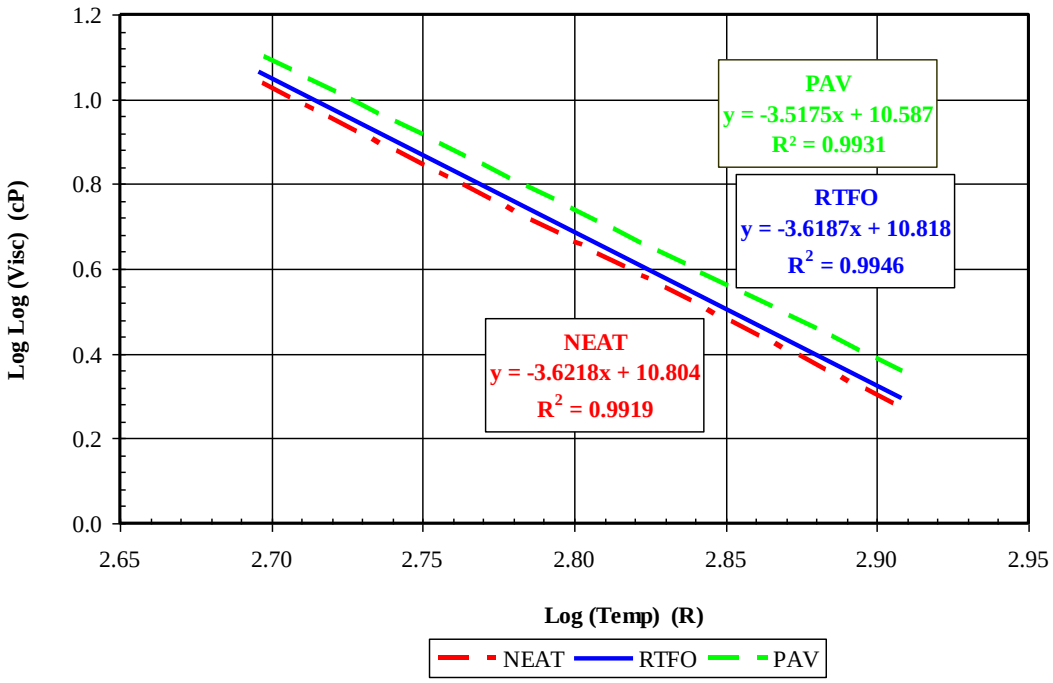


**Figure 14. Viscosity – temperature relationship for PG 58-28 binder.**

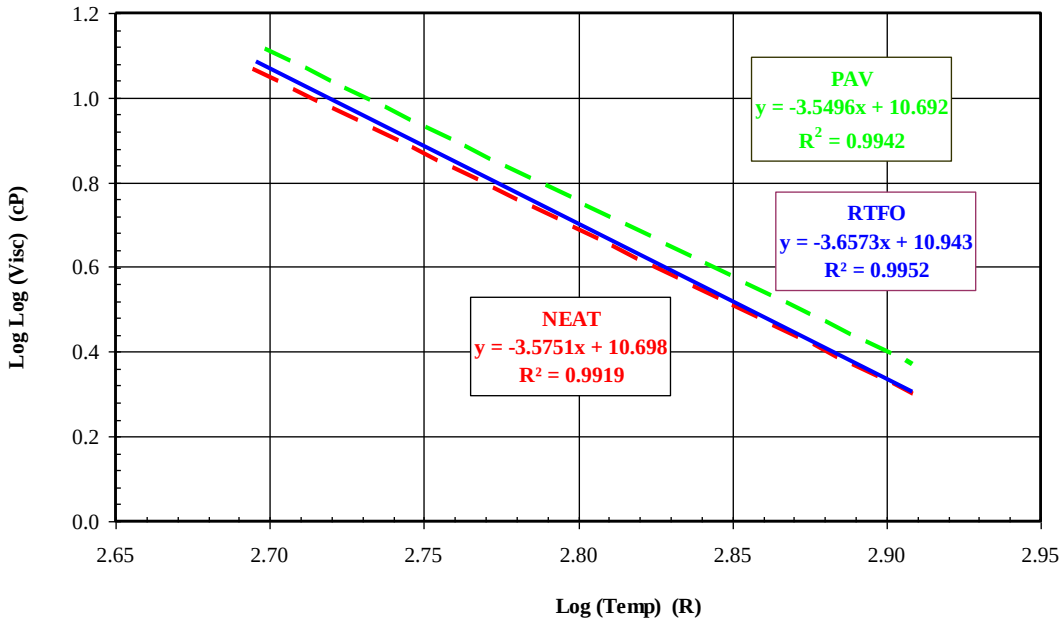


**Figure 15. Viscosity – temperature relationship for PG 64-22 binder.**

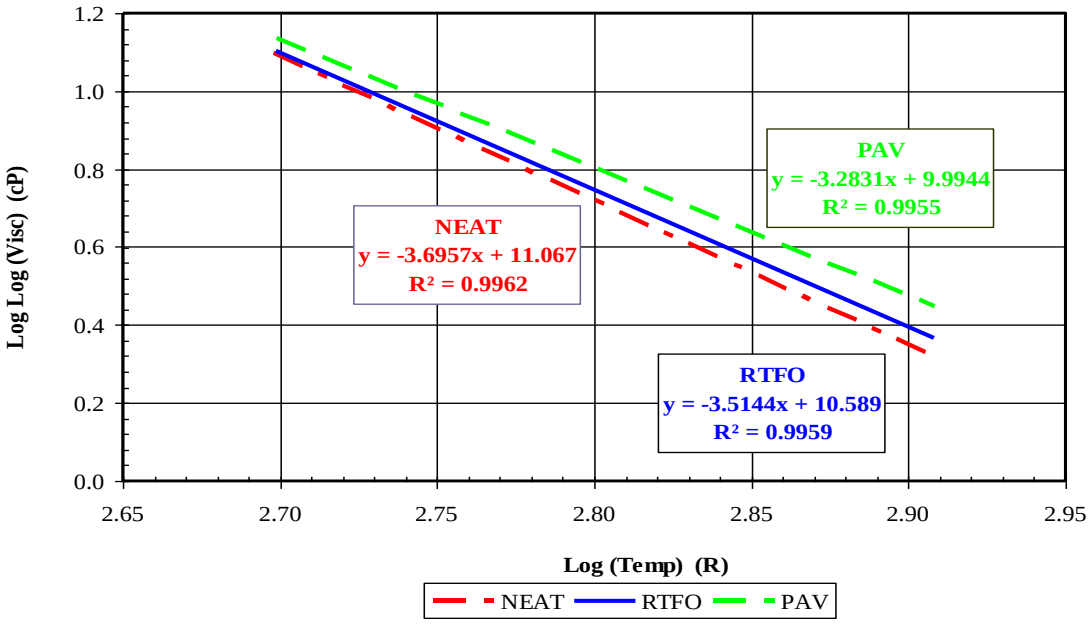


**Figure 16. Viscosity – temperature relationship for PG 76-16 binder.**

### 4.5 MACTEC Mix Design and Aggregate Blend Results

The 19mm Superpave mix design was prepared by MACTEC for the project according to the requirements of the Arizona Uniform Standard Specifications for Public Works Construction Section 710 (100). The Superpave mix design prepared herein is to provide typical paving materials used for paving arterial roads. While three different AC mixes were designed each of which used a particular binder type: PG 58-28, PG 64-22, and PG 76-16, the same aggregate gradation was consistently used for all mix designs. Table 15 shows the designed aggregate gradation along with the minimum and maximum design specifications. Figure 17 illiterates the designed aggregate gradation distribution curve.

Table 16 includes the composite aggregate prosperities that were obtained by MACTEC. The summary of the key volumetric properties from the mix design results using three binders are presented in Table 17.

**Table 15. Designed Aggregate Gradation and Specification Limits Provided by MACTEC.**

| Sieve Size | %Passing | | |
|---|---|---|---|
| | Design | Minimum | Maximum |
| 1 in. | 100.0 | 100.0 | 100.0 |
| ¾ in. | 95.0 | 90.0 | 100.0 |
| ½ in. | 80.0 | 43.0 | 89.0 |
| 3/8 in. | 59.0 | | |
| No. 4 | 39.0 | | |
| No. 8 | 29.0 | 24.0 | 36.0 |
| No. 16 | 23.0 | | |
| No. 30 | 17.0 | | |
| No. 50 | 10.0 | | |
| No. 100 | 5.0 | | |
| No. 200 | 3.3 | 2.0 | 6.0 |

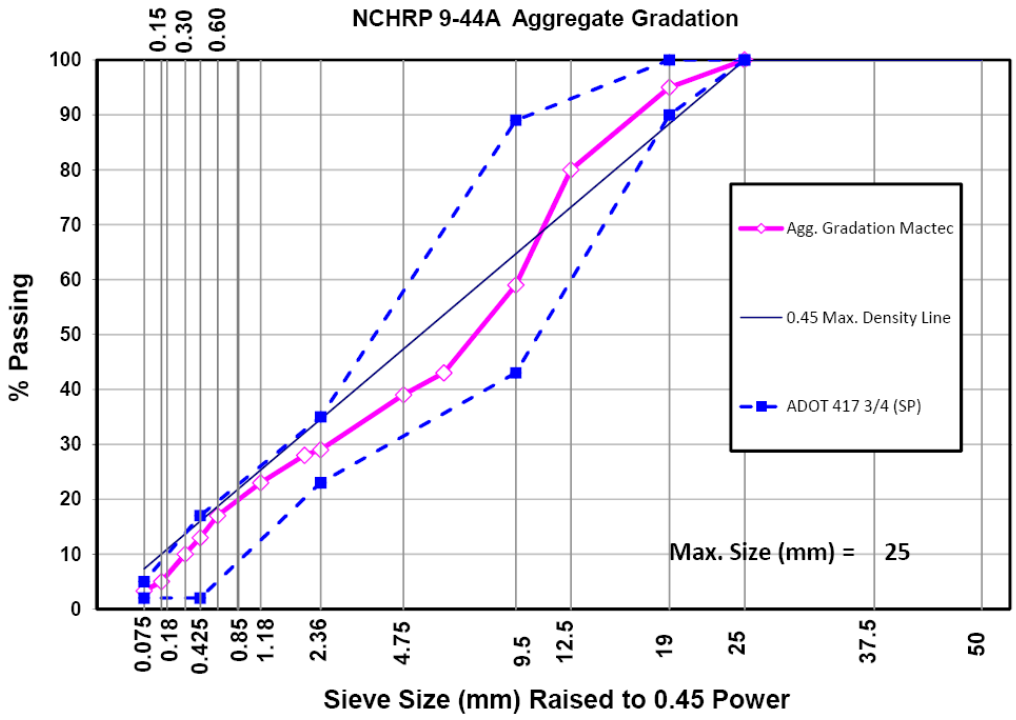


**Figure 17. Designed aggregate gradation distribution curve Provided by MACTEC (27).**

**Table 16. Combosite Aggregate Properties Provided by MACTEC/**

| Property | Value | Specifications |
|---|---|---|
| Bulk (Dry) Sp. Gravity | 2.614 | (2.35-2.85) |
| SSD Sp. Gravity | 2.638 | |
| Apparent Sp. Gravity | 2.677 | |
| Water absorption (%) | 0.90 | (0-2.5) |
| Sand Equivalent Value | 71 | Min 50 |
| Fractured Face One (%) | 99 | Min 85 |
| Fractured Face Two (%) | 96 | Min 80 |
| Flat & Elongation (%) | 1.0 | Max 10 |
| Uncompacted Voids (%) | 46.8 | Min 45 |
| L.A. Abrasion @ 500 Rev. | 16 | Max 40 |

**Table 17. Volumetric Mix Design for Different Binder Types Provided by MACTEC.**

| Volumetric Property | Binder Type | | | Spec. |
|---|---|---|---|---|
| | PG 58-28 | PG 64-22 | PG 76-16 | |
| Target Asphalt Content (%) | 4.8 | 4.5 | 4.7 | 4.5 ~ 5.5 |
| Bulk Specific Gravity ($G_{mb}$) | 2.365 | 2.367 | 2.351 | N/A |
| Theoretical Max. Sp. Gr. ($G_{mm}$) | 2.461 | 2.467 | 2.454 | N/A |
| Design Air Voids (%) | 3.9 | 4.1 | 4.2 | 3.8 ~ 4.2 |
| VMA (%) | 13.9 | 13.5 | 14.3 | Min. 13 |
| VFA (%) | 71.9 | 69.9 | 70.8 | N/A |
| Asphalt Sp. Gr. ($G_b$) | 1.024 | 1.024 | 1.042 | N/A |

# Chapter 5 SPECIMEN PREPARATION AND CALIBRATION OF BEAM FATIGUE MACHINES

This chapter provides a generalized methodology to manufacture testable HMA beams using the Instron compaction machine available in the Advanced Pavements Laboratory at ASU. The chapter also illustrates the beam fatigue apparatus and the calibration procedure used to insure that all testing machines produce accurate and comparable testing results.

## 5.1 Mold Assembly and Specimen Preparation

### *5.1.1 Mold Assembly*

The AASHTO T321 (101) and SHRP M-009 (102), flexural fatigue testing protocol, require a beam of asphalt concrete for testing. The T321 and M-009 procedure require preparation of oversize beams that later have to be sawed to the required dimensions. The final required dimensions are 15 ± 1/4 in. (380 ± 6 mm) in length, 2 ± 1/4 in. (50 ± 6 mm) in height, and 2.5 ± 1/4 in. (63 ± 6 mm) in width. The procedure does not specify a specific method to prepare the beam specimen. Several methods have been used to prepare beams in the laboratory including full scale rolling wheel compaction, miniature rolling wheel compaction, and vibratory loading (103,10).

In this study beams were prepared using vibratory loading applied by a servo-hydraulic loading machine. A beam mold was manufactured with structural steel. The mold consists of a cradle and two side plates as shown in Figure 18. The inside dimensions of the mold are 1/2 inch (12 mm) larger than the required

dimensions of the beam after sawing in each direction to allow for a 1/4 inch (6 mm) sawing from each face.

A top platen made of a series of steel plates welded at the two ends was used to compact the specimen (Figure 19) (8). The loading shaft is connected to the upper steel plate rather than extending it to the bottom plate so that an arch effect is introduced that would assist in distributing the load more uniformly. In addition, the bottom surface of the bottom plate is machined to be slightly concave upward in order to counter balance any bending that might occur during compaction and produce more uniform air void distribution.

**Figure 18. Major components of the mold.**

**Figure 19. Rigid top loading platen.**

### *5.1.2 Specimen Preparation*

*Aggregate Batching*

Aggregates were pre-sieved into different sieve sizes and were stored in labeled, covered 5 gallon plastic buckets until needed. Batches were made using empty, clean 1 gallon metal paint cans. Paint cans were methodically filled with the calculated weights from each aggregate size as per mix design gradation in order to create individual specimens.

*Binder Preparation*

All Binders received at the ASU Advanced Pavement Laboratory arrived in a sealed metal 5 gallon buckets with crimped lid. As a 5 gallon bucket was needed, it was first gently heated at 110$^{o}$C for 30 minutes to slightly liquefy the binder. The binder was then carefully poured into multiple new, clean pint sized metal paint cans. As the pint cans were filled, they were then capped with a lid to cool

for the day and the container identified with a description of the binder type, date of preparation and any appropriate ID number.

*HMA Mixing*

Prior to the specimen mix manufacturing process; batched aggregate cans were placed in a heated oven (295$^{o}$F/145$^{o}$C) overnight to insure that no moisture was present in the aggregate specimens. On the day of the sample mixing, a pint sized can of binder was placed in a heated oven (295$^{o}$F/145$^{o}$C) for approximately 30-45 minutes to gently bring the temperature of the binder up to the desired mixing temperature. Once the binder had reached the ideal mixing temperature, the heated aggregates were then poured into a preheated mixing bucket, and a well was created in the middle of the aggregates with a heated metal spoon. The heated bucket with aggregates was then moved on top of the swing arm balance and the balance was then zeroed out. The lid was then removed from the pint can of heated binder and the heated binder was carefully poured into the well/pocket created within the pile of aggregates. The binder was poured until the weight reaches the desired amount necessary to achieve the exact percent asphalt required. The bucket was then immediately placed into the mixing machine and the heated mixing paddle was attached. The mixer was then engaged and mixing was commenced for 120 seconds (2 minutes).

*Short Term Aging*

The properly mixed HMA was then emptied and evenly spread about 1" thick into a heated metal tray, approximately 2' x 2' and 3" deep in size, and placed uncovered into a preheated 135$^{o}$C convection oven for Short Term Aging. This

procedure was as specified in the AASHTO PP2 procedure (104) aging procedure for Superpave mixture performance testing. The HMA was left uncovered in the oven for a 1 hour period, and then the door opened and the HMA hand mixed and turned over multiple times within the tray with a heated spoon for 15-20 seconds. The door was then shut and the HMA was left to age another hour. After the second hour, the hot, aged mixture was then mixed with the heated spoon again and immediately scooped into the beam mold with the desired weight in order to compact a specimen to the predetermined AV%. The HMA was placed in the mold in two equal weighing lifts. Once the mold was filled, it was returned to an oven for about 15 minutes to achieve the proper compaction temperature before being compacted.

*Obtaining Maximum Theoretical Specific Gravity ($G_{mm}$)*

To begin the manufacturing of testable specimens for a given HMA mixture in agreement with the design (desired) lab volumetrics of the study, the first step was to make a HMA specimen that was heated and mixed within the laboratory, as per the standard mixing protocol, but poured loose on a table to cool overnight. The next day, the cooled HMA was crumbled and separated by hand and the Theoretical Maximum Specific Gravity ($G_{mm}$) was determined using the AASHTO T209 (105) Pycnometer method. This $G_{mm}$ of the specific HMA was used to calculate the Air Voids (AV) all specimens. It was critically important that AASHTO precision-bias statements of repeatability and reproducibility were meticulously followed for the Maximum Theoretical Density determinations on replicate specimens.

*Compacting of HMA Beams*

The heated, filled beam mold was placed on the bottom plate of the loading machine and the top plate was lowered just until contact was made with the top of the mixture layer. A small pressure of 0.2 psi (1.4 kPa) was then applied to seat the specimen. A stress-controlled sinusoidal load was then applied with a frequency of 2 Hz and a peak-to-peak stress of 400 psi (2.8 MPa) for the compaction process.

All beam specimens were made with 4600 grams of the HMA, out of the 5000 gram aggregate batch that was mixed with the binder to achieve the design binder content. The time of compaction of this standardized weight was used, and varied, in order to determine and achieve different compaction density and Air Voids (AV%) of testable specimens after being cut and dried.

After compaction, specimens were left to cool to ambient temperature. The specimens were brought to the required dimensions for fatigue testing by sawing 1/4 inch (6 mm) from each side as shown in Figure 20. The specimens were cut by using water cooled saw machine to the standard dimension of 2.5 in. (63.5 mm) wide, 2.0 in. (50.8 mm) high, and 15 in. (381 mm) long. Finally, Air void was measured by using the saturated surface-dry procedure (106).

**Figure 20. Specimen sawing.**

Specimens were then allowed to dry before testing. Specimen dimensions were obtained by obtaining 3 height and 3 width measurements and recording them in the lab data sheets. Each specimen was clearly identified with its ID number (both on specimen and on data sheets). Wrap finished specimen in a plastic sheet to eliminate any skin aging to occur in the lab, while the specimen was stored until testing.

*Determining Desired Air Voids*

To determine how to produce beam specimens at a target value of 7% air voids, (or at any other air void range desired for the study); three beam specimens were compacted using 0.5 minutes, 3 minutes and 5.5 minutes of compaction time. Note that the specific time used in the laboratory is a direct function of the type of compaction device used. The three specimens were then cut and dried and the air voids of each specimen were obtained using the Bulk Specific Gravity of Bituminous Mixtures Using Saturated Surface Dry Specimens method (106). The

necessary compaction time was determined using a plot comparing the compaction time versus the air void for each specimen as shown in Figure 21. Once the amount of compaction time was established and confirmed to yield a 7% air void beam (or the desired target AV%) multiple specimens were then compacted in bulk using the appropriate compaction time determined for each mix.

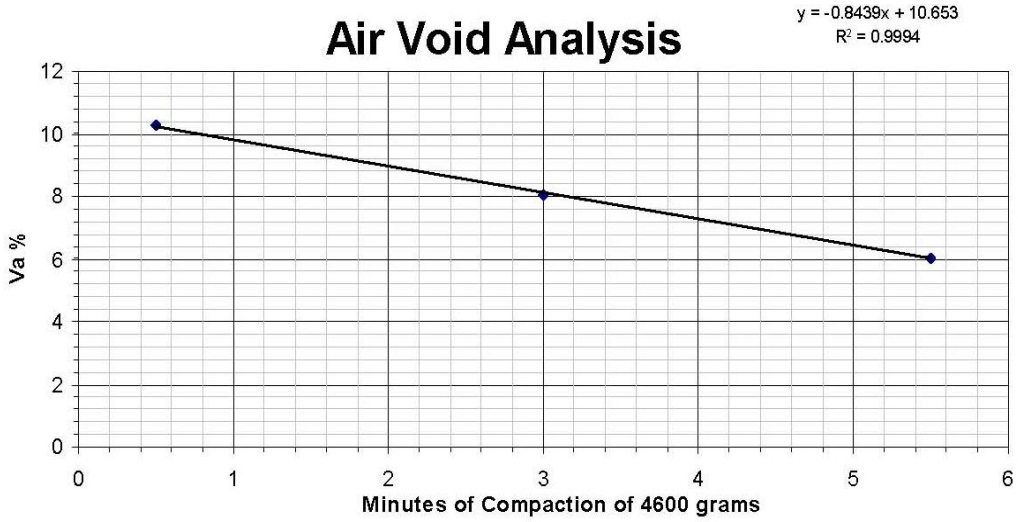


**Figure 21. Comparison of compaction time of 4600 gram beam specimens vs. air void (Va%) of trimmed specimens.**

### 5.2 Flexural Beam Fatigue Apparatus

Flexural fatigue tests were performed according to the AASHTO T321, and SHRP M-009 procedures (101, 102). Figure 22 shows the flexural fatigue apparatus. The device was typically placed inside an environmental chamber to control the temperature during the test.

The cradle mechanism allows for free translation and rotation of the clamps and provides loading at the third points as shown in Figure 22. Pneumatic actuators at the ends of the beam center it laterally and clamp it. Servomotor

driven clamps secure the beam at four points with a pre-determined clamping force. Haversine or sinusoidal loading may be applied to the beam via the built-in digital servo-controlled pneumatic actuator. The innovative floating on-specimen transducer measures and controls the true beam deflection irrespective of loading frame compliance.


**Figure 22. Flexural fatigue apparatus.**

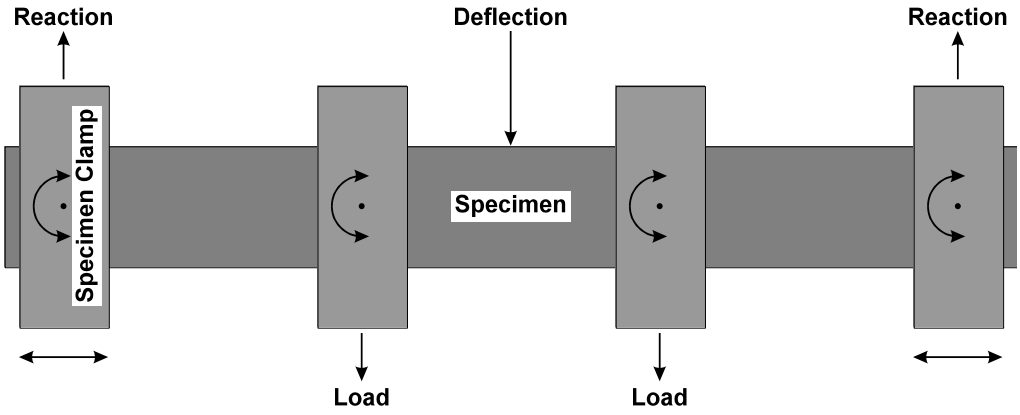


**Figure 23. Loading characteristics of the flexural fatigue apparatus.**

### 5.3 Test Procedure and Calculations

The test was summarized in applying repeated third-point loading cycles as demonstrated in Figure 22 and Figure 23. A controlled- strain sinusoidal loading was applied at a frequency of 10 Hz. The maximum tensile stress and maximum tensile strain are calculated as:

$$\sigma_t = 3\ a\ P / b\ h^2 \quad (19)$$

$$\varepsilon_t = 12\ \delta\ h / (3\ L^2 - 4\ a^2) \quad (20)$$

where,

$\sigma_t$ = Maximum tensile stress, Pa

$\varepsilon_t$ = Maximum tensile strain, m/m

P = Applied load, N

b = Average specimen width, m

h = Average specimen height, m

$\delta$ = Maximum deflection at the center of the beam, m

a = Space between inside clamps, 0.357/3 m (0.119 m)

L = Length of beam between outside clamps, 0.357 m

The flexural stiffness was calculated as follow:

$$S = \sigma_t / \varepsilon_t \quad (21)$$

where,

S = Flexural stiffness, Pa

The phase angle ($\phi$) in degrees was determined as follow:

$$\phi = 360\ f\ s \quad (22)$$

where,

f = Load frequency, Hz

s = Time lag between $P_{max}$ and $\delta_{max}$, seconds

## 5.4 Beam Fatigue Apparatus Calibration

A standard procedure was established to calibrate the testing machines to ensure accurate test results. The following is a brief calibration procedure that was implemented during the project time span. Calibration was performed every two months or when a problem raises indicating that the device was out of calibration.

### *5.4.1 LVDT Calibration Procedure*

1. Mount the LVDT into the LVDT calibrator assembly as shown in Figure 24.
2. Adjust the calibrator to the midpoint position.
3. Open the levels screen on IPC computer display.
4. Move the LVDT so that the computer readout is close to zero volts.
5. Fine tune the zero volts reading by adjusting the calibrator. Note the initial reading on the calibrator.
6. Move the calibrator in even increments and record the computer readout onto the attached calibration sheet.
7. Determine if the calibration check was within tolerance. If not, adjust the calibration gain to bring the calibration within the acceptable tolerance.
8. A sequential listing of all activities completed to achieve compliance to calibration tolerance is recorded.

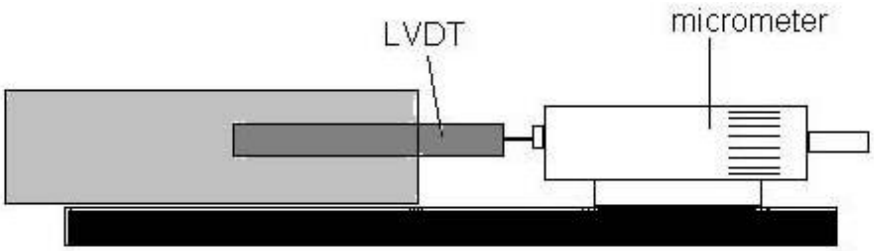


**Figure 24. LVDT Calibration set up.**

### *5.4.2 Load Cell Calibration Procedure*

1. Open the levels screen on IPC computer display.
2. Mount the proving ring onto the top of the Beam Fatigue Apparatus assembly as shown in Figure 25. Zero the dial gauge reading on the proving ring.
3. Apply an offset so that the engineering outputs value was zeroed.
4. Using the large range laboratory scale, record the weight of the dead weights to be used in the calibration verification check.
5. Carefully apply the dead load weights to the machine and proving ring assembly. Record the readouts on the calibration sheet.
6. Determine if the calibration check was within tolerance. If not, adjust the calibration gain to bring the calibration within the acceptable tolerance
7. A sequential listing of all activities completed to achieve compliance to calibration tolerance is recorded.

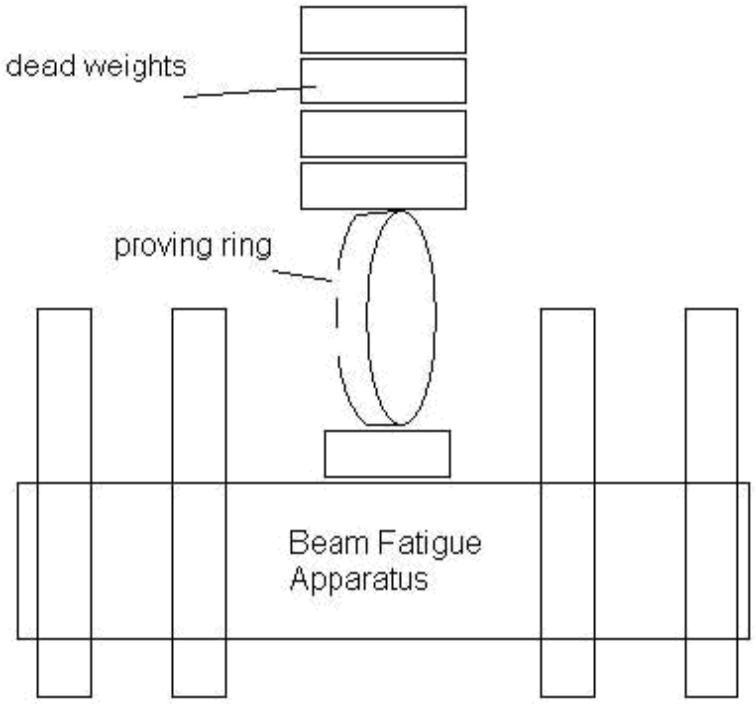


**Figure 25. Calibration set up.**

### *5.4.3 Temperature Calibration Procedure*

1. Adjust the set point temperature on the control unit to a temperature of 4, 20, or 37 degrees C, as needed.
2. Allow enough time for the chamber to come to equilibrium at each temperature.
3. Record the readings for the temperature controller, the computer display (if available), and the temperature calibration meter.
4. Prepare a corrected temperature chart in order to establish the controller set point reading that needs to be selected in order to achieve the three temperature settings required.
5. If the temperature reading is outside of acceptable tolerance, contact either the Laboratory Manager or Laboratory Coordinator in order to coordinate

servicing of the temperature chamber(s) by the Facilities Management department.

6. A sequential listing of all activities completed to achieve compliance to calibration tolerances is recorded.

# Chapter 6 PRELIMINARY QUALITY CONTROL/QUALITY ASSURANCE STUDIES

Two IPC (IPC-1 and IPC-2) beam fatigue devices were used in this study. It was important to insure that both devices measure statistically identical responses during the experimental testing program. In order to accomplish this goal, preliminary statistical ANOVA experiments were designed and implemented to verify this hypothesis. The other issue that the team has encountered and worked hard to resolve was to insure that the machines apply the correct wave form in the bending beam test.

## 6.1 Evaluation of Equality among Machines Using Synthetic Beams with no Rest Period

Before starting the main NCHRP 9-44A experiment, it was prudent to compare both machines to verify the assumption that both machines operate in the same way and produce statistically comparable results. The first evaluation experiment was accomplished with 3 types of synthetic beams with flexural stiffness ranging from 90 ksi to 350 ksi. An experiment was conducted to statistically test this assumption. The primary variable used to measure the equality of the beam measurements was the flexural stiffness at 10,000 repetitions with a zero dwell (rest) time between pulses.

### *6.1.1 Experiment Conditions*

1. Two IPC machines.
2. Three synthetic beams with three levels of stiffness: low, medium, and high.

3. Beams were tested using haversine loads at 10 Hz frequency for 10,000 cycles. The use of a haversine load implies a rest time of 0 seconds.
4. Two strain levels: low (400 micro strains) and high (800 micro strains)
5. One test temperature of 20°C.
6. A full factorial design was used with a total of 24 tests (2 machines x 3 beams x 2 strain levels x 2 replicates).

### *6.1.2 Experiment Results*

Table 18 shows the flexural stiffness of the three beams under different test conditions.

**Table 18. Stiffness of Synthetic Beams (in psi).**

| Machine Type | Beam Stiffness | | | | | |
|---|---|---|---|---|---|---|
| | Low | | Medium | | High | |
| | Low Strain Level | High Strain Level | Low Strain Level | High Strain Level | Low Strain Level | High Strain Level |
| **IPC 1** | 99946 | 96794 | 166500 | 163808 | 356391 | 350240 |
| | 93030 | 93330 | 168694 | 165120 | 361653 | 358960 |
| Average | 96488.0 | 95062.0 | 167597.0 | 164464.0 | 359022.0 | 354600.0 |
| Standard Deviation | 4890.4 | 2449.4 | 1551.4 | 927.7 | 3720.8 | 6166.0 |
| Coefficient of variation, % | 5.1 | 2.6 | 0.9 | 0.6 | 1.0 | 1.7 |
| **IPC 2** | 99957 | 93709 | 173738 | 166747 | 368045 | 368929 |
| | 102855 | 95107 | 174970 | 169706 | 381828 | 377047 |
| Average | 101406.0 | 94408.0 | 174354.0 | 168226.5 | 374936.5 | 372988.0 |
| Standard Deviation | 2049.2 | 988.5 | 871.2 | 2092.3 | 9746.1 | 5740.3 |
| Coefficient of variation, % | 2.0 | 1.0 | 0.5 | 1.2 | 2.6 | 1.5 |

### *6.1.3 Testing Adequacy of Statistical Model*

The model adequacy was determined by the residual analysis (107). Several assumptions were examined as follows.

1. A normal probability plot of the residuals was constructed to determine whether the data depart from the normal assumption or not. If the normal probability plot lies along a straight line, it indicates that the data follow the normal distribution.
2. A second trend was evaluated by plotting the residuals versus the run number. This was constructed to detect any correlations between the residuals. There was no pattern or tendency for positive or negative runs of residuals. Thus, the independence assumption on the error is stisfied.
3. Finally, a report of residuals versus the predicted stiffness was constructed to detemine the homogeneity of variances. There was no pattern of residuals. Thus, the assumption of nonconstant variance was satisfied.

### *6.1.4 Comparison of IPC1 and IPC2 Machines*

The adequacy of the model was checked and the analysis of variance on the IPC1 and IPC2 data are summarized as shown in Table 19. The equality of the IPC1 and IPC2 machines hypotheses were:

$H_0$: $\tau_{IPC1} = \tau_{IPC2} = 0$

$H_1$: at least one $\tau_i \neq 0$

The p-value of the machine type (Factor A) was 0.0014, which is less than 0.05 (significant level of alpha). Therefore, the null hypothesis was rejected and it was concluded that there was significant difference between IPC1 and IPC2 machines.

**Table 19. Analysis of Variance for the Logarithm Transformed IPC1 and IPC2 Data.**

| Source | Sum of Squares | DF | Mean Square | F Value | Prob > F |
|---|---|---|---|---|---|
| Model | 1.34 | 4 | 0.34 | 3769.02 | < 0.0001 significant |
| Machine Type | 1.25E-03 | 1 | 1.25E-03 | 14.01 | 0.0014 |
| Beam Type | 1.34 | 2 | 0.67 | 7526.64 | < 0.0001 |
| Strain Level | 7.85E-04 | 1 | 7.85E-04 | 8.8 | 0.0079 |
| Residual | 1.70E-03 | 19 | 8.92E-05 | | |
| Lack of Fit | 6.81E-04 | 7 | 9.73E-05 | 1.15 | 0.395 not significant |
| Pure Error | 1.01E-03 | 12 | 8.45E-05 | | |
| Correlation Total | 1.35 | 23 | | | |
| Std. Dev. | 9.45E-03 | | R-Squared | 0.9987 | |
| Mean | 5.26 | | Adj R-Squared | 0.9985 | |
| C.V. | 0.18 | | Pred R-Squared | 0.998 | |

Because of the significant difference results obtained in the first experiment, it was necessary to re-calibrate the machines and carefully tune them.

### *6.1.5 Experimental Results after Re-Calibration and Tuning*

The two IPC machines were re-calibrated and the clamps were tightened. Upon tuning each machine, the entire experiment was then repeated. Additionally, the PID settings were set to a similar level for the two machines. In this second

experiment 24 tests were performwd (2 machines x 3 beams x 2 strain levels x 2 replicates). Table 20 summarizes the results of the second experiment.

**Table 20. Stiffness Results (in psi) of the Repeated Experiment After Re-Calibration.**

| Machine Type | Beam Stiffness | | | | | |
|---|---|---|---|---|---|---|
| | Low | | Medium | | High | |
| | Low Strain Level | High Strain Level | Low Strain Level | High Strain Level | Low Strain Level | High Strain Level |
| IPC 1 | 99946 | 96794 | 166500 | 163808 | 356391 | 350240 |
| | 93030 | 93330 | 168694 | 165120 | 361653 | 358960 |
| Average | 96488.0 | 95062.0 | 167597.0 | 164464.0 | 359022.0 | 354600.0 |
| Standard Deviation | 4890.4 | 2449.4 | 1551.4 | 927.7 | 3720.8 | 6166.0 |
| Coefficient of variation, % | 5.1 | 2.6 | 0.9 | 0.6 | 1.0 | 1.7 |
| IPC 2 | 99391 | 98190 | 168211 | 164207 | 357373 | 354662 |
| | 101535 | 95032 | 173583 | 163663 | 360103 | 361799 |
| Average | 100463.0 | 96611.0 | 170897.0 | 163935.0 | 358738.0 | 358230.5 |
| Standard Deviation | 1516.0 | 2233.0 | 3798.6 | 384.7 | 1930.4 | 5046.6 |
| Coefficient of variation, % | 1.5 | 2.3 | 2.2 | 0.2 | 0.5 | 1.4 |

The analysis of variance on the IPC1 and IPC2 data are summarized in Table 21. Similar to the previous analyses, the hypotheses were:

$H_0$: $\tau_{IPC1} = \tau_{IPC2} = 0$

$H_1$: at least one $\tau_i \neq 0$

The null hypothesis failed to be rejected and it was concluded that there was no significant difference between IPC1 and IPC2 machines.

**Table 21. Analysis of Variance for The IPC1 and IPC2 Data.**

| Source | Sum of Squares | DF | Mean Square | F Value | Prob > F |
|---|---|---|---|---|---|
| Model | 2.91E+11 | 4 | 7.28E+10 | 8408.07 | < 0.0001 significant |
| Machine Type | 2.26E+07 | 1 | 2.26E+07 | 2.61 | 0.1227 |
| Beam Type | 2.91E+11 | 2 | 1.46E+11 | 16810.9 | < 0.0001 |
| Strain Level | 6.87E+07 | 1 | 6.87E+07 | 7.94 | 0.011 |
| Residual | 1.65E+08 | 19 | 8.66E+06 | | |
| Lack of Fit | 2.84E+07 | 7 | 4.05E+06 | 0.36 | 0.9102 not significant |
| Pure Error | 1.36E+08 | 12 | 1.13E+07 | | |
| Cor Total | 2.91E+11 | 23 | | | |
| | | | | | |
| Std. Dev. | 2942.26 | | R-Squared | 0.9994 | |
| Mean | 2.07E+05 | | Adj R-Squared | 0.9993 | |

### *6.1.6 Findings from the Experimental Results*

A statistical experiment was performed using synthetic beams to verify an assumption that all machines operate in the same way and produce "Statistically Identical" results. The first trial experiment showed differences in test results among the two machines. The machines were then re-calibrated and tuned and the experiment was repeated. The second experiment showed that there were no significant differences among the results of the two machines. This means that both machines can be used in the study interchangeably.

## 6.2 Evaluation of Equality among Machines Using HMA Beams

Another comparative study was performed to compare both machines to verify the assumption that both machines operate in the same way and produce statistically comparable results. This evaluation experiment was accomplished

using HMA beams similar to the testable HMA samples that are used in the main experiment. The primary variable used to measure the equality of the beam measurements was the initial flexural stiffness with a zero dwell (rest) time between pulses.

### *6.2.1 Experiment Conditions*

1. Two IPC machines.
2. Beams were tested using haversine loads at 10 Hz frequency for 15,000 cycles. The use of a haversine load implies a rest time of 0 seconds.
3. Two strain levels: low (500 micro strains) and high (700 micro strains)
4. Three test temperatures of 40, 70 and 100$^{o}$F.
5. A full factorial design was used with a total of 24 HMA specimens (2 machines x 3 temperatures x 2 strain levels x 2 replicates).

### *6.2.2 Experiment Results*

Table 22 shows the flexural stiffness of the three beams under different test conditions.

**Table 22. Stiffness of HMA Beams (in psi).**

| Machine Type | Test Temperature | | | | | |
|---|---|---|---|---|---|---|
| | 40 F | | 70 F | | 100 F | |
| | Low Strain Level | High Strain Level | Low Strain Level | High Strain Level | Low Strain Level | High Strain Level |
| **IPC 1** | 1713850 | 1685934 | 603145 | 647078 | 154210 | 188782 |
| | 1496119 | 1319385 | 637156 | 776303 | 158065 | 156016 |
| Average | 1604984 | 1502660 | 620151 | 711691 | 156138 | 172399 |
| Standard Deviation | 153959 | 259189 | 24049 | 91376 | 2726.03 | 23168.8 |
| Coefficient of variation, % | 9.59 | 17.25 | 3.88 | 12.84 | 1.75 | 13.44 |
| **IPC 2** | 1529680 | 1561575 | 599774 | 718700 | 152757 | 173428 |
| | 1672471 | 1375957 | 800803 | 573901 | 158557 | 155748 |
| Average | 1601076 | 1468766 | 700289 | 646301 | 155657 | 164588 |
| Standard Deviation | 100969 | 131252 | 142149 | 102388 | 4100.69 | 12501.5 |
| Coefficient of variation, % | 6.31 | 8.94 | 20.30 | 15.84 | 2.63 | 7.60 |

### *6.2.3 Comparison of IPC1 and IPC2 Machines*

The adequacy of the model was checked and the analysis of variance on the IPC1 and IPC2 data are summarized as shown in Table 23. The hypotheses were:

$H_0$: $\tau_{IPC1} = \tau_{IPC2} = 0$

$H_1$: at least one $\tau_i \neq 0$

The null hypothesis failed to be rejected and it was concluded that there was no significant difference between IPC1 and IPC2 machines.

**Table 23. Analysis of Variance betwwen IPC1 and IPC2 using HMA specimens.**

| Source | Sum of Squares | DF | Mean Square | F Value | Prob > F |
|---|---|---|---|---|---|
| Temperature | 8.22556E+12 | 2 | 4.11278E+12 | 443.08 | < 0.0001 significant |
| Strain Level | 261102663 | 1 | 261102663 | 0.03 | 0.869 not significant |
| Machine | 1698938055 | 1 | 1698938055 | 0.18 | 0.674 not significant |
| Error | 1.76364E+11 | 19 | 9282340905 | | |
| Correlation Total | 1.76364E+11 | 23 | | | |
| R-Squared | 0.9790 | | | | |
| Adj R-Squared | 0.9746 | | | | |

### 6.3 Refinement of Beam Fatigue Test Parameters

The ASU research team conducted several pilot studies by running HMA fatigue beam tests to evaluate the different parameters to be used in the main study such as wave form type (haversine vs. sinusoidal) and control mode type (strain control vs. stress control). Another purpose of these pilot studies was to resolve any testing problems that might be encountered before starting the main experiment. All tests were performed on a Salt River Base mix with a PG 64-22 binder, which is the same mix used in the main study as shown in Chapter 4.

The literature indicates that most previous researchers used to run the beam fatigue test without rest period under either a controlled strain or a controlled stress mode. Also, most researchers, especially in the U.S., applied haversine strains or stresses wave forms. In this pilot study, both haversine and sinusoidal strain and stress controlled tests were conducted with and without rest period.

The results have led to the development of solutions to several potentially significant problems and questions.

The beam fatigue test can be performed under these four modes:

1. Haversine controlled strain (108)
2. Haversine controlled stress
3. Sinusoidal controlled strain (101)
4. Sinusoidal controlled stress

Figure 26 shows the haversine and sinusoidal wave forms. The haversine form changes from 0 to $2\varepsilon$ (or $2\square$), whereas the sinusoidal form changes between $\pm\varepsilon$ ($\pm\sigma$). This implies that the haversine wave form bends the beam in one direction, while the sinusoidal form bends the beam in both directions. Of course, each test mode can be performed without or with rest period.

Most of the tests that have been performed in the literature have been performed without rest period. In the last several years, researchers started running tests with rest period to evaluate the healing effect. Note that the haversine stress-controlled test is not typically conducted since the specimen fails very quickly because of the rapid accumulation of permanent deformation.

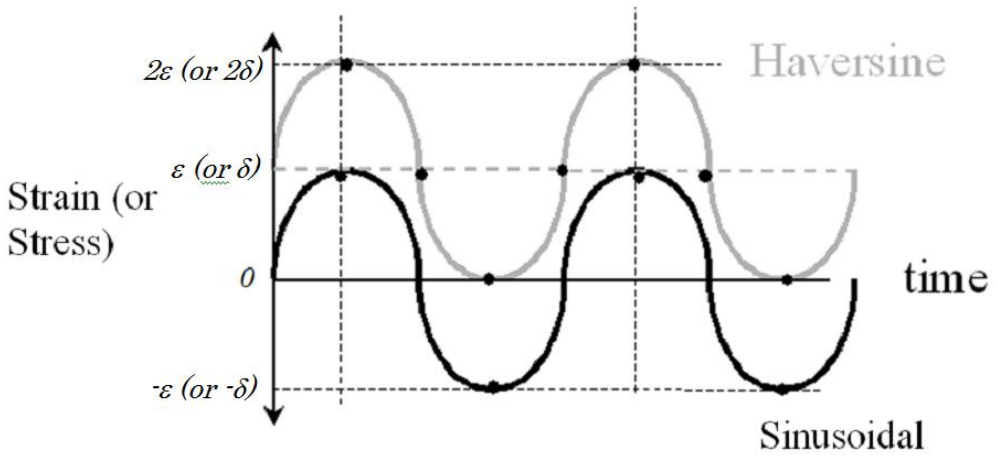


**Figure 26. Haversine and sinusoidal wave forms (109).**

### *6.2.1 Haversine Pulse Tests*

In this part of the study, haversine strain-controlled flexure fatigue tests were performed according to ASTM D-7460. In this test haversine strain-controlled cycles were applied with 0.1 second strain periods for 25,000 repetitions. The following conditions were used.

1. Three test temperatures: 40°F, 70°F, and 100°F
2. Two strain levels: 400 and 800 microstrains
3. Two rest periods: 0 and 10 seconds

This pilot study revealed some issues that need to be studied carefully before continuing on with the NCHRP 9-44A work plan. The results of this pilot study are discussed below.

Figure 27 shows that the test with rest period in some cases resulted in faster damage and lower fatigue life than the test without rest period. This, of course, was completely opposite to the major hypothesis of the endurance limit

study, which is based upon the premise that it is the rest period that "heals" the damage in the asphalt and extends the fatigue life of the material. In other cases, beams subjected to rest period failed in the middle of the test as shown in Figure 28 and Figure 29. The fatigue machines were re-calibrated and many tests were repeated several times, but the problems were not solved completely.

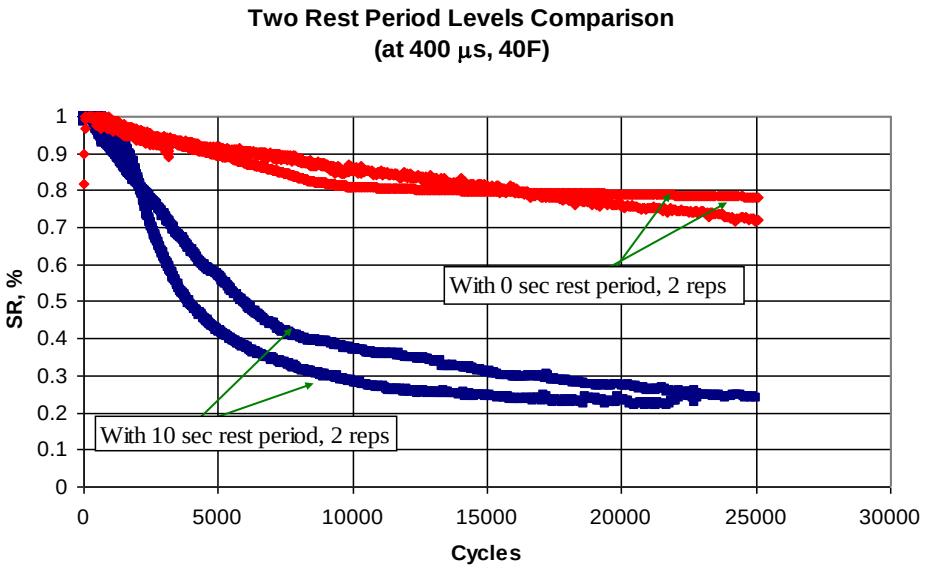


**Figure 27. Stiffness ratio versus loading cycles with and without rest periods (haversine strain controlled test, 400 microstrains, 40°F).**

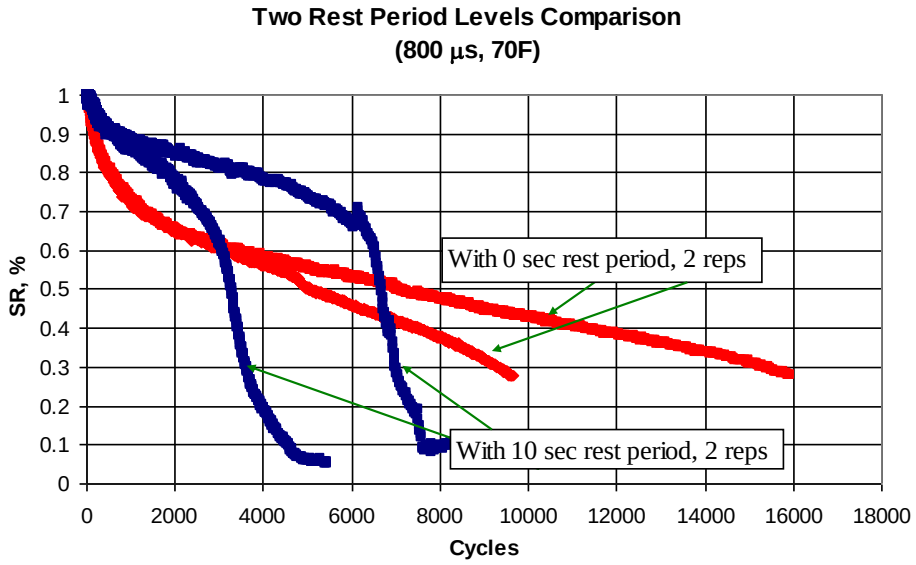


**Figure 28. Stiffness ratio versus loading cycles with and without rest periods (haversine strain controlled test, 800 microstrains, 70°F).**

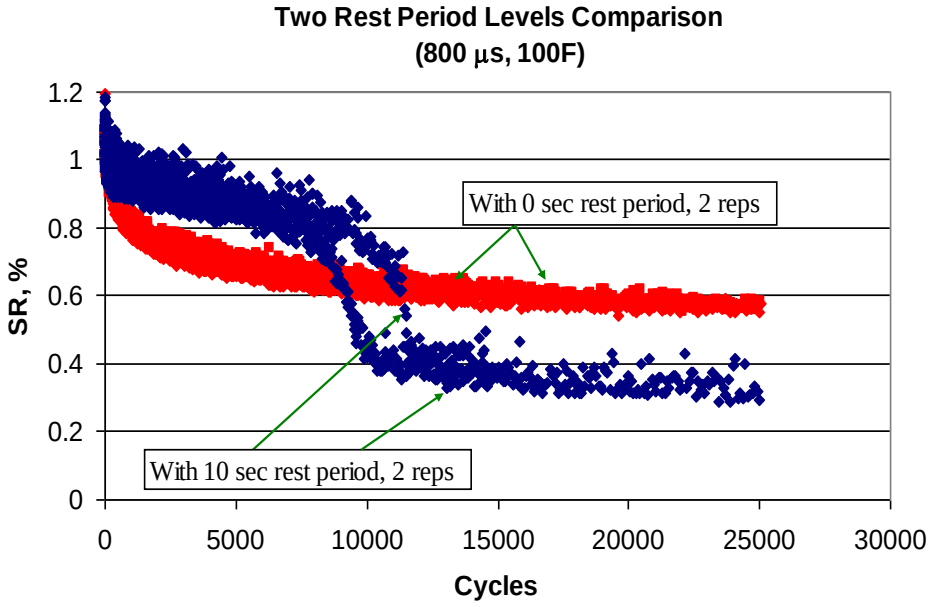


**Figure 29. Stiffness ratio versus loading cycles with and without rest periods (haversine strain controlled test, 800 microstrains, 100°F).**

The shape of the deflection and force pulses were examined in more details in order to find out the reasons for these results. In the strain controlled

haversine tests without rest period, it was observed that the resulting load pulses started as haversine. After only a few cycles, the load pulses transformed to sinusoidal loads, which transferred approximately half the load in one direction and the other half in the other direction as shown in Figure 30. This means that although we were trying to bend the beam in one direction, the beam actually bended in both directions.

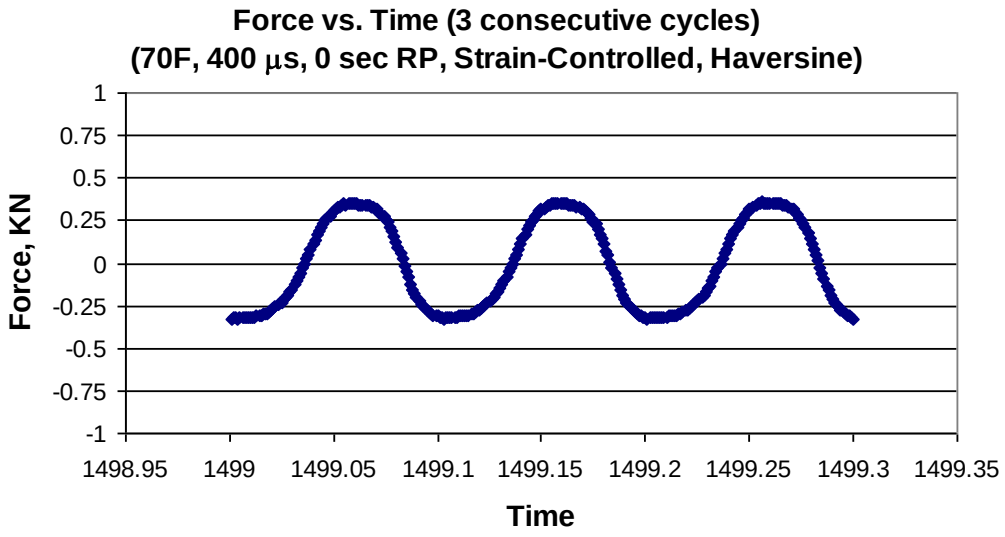


**Figure 30. Force vs. time for a strain controlled test with haversine pulse without rest period.**

This phenomenon was explained by Pronk et al. (109, 111). Due to the viscous character of the material, creep (permanent deformation) occurs in the beam. At the end of the first cycle the beam will go back to the original shape, but the neutral axis will be shifted as shown in Figure 31. This position resembles the new (shifted) neutral axis of the beam, which will shift the strain in future cycles. This implicates that although a haversine *displacement* signal occurs, the

*strains and stresses* in the beam will be pure sinusoidal (compression and tension). The amplitude of the sinusoidal strain signal will be equal (or even less) than half the original value of the haversine at the start of the test. In the new neutral position half of the beam material will be under compression, while the other half is subjected to tension.

Although the tension and compression are reversed every cycle, the compression might have a beneficial effect on the fatigue life. This means that there are two factors working against each other as far as fatigue and healing are concerned.

1. The reversed bending accelerates the fatigue failure because of the reversed stress in each cycle.
2. The compression during half of the cycle accelerates healing.

Depending on which factor has larger effect, the beam could experience either short or long fatigue life.

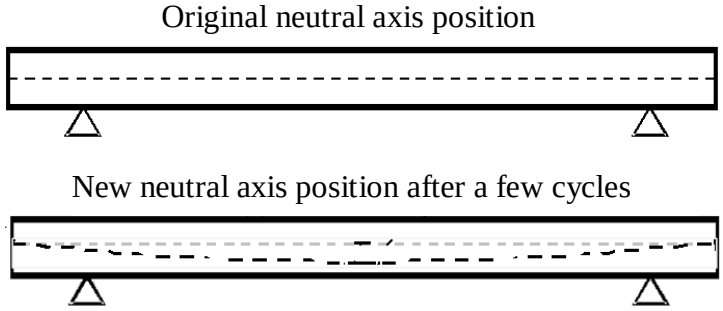


**Figure 31. Viscous response will cause a shift of the neutral axis.**

This phenomenon, however, does not occur in the case with rest period. In the strain-controlled haversine tests with rest period, the load pulses are maintained to be close to haversine until the end of the test as shown in Figure 32. This happens because of the relaxation that occurs during the rest period even when the beam is subjected to creep. This implies that the bottom of the beam is mostly under tension, which may accelerate the fatigue failure. Again, two factors are working against each other in this case.

1. The continuous tension at the bottom of the beam accelerates the fatigue failure.
2. The rest period accelerates healing.

Depending on which factor has larger effect, the beam could experience either short or long fatigue life.

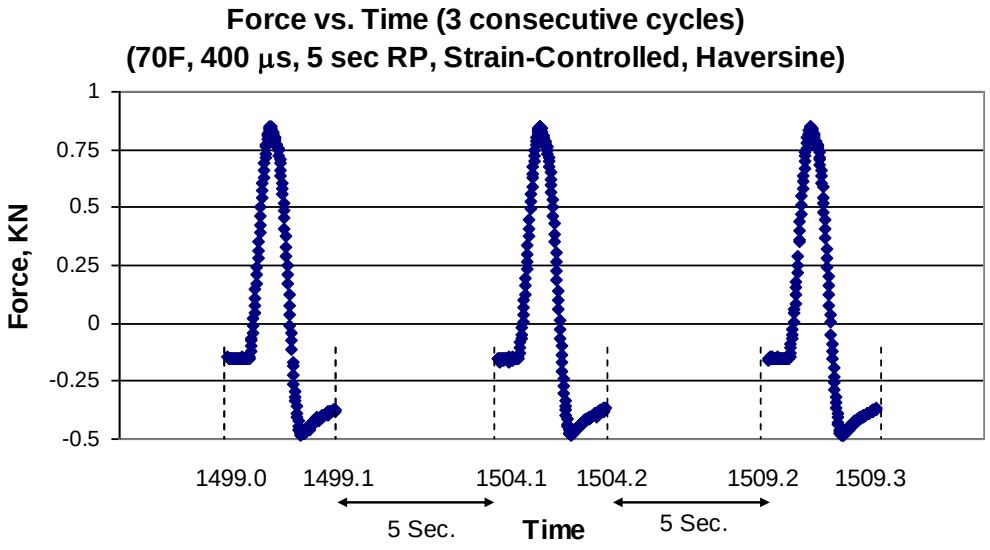


**Figure 32. Force vs. time for a strain controlled test with haversine pulse with rest period.**

In conclusion, the haversine test does not produce consistent results whether the test is run with or without rest period. The comparison in this case might produce erroneous results depending on the mix type, test temperature, strain level, and the duration of the rest period. In addition, the shift from haversine to sinusoidal in the stress and strain signals might induce additional variability, which makes it difficult to compare the results of tests under different conditions (26).

### *6.2.2 Sinusoidal Pulse Tests*

Because of the inconsistency of the haversine test results, a number of sinusoidal strain- and stress-controlled tests were performed without and with rest period. Figure 33 and

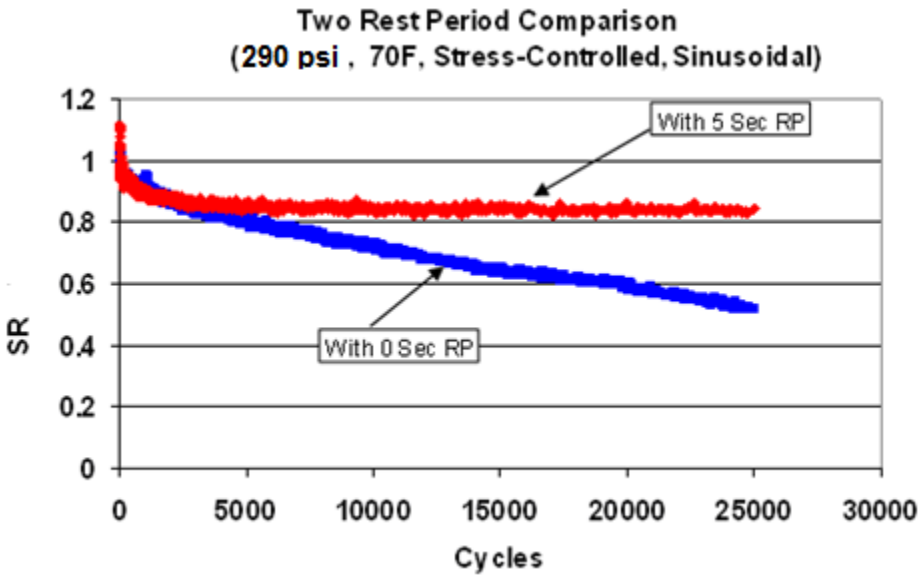


Figure 34 show the stiffness ratio versus number of loading cycles with and without rest periods using sinusoidal strain and stress controlled tests,

respectively. The two figures show that the test with a 5-second rest period resulted in a longer fatigue life than the test without rest period as expected.

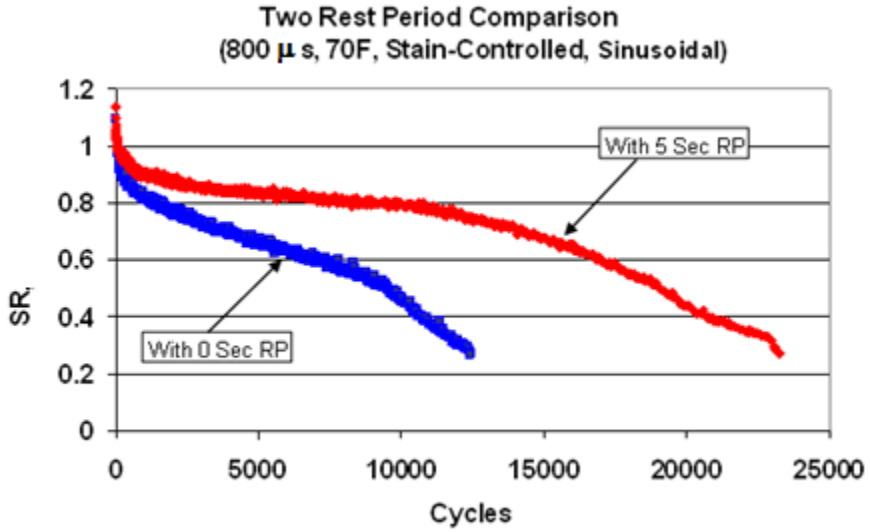


**Figure 33. Stiffness ratio versus loading cycles with and without rest periods (sinusoidal strain-controlled, 70°F).**

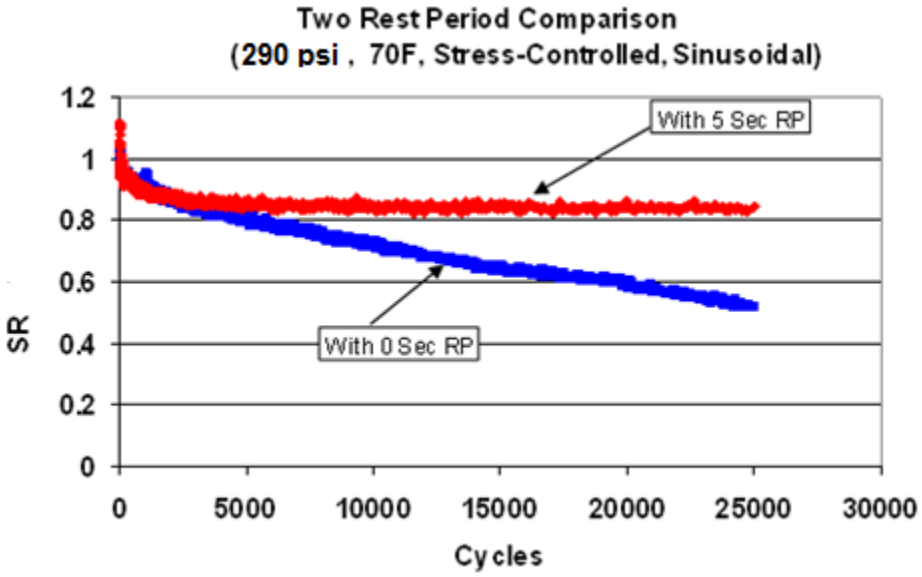


**Figure 34. Stiffness ratio versus loading cycles with and without rest periods (sinusoidal stress-controlled, 290 psi, 70°F).**

The force and displacement cycles were examined for the sinusoidal pulse tests at different conditions. Figure 35 and Figure 36 show the force and

displacement versus time for the strain-controlled tests with sinusoidal pulses without and with rest period, respectively. Unlike the haversine tests, the figures show consistent sinusoidal force and displacement cycles throughout the test. Note that for this strain-controlled test (Figure 36), there is a small amount of force at the beginning of the rest period, but it dissipates at the end of the rest period.

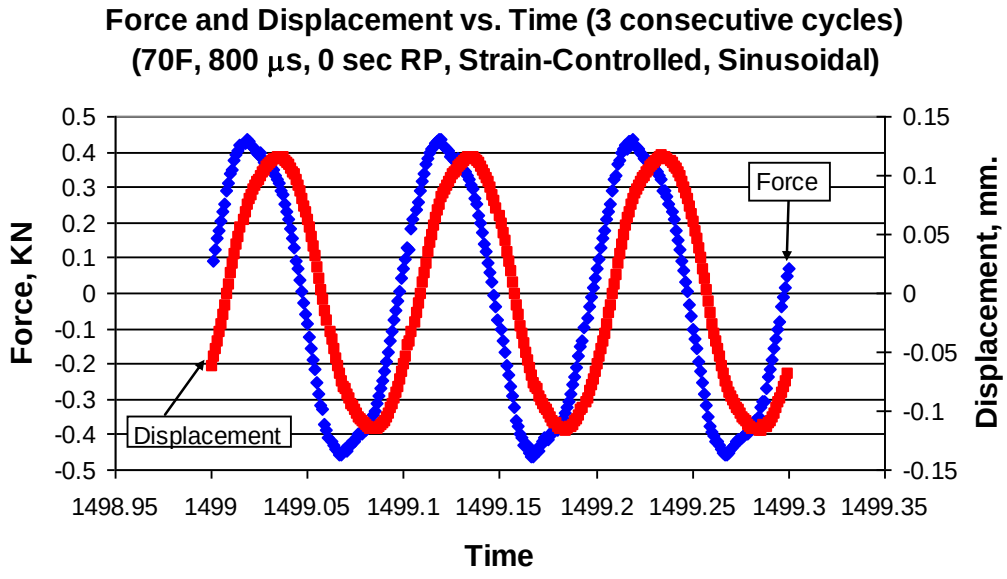


**Figure 35. Force vs. time for a strain controlled test with sinusoidal pulse without rest period.**

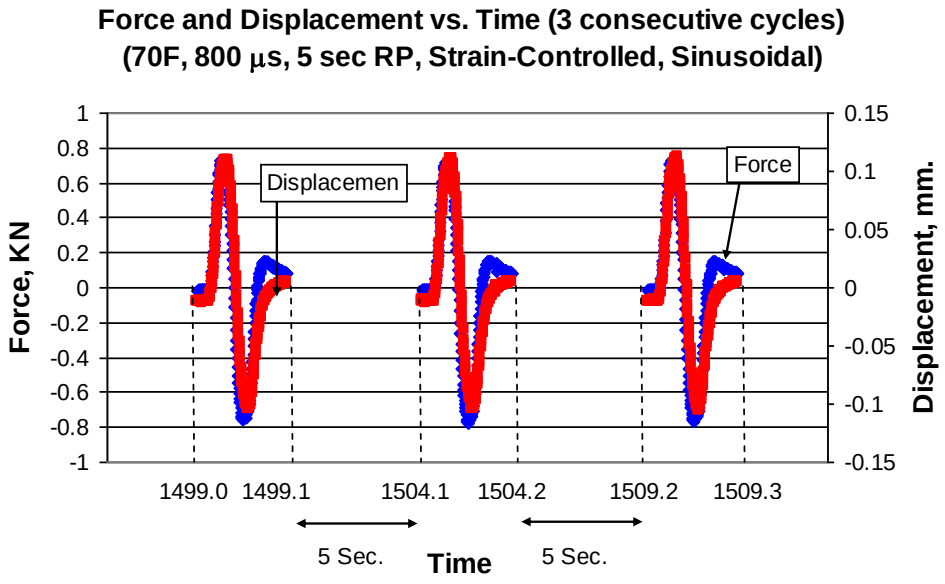


**Figure 36. Force vs. time for a strain controlled test with sinusoidal pulse with rest period.**

Figure 37 and Figure 38 show the force and displacement versus time for the stress-controlled tests with sinusoidal pulse without and with rest period, respectively. Again, the figures show consistent sinusoidal force and displacement cycles throughout the test.

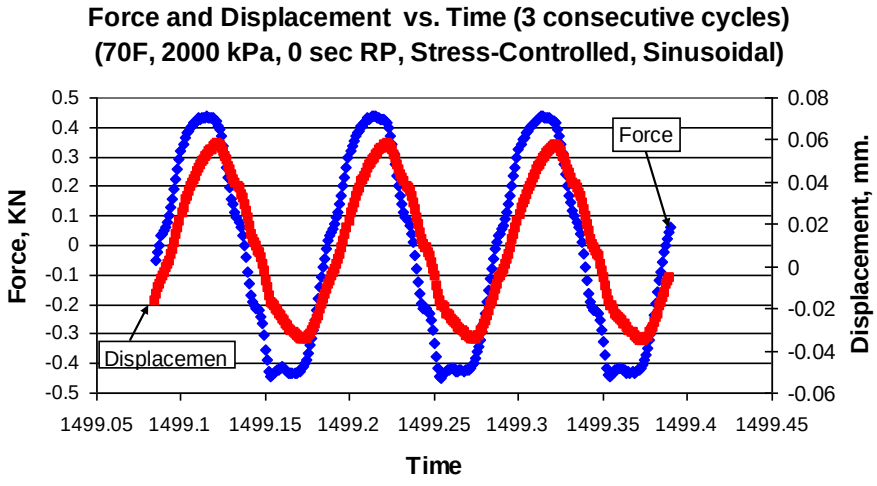


**Figure 37. Force vs. time for a stress controlled test with sinusoidal pulse without rest period.**

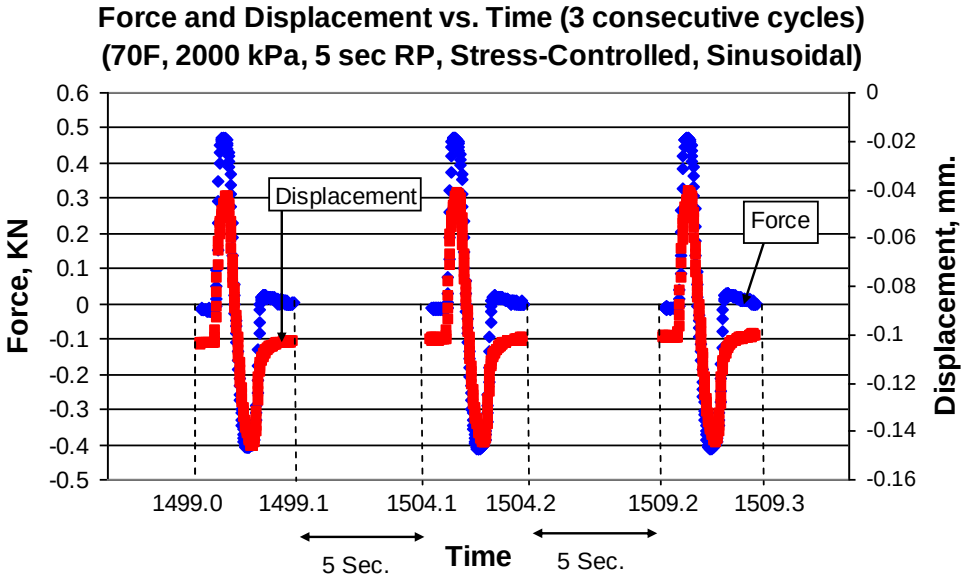


**Figure 38. Force vs. time for a stress controlled test with sinusoidal pulse with rest period.**

Based on these results, it is recommended to use sinusoidal pulse tests instead of the haversine tests in the main experiment. Also, since there is not much difference between strain and stress controls, it is recommended to use strain control to avoid the rapid accumulation of permanent deformation. Thus, it was decided to follow AASHTO T-321 to complete the project.

### *6.2.4 Simulation of Field Condition*

At the bottom of the asphalt layer in the field strain signals look more like a haversine than sinusoidal when a wheel load is passing. Therefore, using haversine signals in lab tests would be more realistic. Based on the previous discussion, however, it is hard to simulate the field condition in the lab since the beam fatigue test with constant haversine deflections will immediately change into tests with constant sinusoidal deflections. It is also important to note that only the surface layer is tested in the lab without consideration of the bottom

layers (base, subbase or subgrade). Asphalt is a viscoelastic material and in contrast with the road there is no 'elastic' bottom layer in the lab fatigue test to 'push' the specimen back to its original position after the load is removed (109). Since neither the haversine wave nor the sinusoidal wave exactly simulates the field condition, it is important to use sinusoidal waves to obtain consistent results as discussed before.

### *6.2.5 Dissipated Energy Calculations*

The dissipated energy during the flexure fatigue test calculation requires a time lag between stress and strain. For example, a linear elastic material will not have dissipated energy since the stress and strain are in-phase. For the beam fatigue test without rest period, the dissipated energy can be calculated since there is a phase lag between stress and strain as shown in Figure 35 and Figure 37. However, if the rest period is introduced, the HMA material relaxes during the rest period and stress and strain will be almost in-phase at the beginning of each cycle as shown in Figure 36 and Figure 38. Therefore, the dissipated energy calculated for the test with rest period is expected to be less accurate than the case without rest period. In this study, it was decided not to use the dessipated energy approach.

## 6.3 Verification of Equality among Machines Using Sinusoidal Waveform and Synthetic Beams with 5 Second Rest Period

After deciding to use the sinusoidal strain control test, the ASU research team conducted an additional pilot study by running beam fatigue tests to verify the assumption of equality among beam fatigue testing machines using synthetic

beams. It was also decided to use a 5 second rest period, which is the same rest period that will be used in the main experiment. Another purpose of this pilot study was to solve any testing problems that might be encountered before starting the main experiment.

### *6.3.1 Experimental Conditions*

The following experimental conditions were used.

1. Two machines: IPC1 and IPC2.
2. Two synthetic beams with two levels of stiffness: low and high.
3. Sinusoidal load at a 10 Hz frequency with a rest time of 5 seconds between pulses for 2,500 cycles.
4. One strain level of 800 micro strains
5. One test temperature of 20°C.

A complete factorial experiment was conducted with a total of 12 tests (2 machines x 2 beams x 1 strain levels x 3 replicates).

### *6.3.2 Comparison of IPC1 and IPC2 machines*

A statistical analysis similar to the previous analyses was performd following the same procedure. A comparison analysis of IPC1 and IPC2 machines were made. Table 24 summarizes the statistical results.

**Table 24. Results of the Statistical Analysis of the Machine Type Comparisons.**

| | Sum of Squares | DF | Mean Square | F Value | Prob > F |
|---|---|---|---|---|---|
| IPC1 vs. IPC2 | 8.52E+09 | 1 | 8.52E+09 | 0.98 | 0.3485 |

The results showed that there are no significant differences among the results of the two machines. This shows that both machines can be used in the study interchangeably, which can improve the test production.

### 6.4 Recommendation for the Main Experiment

- Strain-controlled sinusoidal tests will be performed in the main experiment according to AASHTO T-321 procedure.
- The dissipated energy approach is not suitable for the test with rest period. Instead, the stiffness based method should be used.
- Use the IPC1 and IPC2 machines since there are no statistical differences between them.

# Chapter 7 HMA ENDURANCE LIMIT AND HEALING

## 7.1 Background

The main purpose of this chapter is to develop a mathematical procedure to determine HMA endurance limit based on healing. The proposed mathematical procedure would relate the HMA healing phenomenon to the endurance limit, which makes this procedure unique compared to previous research projects that studied these concepts separately. Six factors that affect fatigue response of asphalt mixtures were evaluated, which are binder type, binder content, air voids, temperature, magnitude of the rest period applied after each loading cycle, and number of cycles to failure for the test without rest period ($N_f$). The procedure was implemented using test results from representative asphalt concrete mixtures. As mentioned earlier in Chapter 4, the healing index (HI) can be defined as the difference between the stiffness ratios (SR) for the tests with and without rest period at the number of cycles to failure for the test without rest period ($N_{f\ w/o\ RP}$) as shown in Figure 7 and Equation 15 in Chapter 3.

According to this HI definition, SR needs to be recorded for both tests with and without rest period at $N_{f\ w/o\ RP}$ as shown in Figure 7. Also, extrapolation was used to predict the SR for the test with rest period at $N_f$ w/o RP since it was decided to run all tests with rest period up to 20,000 cycles only. Figure 8 in Chapter 3 shows the extrapolation process to determine SR for the tests with rest-period at $N_{f\ w/o\ RP}$.

### 7.2 Procedure for Determining Healing-Based Endurance Limit

Since a fractional factorial design of experiment was implemented as discussed in Chapter 3, it was expected that some test combinations would not be tested. Hence, in case of running a test with rest period at certain conditions and no matching test without rest period exists, there is a need to predict $N_{f\ w/o\ RP}$ in order to extend the test with rest period to that $N_{f\ w/o\ RP}$ to get SR. Therefore, a regression model based on all tests without rest period only was developed to predict $N_f$ without RP at any required test combination, which would allow to decide the amount of extrapolation needed for the tests with rest period. Four methods were attempted to develop a fatigue model. Three of these methods used the AASHTO MEPDG $K_1$, $K_2$, and $K_3$ format, while the fourth method used a linear regression procedure that directly correlates the binder content, air void content, and the applied strain with the $N_f$ w/o RP value. More details are explained in the following section.

Once the $N_{f\ w/o\ RP}$ is predicted, the required extrapolation for the test with rest period can be completed and SR can be determined for both tests with and without rest period. After determining the SR values, all data points were used to establish the general SR model. The following is the general form of the SR model based on the six factors:

$$SR = a_1 + a_2\,AC + a_3\,V_a + a_4\,(BT) + a_5\,(RP) + a_6\,(T) + a_7\,N_{f\ w/o\ RP} + \text{2-factor interactions} + \text{3-factor interactions} \quad (23)$$

where

- SR = Stiffness Ratio

- $a_1$, $a_2$ ... $a_n$ = Regression coefficients
- AC = Percent asphalt content
- $V_a$ = Percent air voids
- BT = Binder type
- RP = Rest period (sec)
- $N_{f\ w/o\ RP}$ = Number of cycles to failure (test without rest period)

Once the SR model is developed, HI for any test combination can be computed as shown in Equation 23. Subsequently, the next step is to correlate the computed healing index to the endurance limit. All HI data points can be plotted versus the strain levels that were used for each test at each temperature separately since it is expected to have different endurance limit values by changing the temperature. Figure 39 illustrates a schematic relationship between healing index and strain at each temperature.

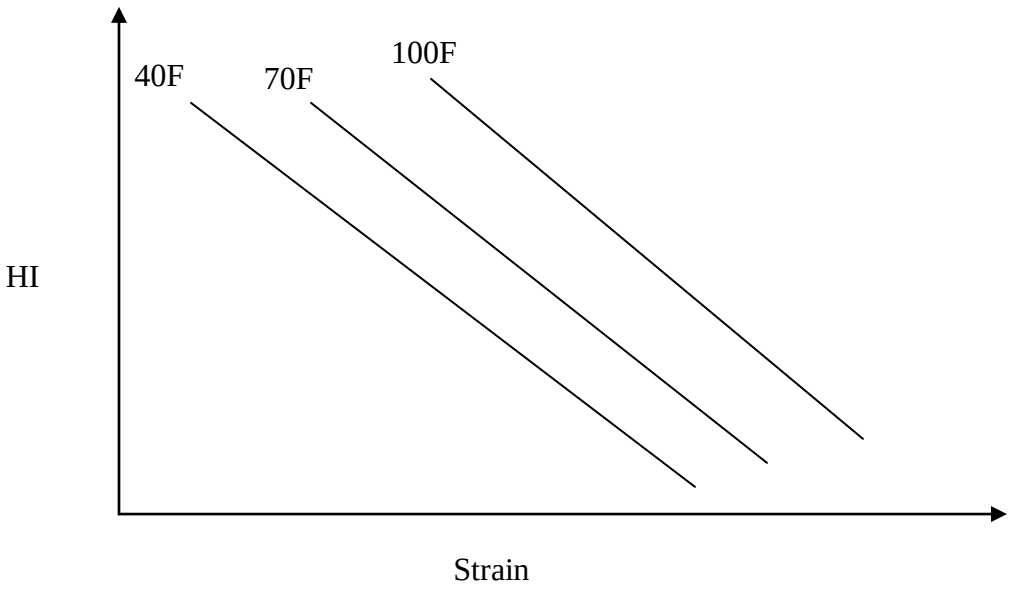


**Figure 39. Healing index versus strain levels at 3 test temperatures.**

It is proposed that the endurance limit will occur when no damage is incurred using the test with rest period. This implies that the endurance limit can be estimated at a HI of 0.5; which means $SR_{w/o\ RP}$ = 0.5 and $SR_{w/\ RP}$ = 1.0 (no damage). Figure 40 shows a schematic of the estimated endurance limit at each temperature.

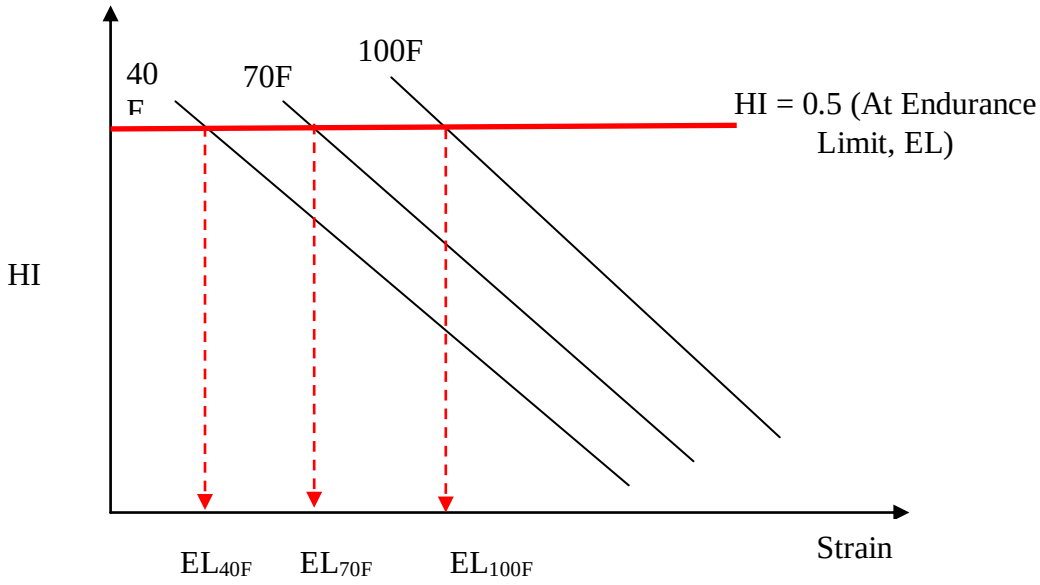


**Figure 40. Endurance limit determination at each temperature based on HI.**

### 7.3 First Generation Integrated Stiffness Ratio Model

The following is first attempt to implement the proposed endurance limit procedure using test results from all three mixtures made of PG 58-28, PG 64-22 and PG 76-16 binders.

#### *7.3.1 Developing $N_f$ Model*

In order to determine the two levels of $N_{f\ w/o\ RP}$ to be used in the experiment, fatigue tests were performed at the optimum mix design conditions (4.5% asphalt

content and 7% air voids) without rest period up to failure (50% stiffness ratio) at the three temperatures of 40, 70 and 100°F as shown in Figure 41 to Figure 43 for the PG 58-28, PG 64-22, and PG 76-16, respectively. These figures were used to determine the recommended strain levels at each temperature. The criterion of selecting the two strain levels at each temperature was to reach an $N_f$ value (for tests without rest period) of a reasonable number of cycles of 30,000 and 100,000 at the high and low strain levels, respectively.

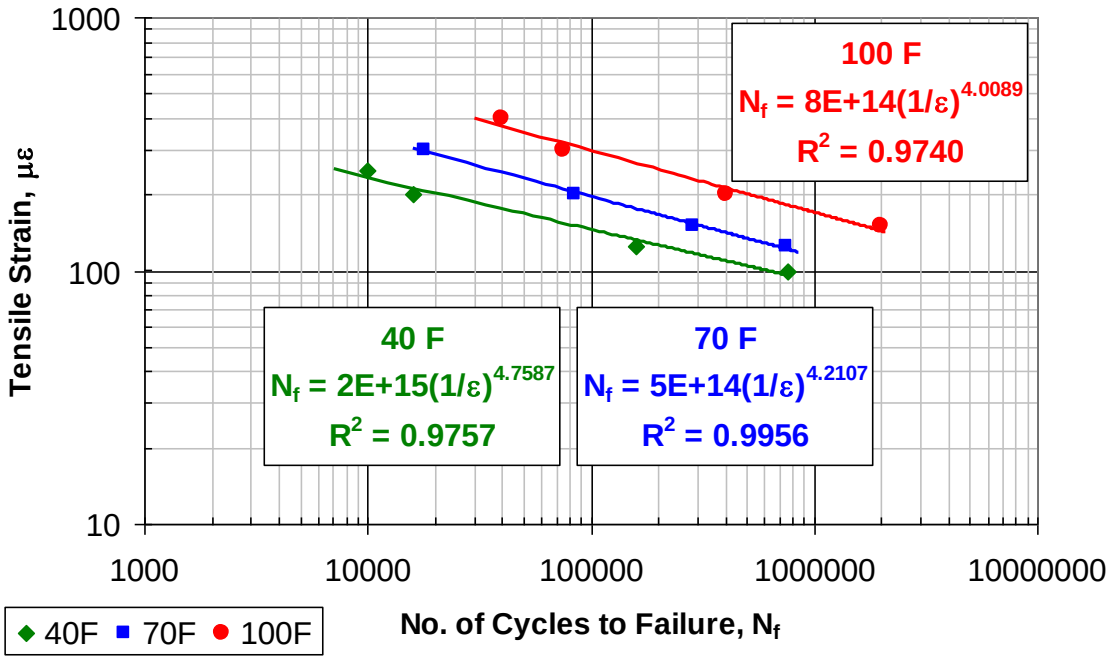


**Figure 41. Tensile strain vs. number of cycles to failure for the PG 58-28 mixture.**

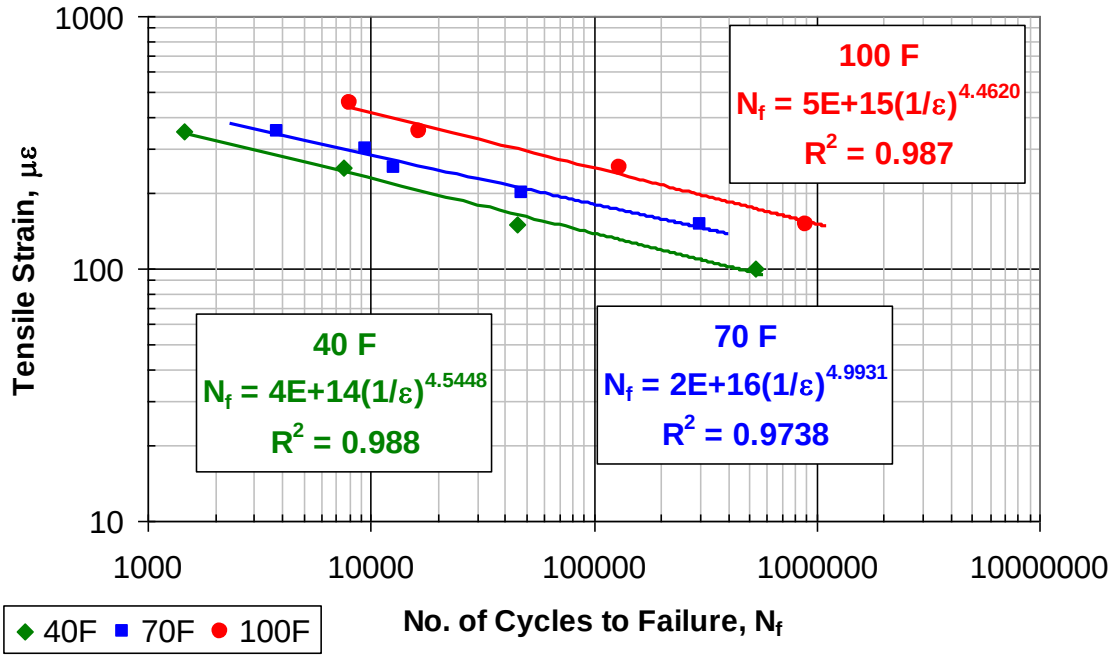


**Figure 42. Tensile strain vs. number of cycles to failure for the PG 64-22 mixture.**

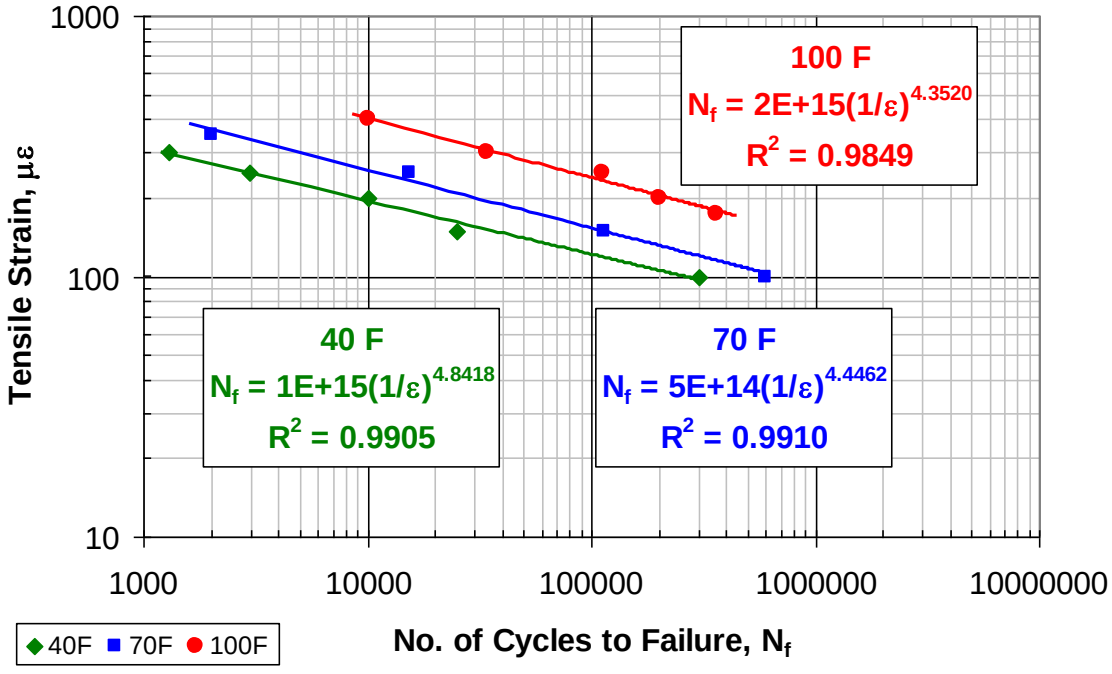


**Figure 43. Tensile strain vs. number of cycles to failure for the PG 76-16 mixture.**

Table 25 summarizes the strains for the three mixtures at the three test temperatures in order to complete the test within 30,000 and 100,000 cycles.

**Table 25. Strains for the Three Mixtures at the Three Test Temperatures.**

| T, F | $N_f$, cycles | Strain, μs | | |
|---|---|---|---|---|
| | | PG 58-28 | PG 64-22 | PG 76-16 |
| 40 | 100,000 | 145 | 100 | 138 |
| | 30,000 | 170 | 150 | 175 |
| 70 | 100,000 | 200 | 137.5 | 188 |
| | 30,000 | 263 | 200 | 238 |
| 100 | 100,000 | 295 | 313 | 238 |
| | 30,000 | 415 | 388 | 325 |

As mentioned above, four methods were attempted to predict $N_f$ w/o RP for the missing cells. The following are the first 3 methods that were used to calculate the $K_1$, $K_2$, and $K_3$ model coefficients. Data from PG 64-22 mixture were used to check these different methods:

*Method 1: One general $K_1$, $K_2$, $K_3$ for all data points*

In this method, tests without rest period were used as one set to determine one general model with a single $K_1$, $K_2$, $K_3$ set similar to the AASHTO MEPDG procedure. The STATISTICA (128) software was used in the statistical analysis. The following is the model that was developed:

$$N_f = 8.49227 * (1/\varepsilon)^{2.7179} * (1/E_0)^{0.9252} \quad (24)$$
$$R^2 = 0.4306$$

where ε is the initial strain and $E_0$ is the initial stiffness.

Figure 44 shows the measured versus predicted $N_f$ using the developed model. It is noticed that the model had a low prediction accuracy indicated by the low $R^2$ value ($R^2$=0.43). Developing one model for all the without-rest-period PG

64-22 mixture data points that have different binder contents and air voids might be a major reason of decreasing the accuracy of the model.

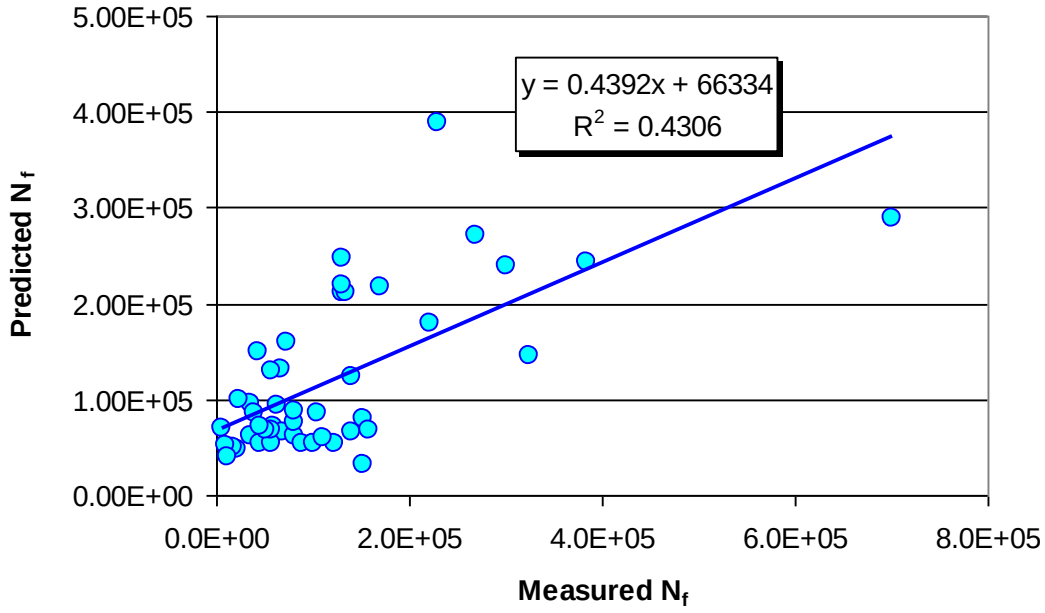


**Figure 44. Measured versus predicted $N_f$ (Method 1).**

*Method 2: Different $K_1$ for each binder content and air void combination and a single set of $K_2$ and $K_3$ values*

The main difference between this method and the previous one is that $K_1$ was calculated using the AASHTO MEPDG equation based on the binder content (AC) and air voids ($V_a$) data.

Since there were 4 different combinations of AC and $V_a$ used, four values of $K_1$ were calculated. Using STATISTICA, a single $K_2$ and $K_3$ set was determined. The following are the models that were developed:

For 4.2 AC and 4.5 $V_a$:

$$N_f=0.000429*(1/\varepsilon)^{4.5564}*(1/E_0)^{1.2635} \quad (25)$$

For 4.2 AC and 9.5 $V_a$

$$N_f=0.0000602*(1/\varepsilon)^{4.5564}*(1/E_0)^{1.2635} \quad (26)$$

For 5.2 AC and 4.5 $V_a$

$$N_f=0.000777*(1/\varepsilon)^{4.5564}*(1/E_0)^{1.2635} \quad (27)$$

For 5.2 AC and 9.5 $V_a$

$$N_f=0.000102*(1/\varepsilon)^{4.5564}*(1/E_0)^{1.2635} \quad (28)$$

Overall $R^2=0.3504$

Figure 45 shows the measured versus predicted $N_f$ values based on the second method. More reasonable values for the three coefficients were obtained using this method since it counted for the difference in binder contents and air voids. However, lower prediction accuracy was obtained, which indicates the need of having a specific coefficient set for each combination.

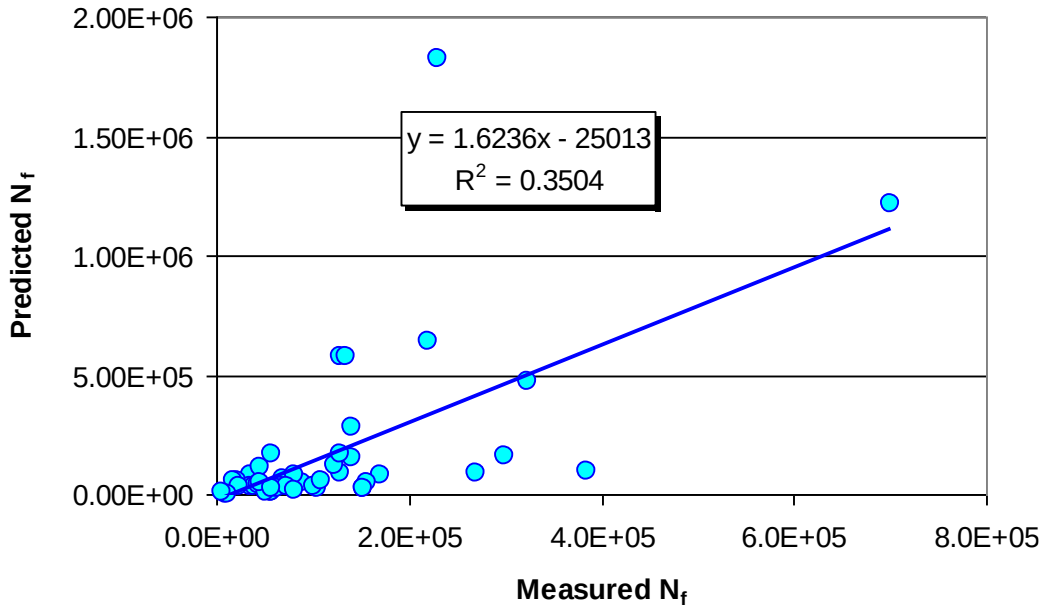


**Figure 45. Predicted versus measured $N_f$ (Method 2).**

*Method 3: Different $K_1$, $K_2$, and $K_3$ sets for each AC-$V_A$ combination*

In this case, the data points were separated into 4 groups according to their AC-$V_A$ properties. Each one of the four groups had a different set of $K_1$, $K_2$, and $K_3$. The following are the models that were developed:

For 4.2 AC and 4.5 $V_a$:

$$N_f=2972.382*(1/\varepsilon)^{1.7978}*(1/E_0)^{0.8135} \quad (29)$$

For 4.2 AC and 9.5 $V_a$

$$N_f=1.15*10\text{^}-21*(1/\varepsilon)^{13.7971}*(1/E_0)^{4.06539} \quad (30)$$

For 5.2 AC and 4.5 $V_a$

$$N_f=42.21357*(1/\varepsilon)^{1.9939}*(1/E_0)^{0.56654} \quad (31)$$

For 5.2 AC and 9.5 $V_a$

$$N_f=0.84045*(1/\varepsilon)^{2.7715}*(1/E_0)^{0.8039} \quad (32)$$

Overall $R^2$=0.6169

Figure 46 shows the measured versus measured $N_f$ values using the third method. It is noticed that by treating each AC-$V_a$ combination as a different mix, the overall prediction accuracy went up ($R^2$ = 0.62).

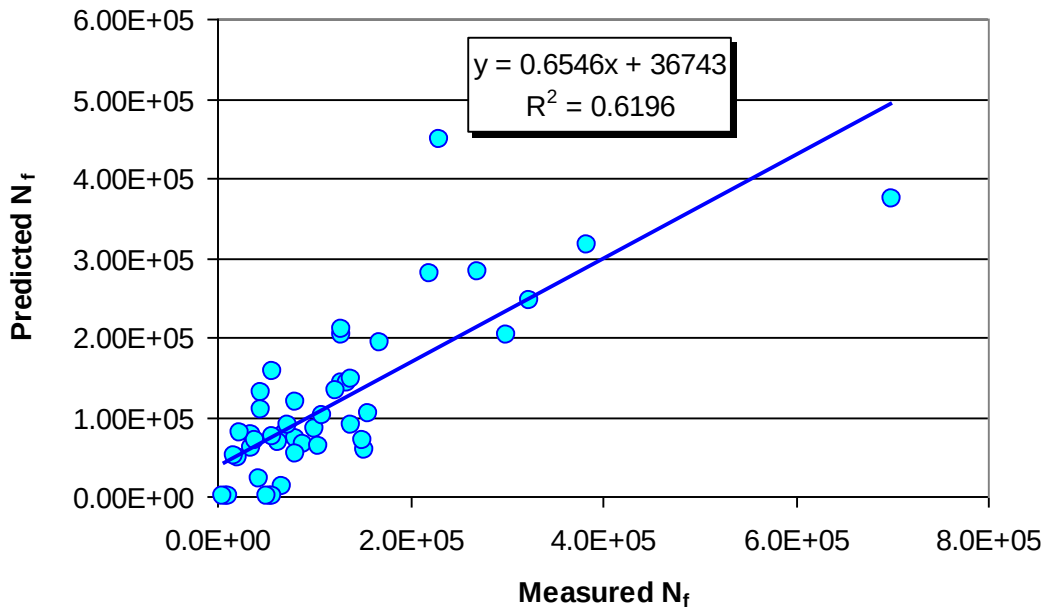


**Figure 46. Measured versus predicted $N_f$ (Method 3).**

*Method 4: Different $N_f$ model for each temperature*

It was noticed that in Method 3, the values of the $K_1$, $K_2$, and $K_3$ coefficients obtained were unreasonable. The main reason of having out-of-range coefficients was the lack of enough data points required to develop each model because of the fractional factorial design. For example, in some temperatures only one strain level was used. This can lead the statistical program to produce unreasonable values of the coefficients. As a result, in Method 4 a linear regression model was developed for each temperature. These models had the mathematical form as presented in Equation 33.

$$\text{Log}\,(N_{f\ w/o\ RP}) = a + b\,AC + c\,V_a + d\,\varepsilon \qquad (33)$$

The three $N_f$ models (3 mixtures x 3 temperatures) have $R^2$ values ranging from 0.624 to 0.964, which are much higher than those of the previous three

methods. The analysis also showed that these models are more rational and accurate than the models obtained in the first 3 methods.

Figure 47 shows a comparison between the first 3 AASHTO MEPDG methods and the above mentioned method (Method 4). Therefore, the forth method was used in the rest of the study.

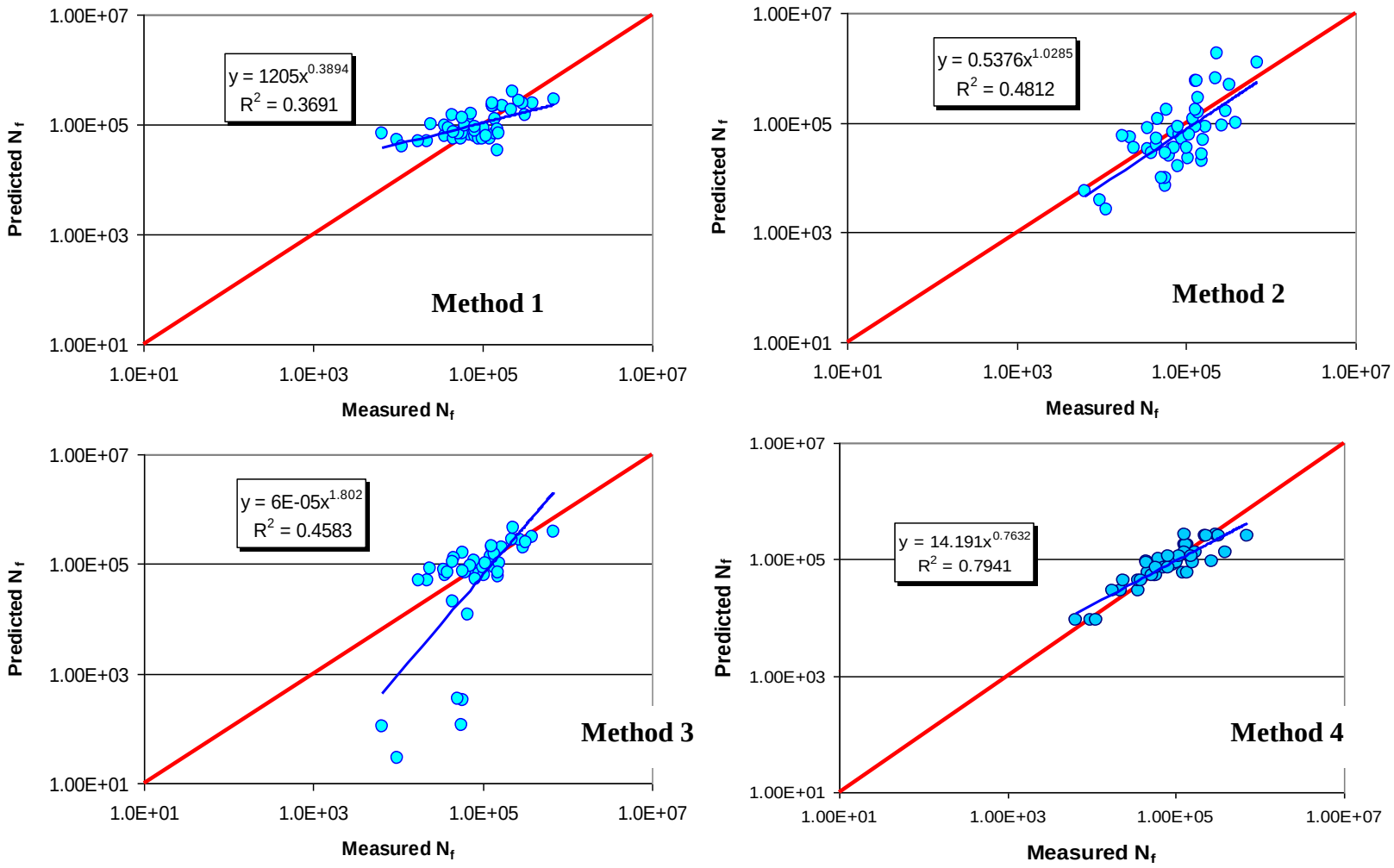


**Figure 47. Measured versus predicted $N_f$ using the 3 predicted AASHTO MEPDG models and the AC- $V_a$ based model.**

### *7.3.2 Developing First Generation SR Model*

The SR values were determined at the $N_{f\ w/o\ RP}$ values for all 288 data points and used to develop the integrated stiffness ratio model for the three mixtures. All data points are presented in Appendix A. The general form of the SR model based on the six factors is shown in Equation 55.

The JMP software (98) was used in developing the integrated model by trying different combinations of factors. The significant factors are selected if the individual p-values are less than the significant level of 0.05 (the yellow highlighted cells). Hierarchy was kept in the model, which means that if there is a significant interaction between two factors, their individual effects were included in the model even if it is not significant. Table 26 shows the final results for the model after removing the insignificant factors.

**Table 26. Results for the Selected Significant Factors for the First Generation SR Model.**

| Source | DF | F Ratio | Prob > F |
|---|---|---|---|
| Binder Type | 2 | 166.5917 | 0.0298* |
| Binder Content(4.2,5.2) | 1 | 36.3884 | <.0001* |
| Air Voids(4.5,9.5) | 1 | 27.6618 | <.0001* |
| Nf(50000,150000) | 1 | 126.4891 | <.0001* |
| Rest Period(0,5) | 1 | 10766.64 | <.0001* |
| Temperature | 2 | 32.9617 | <.0001* |
| Binder Type*Binder Content | 2 | 4.7033 | 0.0111* |
| Binder Type*Rest Period | 2 | 118.8344 | <.0001* |
| Binder Type*Temperature | 4 | 17.5194 | <.0001* |
| Binder Content*Rest Period | 1 | 40.4089 | <.0001* |
| Air Voids*Rest Period | 1 | 34.3220 | <.0001* |
| Air Voids*Temperature | 2 | 8.3959 | 0.0003* |
| Nf*Rest Period | 1 | 129.0273 | <.0001* |
| Nf*Temperature | 2 | 17.0101 | <.0001* |
| Rest Period*Temperature | 2 | 30.9743 | <.0001* |
| Binder Type*Binder Content*Temperature | 4 | 2.5896 | 0.0376* |
| Binder Type*Rest Period*Temperature | 4 | 16.7807 | <.0001* |
| Air Voids*Rest Period*Temperature | 2 | 7.5962 | 0.0006* |
| Nf*Rest Period*Temperature | 2 | 12.6873 | <.0001* |

*Significant factor

**Summary of Fit**

| Parameter | Value |
|---|---|
| RSquared | 0.981223 |
| Adjusted RSquared | 0.97827 |
| Root Mean Square Error | 0.024834 |
| Mean of Response | 0.673556 |
| Observations | 288 |

Three factors needed to be altered from being recognized as categorical factors to numerical factors: $N_f$, temperatures, and binder type. Although the $N_f$ values were estimated in advance using the optimum design conditions, the actual testing resulted in a relatively a large range of $N_f$ values. Because of the large variability of the $N_f$ values $N_f$ was initially treated as a categorical variable (Low and High). If $N_f$ is treated as categorical variable, it would not allow the user to

use specific $N_f$ values other than those used in the study. In order to resolve this issue, an average "low" value and an average "high" value of $N_f$ were calculated based on all data points for all three mixtures. The average low level of $N_f$ was 50,000 cycles, whereas the average high level of $N_f$ was 150,000 cycles.

In addition, temperature was also treated as a categorical variable in the preliminary stage of developing the model because of the inability of the fractional factorial statistical software to deal with three numerical levels of temperatures (40, 70, and 100$^o$F) and other variables as two numerical levels. As a result, the software produced a certain coefficient for each of the three temperatures. To convert temperature from a categorical to a numerical variable, relationships between the three levels of temperature (40, 70, and 100$^o$F) and the categorical coefficients were developed. While converting the binder type from categorical variable to numerical, it was decided to use the elastic modulus (stiffness) values obtained from the E* test at 70F and 10 Hz at the optimum design condition (4.7% AC and 7% $V_a$) for each mix. The values that were used in the analysis were 785, 1017, and 1905 ksi for PG 58-28, PG 64-22, and PG 76-16 mixtures, respectively. Figure 48 shows the categorical coefficients versus temperatures.

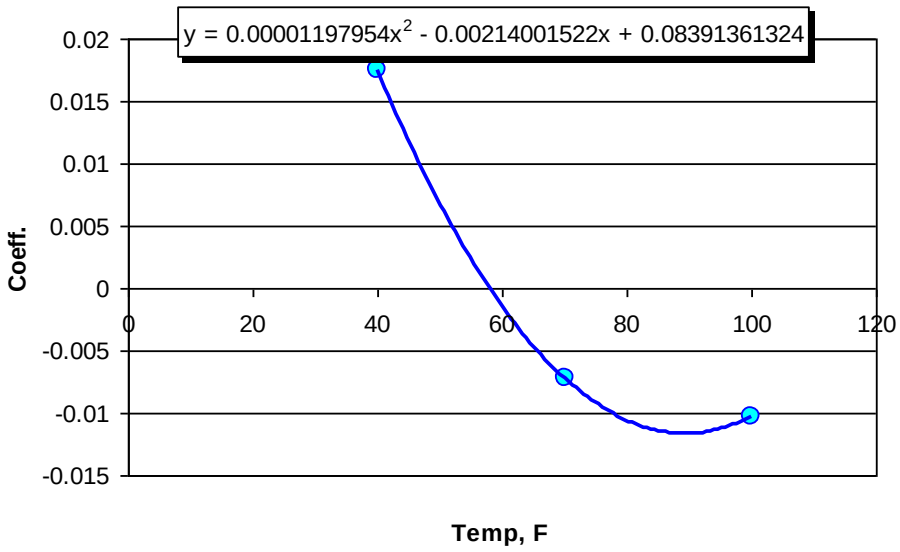


(a)

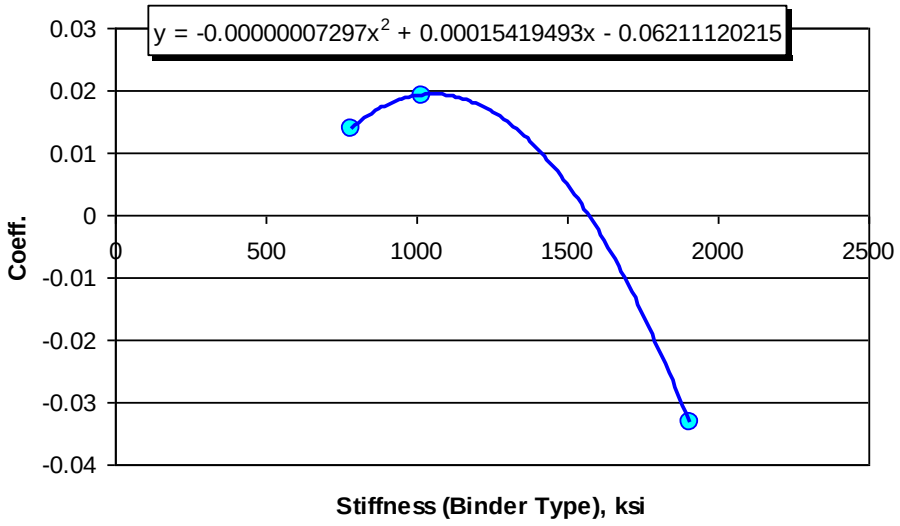


(b)

**Figure 48. Categorical coefficients versus temperatures for the integrated model: (a) coefficient for Stiffness (Binder Type), (b) coefficient for Temperature, (c) coefficient for Binder Type*Binder Content, and (d) Temperature*Air Voids.**

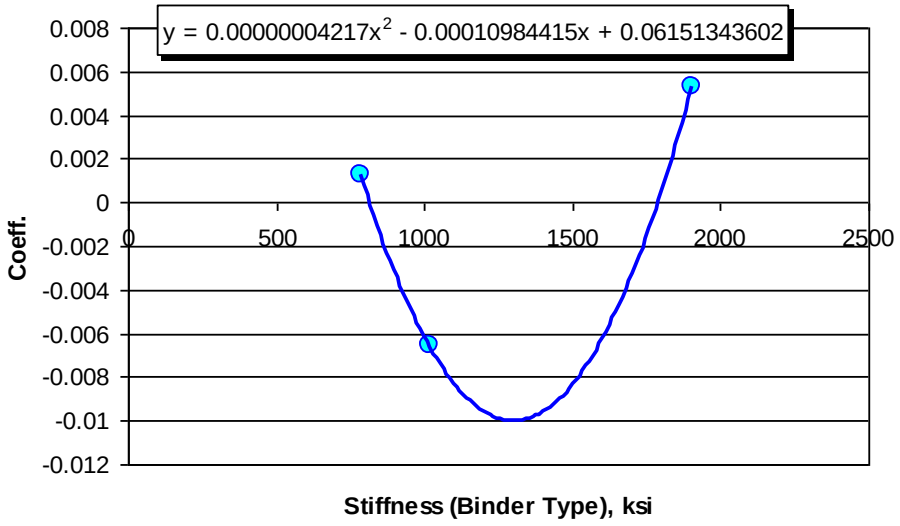


(c)

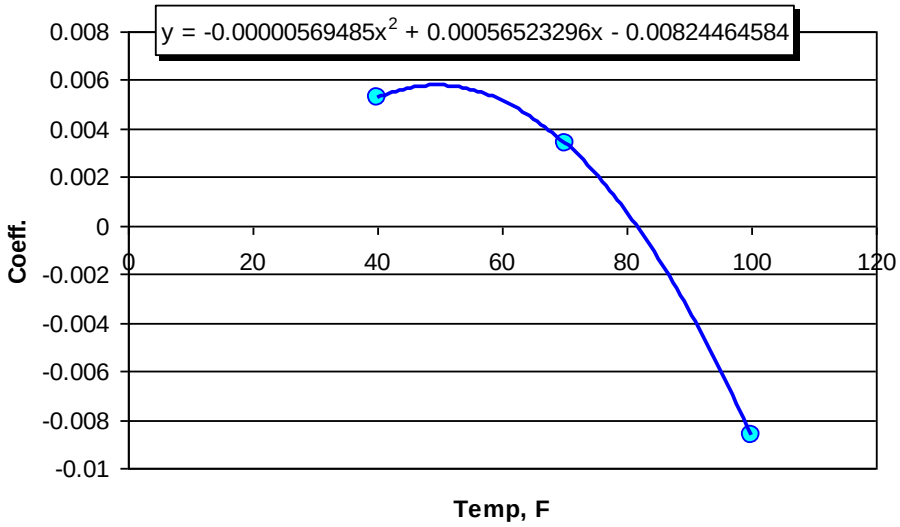


(d)

**Figure 48. (Continued). Categorical coefficients versus temperatures for the integrated model: (a) coefficient for Stiffness (Binder Type), (b) coefficient for Temperature, (c) coefficient for Binder Type*Binder Content, and (d) Temperature*Air Voids.**

The values of $N_f$, temperature and binder type (stiffness) were replaced by the developed relations. As a result, the finalized integrated model was developed as shown below.

$$SR = 0.1564774 + (0.00079*BT) + (0.070059744*AC) + (0.00393*V_a) + (0.10095*RP) - (1.268*10^{-7}*N_f) - (0.0024676*T) - (0.0001677*BT*AC) + (3.29961x10^{-5}*BT*RP) + (3.488*10^{-6}*BT*T) + (0.00794848*AC*RP) - (0.0042225*V_a*RP) + (0.0006044*AC*T) - (0.0001035*V_a*T) - (2.889*10^{-8}*RP*N_f) + (2.9191*10^{-9}*N_f*T) - (0.0025*RP*T) - (3.97*10^{-7}*BT^2) - (1.20135*10^{-5}*T^2) + (8.434*10^{-8}*BT^2*AC) - (2.8756*10^{-8}*BT^2*RP) + (1.9558*10^{-6}*AC*T^2) + (6.6137*10^{-7}*V_a*T^2) - (1.582*10^{-11}*N_f*T^2) + (1.262x10^{-5}*RP*T^2) - (1.176*10^{-6}*V_a*RP*T^2) + (3.124*10^{-12}*N_f*RP*T^2) - (7.4*10^{-7}*BT*AC*T) + (3.92*10^{-7}*BT*RP*T) + (0.00013185*V_a*RP*T) + (2.19*10^{-9}*N_f*RP*T) \quad (34)$$

Figure 49 shows the integrated model's adequacy using the residual versus predicted plot and the residual versus row plot. The fitting model meets the requirement of normal distribution with constant variance. Figure 50 demonstrates measured versus predicted SR values based on the integrated model. The $R^2$ value of the developed model was very high (0.980), which is a good indication of the accuracy of the model.

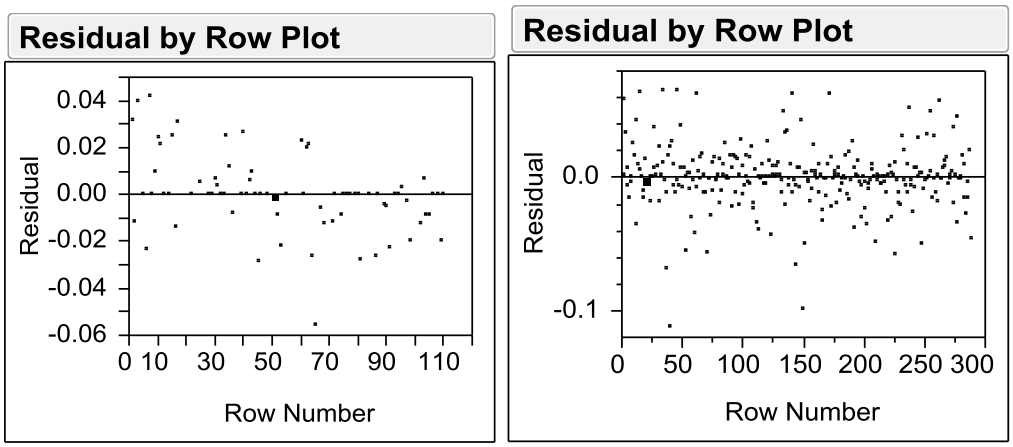


**Figure 49. Residual vs. predicted and residual vs. row for the integrated model.**

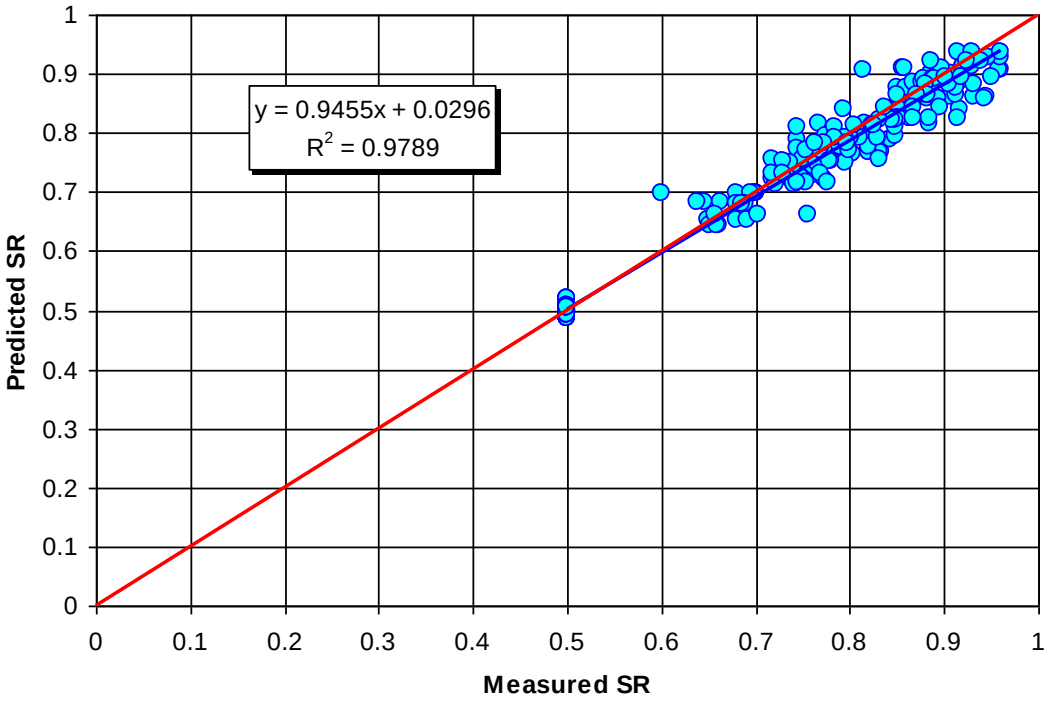


**Figure 50. Measured versus predicted SR values based on the integrated SR model for all three mixtures.**

### *7.3.3 Prediction of Healing Index and Endurance Limit*

Using the developed integrated SR model in Section 7.3.2, the healing index values for all test combinations were computed using Equation 54. Subsequently,

the following step was to relate the computed healing index to the endurance limit. The HI data points were plotted versus strain that were used for each mixture at each temperature separately since it is expected to have different endurance limit values for different mixtures and different temperatures. Figures 51-59 illustrate the relationship between healing index and strain level for each mixture at each temperature (3 mixtures x 3 temperatures). Note that there are two strain levels for each temperature. The relationship between the healing index and strain was assumed logarithmic.

As stated previously in the endurance limit procedure, it was proposed that the endurance limit will occur when a complete healing is achieved during the rest period. This implies that the endurance limit can be estimated at a HI value of 0.5, which means $SR_{w/o\ RP}$ is equal to 0.5 and $SR_{w/\ RP}$ is equal to 1.0 (no damage). Referring to Figure 7, the fatigue curve for the test with rest period will be a horizontal line indicating that the value of the stiffness ratio will always be 1.0.

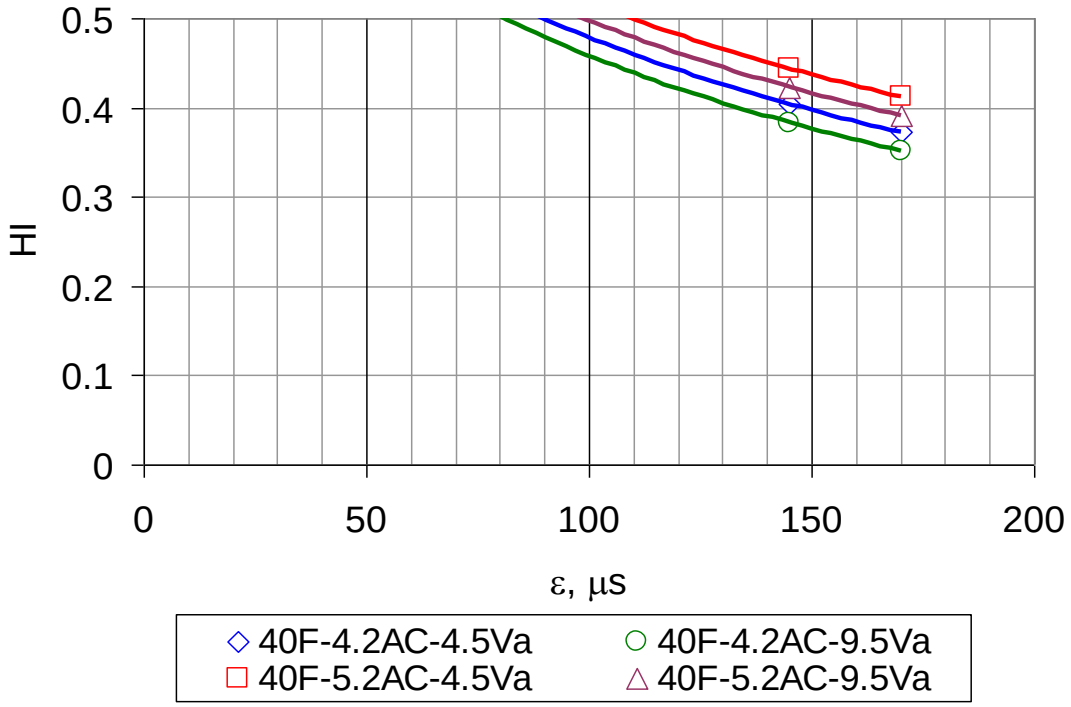


**Figure 51. Healing Index versus strain levels for the PG 58-28 Mixture at 40 F.**

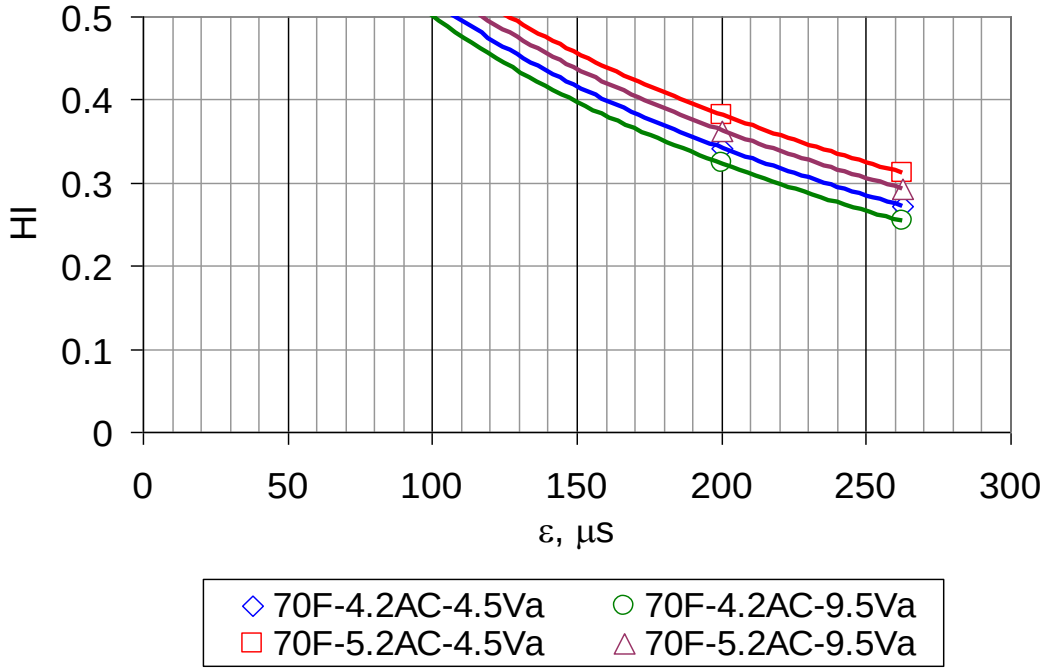


**Figure 52. Healing Index versus strain levels for the PG 58-28 Mixture at 70 F.**

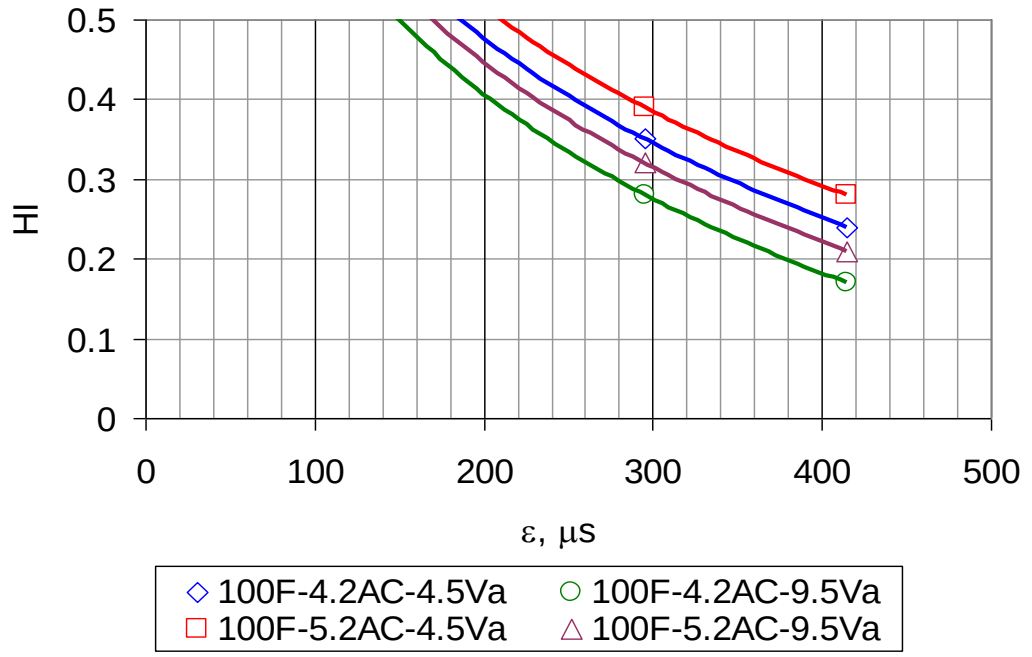


**Figure 53. Healing Index versus strain levels for the PG 58-28 Mixture at 100 F.**

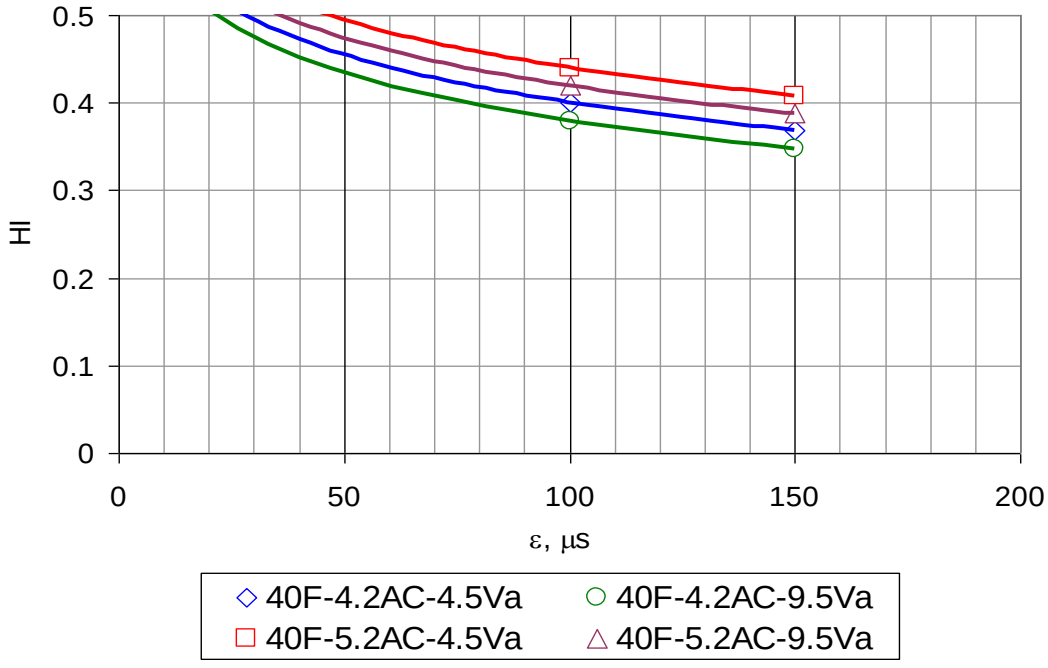


**Figure 54. Healing Index versus strain levels for the PG 64-22 Mixture at 40 F.**

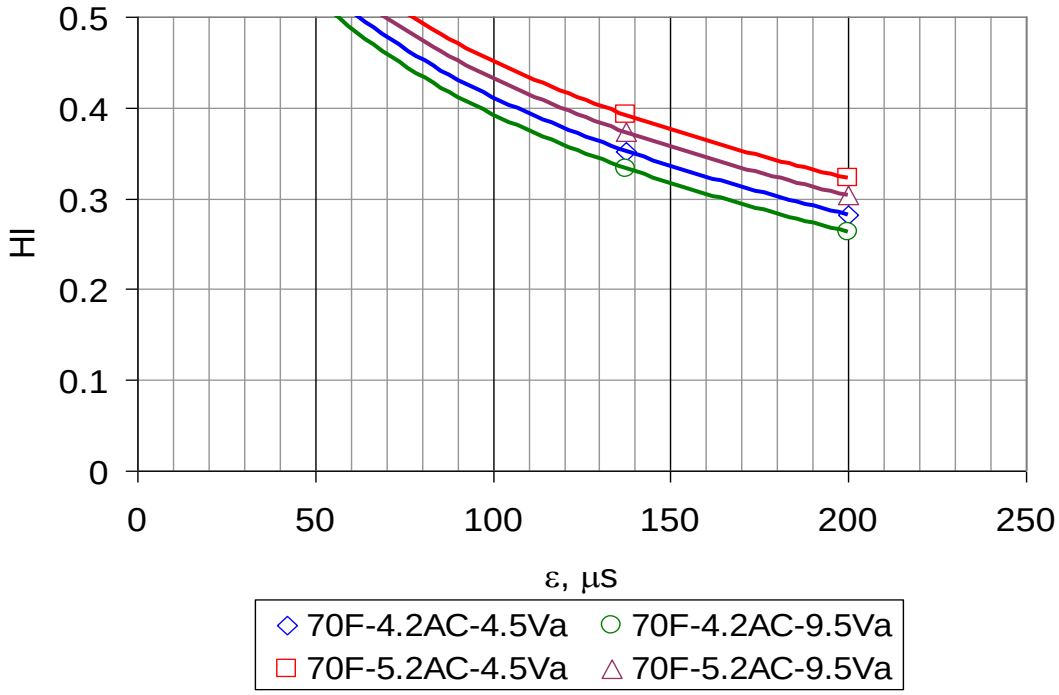


**Figure 55. Healing Index versus strain levels for the PG 64-22 Mixture at 70 F.**

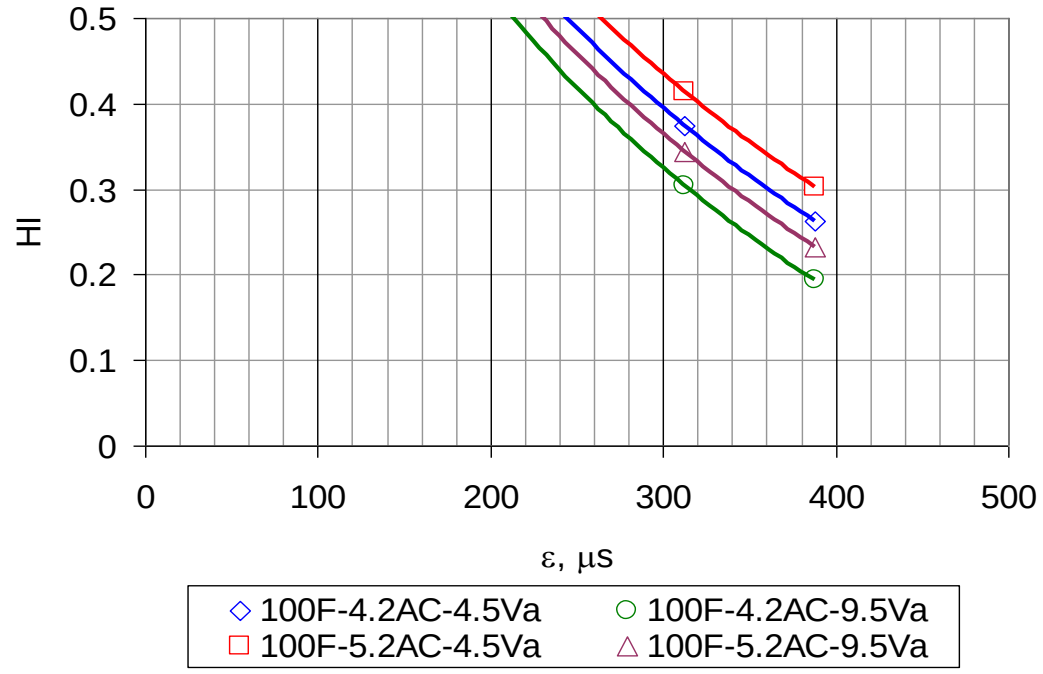


**Figure 56. Healing Index versus strain levels for the PG 64-22 Mixture at 100 F.**

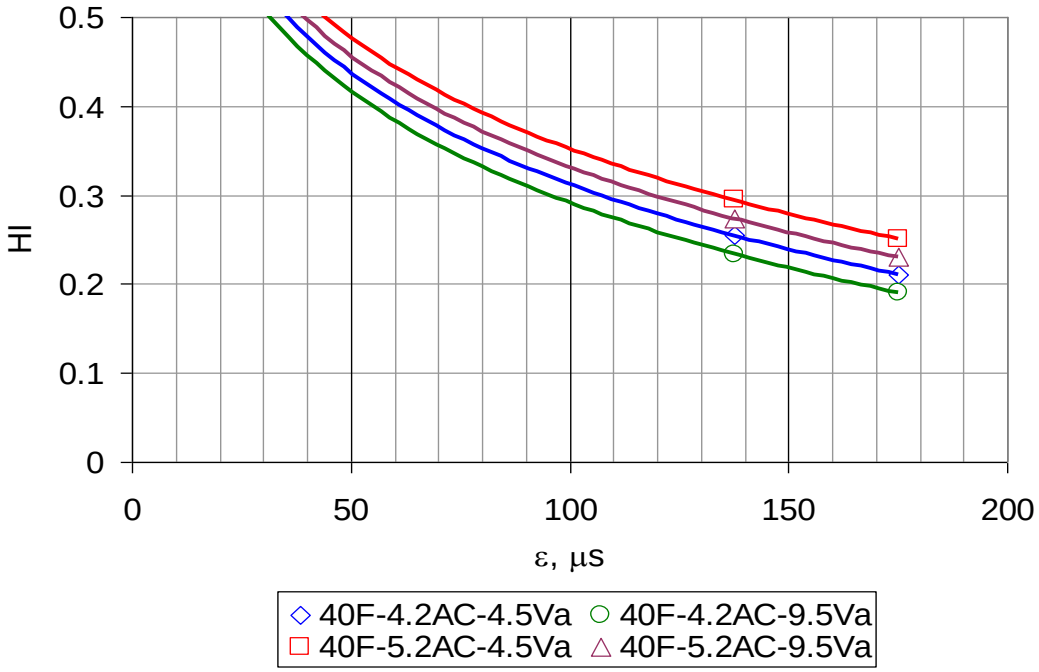


**Figure 57. Healing Index versus strain levels for the PG 76-16 Mixture at 40 F.**

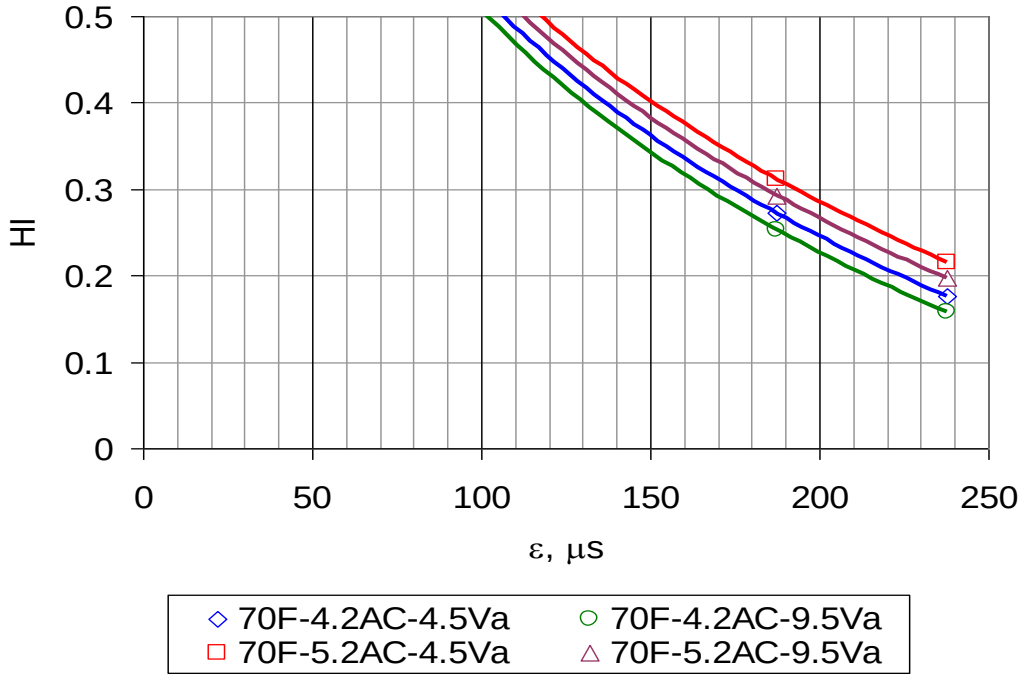


**Figure 58. Healing Index versus strain levels for the PG 76-16 Mixture at 70 F.**

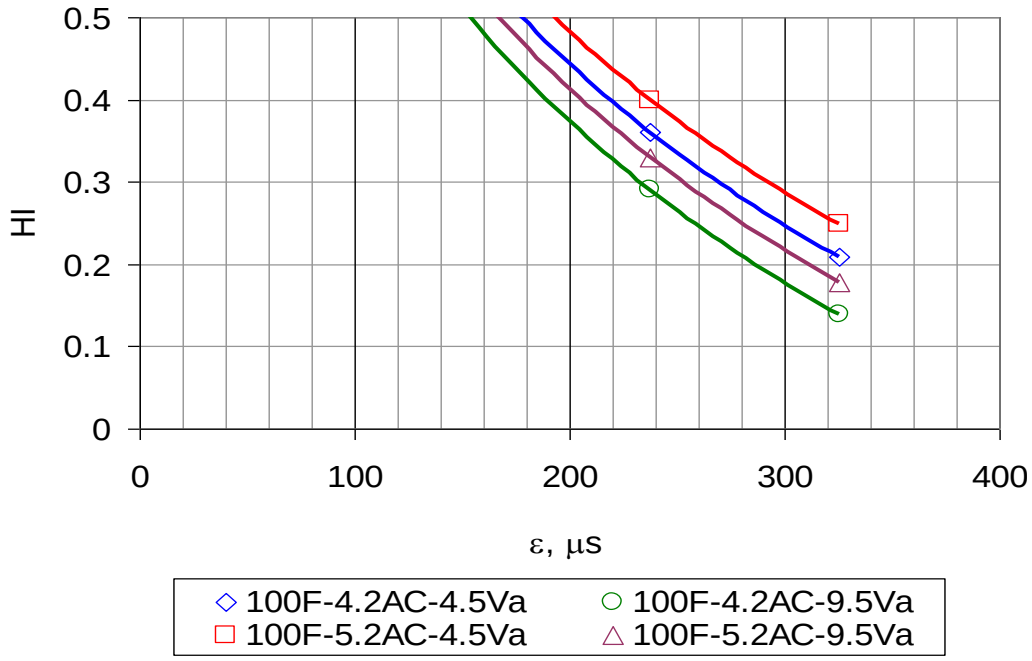


**Figure 59. Healing index versus strain levels for the PG 76-16 Mixture at 100 F.**

Figure 60 shows an example of the estimated endurance limits for all possible factor combinations based on the developed SR model at a 5-second rest period. The endurance limit ranged from 22 micro strains (at 40 F) to 264 micro strains (at 100 F). As expected, increasing the binder content increased the endurance limit, while increasing the air voids decreased the endurance limit. It was also noted that the endurance limit increases by increasing the temperature.

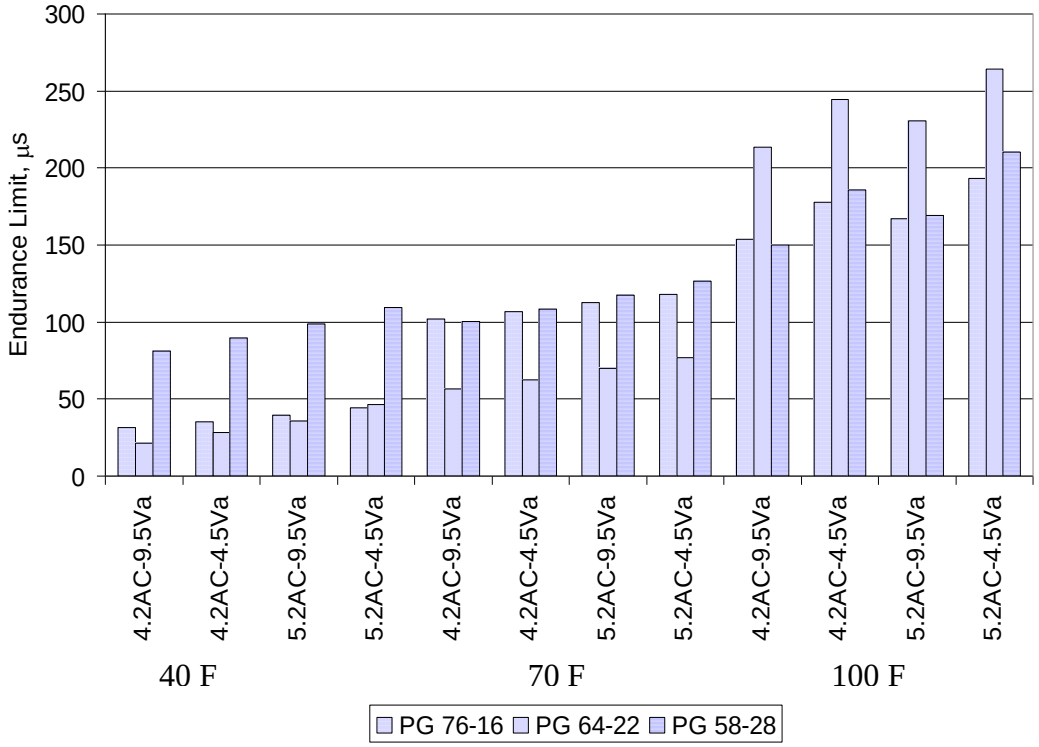


**Figure 60. Endurance limits for different factor combinations for a 5-second rest period using the first generation SR model.**

## 7.4 Second Generation Integrated Stiffness Ratio Model

### *7.4.1 Model Simplification Using Initial Stiffness*

Since the first generation integrated model developed in the previous section was extensive and contained many factor interactions, there was a need to further simplify it. Since binder content, air voids, binder type, and temperature affect stiffness, they were all replaced by the initial stiffness. This is a rather innovative approach that relates the endurance limit to a basic material property such as material stiffness together with the rest period that allows for healing.

### *7.4.2 Introducing Other Rest Periods and Strain Levels*

Since the first generation SR model was based on two levels of rest period and two levels of strain, the mathematical relationship between endurance limit and these two factors cannot incorporate nonlinearity. In section 7.3.3, a logarithmic function was arbitrarily used without good justification. If a linear relationship is assumed, increasing the rest period from 5 seconds to 10 seconds would double the endurance limit. This would contradict the results of previous studies as discussed in Chapter 2. Previous studies demonstrated that increasing the rest period above a certain optimum value would not add a significant gain in the HMA healing, which means no improvement would occur to the endurance limit value. In order to check the nature of the relationship between endurance limit, rest period and strain level, an additional study is performed. In this additional study two other rest periods levels and another strain level were introduced. Another objective of this additional study was to fill some of the missing cells in the main experiments that were not performed because of the use of a fractional factorial statistical design. This additional study allows for gaining more data points in developing the relationship between healing and endurance limit. It would also allow for compiling all the data together to have a regression model for the stiffness ratio that accounts for three strain levels and the four rest periods.

A design of experiment was used to randomly select the intended data points. The combined study considers the following factors:

- Binder type (3 levels: PG 58-28, PG 64-22, PG 76-16)

- Binder content (2 levels: optimum ± 0.5 %)
- Air void (2 levels: 4.5, 9.5 %)
- Strain level (3 levels: L, M, H)
- Temperature (3 levels: 40, 70, 100$^{o}$F)
- Rest period (4 levels: 0, 1, 5, 10 sec)

Table 27 shows the amount of testing performed in this part of the study, which includes:

1. 47 test combinations for the additional study to introduce new levels for rest period and strain level.
2. 43 test combinations for 0 second rest period to complete the missing cells from the main experiment.

**Table 27. Design of Experiment of the Additional Study***

| Temp, F | Strain Level, με | Rest Period, sec | PG 76-16 | | | | | | | | PG 64-22 | | | | | | | | PG 58-28 | | | | | | | |
|---|---|---|---|---|---|---|---|---|---|---|---|---|---|---|---|---|---|---|---|---|---|---|---|---|---|---|
| Binder Type | | | | | | | | | | | | | | | | | | | | | | | | | | |
| Binder Content, % | | | 4.2 | | | | 5.2 | | | | 4.2 | | | | 5.2 | | | | 4.2 | | | | 5.2 | | | |
| Air Voids, % | | | 4.5 | | 9.5 | | 4.5 | | 9.5 | | 4.5 | | 9.5 | | 4.5 | | 9.5 | | 4.5 | | 9.5 | | 4.5 | | 9.5 | |
| 40 | L | 0 | | | | | | | | | | | | | | | | | | | | | | | | |
| | | 1 | | | | | | | | | | | | | | | | | | | | | | | | |
| | | 5 | | | | | | | | | | | | | | | | | | | | | | | | |
| | | 10 | | | | | | | | | | | | | | | | | | | | | | | | |
| | M | 0| | | | | | | | | | | | | | | | | | | | | | | | |
| | | 1 | | | | | | | | | | | | | | | | | | | | | | | | |
| | | 5 | | | | | | | | | | | | | | | | | | | | | | | | |
| | | 10 | | | | | | | | | | | | | | | | | | | | | | | | |
| | H | 0 | | | | | | | | | | | | | | | | | | | | | | | | |
| | | 1 | | | | | | | | | | | | | | | | | | | | | | | | |
| | | 5 | | | | | | | | | | | | | | | | | | | | | | | | |
| | | 10 | | | | | | | | | | | | | | | | | | | | | | | | |
| 70 | L | 0 | | | | | | | | | | | | | | | | | | | | | | | | |
| | | 1 | | | | | | | | | | | | | | | | | | | | | | | | |
| | | 5 | | | | | | | | | | | | | | | | | | | | | | | | |
| | | 10 | | | | | | | | | | | | | | | | | | | | | | | | |
| | M | 0 | | | | | | | | | | | | | | | | | | | | | | | | |
| | | 1 | | | | | | | | | | | | | | | | | | | | | | | | |
| | | 5 | | | | | | | | | | | | | | | | | | | | | | | | |
| | | 10 | | | | | | | | | | | | | | | | | | | | | | | | |
| | H | 0 | | | | | | | | | | | | | | | | | | | | | | | | |
| | | 1 | | | | | | | | | | | | | | | | | | | | | | | | |
| | | 5 | | | | | | | | | | | | | | | | | | | | | | | | |
| | | 10 | | | | | | | | | | | | | | | | | | | | | | | | |
| 100 | L | 0 | | | | | | | | | | | | | | | | | | | | | | | | |
| | | 1 | | | | | | | | | | | | | | | | | | | | | | | | |
| | | 5 | | | | | | | | | | | | | | | | | | | | | | | | |
| | | 10 | | | | | | | | | | | | | | | | | | | | | | | | |
| | M | 0 | | | | | | | | | | | | | | | | | | | | | | | | |
| | | 1 | | | | | | | | | | | | | | | | | | | | | | | | |
| | | 5 | | | | | | | | | | | | | | | | | | | | | | | | |
| | | 10 | | | | | | | | | | | | | | | | | | | | | | | | |
| | H | 0 | | | | | | | | | | | | | | | | | | | | | | | | |
| | | 1 | | | | | | | | | | | | | | | | | | | | | | | | |
| | | 5 | | | | | | | | | | | | | | | | | | | | | | | | |
| | | 10 | | | | | | | | | | | | | | | | | | | | | | | | |

* Highlighted cells show additional tests performed.

One of the main issues regarding pursuing the additional study was the large amount of required tests. A statistical study using the PG 64-22 data points was performed to obtain the appropriate number of replicates for each test combination.

Statistical analysis was used to determine an appropriate number of replicates needed in the additional study. The stiffness ratios of the mixture were analyzed using the following factors: temperature, binder content, air voids, rest period, and strain. A statistical analysis was used (99) to determine the minimum number of replicates to maintain the required accuracy. The results concluded

that two replicates only for each test combination are needed to complete the additional study. Therefore, 180 tests (90 test combinations x 2 replicates) were conducted.

### *7.4.3 Developing Second Generation SR Model*

All the data from the main study (Section 7.3.2) and the additional study (Section 7.4.2) were combined in one master database that contained a total of 468 beam fatigue tests. The combined data were then used to build a simplified integrated stiffness ratio model that replaces four factors (binder type, binder content, air voids, and temperature) with the initial stiffness of the mixture, $E_o$. It also accounts for the nonlinear effects of rest period and the applied strain on the healing and endurance limit of the material.

Two main statistical software were utilized to build the regression model: STATISTICA and Excel. STATISTICA was used to come up with the best initial values for the coefficients. An optimization process was performed using Excel to minimize the sum of squared error followed by setting the sum of error equal to zero.

Several trials were made to determine the best mathematical form that relates the three independent variables (rest period, strain level, and stiffness) with SR. It was found that there is a need for a logarithmic transformation for both strain and stiffness values. It was also concluded that the best mathematical from to relate SR with rest period was the tangent hyperbolic (Tanh) function since it was noticed that there was no extra healing gained by applying 10 seconds rest

period compared to 5 seconds observed during the laboratory tests as shown in Figure 61. This also supports the literature that showed an optimum rest period beyond which no more healing is gained (see Figure 61).

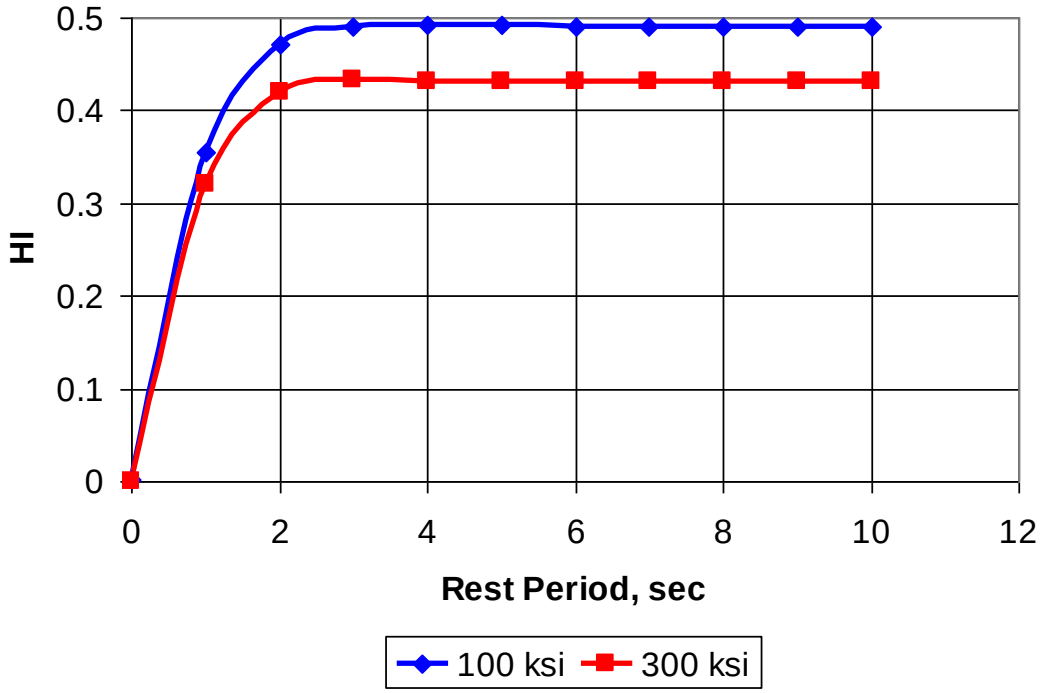


**Figure 61. Healing index versus rest period at two stiffness levels.**

Regression analysis was used to generate the second generation SR model that accounts for HMA stiffness and nonlinearity. The first trial was obtained with an $R^2$ value of 0.917. The model was further refined by removing the outlier data using the method suggested my Montgomery (99).

The analysis was then repeated based on the remaining 458 data points and the following second generation was obtained.

$$SR=0.6543-0.0594*\log(E_o)-0.00640*\log(\varepsilon)+2.0263*\tanh(0.7718*RP)$$
$$+0.0250*\log(E_o)*\log(\varepsilon)-0.1260*\log(E_o)*\tanh(0.6603*RP)-$$
$$0.5915*Log(\varepsilon)*\tanh(0.7446*RP) \quad (35)$$

Using this model, the $R^2$ improved from 0.917 to 0.933 and the skewness of the data was significantly reduced. Figure 62 shows predicted versus measured SR after removing the outliers.

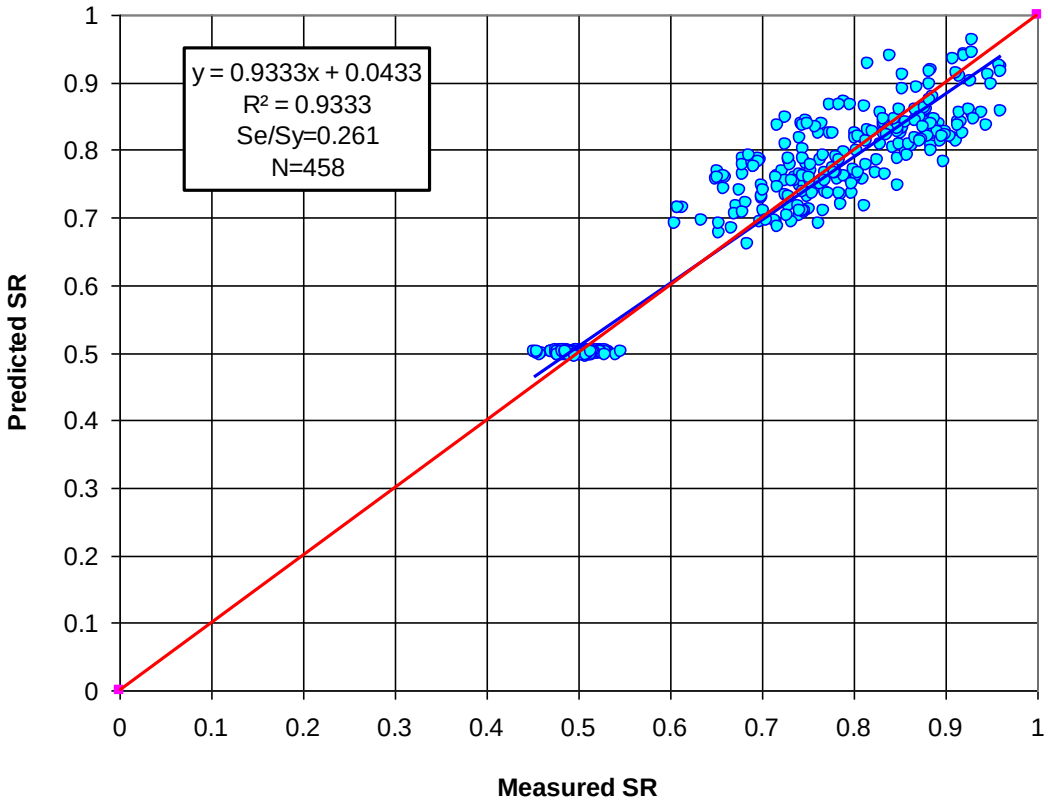


**Figure 62. Measured versus predicted SR for the second generation model.**

Figure 63 to Figure 67 demonstrate the SR versus strain at several rest periods. Similar to the first generation model discussed in Section 7.3.2, the

endurance limit occurs when complete healing happens during the rest period when the stiffness ratio is 1.0.

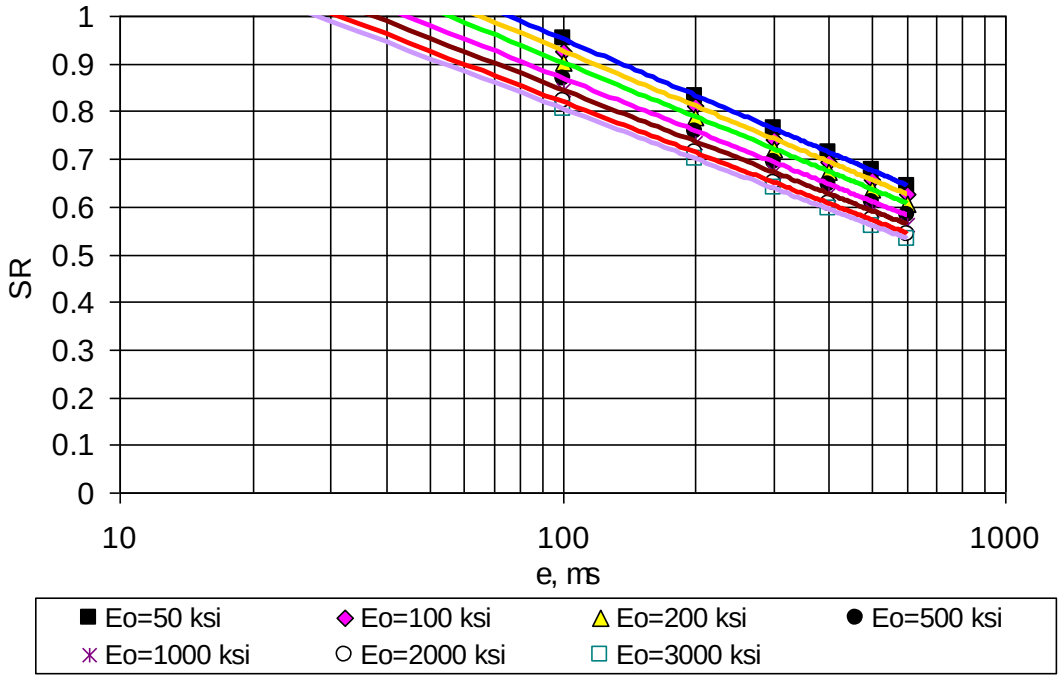


**Figure 63. SR vs. strain for several initial stiffness values and 1 second rest period.**

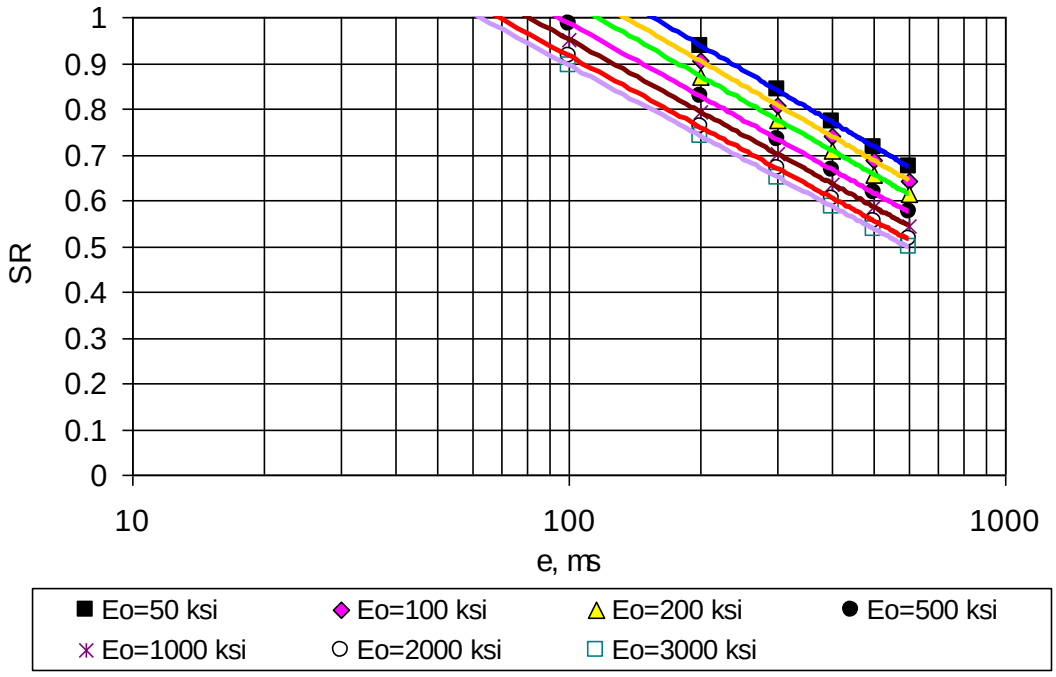


**Figure 64. SR vs. strain for several initial stiffness values and 2 second rest period.**

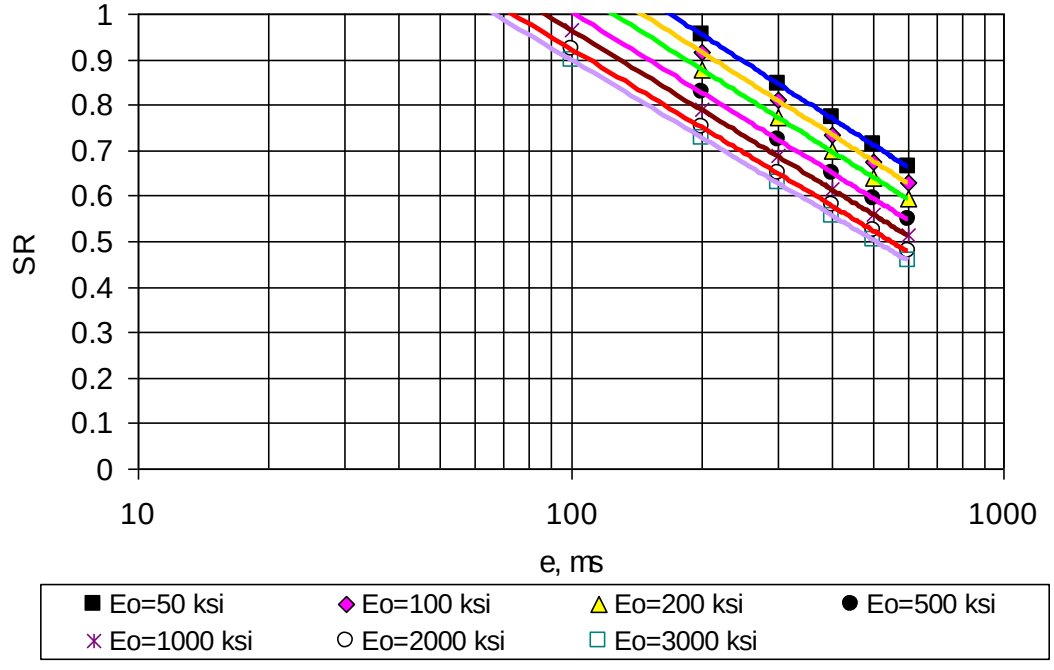


**Figure 65. SR vs. strain for several initial stiffness values and 5 second rest period.**

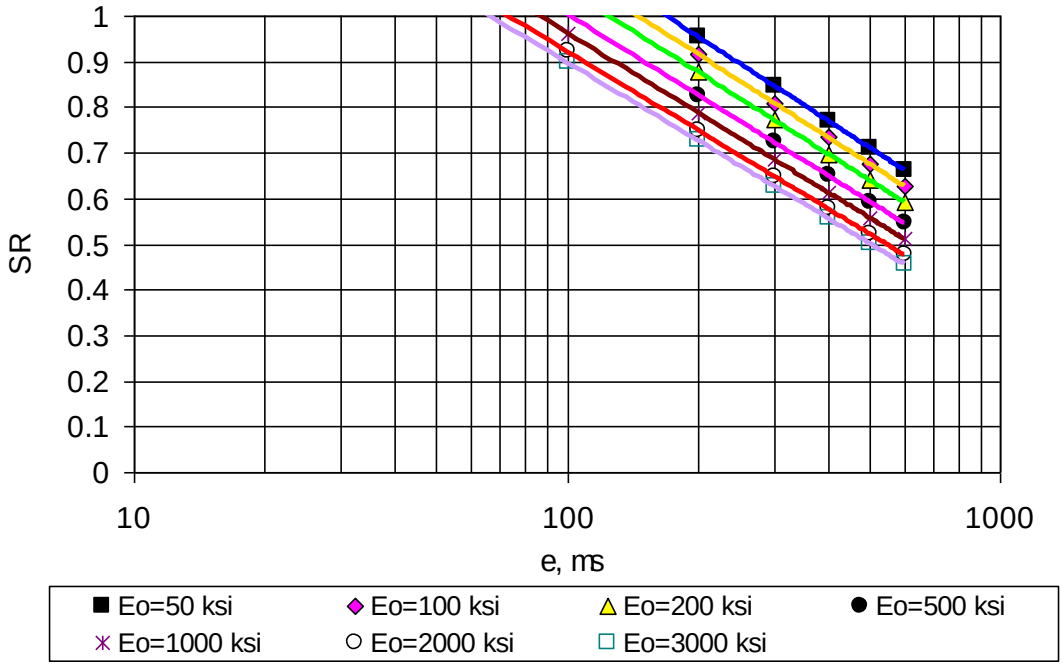


**Figure 66. SR vs. strain for several initial stiffness values and 10 second rest period.**

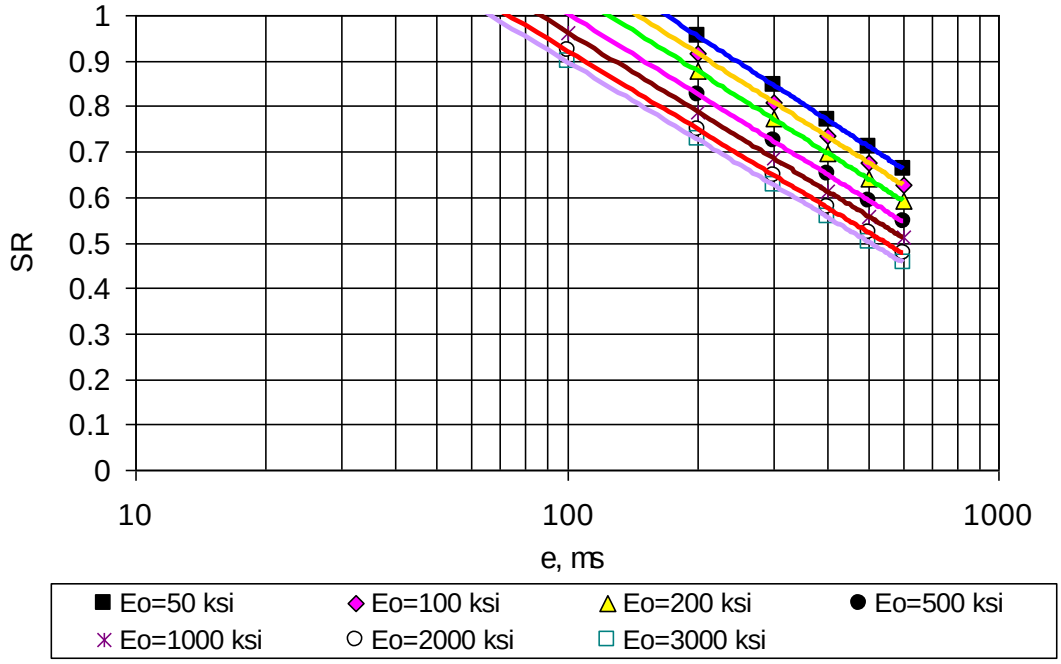


**Figure 67. SR vs. strain for several initial stiffness values and 20 second rest period.**

Figure 68 illustrates the summary of the endurance limit values for several rest periods and stiffness values. The endurance limit values ranged from 30 micro strains (1 seconds rest period and 3,000 ksi stiffness) to 170 micro strains (5 seconds and 50 ksi stiffness). It was noticed that the endurance limit values at 5 seconds were the same as 10 and 20 seconds. This indicates that no more improvement on endurance limit occurs beyond 5 seconds. In addition, the endurance limit increases by decreasing the stiffness of the mixture. In other words, softer mixtures allow for larger strains to be applied without causing fatigue damage to the HMA layer. The value of the allowed strain that does not cause fatigue damage increases as the rest period between load applications increases up to 5 seconds.

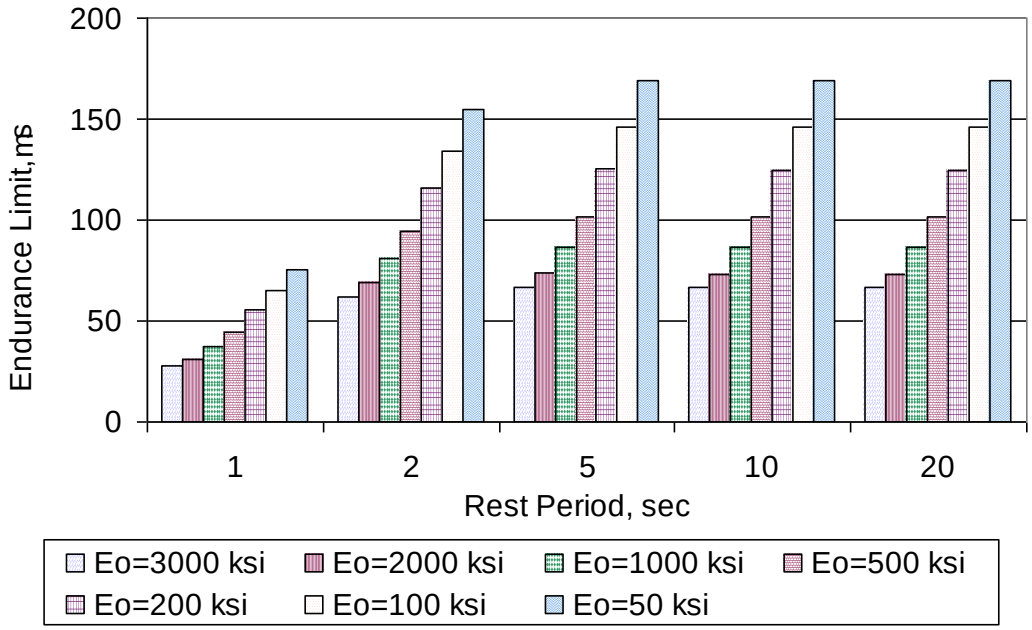


**Figure 68. Summary of endurance limit values for several rest periods and stiffness values (based on second generation SR model).**

## 7.5 Third Generation Integrated Stiffness Ratio Model

The data points of the second generation SR model discussed in Section 7.4.3 were collected at $N_{f\ w/o\ RP}$. Since the applied strain was pre-selected to reach failure for the test without rest period at a certain value of number of cycles ($N_{f\ w/o\ RP}$) as discussed in Section 7.3.1, the strain and $N_{f\ w/o\ RP}$ were highly correlated. This issue resulted in removing either strain or $N_{f\ w/o\ RP}$ from the second generation model since these two factors are co-linear. In order to include N in the third generation model, SR data were collected at three different locations along the SR-N relationship for each test in order to remove the statistical co-linearity between strain and N. Figure 69 shows the typical SR-N relationships for the tests with and without rest period and the locations where data points were selected. For each curve, two of the points were taken during the test, while the third point was taken at $N_{f\ w/o\ RP}$. Note that the test results with rest period are extrapolated to $N_{f\ w/o\ RP}$ as discussed in Chapter 7.

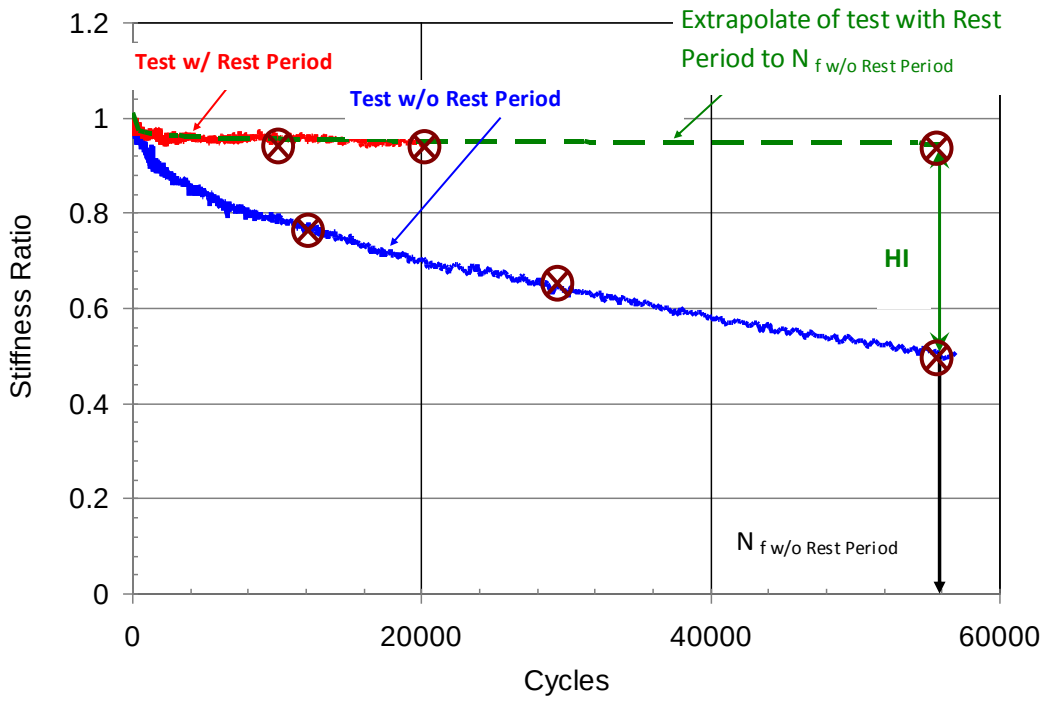


**Figure 69. Selection of data point locations.**

In this third generation, a total of 1,404 data points were used (468 tests x 3 data points/test) to build the model. The $R^2$ value of the developed model was 0.893. A statistical analysis (127) was then used to remove the outliers in order to improve the accuracy of the model. Consequently, 12 data points were excluded from the analysis, which increased the $R^2$ value from 0.893 to 0.904. Figure 70 shows predicted versus measured SR after removing the outliers.

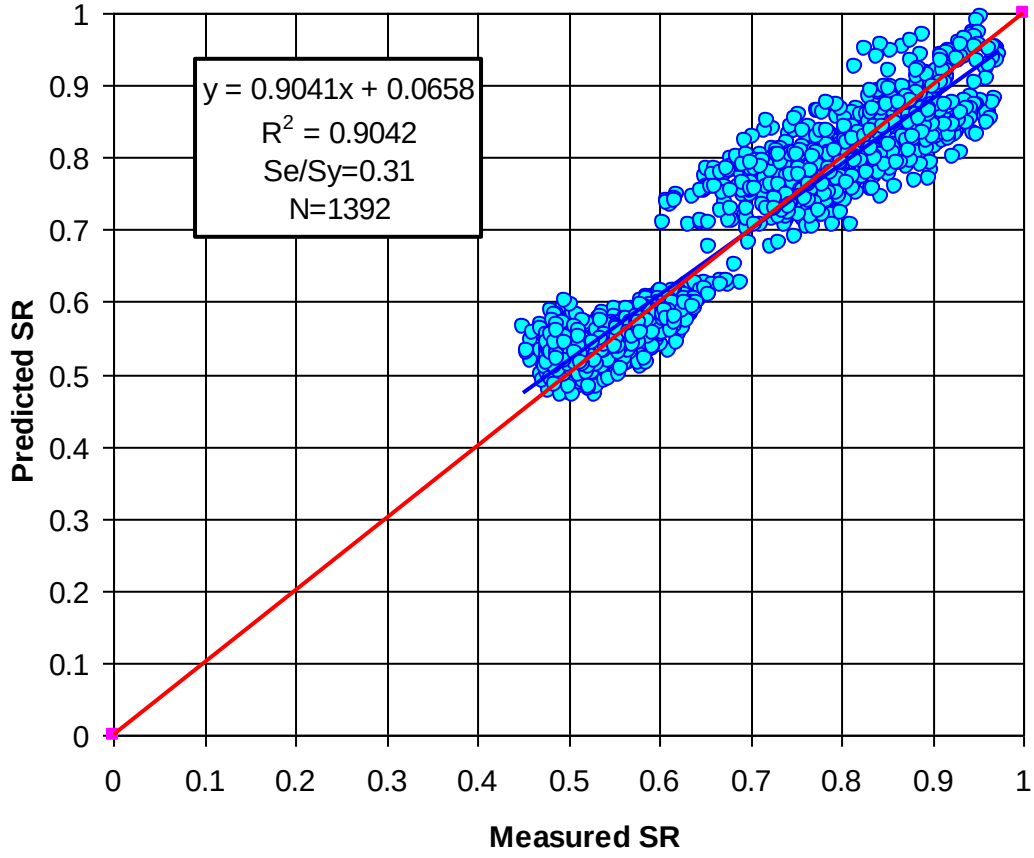


**Figure 70. Measured versus predicted SR for the third generation SR Model after removing data outliers.**

The third generation integrated stiffness ratio model after removing the outliers is shown below.

$$SR=1.7897-0.1361*\log(E_o)-0.3258*\log(\varepsilon)-0.1299*\log(N)+1.4104*\tanh(0.8470*RP)+0.0302*\log(E_o)*\log(\varepsilon)-0.0953*\log(E_o)*\tanh(0.7153*RP)-0.4747*\log(\varepsilon)*\tanh(0.6965*RP)+0.0044*\log(N)*\log(E_o)+0.0212*\log(N)*\log(\varepsilon)+0.59*\log(N)*\tanh(0.2671*RP) \quad (36)$$

By substituting the stiffness ratio with 1.0 (no damage condition), the endurance limit can be predicted for different values of $E_o$, RP.

### *7.5.1 Effect of N on Endurance Limit*

After N was included in the model, it was important to know the effect of changing the value of N on the endurance limit. A sensitivity analysis study was performed, where SR was plotted versus strain and rest period for different $E_o$ values and three levels of N (20,000, 100,000, 200,000 cycles).

Based on Figures 71 and 72, the number of loading cycles has little of no effect on the SR value for tests with rest period, especially at large values of N. Since the endurance limit is obtained at a SR value of 1.0, the number of loading cycles also has little or no effect on the endurance limit. As a result, the endurance limit was calculated at a conservative value of 200,000 cycles in the rest of the study.

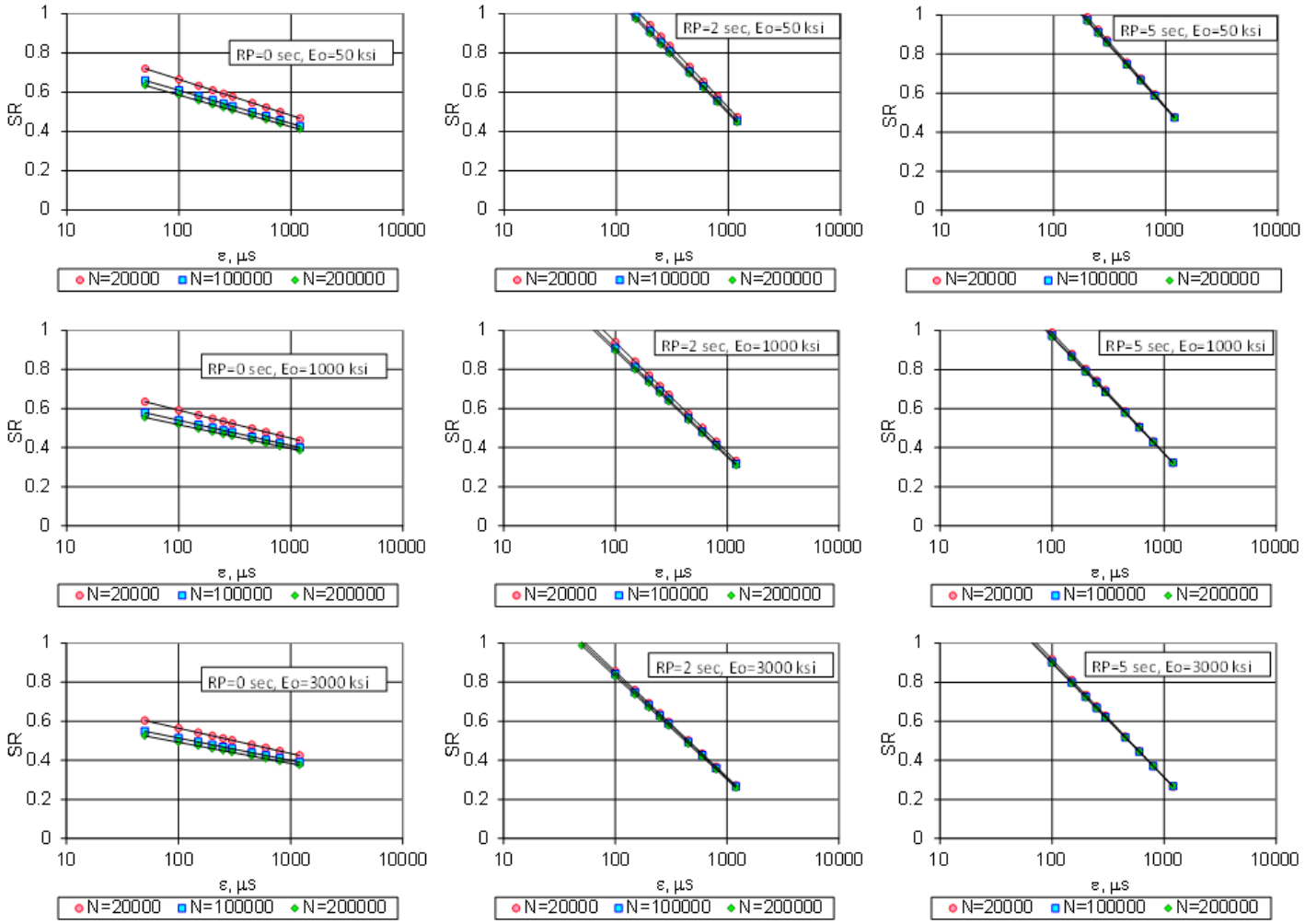


**Figure 71. SR vs. ε at different values of rest period, stiffness and N.**

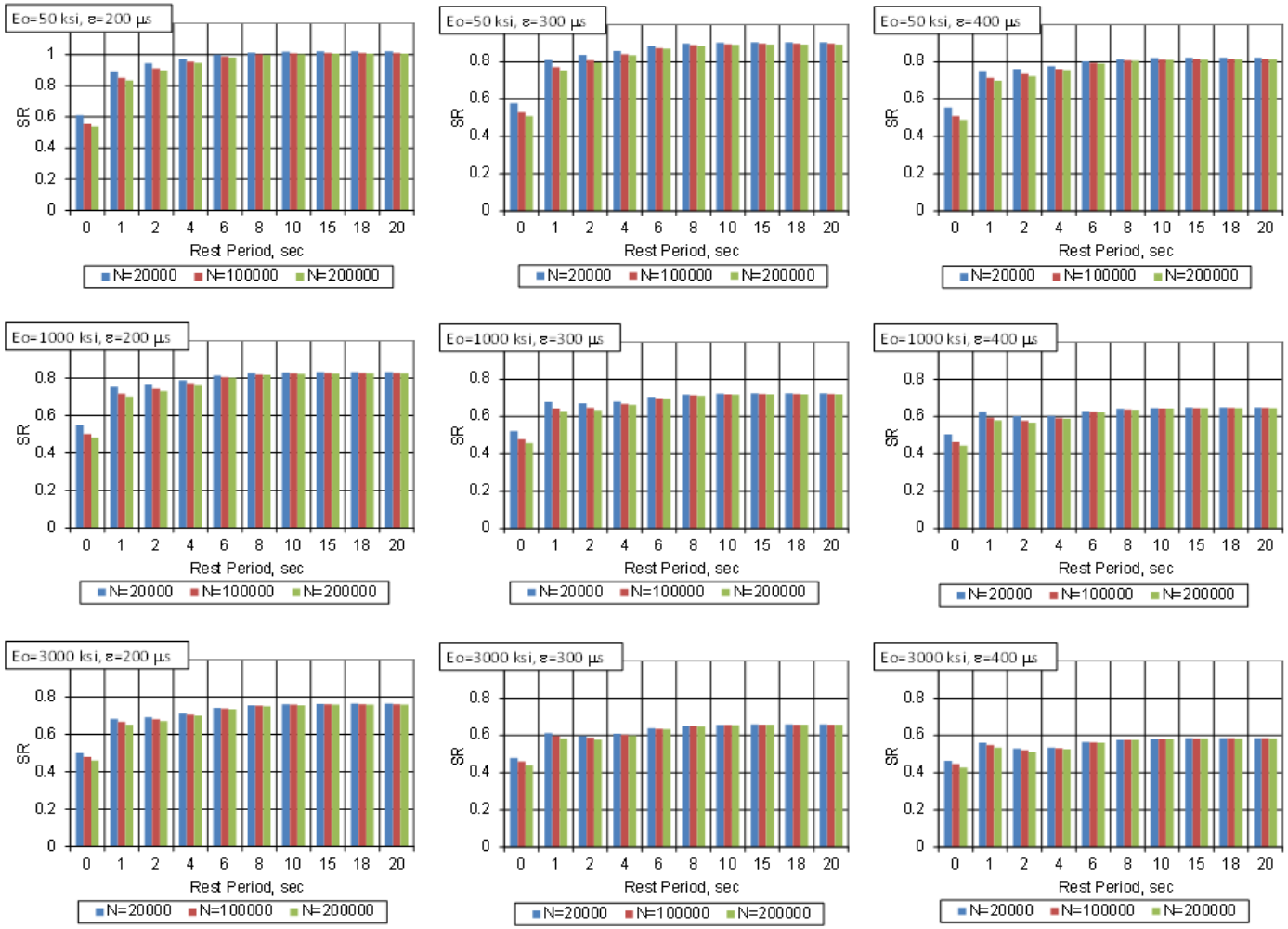


**Figure 72. SR vs. rest period at different values of strain, stiffness and N.**

### *7.5.2 Predicting Endurance Limit using Third Generation SR Model*

Figure 73 to Figure 77 demonstrate stiffness ratio versus strain level at several rest periods. The endurance limit occurs when complete healing happens during the rest period at an SR value of 1.0.

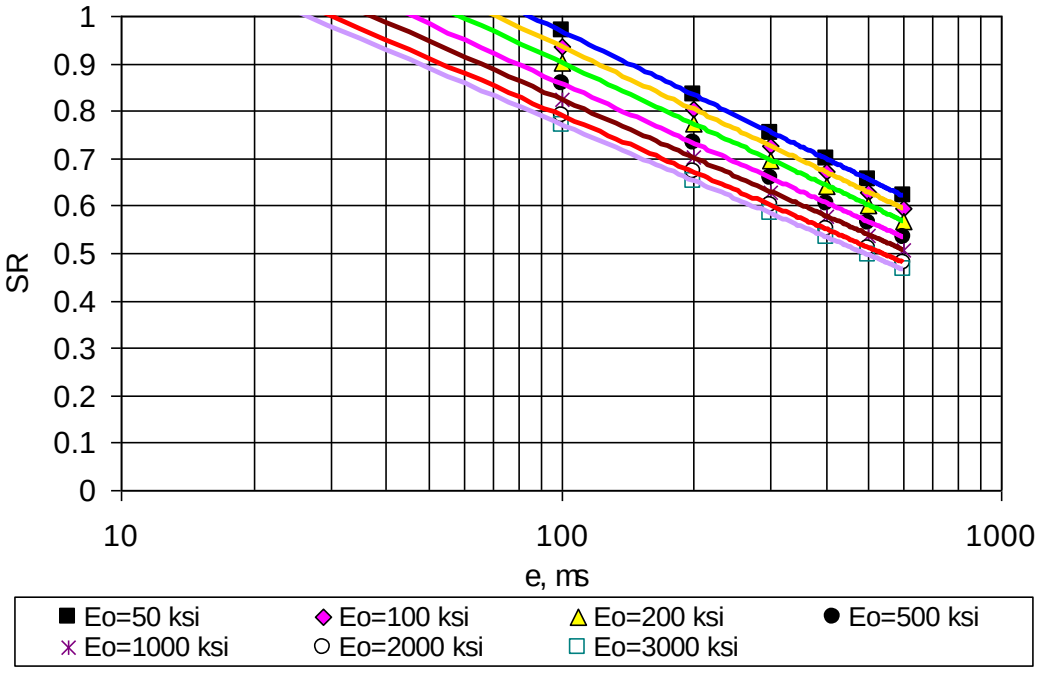


**Figure 73. Strain versus SR for several initial stiffness values (RP = 1 sec, N=200,000 cycles).**

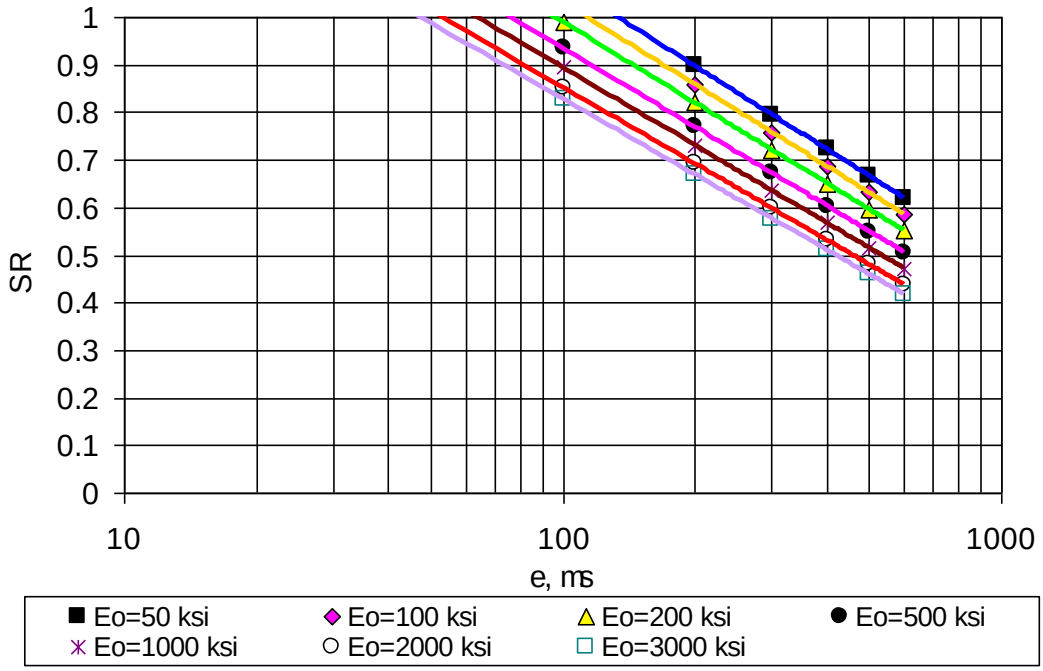


**Figure 74. Strain versus SR for several initial stiffness values (RP = 2 sec, N=200,000 cycles).**

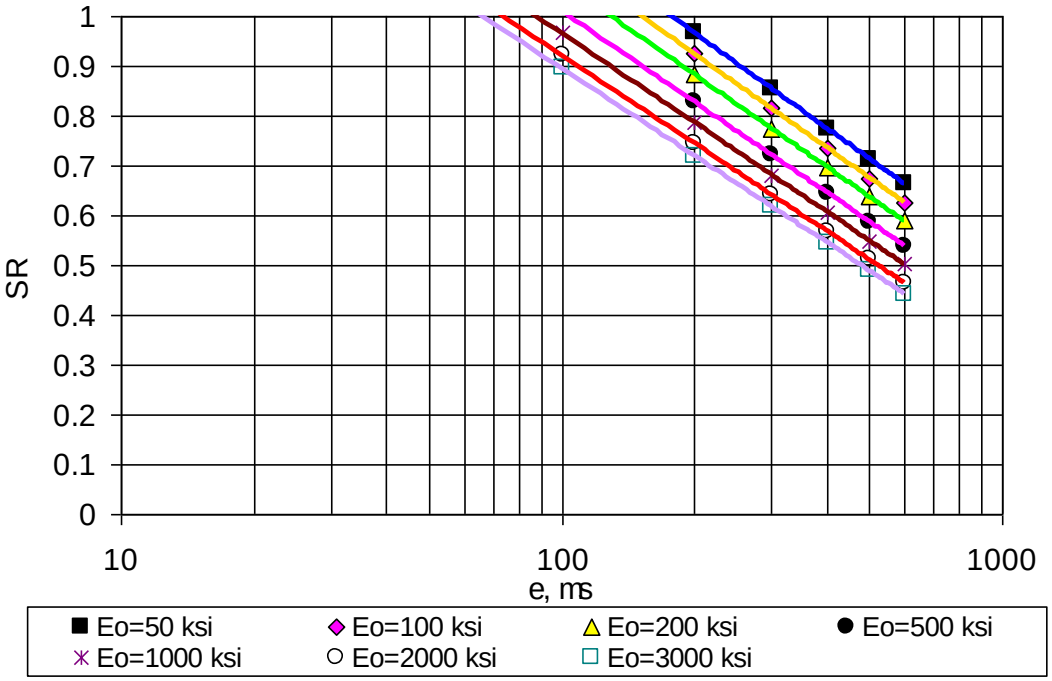


**Figure 75. Strain versus SR for several initial stiffness values (RP = 5 sec, N=200,000 cycles).**

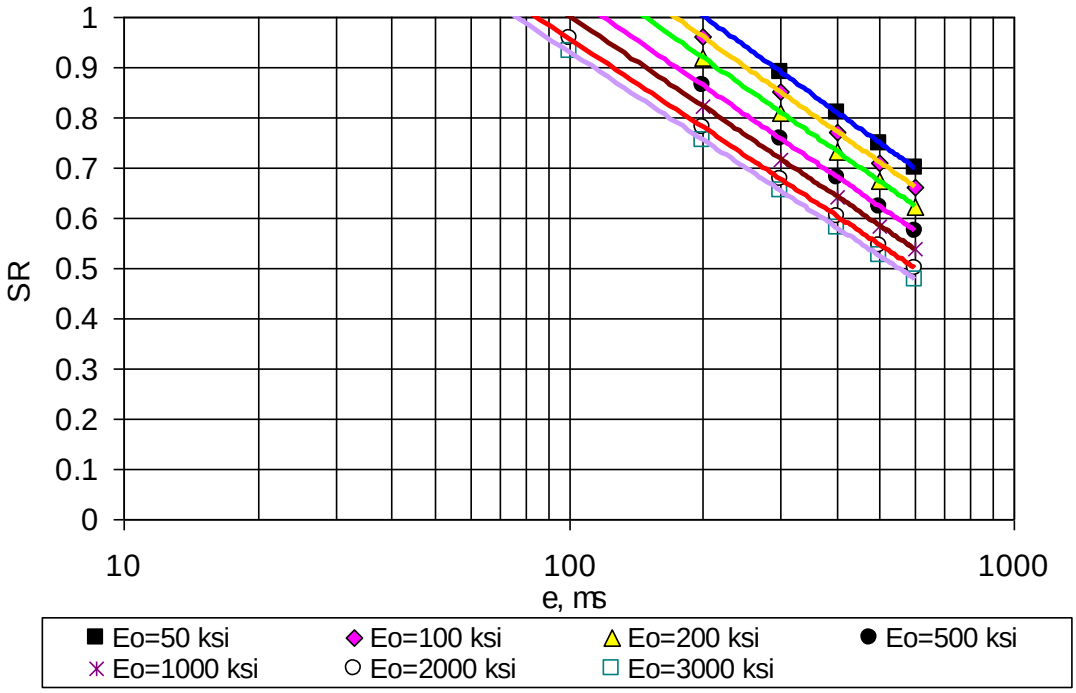


**Figure 76. Strain versus SR for several initial stiffness values (RP = 10 sec, N=200,000 cycles).**

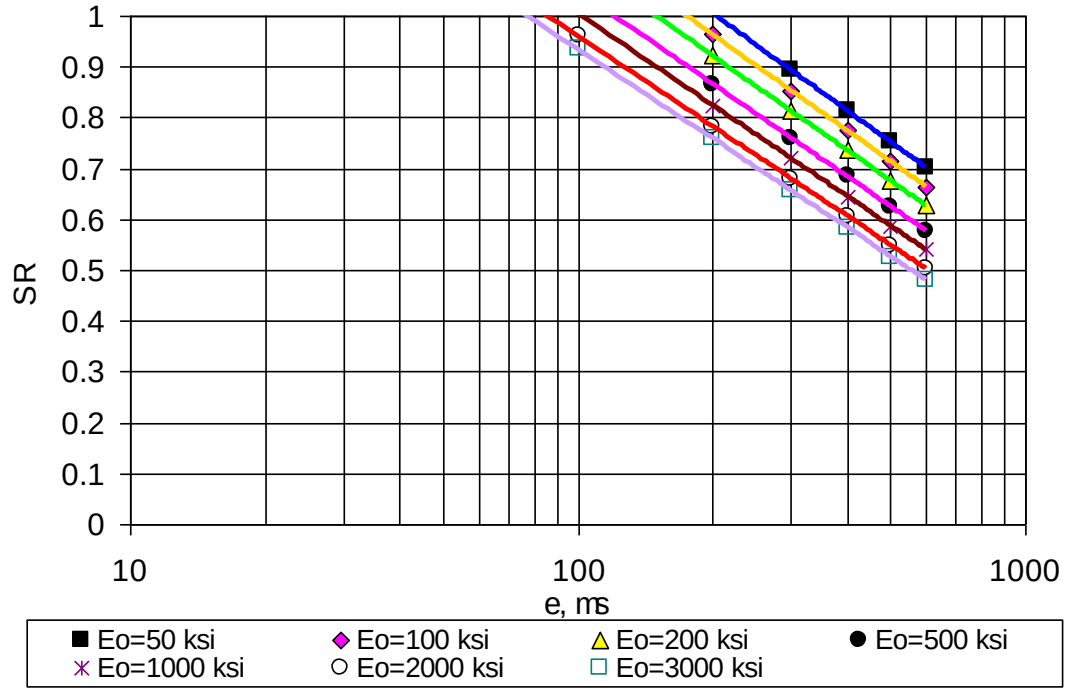


**Figure 77. Strain versus SR for several initial stiffness values (RP = 20 sec, N=200,000 cycles).**

Figure 78 illustrates the summary of the endurance limit values for several rest periods and stiffness levels. The endurance limit values ranged from 26 micro strains (1 seconds rest period and 3,000 ksi stiffness) to 204 micro strains (20 seconds and 50 ksi stiffness). It was noticed that the endurance limit values at rest periods of 10 and 20 seconds were the same. This indicates that no more improvement on endurance limit occurs beyond 10 seconds.

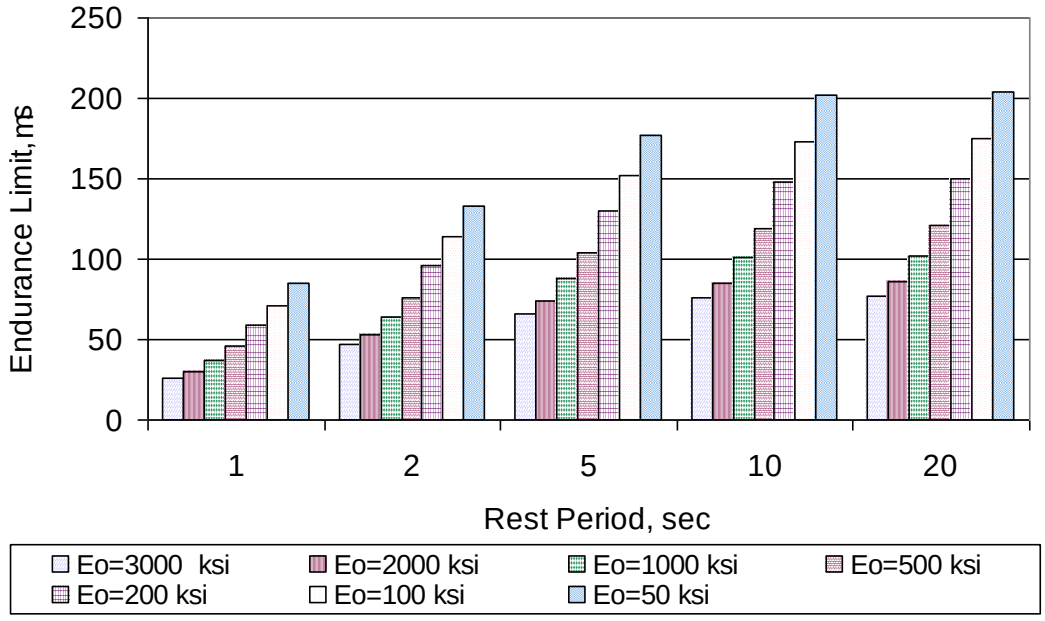


**Figure 78. Summary of endurance limit values versus several rest periods and stiffness values (based on third generation SR model).**

### *7.5.3 Comparison between Endurance Limits of Second and Third Generation Models*

After developing the third generation model, it was important to compare the predicted endurance limit values between this model and the second generation

model developed in Section 7.4.3 because of their similarities. Table 28 shows a comparison between predicted endurance limit values using the two models at several values of rest period and stiffness. The table shows that the percent difference between the endurance limits of the second and third models ranges from -20% – 24%. It can be concluded that both models produce comparable endurance limit results.

**Table 28. Predeicted Endurance Limit Values using the Second and Third Generation SR models.**

| Rest Period, Sec | Stiffness, ksi | Predicted EL, μs | | Percent Difference* |
|---|---|---|---|---|
| | | Second Generation | Third Generation | |
| 1 | 3,000 | 26 | 28 | 7 |
| 1 | 2,000 | 30 | 31 | 3 |
| 1 | 1,000 | 37 | 37 | 0 |
| 1 | 500 | 46 | 44 | -5 |
| 1 | 200 | 59 | 55 | -7 |
| 1 | 100 | 71 | 65 | -9 |
| 1 | 50 | 85 | 76 | -12 |
| 2 | 3,000 | 47 | 62 | 24 |
| 2 | 2,000 | 53 | 69 | 23 |
| 2 | 1,000 | 64 | 81 | 21 |
| 2 | 500 | 76 | 95 | 20 |
| 2 | 200 | 96 | 116 | 17 |
| 2 | 100 | 114 | 134 | 15 |
| 2 | 50 | 133 | 155 | 14 |
| 5 | 3,000 | 66 | 67 | 1 |
| 5 | 2,000 | 74 | 73 | -1 |
| 5 | 1,000 | 88 | 87 | -1 |
| 5 | 500 | 104 | 102 | -2 |
| 5 | 200 | 130 | 125 | -4 |
| 5 | 100 | 152 | 146 | -4 |
| 5 | 50 | 177 | 169 | -5 |
| 10 | 3,000 | 76 | 66 | -15 |
| 10 | 2,000 | 85 | 73 | -16 |
| 10 | 1,000 | 101 | 86 | -17 |
| 10 | 500 | 119 | 102 | -17 |
| 10 | 200 | 148 | 125 | -18 |
| 10 | 100 | 173 | 146 | -18 |
| 10 | 50 | 202 | 169 | -20 |
| 20 | 3,000 | 77 | 66 | -17 |
| 20 | 2,000 | 86 | 73 | -18 |
| 20 | 1,000 | 102 | 86 | -19 |
| 20 | 500 | 121 | 102 | -19 |
| 20 | 200 | 150 | 125 | -20 |
| 20 | 100 | 175 | 146 | -20 |
| 20 | 50 | 204 | 169 | -21 |

*Percent Difference = 100 * ($EL_{3rd\ gen} - EL_{2nd\ gen}$) / $EL_{3rd\ ge}$

# CHAPTER 8 INCORPORATING ENDURANCE LIMIT IN THE MEPDG

After developing the third generation stiffness ratio model (Equation 36), the following step was to incorporate the predicted endurance limit values in the strain-$N_f$ fatigue relationships in the MEPDG software.

## *8.1 Incorporating Endurance Limit in Strain-$N_f$ Fatigue Relationships*

The developed third generation model (Equation 36) follows the following form:

$$SR = f(E_o, \varepsilon, N, RP) \quad (37)$$

where,

SR = Stiffness ratio = 1 – Damage Level

$E_o$ = Initial flexural stiffness

$\varepsilon$ = Applied strain

N = Number of loading cycles to reach a certain level of damage

PR = Rest period

One of the main advantages of this model over the second generation model is its ability to predict N at any level of damage. The number of loading cycles required to reach failure ($N_f$), assuming that failure occurs at 50% damage, can be achieved by substituting the stiffness ratio with 0.5 in this model. In this part of the study, the third generation model was used to calculate the values of Nf for different values of flexural stiffness, applied strain, and rest period as illustrated in the left side of Figures 79-81.

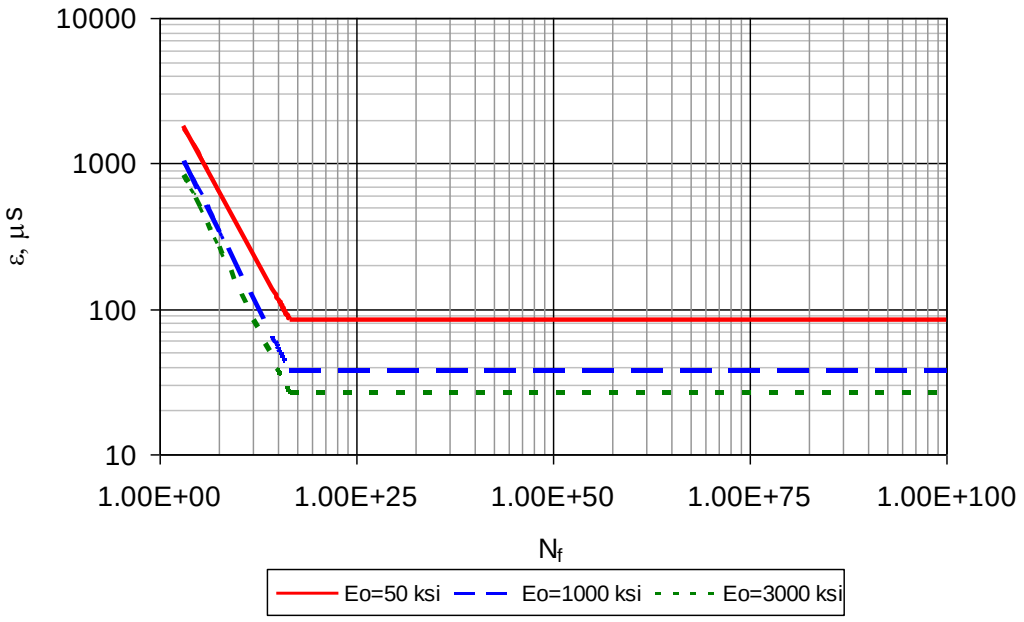


**Figure 79. ε-$N_f$ relationship for different stiffness values based on third generation SR model (1 sec RP).**

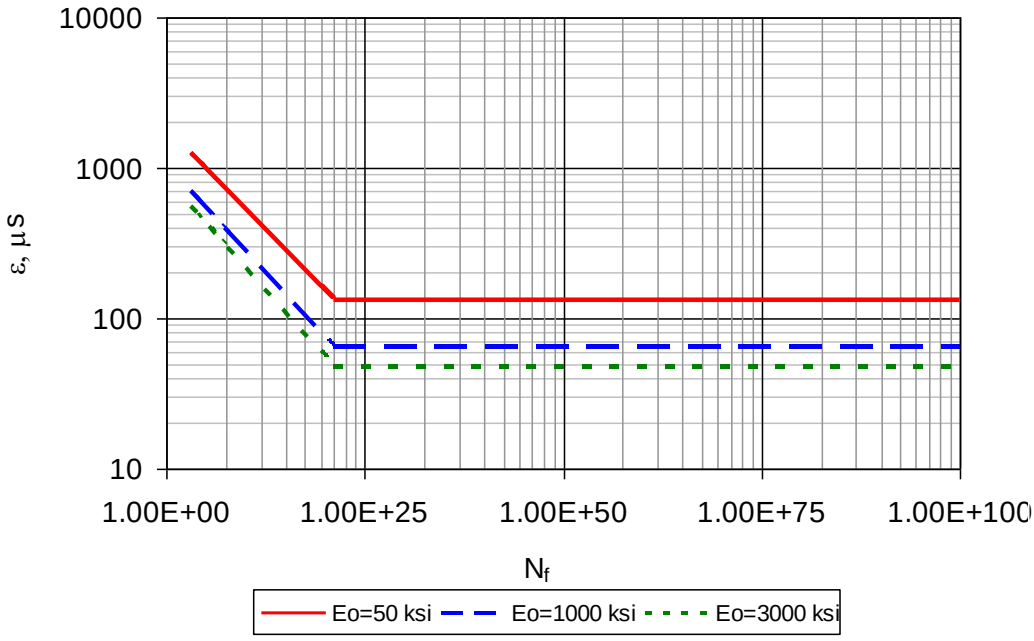


**Figure 80. ε-$N_f$ relationship for different stiffness values based on third generation SR model (2 sec RP).**

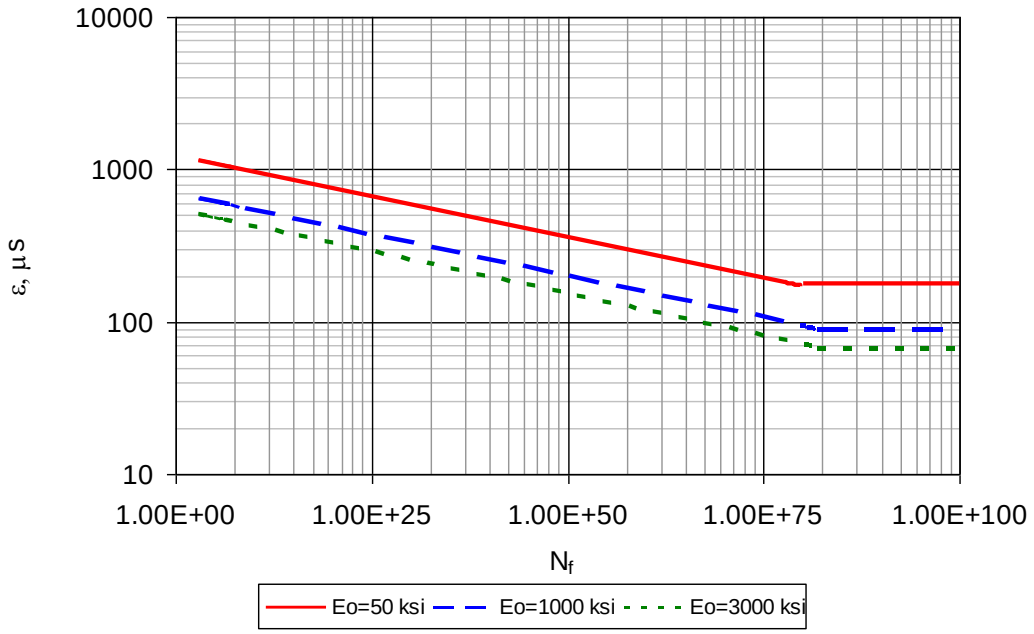


**Figure 81. ε-Nf relationship for different stiffness values based on third generation SR model (5 sec RP).**

Table 29 shows the developed $K_1$, $K_2$, $K_3$ coefficients for 1, 2, and 5 seconds rest periods, respectively, obtained by substituting SR of 0.5 and the appropriate values of RP in Equation 36. It is noticed that the $K_2$ value increases by increasing the rest period. This indicates that introducing a rest period between loading cycles allows the HMA to heal, which allows much higher number of cycles to fail the HMA layer compared to the case of not applying a rest period. Note that the $K_1$, $K_2$, $K_3$ values are different than the traditional values because of the incorporation of the rest period between loading cycles.

**Table 29. $K_1$, $K_2$, $K_3$ Fatigue Model Coeffecients Obtained from the Third Generation Model.**

| Rest Period | $K_1$ | $K_2$ | $K_3$ |
|---|---|---|---|
| 1 | 8.14E-09 | 7.093 | 1.511 |
| 2 | 7.87E-22 | 12.959 | 2.654 |
| 5 | 1.46E-22 | 13.520 | 2.684 |

The third general model (Equation 36) can also be used to determine the endurance limit, which is the strain at a combination of the following parameters:

1. Flexural stiffness.
2. A stiffness ratio of 1.0, indicating no damage.
3. Number of loading cycles. The discussion in Chapter 7 indicates that the endurance limit is not affected by the number of cycles, especially if the number of cycles is large.
4. Rest period.

The endurance limit was then calculated to for different conditions and added to the $\varepsilon$-$N_f$ relationships shown in Figures 79-81. This means that the $\varepsilon$-$N_f$ curves cannot be extended to very low strain values, but need to stop once the endurance limit is reached. Thus, if the applied strain is below the endurance limit, no fatigue damage will occur. Figures 79-81 show that the endurance limit is between 28-76 micro strains for a 1 second rest period and increases to 62-155 micro strains at 2 second rest period and 67-169 micro strains at 5 second rest period. This means that increasing the spacing between trucks allows for more

healing and, therefore, larger truck loads that can be accommodated without fatigue damage.

## *8.2 Incorporating Endurance Limit in the MEPDG*

The current MEPDG software (DARWIN-ME) requires the designer to input the following design parameters related to fatigue performance.

1. $K_1$, $K_2$, $K_3$ coefficients
2. A single value of endurance limit.

In this NCHRP study, the rest period between loading cycles was introduced, which matches the real traffic loads in the field. Section 8.1 shows that both the set of $K_1$, $K_2$, $K_3$ coefficients and the endurance limit value vary depending on the rest period between loading cycles. In the MEPDG software, a simulation is performed every two hours during the pavement service life. Therefore, the incorporation of the endurance limit into the MEPDG software requires additional software that calculates the $K_1$, $K_2$, $K_3$ coefficients and endurance limit values for the rest period associated with each 2-hour MEPDG simulation and feeds them into the MEPDG software during the analysis process.

The parameters that are needed in the proposed software are discussed below.

### *Rest Period (RP)*

The rest period is a function of the average annual daily truck traffic (AADTT) during the 2-hour simulation period. The rest period between truck axles in

seconds is calculated as an average value every two hours of MEPDG simulation. This would require the calculation of the actual truck spectrum for the hours of the day as shown in Figure 82 and dividing the day to 2-hour increments.

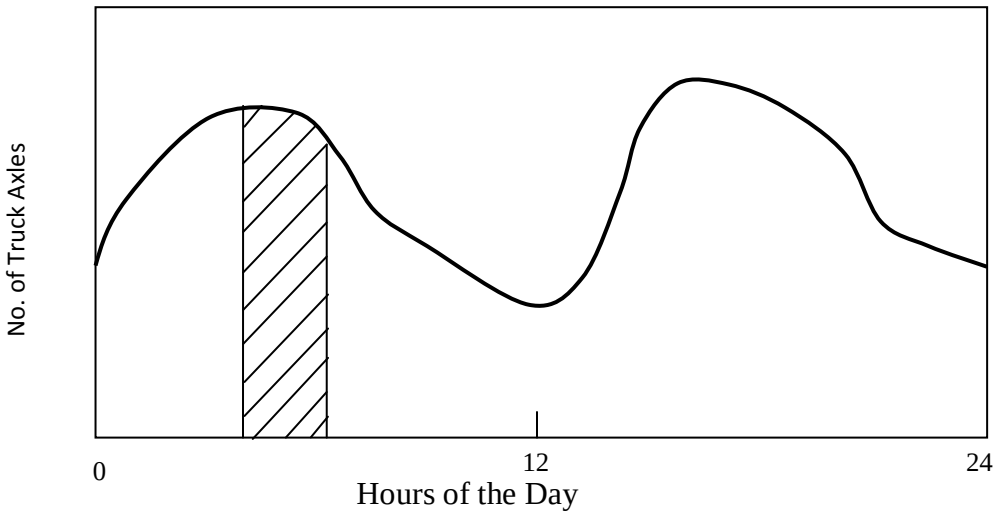


**Figure 82. Example of truck axle distribution during the 24 hours of the day.**

The RP value (in seconds) in this case can be calculated as follows:

$$RP = 3{,}600 \times 2 / \sum(N_T * N_A) \quad (39)$$

where,

$N_T$ = Number of trucks in the 2-hour increment considered in the analysis

$N_A$ = Average number of axles in each truck

***$K_1$, $K_2$, $K_3$ coefficients***

Using the third generation model (Equation 36), the number of cycles to failure ($N_f$) can be obtained every 2-hour simulation period by substituting the stiffness

ratio with 0.5 (50% damage) for different values of flexural stiffness ($E_o$), applied strain ($\varepsilon$), and rest period (RP). The $E_o$ value is calculated from the dynamic modulus value used in the MEPDG software. The strain versus $N_f$ data points are then generated and fed to a statistical package (for example Statistica) in order to run a nonlinear estimation to estimate the $K_1$, $K_2$, $K_3$ coefficients.

***Endurance Limit***

Similarly, the endurance limit can be obtained every 2-hour of MEPDG simulation using the third general model (Equation 36) for a stiffness ratio of 1.0 (no fatigue damage) and a large value of N such as 200,000 cycles.

***Calculating Fatigue Damage***

The fatigue damage is then calculated every two hours during MEPDG simulation. The model used for the calculation of the fatigue damage in the MEPDG is as follows:

$$N_f = C \times K_1 (1/\varepsilon_t)^{K_2} (1/E_o)^{K_3} \quad (40)$$

where:

$N_f$ = Number of repetitions to reach fatigue failure

$\varepsilon_t$ = Strain at the critical location

$E_o$ = Flexure stiffness of the HMA

$K_1$, $K_2$, $K_3$ = Laboratory fatigue coefficients

C = Laboratory to field adjustment factor

The MEPDG software divides the HMA layer into sublayers. The JULEA program then calculates the critical tensile strain every two hours. The estimation of the fatigue damage in the MEPDG software is based on Miner's law given by the following Equation.

$$D_{i=1-T} = \Sigma (n_i / N_i) \quad (41)$$

where:

$D_{i=1-T}$ = Cumulative damage for periods 1 through T

T = Total number of periods

$n_i$ = Actual traffic for period i

$N_i$ = Traffic allowed under conditions prevailing in period i

The endurance limit is calculated every two hours as discussed before. At the same time, the critical strain value of the HMA layer (or sublayer) for each truck axle for this period is calculated using the JULEA program. If the critical strain calculated from the JULEA program is less than the fatigue endurance limit, the axle should not be counted in the analysis for this period, which means that there is no fatigue damage caused by this axle. However, if the critical strain is greater than the fatigue endurance limit, the axle is counted as causing fatigue damage during this period.

# Chapter 9 SUMMARY, CONCLUSIONS, AND RECOMMENDATIONS FOR FURTHER RESEARCH

## 9.1 Summary

Building perpetual pavements has been one of goals of the highway community for many years. The concept of perpetual pavement requires the knowledge of the endurance limit of hot-mix asphalt. The main purpose of this study was to validate the endurance limit for HMA using laboratory beam fatigue tests with rest periods between loading cycles. A comprehensive study was performed to estimate the endurance limit of typical HMA due to healing that occurs during the rest periods. Six main factors were selected for evaluation: binder type, binder content, air voids, test temperature, duration of the rest period between loading cycles, and strain level. A 6-factor fractional factorial statistical design was used in order to reduce the number of tests and still obtain the necessary results.

The binder and aggregate used in this study were characterized by a local commercial laboratory followed by a Superpave mix design. Before testing, the two beam fatigue machines were calibrated and several QA/QC studies were performed to insure comparable test results and to verify the proper testing conditions. Both beam fatigue machines produced statistically same results.

Extensive laboratory displacement-controlled flexure fatigue tests were performed according to AASHTO T321-03 test procedure. Hot mix asphalt was used with 3 unmodified binder types, 2 binder contents, 2 levels of air void, 3 levels of applied strain, 3 test temperatures and 4 values of rest periods between

loading cycles. The stiffness ratio was obtained for different conditions and the healing index was determined. The results were statistically analyzed and the endurance limits were obtained at a stiffness ratio value of 1.0. The study assumes that the endurance limit is obtained due to healing that occurs during the rest period between loading cycles. Three rational predictive model generations were developed that can predict the stiffness ratio at various test conditions which can be related to the healing gained during the rest period. The strain level that allows for complete healing was obtained to estimate the endurance limit below which a very large number of load repetitions can be applied to the pavement without fatigue damage.

After developing the third generation stiffness ratio model, the predicted endurance limit values were integrated in the strain-$N_f$ fatigue relationships as a step toward incorporating the endurance limit in the MEPDG software.

**9.2 Conclusions**

The following are the conclusions drawn from the three stiffness ratio model generations developed in this study.

1. HMA exhibits endurance limit that varies with mixture properties and pavement design conditions. There is no single value of the endurance limit for all conditions. The endurance limit varies depending on the applied strain, binder type, binder content, air void, temperature and the frequency of the load application.
2. The endurance limit ranged from 22 micro strains to 264 micro strains.

3. Softer binder mixtures exhibit higher endurance limit values than stiffer binder mixtures.
4. High binder contents and low air voids produced the highest endurance limit values compared to low binder contents and high air voids, which showed the lowest endurance limit.
5. Endurance limit values were higher at high temperatures, which correspond to soft mixtures compared to low temperatures that correspond to stiff mixtures.
6. HMA stiffness is a good mixture property that represents other volumetric parameters. It can represent the same effect of four combined pavement mixture variables: binder type, binder content, air voids, and temperature.
7. The true relationship between the rest period and healing index is tangent hyperbolic function, which indicates that there is no additional healing gained after reaching a certain rest period. Based on the results of this study, the rest period that ensures complete healing ranges from 5 to 10 seconds based on pavement design conditions.
8. Number of loading cycles has little effect on endurance limit for tests with rest period. This concludes that the endurance limit can be determined based on a relatively short number of cycles since damage will be always healed at the end of each loading cycle.

9. The relationship between strain and number of cycles to failure for tests with rest period can be predicted for any rest period-stiffness combination by setting the stiffness ratio at 50 percent in the developed model.
10. The predicted endurance limit values based on second and third generation models were comparable. Therefore, either model can be used to obtain the endurance limit of typical hot mix asphalts.

Using the results of this study with the developed methodology to incorporate endurance limit in the MEPDG, will lead to design perpetual pavements that can sustain a large number of truck loads. If traffic volumes and vehicle weights are controlled, a very large number of vehicle repetitions can be applied without causing fatigue damage to the HMA layer.

### 9.3 Recommendations for Further Research

This research effort resulted in developing a simplified integrated prediction model to predict healing and endurance limit for conventional HMA mixtures. In order to gain more understanding of the endurance limit for asphalt mixtures, the following items are recommended:

- Filed validation studies are highly recommended as a prudent step in implementing the developed integrated model. This can be achieved by monitoring perpetual pavements designed using the integrated models developed in this study.

- A validation database needs to be developed to confirm that the relationship between pavement mixture parameters and endurance limit is adequate and appropriate.
- It is recommended to implement the developed healing-based endurance limit method to determine the endurance limit for other types of mixes such as warm mix asphalt, asphalt rubber, and polymer modified mixtures.

## REFERENCES


1. Monismith, C. L., J. A. Epps, and F. N. Finn. "Improved Asphalt Design." Proceedings, Journal of the Association of Asphalt Paving Technologists Vol. 54, 1985.

2. Monismith, C. L. and D. B. McLean, "Technology of Thick Lift Construction: Structural Design Considerations" Proceedings, Association of Asphalt Paving Technologists, Vol 41, pp. 258-304, 1972.

3. Carpenter S. H. K. Ghuzlan, and S. Shen, "Fatigue Endurance Limit for Highway and Airport Pavements," Transportation Research Record: Journal of the Transportation Research Board, No. 1832, TRB, National Research Council, Washington, D.C., pp. 131-138, 2003

4. Advanced Pavement Laboratory, National Cooperative Highway Research Program Project NCHRP 9-44, Research Plan, Washington, DC, Nov. 2008.

5. Marshall R. Thompson, Samuel H. Carpenter, "Considering Hot-Mix-Asphalt Fatigue Endurance Limit in Full-Depth Mechanistic-Empirical Pavement Design", International conference on perpetual pavement, Ohio 2006.

6. Carpenter, S. H., and S. Shen, "A Dissipated Energy Approach to Study HMA Healing in Fatigue," Journal of the Transportation Research Board, 2006.

7. Prowell, B. et al., "Endurance Limit of Hot Mix Asphalt Mixtures to Prevent Fatigue Cracking in Flexible Pavements," NCHRP 9-38, Updated Draft Final Report, NCHRP, May 2008.

8. Abojaradeh, M., "Effective Fatigue Models for Arizona Asphalt Concrete Mixtures," Ph.D. Dissertation, Arizona State University, Tempe, AZ. December 2003.

9. Long-Term Pavement Performance Program, "Distress Identification Manual for the Long-Term Pavement Performance Project," Report No. SHRP-P-338, Strategic Highway Research Program, National Research Council, Washington, DC, 1993.

10. SHRP, A-404. "Fatigue Response of Asphalt-Aggregate Mixes". Strategic Highway Research Program, National Research Council, 1994.

11. Finn, F. N., C. L. Saraf, R. Kulkarni, K. Nair, W. Smith, and A. Abdullah. "The Use of Distress Prediction Subsystem for the Design of Pavement Structure." Proceedings, Fourth International Conference on the Structural Design of Asphalt Pavements, University of Michigan, Ann Arbor, 1977.

12. Shell, "Shell Pavement Design Manual Asphalt Pavements and Overlays for Road Traffic," Shell International Petroleum, London, 1978.

13. Asphalt Institute. "Research and Development of the Asphalt Institute's Thickness Design Manual (MS-1)," Ninth Edition. Research Report No. 82-2 RR-82-2 College Park, MD Aug. 1982.

14. Chomton, J. S., and P. J. Valayer. "Applied Rheology of Asphalt Mixes, Practical Applications." Proceedings, Third International Conference on the Structural Design of Asphalt Pavements, London, Vol. I., 1972.

15. Van Dijk, W., "Practical Fatigue Characterization of Bituminous Mixes." Proceedings Journal of the Association of Asphalt Paving Technologists. Phoenix, Arizona, Vol. 44. , p.38, 1975.

16. Van Dijk, W., and W. Visser. "The Energy Approach to Fatigue for Pavement Design." Proceedings Journal of the Association of Asphalt Paving Technologists Vol. 46. pp. 1-40, 1977.

17. Pronk, A.C., and P.C. Hopman, "Energy Dissipation: The Leading Factor of Fatigue". Highway Research: Sharing the Benefits. Proceedings of the Conference the United States Strategic Highway Research Program. London, 1990.

18. Tayebali, A. A., J. A. Deacon, and C. L. Monismith. "Development and Evaluation of Surrogate Fatigue Models for SHRP A-003A Abridged Mix Design Procedure." Journal of the Association of Asphalt Paving Technologists Vol. 64, pp. 340-366, 1995.

19. Tayebali, A.A., John A. Deacon, John S. Coplantz, and Carl L. Monismith. "Modeling Fatigue Response of Asphalt-Aggregate Mixtures". Asphalt Paving Technology, Vol. 62, 1993.

20. NCHRP. 2004. "Guide for Mechanistic-Empirical Design of New and Rehabilitated Pavement Structures, Project 37-1A". Washington DC: National Cooperative Highway Research Program, Transportation Research Board, National Research Council.

21. Bazin, P., and J.B. Saunier. Deformability, "Fatigue and Healing Properties of Asphalt Mixes". Proceedings, Second International Conference on the Structural design of Asphalt Pavements.University of Michigan, 1967.

22. Pell, P.S. and K.E. Cooper, "The Effect of Testing and Mix Variables on the Fatigue Performance of Bituminous Materials". Proceedings, Asphalt Paving Technology, Vol. 44, 1975.

23. Tayebali, A.A., G.M. Rowe and J.B. Sousa, "Fatigue Response of Asphalt-Aggregate Mixtures". Proceedings, Asphalt Paving Technology, Vol. 61, pp. 333-360, 1992.

24. Rowe, G.M., "Performance of Asphalt Mixtures in the Trapezoidal Fatigue Test". Proceedings, Asphalt Paving Technology, Vol. 62, 1993.

25. Tangella, SCSR, et al., "Summary Report on Fatigue Response of Asphalt Mixtures," Report No. SHRP-A-312, Strategic Highway Research Program, Washington, D.C., Feb. 1990.

26. Pronk, A.C., "Comparison of 2 and 4 point fatigue tests and healing in 4 point dynamic bending test based on the dissipated energy concept". Proceedings of the eighth international conference on asphalt pavements, Seattle, Washington, pp. 987-994, 1997.

27. NCHRP Project 944-A. Validating an Endurance Limit for HMA Pavements: Laboratory Experiment and Algorithm Development, Quarterly Progress Report, Arizona State University, Tempe, Arizona, June, 2010.

28. Tsai, B.-W., V.N. Kannekanti, and J.T. Harvey, "The Application of Genetic Algorithm in Asphalt Pavement Design," Accepted for publication by Transportation Research Record: Journal of the Transportation Research Record Board, TRB, National Research Council, Annual Meeting CD-Rom, Washington, D.C., 2004.

29. Tsai, B.-W., J.T. Harvey, and Monismith, C. L., "The Application of Weibull Theory in Asphalt Concrete Fatigue Performance Prediction," Transportation Research Record: Journal of the Transportation Research Record Board, TRB, National Research Council, Annual Meeting CD-Rom, Washington, D.C., 2003.

30. Tsai, B.-W., J.T. Harvey, and Monismith, C. L., "Characterization of Mix Fatigue Damage Process Using Three-Stage Weibull Equation and Tree-Based Model," Transportation Research Record: Journal of the Transportation Research Record Board, TRB, National Research Council, Annual Meeting CD-Rom, Washington, D.C., 2005.

31. Biligiri, K., Kaloush, K., Mamlouk, M., Witczak, M., "Rational Modeling of Tertiary Flow for Asphalt Mixtures". Journal of the Transportation Research Board, No. 2001, pp 63-72. Washington, D.C., 2007.

32. Harvey, J., Bor-Wen Tsai. "Effect of Asphalt Content and Air Void Content on Mix Fatigue and Stiffness." Transportation Research Record No: 1543, Washington, D.C. pp. 38-45, 1996.

33. Tayebali, A. A., G.M. Rowe, and J.B. Sousa. "Fatigue Response of Asphalt Aggregate Mixtures." Journal of the Association of Asphalt Paving Technologists Vol: 61. pp. 333-360, 1994.

34. Sousa, J.B., Pais, J.C., Prates, M.,Barros, R., langlios, P., and Leclerc, AM. "Effect of Aggregate Gradation on Fatigue Life of Asphalt Concrete Mixes." Transportation Research Record No: 1630, Washington, D.C., 1998.

35. Button, J.W. and Lytton, R.L. "Evaluation of Fabrics, Fibers and Grids in Overlays". Sixth International Conference on the Structural Design of Asphalt Pavements. Ann Arbor, Michigan, 1987.

36. Pell, P.S. “Characteristics of Fatigue behavior” Highway Research Special Report No. 140, National Research Council, Washington D.C., pp. 49-64, 1973.

37. Monismith, C.L. and J.A. Deacon. “Fatigue of asphalt paving mixtures”. Journal of Transportation Engineering, 95(2): pp. 317-345, 1969.

38. Monismith, C L, Secor, K E and Blackmer, W., “Asphalt mixture behaviour in repeated flexure”, Proceedings of Association of Asphalt Paving Technologists, Vol. 30, pp.188-222, 1961.

39. Raithby, K.D. and A.B. Sterling “The effect of rest periods on the fatigue performance of a hot-rolled asphalt under repeated loading”. Journal of the Association of Asphalt Paving Technologists, 39: 134-152, 1970.

40. McElvane, J., and Pell, P. S. "Fatigue Damage of Asphalt, Effect of Rest Periods." Highways and Road Construction, 1973.

41. Verstraeten, J., J. E. Romain, and V. Veverka, “The Belgian Road Research Center’s Overall Approach Structural Design”, Fourth International Conference on The Structural Design of Asphalt Pavements, Vol. 1, Proc., Ann Arbor, MI, Aug 1977.

42. Francken, L., “Fatigue Performance of Bituminous Road Mix under Realistic Conditions” Transportation Research Record 712. Washington D.C., pp.30-37, 1979.

43. Hsu, T. W. and K. H. Tseng, “Effect of Rest Periods on Fatigue Response of Asphalt Concrete Mixtures.” Journal of Transportation Engineering, ASCE. Vol. 122, No. 4, 1996.

44. Breysse, D.; C. De La Roche, V. Domec and J.J. Chauvin. “Influence of rest time on recovery and damage during fatigue testes on bituminous composites”. In Materials and Structures, Vol. 36, pp. 648-651, 2003.

45. Castro, M. and Sanchez, J.A. Fatigue and Healing of Asphalt Mixtures: Discriminate Analysis of Fatigue Curves, Journal of Transportation Engineering, ASCE, Vol. 132, No. 2, pp. 168-174, 2006.

46. Raithby, K. D. and Sterling, A. B. “Some Effects of Loading History on the Performance of Rolled Asphalt”, TRRL-LR 496, Crowthorne, England, 1972.

47. Bonnaure, F., Huibbers, A.H.J.J., and Booders, A. "A Laboratory Investigation of the Influence of Rest Periods on Fatigue Characteristics of Bituminous Mixes." Proceedings, the Association of Asphalt Paving Technologists, Vol. 51, 104, 1982.

48. Harvey, J., "University of California - Berkeley SHRP A-003A Asphalt Concrete Specimen Preparation Manual, Version 3.0," SHRP Technical Memorandum No. TMUCB- A-003A-91-2, Berkeley, 1991.

49. Pell, P. S. and Hanson, J. M. "Behavior of Bituminous Road Base Materials under Repeated Loading," Proceedings, Association of Asphalt Paving Technologists, 201, 229, 1973.

50. Bonnot, J. "Asphalt Aggregate Mixtures." Transportation Research Record1096, Transportation Research Board, Washington, D. C., pp. 42-50, 1986.

51. Majidzadeh, K., Kauffmann, E. M., and Ramsamooj, D. V. “Application of fracture mechanics in the analysis of pavement fatigue.” Proc., Association of Asphalt Paving Technologists, Association of Asphalt Paving Technologists, White Bear Lake, Minn., 40, 227–246, 1971.

52. Barksdale, R.D. and Miller, J. H., III. “Development of Equipment and Techniques for Evaluating Fatigue and Rutting Characteristics of Asphalt Concrete Mixes”. Report SCEGIT-77-147. School of Civil Engineering, Georgia Institute of Technology, Atlanta, 1977.

53. Sousa, J.B. “Dynamic Properties of Pavement Materials.” Ph.D. thesis, University of California, Berkeley, 1986.

54. Raithby, K. D. and Ramshaw, J. T. “Effect of Secondary Compaction on the Fatigue Performance of a Hot-Rolled Asphalt, TRRL-LR 471, Crowthorne, England, 1972.

55. Kunst, P.A.J.C. “Surface Cracking on Asphalt Layers, Working Committee B12, Hoevelaken, Holland, 1989.

56. Kennedy, T. W. "Characterization of Asphalt Pavement Materials Using the Indirect Tensile Test," Proceedings, The Association of Asphalt Paving Technologists, Vol. 56, 1977.

57. Moore, R. K. and T. W. Kennedy. “Tensile Behavior of Subbase Materials under Repetitive Loading.” Research Report 98-12, Center for Highway Research, University of Texas at Austin, Austin, TX, 1971.

58. Navarro, D. and T, W. Kennedy. "Fatigue and Repeated-Load Elastic Characteristics of In-service Asphalt-Treated Pavement.” Research Report No.183-2, Center for Highway Research, the University of Texas at Austin, 1975.

59. Cowher, K. “Cumulative Damage of Asphalt Materials under Repeated-Load Indirect Tension.” Research Report Number 183-3. Center for Highway Research – University of Texas at Austin, 1975.

60. Suresh, S., “Fatigue of Materials” 2nd Edition. Cambridge University Press, USA, pp 1-679, 1998.

61. Phillips, M.C. Multi-Step Models for Fatigue and Healing, and Binder Properties Involved in Healing. Proceedings, Eurobitume Workshop on Performance Related Properties for Bituminous Binders, Luxembourg, Paper No. 115, 1998.

62. Jacobs, M.M.J. “Crack Growth in Asphaltic Mixes,” PhD. Thesis, Delft University of Technology, Netherlands, 1995.

63. Lytton, R. L. “Characterizing Asphalt Pavements for Performance” Transportation Research Record, 1767, Transportation Research Board, Washington, D. C., pp. 5-16, 2000.

64. S. Pager and M. Tirrell, J. Chem. Phys., 5194-5198, 1981.

65. Peterson J.C., “Chemical Composition of Asphalt Related to Asphalt Durability: State of the Art”, Transportation Research Record, Vol #999, 1984.

66. Ensley, Keith E. "A Kinetic Investigation of Association in Asphalt," Colloid Interface Sci., vol. 53, pp. 452-460, 1975.

67. Kim, Y.R., D.N. Little, and F.C. Benson “Chemical And Mechanical Evaluation On Healing Mechanism Of Asphalt Concrete”. Journal of the Association of Asphalt Paving Technologists (AAPT), Vol. 59. pp. 241-276, 1990.

68. Bazin, P., and Saunier, J.B. "Deformability, fatigue and healing properties of asphalt mixes." Proceedings of the Second International Conference on the Structural Design of Asphalt Pavements, Ann Arbor, Michigan, USA, pp. 553-569. 1967.

69. Kim, Y, R. and Little, D, N. “Evaluation of Healing in asphalt concrete by means of the theory of nonlinear viscoelasticity”, Journal of Transportation Research Record: Transportation Research Board, No. 1228, pp. 198-210, 1989.

70. Kim, Y., Little, D. N. and Lytton, R. L. “Effect of Moisture Damage on Material Properties and Fatigue Resistance of Asphalt Mixtures.” In Transportation Research Record 1832, TRB, National Research Council, Washington, D.C., pp. 48-54, 2004.

71. Kim, Y. and Y.R. Kim, "Evaluation of Microcrack Damage Growth and Healing of Asphalt Concrete Pavements Using Stress Wave Method," Proceedings of the 11th ASCE Engineering Mechanics Specialty Conference, pp. 612-615, 1996.

72. Schapery R. A. Correspondence Principles and a Generalized J-Integral for Large Deformation and Fracture Analysis of Viscoelastic Media, International Journal of Fracture Mechanics, Vol. 25, No. 3, pp. 195-223, 1984.

73. Schapery, R. A. ‘‘On the mechanics of crack closing and bonding in linear viscoelastic media.’’ International Journal of Fracture, 39, pp. 163–183, 1989.

74. Wöhler, A. "Versuche uber die Festigkeit der Eisenbahnwagenachsen"; English summary (1867). Engineering, 4, 160-161, 1860.

75. Prot, E. M. "Rev Metallurgie." translated by Ward, E.J. WADC Tech Rep, pp. 52-148, 1948.

76. Lagace, P. A., and Allen, M. W. "Evaluation of the Alternative Manufacturing Methods for Bonding Graphite/epoxy composites." 30th National SAMPE Symposium, 1985.

77. Monismith, C. L., and D. B. McLean, “Structural Design Considerations”, Proceedings of the Association of Asphalt Paving Technologists, Vol. 41, 1972.

78. Maupin, G. W., Jr. and J. R. Freeman, Jr. “Simple Procedure for Fatigue Characterization of Bituminous Concrete” Final Report No. FHWA-RD-76-102, Federal Highway Administration, Washington, DC 1976.

79. Nunn, M. “Long-life Flexible Roads”. Proceedings of the 8th International Conference on Asphalt Pavements, Vol. 1. University of Washington, Seattle, WA, Pp. 3-16, August 1997.

80. Nishizawa, T., S. Shimeno, and M. Sekiguchi. “Fatigue Analysis of Asphalt Pavements with Thick Asphalt Mixture Layer”, Proceedings of the 8th International Conference on Asphalt Pavements, Vol. 2. University of Washington, Seattle, WA,. Pp. 969-976, August 1997.

81. Wu, Z., Z. Q. Siddique, and A. J. Gisi. “Kansas Turnpike – An Example of Long Lasting Asphalt Pavement”. Proceedings International Symposium on

Design and Construction of Long Lasting Asphalt Pavements. National Center for Asphalt Technology, Auburn, Pp. 857-876, AL 2004.

82. Mahoney, J. P., "Study of Long-Lasting Pavements in Washington State, Transportation Research Circular No. 503", Perpetual Bituminous Pavements, Transportation Research Board, pp 88-95, Washington, DC 2001.

83. Newcomb, D. Perpetual Pavements: A Synthesis. APA 101, Asphalt Pavement Alliance, Lanham, MD 2002.

84. Monismith, C. L., J. A. Epps, et al., "Asphalt Mixture Behavior in Repeated Flexure." Report No. TE 70-5, Institute of Transportation and Traffic Engineering, University of California, Berkley, 303 pp., 1970.

85. Monismith, C. L., and Long, F., "Overlay Design for Cracked and Seated Portland Cement Concrete (PCC) Pavement—Interstate Route 710." Technical Memorandum TM UCB PRC99-3, Pavement Research Center, Institute for Transportation Studies, University of California, Berkeley, 1999.

86. Von Quintus, Harold L., J.A. Scherocman, C.S. Hughes, and T.W. Kennedy, Asphalt- Aggregate Mixture Analysis System: AAMAS, NCHRP Report No. 338, National Cooperative Highway Research Program, National Research Council, Washington, DC, March 1991.

87. Von Quintus, Harold L. "Application of the Endurance Limit Premise in Mechanistic-Empirical Based Pavement Design Procedures", July 2006.

88. Carpenter, S.H. "Fatigue Performance of IDOT Mixtures, Civil Engineering Studies", Illinois Center for Transportation Series No 07.-007, University of Illinois at Urbana-Champaign, July, 2006.

89. Newcomb, D.E., Buncher, M., and Huddleston, I.J., "Concepts of Perpetual Pavements," Transportation Research Circular Number 503, Perpetual Bituminous Pavements, Transportation Research Board, Washington, D.C., December, 2001.

90. Advanced Asphalt Technologies, LLC, "Hot Mix Asphalt Endurance Limit Workshop: Executive Summary," National Cooperative Highway Research Program Project 9-44, November, 2007.

91. Kim, B. and Roque, R., "Evaluation of Healing Property of Asphalt Mixtures," Transportation Research Record No. 1970, Transportation Research Board, Washington, D.C., 2006.

92. Romanoschi, S., Gisi, A., Portillo, M., and Dumitru, C., "First Findings from the Kansas Perpetual Pavements Experiment" Transportation Research Record: Journal of the Transportation Research Board, No. 2068, Washington, D.C., 2008, pp. 41–48.

93. Bhattacharjee, S., Swamy, A., and Daniel, J., "Application of Elastic–Viscoelastic Correspondence Principle to Determine Fatigue Endurance Limit of Hot-Mix Asphalt". Transportation Research Record: Journal of the Transportation Research Board, No. 2126, Washington, D.C., 2009, pp. 12–18.

94. Nunn, M. and Ferne, B.W., "Design and Assessment of Long-Life Flexible Pavements," Transportation Research Circular Number 503, Perpetual Bituminous Pavements, Transportation Research Board, Washington, D.C., December, 2001.

95. Brown, S.R., Thom, N.H., and Hakim, B.A., "Performance and Rehabilitation of Heavy-duty Pavements in the UK: Some Case Studies," Proceedings, International Symposium of Design and Construction of Long Lasting Asphalt Pavements, National Center for Asphalt Technology, Auburn, AL, 2004.

96. Uhlmeyer, J.S., Willoughby, K., Pierce, L.M., and Mahoney, J.P., "Top-Down Cracking in Washington State Asphalt Concrete Wearing Courses," Transportation Research Record No. 1730, Transportation Research Board, Washington, D.C., 2000.

97. R.L. Plackett and J.P. Burman, "The Design of Optimum Multifactorial Experiments", Biometrika 33 (4), pp. 305-25, June 1946.

98. JMP software, SAS Institute Inc, http://www.jmp.com/.

99. Montgomery, Douglas C., Design and Analysis of Experiments, Wiley, 2008.

100. Uniform Standard Specifications for Public Works Construction Sponsored and Distributed By the Maricopa Association of Governments, 2011, AZ.

101. AASHTO Designation: T321-03. Determining the Fatigue Life of Compacted Hot-Mix Asphalt (HMA) Subjected to Repeated Flexural Bending.

102. SHRP Designation: M-009. Standard Method of Test for Determining the Fatigue Life of Compacted Bituminous Mixtures Subjected to Repeated Flexural Bending.

103. Harvey, J., et al., "Evaluation of Fatigue and Permanent Deformation Properties of Several Asphalt-Aggregate Field Mixes Using Strategic Highway Research Program A-003A Equipment," Record 1454, Transportation Research Board, Washington, D.C., 1994.

104. AASHTO. AASHTO PP2 – Standard Practice for Mixture Conditioning of Hot-Mix Asphalt (HMA). American Association of State Highway and Transportation Officials, Washington D.C., United States of America, p. 34-36, 1994.

105. American Association of State Highway and Transportation Officials. "Theoretical Maximum Specific Gravity And Density Of Bituminous Paving Mixtures" Test Method AASHTO T 209, Washington D.C.,

106. American Association of State Highway and Transportation Officials. Bulk Specific Gravity of Bituminous Mixtures Using Saturated Surface Dry Specimens, Test Method AASHTO T 166 – 00, Standard Specifications for Transportation Materials and Methods of Sampling and Testing, Part II – Tests, Twentieth Edition, 2000.

107. Montgomery, D. C., Design and Analysis of Experiments, Wiley, 2008.

108. ASTM, "Standard Test Method for Determining Fatigue Failure of Compacted Asphalt Concrete Subjected to Repeated Flexural Bending," Test

method ASTM D7460, ASTM International, 100 Barr Harbor Drive, West Conshohocken, Pennsylvania, USA.

109. Pronk A.C., "Haversine Fatigue Testing in Controlled Deflection Mode: Is It Possible?" Presented at the Transportation Research Board meeting, 2010.

110. Pronk A.C. and S.M.J.G Erkens., "A note on fatigue bending tests using a haversine loading", International Journal on Road Design, Vol. 2, Issue 4, 2001.

111. Shen, S. and S. H. Carpenter, "Application of Dissipated Energy Concept in Fatigue Endurance Limit Testing," Transportation Research Record, Journal of Transportation Research Board, No. 1929, pp. 165 – 173, 2005.

112. AASHTO Provisional Standards, "Standard Test Method for Determination the Fatigue Life of Compacted Hot Mix Asphalt (HMA) Subjected to Repeated Flexural Bending". TP8-94, September 1994.

113. Ghuzlan, K., S.H. Carpenter, "Energy-Derived, Damage-Based Failure Criterion for Fatigue Testing". Transportation Research Record No: 1723, Washington, D.C., pp. 141-149, 2001.

114. Pronk, A. C., and P. C. Hopman. "Energy Dissipation: The Leading Factor of Fatigue." Proceedings, United State Strategic Highway Research Program – Sharing the Benefits, October 29-31 London, 1990.

115. Asphalt Institute. "Thickness Design Asphalt Pavements for Highways and Streets." Manual Series No.1, MS-1. Lexington, KY. 1991.

116. Huang, Y.H. "Pavement Analysis and Design," Prentice Hall, Englewood Cliffs, N.J. 1993.

117. Van Dijk, W., and W. Visser. "The Energy Approach to Fatigue for Pavement Design." Proceedings Journal of the Association of Asphalt Paving Technologists Vol. 46. pp. 1-40, 1977.

118. Rowe, G. M., and M. G. Bouldin. "Improved Techniques to Evaluate the Fatigue Resistance of Asphalt Mixtures". EUROBITUME Conference Barcelona, Spain,.Septemper 2000.

119. Epps, J.A. and C.L. Monismith. "Influence of mixture variables on the flexural fatigue properties of asphalt concrete". Journal of the Association of Asphalt Paving Technologists, 38: 423-464, 1969.

120. Monismith, C. L. "Asphalt Mixture Behavior in Repeated Flexure, Report No. TE 66-66, ITIE", to California Division of Highways, University of California, 1966.

121. Said, S.F., "Variable in Roadbase Layer Properties Conducting Indirect Tensile Test", Eight International Conference on The Structural Design of Asphalt Pavements, Vol. 2 Proc., Seattle, Washington, August 1997.

122. Verstraeten, J., "Influence des caractéristiques du bitume sur les propriétés en fatigue des mélanges bitumineux". RILEM, 1976.

123. W. N. Houston, M. W. Mirza, C. E. Zapata, and S. Raghavendra "Simulating The Effects Of Hot Mix Asphalt Aging For Performance Testing And Pavement Structural Design" NCHR Research Results Digest 324, October 2007.

124. NCHRP Project 944-A. Validating an Endurance Limit for HMA Pavements: Laboratory Experiment and Algorithm Development, Quarterly Progress Report, Arizona State University, Tempe, Arizona, June, 2010.

125. Stat-Ease, Inc. http://www.statease.com/

126. Box, G. E. P., Cox, D. R., "An Analysis of Transformations", Journal of the Royal Statistical Society, Series B 26(2), pp.211-252, 1964.

127. Montgomery, D. C., Peck, E. A., and Vining, G. G., Introduction to Linear Regression Analysis, Wiley, 2001.

128. STATISTICA software, StateSoft, http://www.statsoft.com/#.

129. Minitabe software, http://www.minitab.com/en-US/default.aspx

# APPENDIX A

# SUMMARY OF BEAM FATIGUE TEST RESULTS

Table A-1 shows a summary of results obtained from the beam fatigue experiment. The following is a description of the different columns used in the table.

- Serial Number.
- Specimen ID: Actual ID marked on each specimen for identification.
- Machine Used: IPC-1 and IPC-2.
- Temperature: Three test temperatures of 40, 70, and 100 F were used
- PG Binder Grade: PG 76-16, PG 64-22, and PG 58-22.
- AC%: Two binder contents of 4.2 and 5.2 % were used.
- Target $V_a$%: 4.5 and 9.5%.
- Applied Strain: A constant-strain sinusoidal loading was applied at a frequency of 10 Hz according to the AASHTO T-321 procedure. The values shown in the table are half of the peak-to-peak values.
- Initial Stress: The tensile stress calculated at the $50^{th}$ cycle of each test.
- Initial Stiffness: The initial flexural stiffness calculated at the $50^{th}$ cycle of each test. The relationships between strain, stress and flexural stiffness are shown in Equations A-1, A-2 and A-3.

$$\varepsilon_t = 12\,\delta\,h / (3\,L^2 - 4\,a^2) \qquad \text{(A-1)}$$

$$\sigma_t = 3\,a\,P / b\,h^2 \qquad \text{(A-2)}$$

$$S_o = \sigma_t / \varepsilon_t \qquad \text{(A-3)}$$

where,

$\varepsilon_t$ = Applied strain
$\sigma_t$ = Initial stress
$S_o$ = Initial flexural stiffness
P = Load
b = Average specimen width
h = Average specimen height
$\delta$ = deflection at the center of the beam
a = Space between inside clamps
L = Length of beam between outside clamps

- Rest Period: 0, 1, 5, and 10 seconds.
- $N_f$ (at SR=0.5): All tests without rest period were conducted until failure (stiffness ratio of 0.5). Values shown in this column are for tests without rest period only.

- Cycle Number: Three points were selected on the SR-N relationship for each test, at which the stiffness ratios were used in the analysis. Two of these points were taken during the test, while the third point was taken at $N_{f\ w/o\ RP}$. Note that the results of the tests with rest period were extrapolated to $N_{f\ w/o\ RP}$ as discussed in Chapter 7.
- Stiffness Ratio at Cycle Number: The stiffness ratios at the corresponding cycle numbers are recorded in the table and used in the analysis.

**Table A-1. Beam Fatigue Test Results**

| Serial Number | Specimen ID | Machine Used | Temperature, F | PG Binder Grade | AC % | Target $V_a$ % | Applied Strain, µs | Initial Stress, psi | Initial Stiffness, ksi | Rest Period, Sec | $N_f$ (at SR=0.5) | Cycles Number | | | Stiffness Ratio at Cycle Number | | |
|---|---|---|---|---|---|---|---|---|---|---|---|---|---|---|---|---|---|
| | | | | | | | | | | | | $N_1$ | $N_2$ | $N_3$ | $SR_{N1}$ | $SR_{N2}$ | $SR_{N3}$ |
| 1 | 21 | IPC-1 | 40 | 76-16 | 4.2 | 4.5 | 175 | 294.5 | 1682.8 | 0 | 27676 | 24405 | 5000 | 10000 | 0.519 | 0.634 | 0.591 |
| 2 | 24 | IPC-1 | 40 | 76-16 | 4.2 | 4.5 | 175 | 339.6 | 1940.7 | 0 | 32190 | 24405 | 10000 | 15000 | 0.523 | 0.601 | 0.577 |
| 3 | 17 | IPC-2 | 40 | 76-16 | 4.2 | 4.5 | 175 | 391.8 | 2238.9 | 0 | 13350 | 24405 | 5000 | 7500 | 0.482 | 0.578 | 0.548 |
| 4 | 7 | IPC-1 | 40 | 76-16 | 4.2 | 9.5 | 137.5 | 185.1 | 1346.3 | 0 | 286070 | 231971 | 30000 | 100000 | 0.522 | 0.622 | 0.566 |
| 5 | 16 | IPC-2 | 40 | 76-16 | 4.2 | 9.5 | 137.5 | 206.1 | 1499.2 | 0 | 219610 | 231971 | 30000 | 100000 | 0.493 | 0.594 | 0.533 |
| 6 | 20 | IPC-2 | 40 | 76-16 | 4.2 | 9.5 | 137.5 | 172.5 | 1254.7 | 0 | 190232 | 231971 | 30000 | 100000 | 0.470 | 0.572 | 0.507 |
| 7 | 22 | IPC-2 | 40 | 76-16 | 5.2 | 4.5 | 137.5 | 223.8 | 1627.7 | 0 | 342760 | 341261 | 50000 | 100000 | 0.500 | 0.589 | 0.556 |
| 8 | 6 | IPC-1 | 40 | 76-16 | 5.2 | 4.5 | 137.5 | 226.8 | 1649.1 | 0 | 320000 | 341261 | 50000 | 100000 | 0.480 | 0.572 | 0.537 |
| 9 | 2 | IPC-1 | 40 | 76-16 | 5.2 | 4.5 | 137.5 | 245.9 | 1788.5 | 0 | 361023 | 341261 | 50000 | 100000 | 0.530 | 0.612 | 0.581 |
| 10 | 20 | IPC-2 | 40 | 76-16 | 5.2 | 9.5 | 175 | 233.7 | 1335.3 | 0 | 22790 | 18000 | 5000 | 10000 | 0.532 | 0.635 | 0.592 |
| 11 | 23 | IPC-2 | 40 | 76-16 | 5.2 | 9.5 | 175 | 194.7 | 1112.8 | 0 | 19590 | 18000 | 5000 | 10000 | 0.502 | 0.609 | 0.563 |
| 12 | 9 | IPC-1 | 40 | 76-16 | 5.2 | 9.5 | 175 | 263.7 | 1506.9 | 0 | 11620 | 18000 | 3000 | 5000 | 0.480 | 0.610 | 0.572 |
| 13 | 20 | IPC-1 | 70 | 76-16 | 4.2 | 4.5 | 237.5 | 173.6 | 731.03 | 0 | 14640 | 15757 | 5000 | 10000 | 0.493 | 0.590 | 0.541 |
| 14 | 11 | IPC-2 | 70 | 76-16 | 4.2 | 4.5 | 237.5 | 172.9 | 728.12 | 0 | 9020 | 15757 | 3000 | 5000 | 0.470 | 0.591 | 0.550 |
| 15 | 12 | IPC-2 | 70 | 76-16 | 4.2 | 4.5 | 237.5 | 203.9 | 858.55 | 0 | 23612 | 15757 | 5000 | 10000 | 0.532 | 0.636 | 0.594 |
| 16 | 12 | IPC-1 | 70 | 76-16 | 4.2 | 9.5 | 187.5 | 128.0 | 682.58 | 0 | 75470 | 80410 | 25000 | 45000 | 0.486 | 0.556 | 0.521 |
| 17 | 24 | IPC-1 | 70 | 76-16 | 4.2 | 9.5 | 187.5 | 112.3 | 598.79 | 0 | 94520 | 80410 | 30000 | 45000 | 0.524 | 0.584 | 0.563 |

| | | | | | | | | | | | | | | | | | |
|---|---|---|---|---|---|---|---|---|---|---|---|---|---|---|---|---|---|
| 18 | 11 | IPC-2 | 70 | 76-16 | 4.2 | 9.5 | 187.5 | 136.7 | 728.84 | 0 | 71239 | 80410 | 25000 | 35000 | 0.479 | 0.548 | 0.528 |
| 19 | 3 | IPC-1 | 70 | 76-16 | 5.2 | 4.5 | 187.5 | 152.8 | 814.8 | 0 | 162180 | 163845 | 30000 | 80000 | 0.501 | 0.588 | 0.537 |
| 20 | 14 | IPC-2 | 70 | 76-16 | 5.2 | 4.5 | 187.5 | 126.6 | 675.1 | 0 | 152896 | 163845 | 40000 | 70000 | 0.485 | 0.558 | 0.528 |
| 21 | 16 | IPC-2 | 70 | 76-16 | 5.2 | 4.5 | 187.5 | 109.7 | 584.88 | 0 | 176459 | 163845 | 40000 | 70000 | 0.521 | 0.591 | 0.563 |
| 22 | 23 | IPC-1 | 70 | 76-16 | 5.2 | 4.5 | 237.5 | 200.4 | 843.84 | 0 | 67950 | 50076 | 20000 | 30000 | 0.536 | 0.602 | 0.580 |
| 23 | 17 | IPC-2 | 70 | 76-16 | 5.2 | 4.5 | 237.5 | 122.9 | 517.27 | 0 | 56707 | 50076 | 10000 | 25000 | 0.514 | 0.617 | 0.565 |
| 24 | 28 | IPC-1 | 70 | 76-16 | 5.2 | 4.5 | 237.5 | 111.8 | 470.81 | 0 | 25570 | 50076 | 5000 | 10000 | 0.460 | 0.594 | 0.545 |
| 25 | 7 | IPC-1 | 70 | 76-16 | 5.2 | 9.5 | 237.5 | 151.3 | 637.19 | 0 | 15434 | 17388 | 3000 | 6000 | 0.495 | 0.630 | 0.581 |
| 26 | 11 | IPC-2 | 70 | 76-16 | 5.2 | 9.5 | 237.5 | 127.1 | 534.96 | 0 | 20520 | 17388 | 6000 | 10000 | 0.514 | 0.607 | 0.574 |
| 27 | 14 | IPC-2 | 70 | 76-16 | 5.2 | 9.5 | 237.5 | 115.4 | 485.96 | 0 | 16210 | 17388 | 4000 | 8000 | 0.498 | 0.614 | 0.565 |
| 28 | 19 | IPC-1 | 100 | 76-16 | 4.2 | 4.5 | 237.5 | 43.2 | 182 | 0 | 82320 | 132241 | 20000 | 40000 | 0.462 | 0.555 | 0.513 |
| 29 | 23 | IPC-2 | 100 | 76-16 | 4.2 | 4.5 | 237.5 | 47.8 | 201.47 | 0 | 189080 | 132241 | 50000 | 90000 | 0.532 | 0.592 | 0.564 |
| 30 | 26 | IPC-1 | 100 | 76-16 | 4.2 | 4.5 | 237.5 | 50.4 | 212.34 | 0 | 125324 | 132241 | 40000 | 60000 | 0.489 | 0.554 | 0.532 |
| 31 | 17 | IPC-1 | 100 | 76-16 | 4.2 | 9.5 | 325 | 53.5 | 164.71 | 0 | 12140 | 24314 | 3000 | 6000 | 0.451 | 0.593 | 0.538 |
| 32 | 22 | IPC-2 | 100 | 76-16 | 4.2 | 9.5 | 325 | 26.1 | 80.292 | 0 | 35390 | 24314 | 6000 | 15000 | 0.532 | 0.641 | 0.588 |
| 33 | 4 | IPC-2 | 100 | 76-16 | 4.2 | 9.5 | 325 | 35.5 | 109.14 | 0 | 25413 | 24314 | 7500 | 10000 | 0.498 | 0.591 | 0.572 |
| 34 | 24 | IPC-2 | 100 | 76-16 | 5.2 | 4.5 | 325 | 51.7 | 159.17 | 0 | 124920 | 125898 | 30000 | 50000 | 0.496 | 0.575 | 0.547 |
| 35 | 19 | IPC-1 | 100 | 76-16 | 5.2 | 4.5 | 325 | 38.2 | 117.46 | 0 | 132093 | 125898 | 30000 | 60000 | 0.513 | 0.589 | 0.553 |
| 36 | 20 | IPC-1 | 100 | 76-16 | 5.2 | 4.5 | 325 | 62.4 | 192.08 | 0 | 120680 | 125898 | 30000 | 60000 | 0.486 | 0.566 | 0.527 |
| 37 | 22 | IPC-1 | 100 | 76-16 | 5.2 | 9.5 | 237.5 | 23.0 | 97.007 | 0 | 191270 | 165576 | 50000 | 70000 | 0.523 | 0.585 | 0.568 |
| 38 | 10 | IPC-1 | 100 | 76-16 | 5.2 | 9.5 | 237.5 | 22.3 | 94.045 | 0 | 121150 | 165576 | 40000 | 60000 | 0.478 | 0.544 | 0.521 |
| 39 | 31 | IPC-2 | 100 | 76-16 | 5.2 | 9.5 | 237.5 | 25.6 | 107.87 | 0 | 184309 | 165576 | 40000 | 80000 | 0.519 | 0.592 | 0.558 |
| 40 | 24 | IPC-1 | 100 | 76-16 | 5.2 | 9.5 | 325 | 40.2 | 123.81 | 0 | 101540 | 105003 | 25000 | 50000 | 0.496 | 0.575 | 0.537 |
| 41 | 8 | IPC-1 | 100 | 76-16 | 5.2 | 9.5 | 325 | 30.4 | 93.668 | 0 | 115250 | 105003 | 25000 | 50000 | 0.516 | 0.595 | 0.559 |
| 42 | 13 | IPC-2 | 100 | 76-16 | 5.2 | 9.5 | 325 | 29.9 | 91.939 | 0 | 98220 | 105003 | 25000 | 45000 | 0.472 | 0.557 | 0.523 |

| | | | | | | | | | | | | | | | | | |
|---|---|---|---|---|---|---|---|---|---|---|---|---|---|---|---|---|---|
| 43 | 9 | IPC-1 | 40 | 76-16 | 4.2 | 4.5 | 137.5 | 306.7 | 2230.2 | 5 | | 320471 | 10000 | 20000 | 0.743 | 0.829 | 0.811 |
| 44 | 10 | IPC-1 | 40 | 76-16 | 4.2 | 4.5 | 137.5 | 262.4 | 1908 | 5 | | 320471 | 10000 | 20000 | 0.726 | 0.818 | 0.799 |
| 45 | 14 | IPC-2 | 40 | 76-16 | 4.2 | 4.5 | 137.5 | 280.7 | 2041.1 | 5 | | 320471 | 10000 | 20000 | 0.749 | 0.833 | 0.816 |
| 46 | 1 | IPC-2 | 40 | 76-16 | 4.2 | 4.5 | 175 | 350.0 | 2000 | 5 | | 22819 | 10000 | 20000 | 0.699 | 0.731 | 0.704 |
| 47 | 4 | IPC-2 | 40 | 76-16 | 4.2 | 4.5 | 175 | 339.1 | 1937.9 | 5 | | 22819 | 10000 | 20000 | 0.679 | 0.713 | 0.685 |
| 48 | 6 | IPC-1 | 40 | 76-16 | 4.2 | 4.5 | 175 | 335.7 | 1918.2 | 5 | | 22819 | 10000 | 20000 | 0.696 | 0.729 | 0.701 |
| 49 | 8 | IPC-1 | 40 | 76-16 | 4.2 | 9.5 | 175 | 213.4 | 1219.4 | 5 | | 5000 | | | 0.717 | | |
| 50 | 21 | IPC-2 | 40 | 76-16 | 4.2 | 9.5 | 175 | 248.9 | 1422 | 5 | | 5000 | | | 0.703 | | |
| 51 | 15 | IPC-2 | 40 | 76-16 | 4.2 | 9.5 | 175 | 263.6 | 1506.5 | 5 | | 5000 | | | 0.695 | | |
| 52 | 10 | IPC-1 | 40 | 76-16 | 5.2 | 4.5 | 175 | 276.7 | 1581.4 | 5 | | 24263 | 10000 | 20000 | 0.790 | 0.814 | 0.796 |
| 53 | 13 | IPC-1 | 40 | 76-16 | 5.2 | 4.5 | 175 | 325.9 | 1862.1 | 5 | | 24263 | 10000 | 20000 | 0.781 | 0.806 | 0.786 |
| 54 | 18 | IPC-2 | 40 | 76-16 | 5.2 | 4.5 | 175 | 266.9 | 1525 | 5 | | 24263 | 10000 | 20000 | 0.803 | 0.825 | 0.808 |
| 55 | 2 | IPC-2 | 40 | 76-16 | 5.2 | 9.5 | 137.5 | 186.3 | 1354.7 | 5 | | 243051 | 10000 | 20000 | 0.774 | 0.845 | 0.830 |
| 56 | 4 | IPC-2 | 40 | 76-16 | 5.2 | 9.5 | 137.5 | 173.0 | 1258.2 | 5 | | 243051 | 10000 | 20000 | 0.790 | 0.856 | 0.842 |
| 57 | 12 | IPC-1 | 40 | 76-16 | 5.2 | 9.5 | 137.5 | 197.0 | 1432.8 | 5 | | 243051 | 10000 | 20000 | 0.811 | 0.871 | 0.858 |
| 58 | 8 | IPC-1 | 70 | 76-16 | 4.2 | 4.5 | 187.5 | 180.7 | 963.55 | 5 | | 105252 | 10000 | 20000 | 0.726 | 0.796 | 0.775 |
| 59 | 5 | IPC-2 | 70 | 76-16 | 4.2 | 4.5 | 187.5 | 151.3 | 806.97 | 5 | | 105252 | 10000 | 20000 | 0.741 | 0.807 | 0.787 |
| 60 | 13 | IPC-2 | 70 | 76-16 | 4.2 | 4.5 | 187.5 | 136.8 | 729.78 | 5 | | 105252 | 10000 | 20000 | 0.762 | 0.822 | 0.805 |
| 61 | 13 | IPC-1 | 70 | 76-16 | 4.2 | 9.5 | 237.5 | 173.1 | 728.93 | 5 | | 11104 | 3000 | 5000 | 0.680 | 0.740 | 0.717 |
| 62 | 1 | IPC-2 | 70 | 76-16 | 4.2 | 9.5 | 237.5 | 139.0 | 585.37 | 5 | | 11104 | 3000 | 5000 | 0.692 | 0.750 | 0.727 |
| 63 | 6 | IPC-2 | 70 | 76-16 | 4.2 | 9.5 | 237.5 | 198.9 | 837.52 | 5 | | 11104 | 3000 | 5000 | 0.650 | 0.715 | 0.690 |
| 64 | 1 | IPC-1 | 70 | 76-16 | 5.2 | 4.5 | 187.5 | 152.0 | 810.7 | 5 | | 195502 | 10000 | 20000 | 0.811 | 0.869 | 0.856 |
| 65 | 5 | IPC-2 | 70 | 76-16 | 5.2 | 4.5 | 187.5 | 134.5 | 717.47 | 5 | | 195502 | 10000 | 20000 | 0.801 | 0.861 | 0.847 |
| 66 | 9 | IPC-2 | 70 | 76-16 | 5.2 | 4.5 | 187.5 | 149.0 | 794.4 | 5 | | 195502 | 10000 | 20000 | 0.801 | 0.861 | 0.847 |
| 67 | 4 | IPC-1 | 70 | 76-16 | 5.2 | 4.5 | 237.5 | 185.8 | 782.5 | 5 | | 32445 | 10000 | 20000 | 0.737 | 0.776 | 0.753 |

| | | | | | | | | | | | | | | | | | |
|---|---|---|---|---|---|---|---|---|---|---|---|---|---|---|---|---|---|
| 68 | 8 | IPC-1 | 70 | 76-16 | 5.2 | 4.5 | 237.5 | 181.5 | 764.32 | 5 | | 32445 | 10000 | 20000 | 0.717 | 0.758 | 0.734 |
| 69 | 21 | IPC-2 | 70 | 76-16 | 5.2 | 4.5 | 237.5 | 175.5 | 738.95 | 5 | | 32445 | 10000 | 20000 | 0.773 | 0.807 | 0.787 |
| 70 | 19 | IPC-1 | 70 | 76-16 | 5.2 | 9.5 | 187.5 | 105.7 | 563.63 | 5 | | 124280 | 10000 | 20000 | 0.766 | 0.828 | 0.811 |
| 71 | 15 | IPC-1 | 70 | 76-16 | 5.2 | 9.5 | 187.5 | 107.4 | 572.85 | 5 | | 124280 | 10000 | 20000 | 0.745 | 0.814 | 0.795 |
| 72 | 18 | IPC-2 | 70 | 76-16 | 5.2 | 9.5 | 187.5 | 113.1 | 603.42 | 5 | | 124280 | 10000 | 20000 | 0.759 | 0.823 | 0.805 |
| 73 | 2 | IPC-1 | 100 | 76-16 | 4.2 | 4.5 | 237.5 | 57.5 | 241.93 | 5 | | 108407 | 10000 | 20000 | 0.851 | 0.890 | 0.878 |
| 74 | 3 | IPC-1 | 100 | 76-16 | 4.2 | 4.5 | 237.5 | 80.6 | 339.53 | 5 | | 108407 | 10000 | 20000 | 0.863 | 0.899 | 0.888 |
| 75 | 7 | IPC-2 | 100 | 76-16 | 4.2 | 4.5 | 237.5 | 49.5 | 208.41 | 5 | | 108407 | 10000 | 20000 | 0.853 | 0.891 | 0.880 |
| 76 | 16 | IPC-1 | 100 | 76-16 | 4.2 | 4.5 | 325 | 47.5 | 146.28 | 5 | | 46138 | 10000 | 20000 | 0.722 | 0.772 | 0.749 |
| 77 | 18 | IPC-1 | 100 | 76-16 | 4.2 | 4.5 | 325 | 72.9 | 224.23 | 5 | | 46138 | 10000 | 20000 | 0.742 | 0.789 | 0.767 |
| 78 | 22 | IPC-2 | 100 | 76-16 | 4.2 | 4.5 | 325 | 53.8 | 165.41 | 5 | | 46138 | 10000 | 20000 | 0.741 | 0.788 | 0.767 |
| 79 | 18 | IPC-1 | 100 | 76-16 | 4.2 | 9.5 | 237.5 | 45.6 | 192.07 | 5 | | 59581 | 10000 | 20000 | 0.718 | 0.776 | 0.754 |
| 80 | 28 | IPC-1 | 100 | 76-16 | 4.2 | 9.5 | 237.5 | 43.3 | 182.29 | 5 | | 59581 | 10000 | 20000 | 0.750 | 0.801 | 0.781 |
| 81 | 23 | IPC-2 | 100 | 76-16 | 4.2 | 9.5 | 237.5 | 45.0 | 189.34 | 5 | | 59581 | 10000 | 20000 | 0.832 | 0.867 | 0.853 |
| 82 | 14 | IPC-1 | 100 | 76-16 | 4.2 | 9.5 | 325 | 49.0 | 150.64 | 5 | | 25357 | 10000 | 20000 | 0.652 | 0.693 | 0.662 |
| 83 | 5 | IPC-2 | 100 | 76-16 | 4.2 | 9.5 | 325 | 58.3 | 179.34 | 5 | | 25357 | 10000 | 20000 | 0.661 | 0.702 | 0.672 |
| 84 | 10 | IPC-2 | 100 | 76-16 | 4.2 | 9.5 | 325 | 55.1 | 169.65 | 5 | | 25357 | 10000 | 20000 | 0.659 | 0.700 | 0.669 |
| 85 | 15 | IPC-1 | 100 | 76-16 | 5.2 | 4.5 | 237.5 | 44.6 | 187.87 | 5 | | 337869 | 10000 | 20000 | 0.893 | 0.929 | 0.922 |
| 86 | 12 | IPC-2 | 100 | 76-16 | 5.2 | 4.5 | 237.5 | 46.7 | 196.68 | 5 | | 337869 | 10000 | 20000 | 0.944 | 0.963 | 0.959 |
| 87 | 7 | IPC-2 | 100 | 76-16 | 5.2 | 4.5 | 237.5 | 54.3 | 228.53 | 5 | | 337869 | 10000 | 20000 | 0.894 | 0.929 | 0.922 |
| 88 | 29 | IPC-1 | 100 | 76-16 | 5.2 | 4.5 | 325 | 61.4 | 188.93 | 5 | | 143797 | 10000 | 20000 | 0.796 | 0.853 | 0.838 |
| 89 | 31 | IPC-2 | 100 | 76-16 | 5.2 | 4.5 | 325 | 63.9 | 196.59 | 5 | | 143797 | 10000 | 20000 | 0.766 | 0.832 | 0.815 |
| 90 | 32 | IPC-2 | 100 | 76-16 | 5.2 | 4.5 | 325 | 62.2 | 191.52 | 5 | | 143797 | 10000 | 20000 | 0.736 | 0.809 | 0.790 |
| 91 | 33 | IPC-1 | 100 | 76-16 | 5.2 | 9.5 | 237.5 | 32.8 | 137.93 | 5 | | 185694 | 10000 | 20000 | 0.829 | 0.880 | 0.868 |
| 92 | 16 | IPC-2 | 100 | 76-16 | 5.2 | 9.5 | 237.5 | 26.2 | 110.19 | 5 | | 185694 | 10000 | 20000 | 0.796 | 0.856 | 0.842 |

| | | | | | | | | | | | | | | | | | |
|---|---|---|---|---|---|---|---|---|---|---|---|---|---|---|---|---|---|
| 93 | 17 | IPC-2 | 100 | 76-16 | 5.2 | 9.5 | 237.5 | 25.8 | 108.79 | 5 | | 185694 | 10000 | 20000 | 0.785 | 0.849 | 0.834 |
| 94 | 5 | IPC-1 | 100 | 76-16 | 5.2 | 9.5 | 325 | 40.4 | 124.27 | 5 | | 79031 | 10000 | 20000 | 0.679 | 0.753 | 0.728 |
| 95 | 6 | IPC-1 | 100 | 76-16 | 5.2 | 9.5 | 325 | 38.3 | 117.77 | 5 | | 79031 | 10000 | 20000 | 0.689 | 0.760 | 0.736 |
| 96 | 25 | IPC-2 | 100 | 76-16 | 5.2 | 9.5 | 325 | 31.8 | 97.799 | 5 | | 79031 | 10000 | 20000 | 0.686 | 0.758 | 0.734 |
| 97 | 36 | IPC-2 | 40 | 76-16 | 4.2 | 4.5 | 137.5 | 314.3 | 2286.1 | 0 | 294160 | 305580 | 100000 | 200000 | 0.493 | 0.545 | 0.511 |
| 98 | 40 | IPC-1 | 40 | 76-16 | 4.2 | 4.5 | 137.5 | 306.6 | 2229.7 | 0 | 317000 | 305580 | 100000 | 200000 | 0.506 | 0.557 | 0.524 |
| 99 | 34 | IPC-1 | 40 | 76-16 | 4.2 | 4.5 | 195 | 355.1 | 1820.9 | 0 | 5830 | 5405 | 1000 | 2500 | 0.503 | 0.678 | 0.605 |
| 100 | 27 | IPC-2 | 40 | 76-16 | 4.2 | 4.5 | 195 | 313.0 | 1604.9 | 0 | 4980 | 5405 | 1000 | 2500 | 0.496 | 0.669 | 0.594 |
| 101 | 3 | IPC-2 | 40 | 76-16 | 4.2 | 9.5 | 175 | 214.7 | 1226.8 | 0 | 18200 | 19165 | 5000 | 9000 | 0.494 | 0.601 | 0.560 |
| 102 | 2 | IPC-2 | 40 | 76-16 | 4.2 | 9.5 | 175 | 259.4 | 1482 | 0 | 20130 | 19165 | 5000 | 10000 | 0.504 | 0.611 | 0.565 |
| 103 | 39 | IPC-1 | 40 | 76-16 | 5.2 | 4.5 | 175 | 352.5 | 2014.2 | 0 | 28640 | 30415 | 7500 | 15000 | 0.489 | 0.590 | 0.544 |
| 104 | 36 | IPC-1 | 40 | 76-16 | 5.2 | 4.5 | 175 | 342.1 | 1954.6 | 0 | 32190 | 30415 | 5000 | 15000 | 0.512 | 0.636 | 0.568 |
| 105 | 38 | IPC-1 | 40 | 76-16 | 5.2 | 4.5 | 195 | 261.7 | 1341.9 | 0 | 8650 | 7625 | 2000 | 4000 | 0.521 | 0.651 | 0.601 |
| 106 | 37 | IPC-1 | 40 | 76-16 | 5.2 | 4.5 | 195 | 265.9 | 1363.6 | 0 | 6600 | 7625 | 2000 | 3000 | 0.486 | 0.619 | 0.586 |
| 107 | 43 | IPC-2 | 40 | 76-16 | 5.2 | 9.5 | 137.5 | 205.2 | 1492.1 | 0 | 211050 | 220845 | 50000 | 100000 | 0.493 | 0.565 | 0.530 |
| 108 | 34 | IPC-2 | 40 | 76-16 | 5.2 | 9.5 | 137.5 | 211.2 | 1536.2 | 0 | 230640 | 220845 | 50000 | 100000 | 0.514 | 0.585 | 0.551 |
| 109 | 35 | IPC-2 | 40 | 76-16 | 5.2 | 9.5 | 195 | 228.2 | 1170.2 | 0 | 4445 | 4965 | 1500 | 2500 | 0.494 | 0.630 | 0.587 |
| 110 | 39 | IPC-2 | 40 | 76-16 | 5.2 | 9.5 | 195 | 227.0 | 1164 | 0 | 5485 | 4965 | 2000 | 3000 | 0.505 | 0.622 | 0.590 |
| 111 | 29 | IPC-1 | 70 | 76-16 | 4.2 | 4.5 | 187.5 | 137.4 | 732.96 | 0 | 82920 | 108690 | 20000 | 40000 | 0.478 | 0.567 | 0.526 |
| 112 | 33 | IPC-1 | 70 | 76-16 | 4.2 | 4.5 | 187.5 | 159.6 | 851.01 | 0 | 134460 | 108690 | 40000 | 70000 | 0.530 | 0.587 | 0.560 |
| 113 | 37 | IPC-1 | 70 | 76-16 | 4.2 | 9.5 | 237.5 | 166.3 | 700.09 | 0 | 13780 | 12213 | 4000 | 7000 | 0.511 | 0.615 | 0.577 |
| 114 | 9 | IPC-1 | 70 | 76-16 | 4.2 | 9.5 | 237.5 | 161.5 | 679.98 | 0 | 10645 | 12213 | 4000 | 6000 | 0.485 | 0.586 | 0.556 |
| 115 | 19 | IPC-1 | 70 | 76-16 | 4.2 | 9.5 | 262.5 | 150.6 | 573.59 | 0 | 4980 | 4380 | 1000 | 1500 | 0.509 | 0.675 | 0.643 |
| 116 | 25 | IPC-1 | 70 | 76-16 | 4.2 | 9.5 | 262.5 | 181.1 | 689.83 | 0 | 3780 | 4380 | 1000 | 1500 | 0.481 | 0.650 | 0.614 |
| 117 | 30 | IPC-1 | 70 | 76-16 | 5.2 | 9.5 | 187.5 | 115.5 | 615.84 | 0 | 137600 | 126160 | 35000 | 60000 | 0.520 | 0.588 | 0.560 |

| | | | | | | | | | | | | | | | | | |
|---|---|---|---|---|---|---|---|---|---|---|---|---|---|---|---|---|---|
| 118 | 29 | IPC-2 | 70 | 76-16 | 5.2 | 9.5 | 187.5 | 109.9 | 586.17 | 0 | 114720 | 126160 | 30000 | 60000 | 0.485 | 0.562 | 0.524 |
| 119 | 36 | IPC-1 | 70 | 76-16 | 5.2 | 9.5 | 262.5 | 145.4 | 554.04 | 0 | 9405 | 8780 | 2000 | 4000 | 0.524 | 0.656 | 0.607 |
| 120 | 32 | IPC-1 | 70 | 76-16 | 5.2 | 9.5 | 262.5 | 141.3 | 538.14 | 0 | 8155 | 8780 | 2000 | 4000 | 0.487 | 0.628 | 0.574 |
| 121 | 32 | IPC-2 | 100 | 76-16 | 4.2 | 4.5 | 325 | 64.7 | 198.95 | 0 | 55660 | 52290 | 10000 | 25000 | 0.521 | 0.621 | 0.569 |
| 122 | 28 | IPC-2 | 100 | 76-16 | 4.2 | 4.5 | 325 | 60.0 | 184.62 | 0 | 48920 | 52290 | 10000 | 25000 | 0.485 | 0.591 | 0.535 |
| 123 | 31 | IPC-1 | 100 | 76-16 | 4.2 | 9.5 | 237.5 | 33.3 | 140.03 | 0 | 59155 | 61942 | 15000 | 30000 | 0.498 | 0.584 | 0.544 |
| 124 | 38 | IPC-2 | 100 | 76-16 | 4.2 | 9.5 | 237.5 | 33.8 | 142.26 | 0 | 64729 | 61942 | 20000 | 30000 | 0.505 | 0.576 | 0.553 |
| 125 | 33 | IPC-2 | 100 | 76-16 | 5.2 | 4.5 | 237.5 | 42.9 | 180.61 | 0 | 372847 | 342101 | 100000 | 200000 | 0.531 | 0.584 | 0.553 |
| 126 | 35 | IPC-2 | 100 | 76-16 | 5.2 | 4.5 | 237.5 | 41.9 | 176.32 | 0 | 311355 | 342101 | 100000 | 200000 | 0.473 | 0.530 | 0.495 |
| 127 | 34 | IPC-2 | 100 | 76-16 | 5.2 | 4.5 | 415 | 57.0 | 137.36 | 0 | 63280 | 59960 | 20000 | 30000 | 0.513 | 0.581 | 0.558 |
| 128 | 30 | IPC-2 | 100 | 76-16 | 5.2 | 4.5 | 415 | 60.8 | 146.48 | 0 | 56640 | 59960 | 10000 | 20000 | 0.484 | 0.597 | 0.555 |
| 129 | 25 | IPC-2 | 40 | 76-16 | 4.2 | 4.5 | 195 | 396.8 | 2034.9 | 10 | | 5405 | 2000 | 3000 | 0.782 | 0.817 | 0.803 |
| 130 | 31 | IPC-2 | 40 | 76-16 | 4.2 | 4.5 | 195 | 393.1 | 2015.8 | 10 | | 5405 | 2000 | 3000 | 0.811 | 0.841 | 0.829 |
| 131 | 40 | IPC-1 | 40 | 76-16 | 5.2 | 9.5 | 137.5 | 181.3 | 1318.3 | 1 | | 220845 | 10000 | 20000 | 0.730 | 0.814 | 0.795 |
| 132 | 38 | IPC-2 | 40 | 76-16 | 5.2 | 9.5 | 137.5 | 183.0 | 1330.6 | 1 | | 220845 | 10000 | 20000 | 0.763 | 0.836 | 0.820 |
| 133 | 42 | IPC-1 | 40 | 76-16 | 5.2 | 9.5 | 137.5 | 212.7 | 1546.7 | 10 | | 220845 | 10000 | 20000 | 0.878 | 0.916 | 0.907 |
| 134 | 21 | IPC-2 | 40 | 76-16 | 5.2 | 9.5 | 137.5 | 203.7 | 1481.7 | 10 | | 220845 | 10000 | 20000 | 0.880 | 0.917 | 0.909 |
| 135 | 37 | IPC-1 | 40 | 76-16 | 5.2 | 9.5 | 195 | 267.6 | 1372.3 | 5 | | 4965 | 1000 | 2500 | 0.731 | 0.801 | 0.761 |
| 136 | 41 | IPC-2 | 40 | 76-16 | 5.2 | 9.5 | 195 | 249.3 | 1278.6 | 5 | | 4965 | 1000 | 2500 | 0.696 | 0.774 | 0.729 |
| 137 | 15 | IPC-1 | 70 | 76-16 | 4.2 | 4.5 | 237.5 | 190.0 | 800.17 | 1 | | 15757 | 5000 | 10000 | 0.673 | 0.724 | 0.693 |
| 138 | 30 | IPC-2 | 70 | 76-16 | 4.2 | 4.5 | 237.5 | 204.1 | 859.2 | 1 | | 15757 | 5000 | 10000 | 0.613 | 0.673 | 0.637 |
| 139 | 26 | IPC-1 | 70 | 76-16 | 4.2 | 9.5 | 187.5 | 138.5 | 738.45 | 1 | | 80410 | 10000 | 20000 | 0.619 | 0.707 | 0.678 |
| 140 | 27 | IPC-1 | 70 | 76-16 | 4.2 | 9.5 | 187.5 | 124.1 | 662.11 | 1 | | 80410 | 10000 | 20000 | 0.651 | 0.732 | 0.705 |
| 141 | 29 | IPC-2 | 70 | 76-16 | 4.2 | 9.5 | 237.5 | 200.8 | 845.29 | 10 | | 12213 | 5000 | 10000 | 0.726 | 0.760 | 0.733 |
| 142 | 27 | IPC-1 | 70 | 76-16 | 5.2 | 9.5 | 237.5 | 128.9 | 542.9 | 5 | | 17388 | 5000 | 10000 | 0.748 | 0.790 | 0.766 |

| | | | | | | | | | | | | | | | | | |
|---|---|---|---|---|---|---|---|---|---|---|---|---|---|---|---|---|---|
| 143 | 26 | IPC-2 | 70 | 76-16 | 5.2 | 9.5 | 237.5 | 140.5 | 591.46 | 5 | | 17388 | 5000 | 10000 | 0.692 | 0.743 | 0.715 |
| 144 | 28 | IPC-1 | 70 | 76-16 | 5.2 | 9.5 | 262.5 | 182.3 | 694.4 | 10 | | 8780 | 2000 | 4000 | 0.675 | 0.746 | 0.712 |
| 145 | 3 | IPC-2 | 70 | 76-16 | 5.2 | 9.5 | 262.5 | 159.8 | 608.76 | 10 | | 8780 | 2000 | 4000 | 0.700 | 0.765 | 0.734 |
| 146 | 35 | IPC-2 | 100 | 76-16 | 4.2 | 9.5 | 325 | 51.7 | 159.05 | 1 | | 24314 | 10000 | 20000 | 0.608 | 0.653 | 0.618 |
| 147 | 36 | IPC-2 | 100 | 76-16 | 4.2 | 9.5 | 325 | 53.9 | 165.91 | 1 | | 24314 | 10000 | 20000 | 0.609 | 0.653 | 0.618 |
| 148 | 27 | IPC-1 | 100 | 76-16 | 5.2 | 4.5 | 325 | 62.6 | 192.73 | 10 | | 125897 | 10000 | 20000 | 0.733 | 0.804 | 0.785 |
| 149 | 26 | IPC-2 | 100 | 76-16 | 5.2 | 4.5 | 325 | 59.4 | 182.73 | 10 | | 125897 | 10000 | 20000 | 0.801 | 0.854 | 0.840 |
| 150 | 11 | IPC-2 | 100 | 76-16 | 5.2 | 4.5 | 415 | 58.7 | 141.42 | 1 | | 59960 | 10000 | 20000 | 0.654 | 0.725 | 0.697 |
| 151 | 25 | IPC-1 | 100 | 76-16 | 5.2 | 4.5 | 415 | 105.2 | 253.5 | 1 | | 59960 | 10000 | 20000 | 0.684 | 0.749 | 0.724 |
| 152 | 7 | IPC-1 | 40 | 64-22 | 4.2 | 4.5 | 100 | 231.0 | 2310.3 | 0 | 140000 | 135000 | 35000 | 70000 | 0.508 | 0.579 | 0.543 |
| 153 | 3 | IPC-1 | 40 | 64-22 | 4.2 | 4.5 | 150 | 222.5 | 1483.2 | 0 | 36000 | 25263 | 7000 | 15000 | 0.526 | 0.628 | 0.583 |
| 154 | 2 | IPC-2 | 40 | 64-22 | 4.2 | 4.5 | 150 | 294.9 | 1966.2 | 0 | 22150 | 25263 | 5000 | 10000 | 0.485 | 0.603 | 0.556 |
| 155 | 14 | IPC-1 | 40 | 64-22 | 4.2 | 4.5 | 100 | 130.1 | 1300.5 | 0 | 130000 | 135000 | 30000 | 60000 | 0.491 | 0.572 | 0.534 |
| 156 | 15 | IPC-1 | 40 | 64-22 | 4.2 | 4.5 | 150 | 283.6 | 1890.7 | 0 | 17640 | 25263 | 3000 | 9000 | 0.461 | 0.615 | 0.534 |
| 157 | 19 | IPC-2 | 40 | 64-22 | 4.2 | 4.5 | 100 | 129.8 | 1297.5 | 0 | 135000 | 135000 | 30000 | 60000 | 0.500 | 0.580 | 0.543 |
| 158 | 2 | IPC-1 | 40 | 64-22 | 4.2 | 9.5 | 100 | 126.7 | 1267.1 | 0 | 385000 | 228333 | 100000 | 200000 | 0.541 | 0.593 | 0.563 |
| 159 | 4 | IPC-2 | 40 | 64-22 | 4.2 | 9.5 | 100 | 126.7 | 1267.1 | 0 | 170000 | 228333 | 50000 | 90000 | 0.459 | 0.530 | 0.497 |
| 160 | 14 | IPC-2 | 40 | 64-22 | 4.2 | 9.5 | 100 | 125.3 | 1253.1 | 0 | 130000 | 228333 | 40000 | 70000 | 0.486 | 0.552 | 0.521 |
| 161 | 13 | IPC-1 | 40 | 64-22 | 5.2 | 4.5 | 150 | 189.0 | 1260.2 | 0 | 58430 | 91801 | 10000 | 30000 | 0.456 | 0.579 | 0.509 |
| 162 | 30 | IPC-2 | 40 | 64-22 | 5.2 | 4.5 | 150 | 256.4 | 1709.1 | 0 | 122543 | 91801 | 30000 | 60000 | 0.516 | 0.589 | 0.553 |
| 163 | 27 | IPC-2 | 40 | 64-22 | 5.2 | 4.5 | 150 | 207.5 | 1383.2 | 0 | 140000 | 91801 | 30000 | 70000 | 0.521 | 0.597 | 0.554 |
| 164 | 1 | IPC-2 | 40 | 64-22 | 5.2 | 4.5 | 150 | 261.0 | 1740.3 | 0 | 46230 | 91801 | 10000 | 20000 | 0.523 | 0.615 | 0.576 |
| 165 | 1 | IPC-1 | 40 | 64-22 | 5.2 | 9.5 | 100 | 113.9 | 1139.3 | 0 | 300000 | 215000 | 100000 | 200000 | 0.478 | 0.533 | 0.498 |
| 166 | 7 | IPC-2 | 40 | 64-22 | 5.2 | 9.5 | 100 | 110.1 | 1100.9 | 0 | 130000 | 215000 | 30000 | 60000 | 0.519 | 0.593 | 0.558 |
| 167 | 11 | IPC-1 | 40 | 64-22 | 5.2 | 9.5 | 150 | 172.0 | 1146.6 | 0 | 35480 | 33077 | 10000 | 20000 | 0.504 | 0.591 | 0.549 |

| | | | | | | | | | | | | | | | | | |
|---|---|---|---|---|---|---|---|---|---|---|---|---|---|---|---|---|---|
| 168 | 16 | IPC-2 | 40 | 64-22 | 5.2 | 9.5 | 150 | 156.8 | 1045 | 0 | 39400 | 33077 | 10000 | 20000 | 0.516 | 0.604 | 0.563 |
| 169 | 15 | IPC-1 | 40 | 64-22 | 5.2 | 9.5 | 150 | 135.0 | 899.85 | 0 | 24350 | 33077 | 5000 | 10000 | 0.471 | 0.599 | 0.551 |
| 170 | 9 | IPC-1 | 70 | 64-22 | 4.2 | 4.5 | 200 | 120.2 | 601.04 | 0 | 70000 | 80667 | 20000 | 35000 | 0.481 | 0.562 | 0.529 |
| 171 | 4 | IPC-2 | 70 | 64-22 | 4.2 | 4.5 | 200 | 130.1 | 650.65 | 0 | 82000 | 80667 | 20000 | 40000 | 0.502 | 0.583 | 0.545 |
| 172 | 24 | IPC-1 | 70 | 64-22 | 4.2 | 4.5 | 200 | 146.9 | 734.45 | 0 | 90000 | 80667 | 20000 | 45000 | 0.521 | 0.602 | 0.559 |
| 173 | 8 | IPC-1 | 70 | 64-22 | 4.2 | 9.5 | 137.5 | 102.0 | 742.12 | 0 | 44490 | 127417 | 10000 | 20000 | 0.476 | 0.581 | 0.537 |
| 174 | 11 | IPC-1 | 70 | 64-22 | 4.2 | 9.5 | 200 | 150.6 | 752.84 | 0 | 56660 | 55433 | 10000 | 25000 | 0.500 | 0.607 | 0.554 |
| 175 | 16 | IPC-1 | 70 | 64-22 | 4.2 | 9.5 | 137.5 | 117.9 | 857.73 | 0 | 67760 | 127417 | 15000 | 30000 | 0.521 | 0.606 | 0.568 |
| 176 | 17 | IPC-1 | 70 | 64-22 | 4.2 | 9.5 | 200 | 116.1 | 580.49 | 0 | 57830 | 55433 | 10000 | 25000 | 0.504 | 0.611 | 0.558 |
| 177 | 7 | IPC-2 | 70 | 64-22 | 4.2 | 9.5 | 137.5 | 53.8 | 391.25 | 0 | 270000 | 127417 | 50000 | 140000 | 0.516 | 0.592 | 0.544 |
| 178 | 20 | IPC-2 | 70 | 64-22 | 4.2 | 9.5 | 200 | 115.1 | 575.28 | 0 | 51810 | 55433 | 10000 | 25000 | 0.471 | 0.585 | 0.527 |
| 179 | 25 | IPC-1 | 70 | 64-22 | 5.2 | 4.5 | 137.5 | 83.9 | 610.21 | 0 | 221300 | 415210 | 50000 | 100000 | 0.491 | 0.566 | 0.531 |
| 180 | 18 | IPC-2 | 70 | 64-22 | 5.2 | 4.5 | 137.5 | 50.3 | 365.71 | 0 | 700000 | 415210 | 100000 | 300000 | 0.501 | 0.582 | 0.533 |
| 181 | 26 | IPC-1 | 70 | 64-22 | 5.2 | 4.5 | 137.5 | 105.8 | 769.23 | 0 | 324330 | 415210 | 100000 | 200000 | 0.521 | 0.570 | 0.538 |
| 182 | 10 | IPC-1 | 70 | 64-22 | 5.2 | 9.5 | 200 | 90.8 | 453.8 | 0 | 104710 | 106773 | 20000 | 50000 | 0.499 | 0.591 | 0.541 |
| 183 | 21 | IPC-1 | 70 | 64-22 | 5.2 | 9.5 | 200 | 81.7 | 408.49 | 0 | 63090 | 106773 | 10000 | 30000 | 0.476 | 0.596 | 0.529 |
| 184 | 20 | IPC-2 | 70 | 64-22 | 5.2 | 9.5 | 200 | 97.1 | 485.71 | 0 | 152520 | 106773 | 50000 | 100000 | 0.527 | 0.579 | 0.545 |
| 185 | 12 | IPC-1 | 100 | 64-22 | 4.2 | 4.5 | 312.5 | 48.3 | 154.68 | 0 | 157680 | 101233 | 30000 | 75000 | 0.546 | 0.620 | 0.577 |
| 186 | 17 | IPC-1 | 100 | 64-22 | 4.2 | 4.5 | 312.5 | 45.9 | 146.91 | 0 | 45000 | 101233 | 10000 | 20000 | 0.455 | 0.568 | 0.522 |
| 187 | 8 | IPC-2 | 100 | 64-22 | 4.2 | 4.5 | 312.5 | 61.8 | 197.88 | 0 | 101020 | 101233 | 20000 | 50000 | 0.500 | 0.591 | 0.541 |
| 188 | 6 | IPC-2 | 100 | 64-22 | 4.2 | 9.5 | 387.5 | 43.2 | 111.51 | 0 | 9680 | 9180 | 3000 | 4500 | 0.502 | 0.614 | 0.584 |
| 189 | 26 | IPC-1 | 100 | 64-22 | 4.2 | 9.5 | 387.5 | 57.6 | 148.75 | 0 | 11410 | 9180 | 3000 | 5000 | 0.513 | 0.629 | 0.593 |
| 190 | 9 | IPC-2 | 100 | 64-22 | 4.2 | 9.5 | 387.5 | 31.4 | 81.124 | 0 | 6450 | 9180 | 2000 | 3000 | 0.487 | 0.618 | 0.586 |
| 191 | 17 | IPC-1 | 100 | 64-22 | 5.2 | 4.5 | 387.5 | 37.1 | 95.735 | 0 | 110060 | 114283 | 30000 | 50000 | 0.497 | 0.570 | 0.542 |
| 192 | 20 | IPC-1 | 100 | 64-22 | 5.2 | 4.5 | 387.5 | 28.8 | 74.409 | 0 | 80860 | 114283 | 20000 | 40000 | 0.475 | 0.564 | 0.523 |

| | | | | | | | | | | | | | | | | | |
|---|---|---|---|---|---|---|---|---|---|---|---|---|---|---|---|---|---|
| 193 | 22 | IPC-1 | 100 | 64-22 | 5.2 | 4.5 | 387.5 | 70.8 | 182.81 | 0 | 151930 | 114283 | 40000 | 75000 | 0.523 | 0.587 | 0.556 |
| 194 | 2 | IPC-2 | 100 | 64-22 | 5.2 | 9.5 | 312.5 | 19.5 | 62.416 | 0 | 72720 | 70550 | 20000 | 35000 | 0.504 | 0.581 | 0.549 |
| 195 | 6 | IPC-1 | 100 | 64-22 | 5.2 | 9.5 | 312.5 | 24.1 | 77.213 | 0 | 57960 | 70550 | 10000 | 25000 | 0.476 | 0.593 | 0.536 |
| 196 | 5 | IPC-2 | 100 | 64-22 | 5.2 | 9.5 | 312.5 | 37.1 | 118.76 | 0 | 80970 | 70550 | 20000 | 40000 | 0.524 | 0.599 | 0.562 |
| 197 | 10 | IPC-1 | 40 | 64-22 | 4.2 | 4.5 | 100 | 190.0 | 1900.3 | 5 | | 179804 | 10000 | 20000 | 0.815 | 0.869 | 0.856 |
| 198 | 21 | IPC-2 | 40 | 64-22 | 4.2 | 4.5 | 100 | 201.7 | 2016.9 | 5 | | 179804 | 10000 | 20000 | 0.961 | 0.972 | 0.970 |
| 199 | 22 | IPC-2 | 40 | 64-22 | 4.2 | 4.5 | 100 | 193.6 | 1935.7 | 5 | | 179804 | 10000 | 20000 | 0.958 | 0.970 | 0.967 |
| 200 | 12 | IPC-2 | 40 | 64-22 | 4.2 | 9.5 | 150 | 317.9 | 2119 | 5 | | 21419 | 10000 | 20000 | 0.805 | 0.825 | 0.807 |
| 201 | 21 | IPC-2 | 40 | 64-22 | 4.2 | 9.5 | 150 | 214.0 | 1426.7 | 5 | | 21419 | 10000 | 20000 | 0.857 | 0.872 | 0.859 |
| 202 | 23 | IPC-2 | 40 | 64-22 | 4.2 | 9.5 | 150 | 214.9 | 1432.9 | 5 | | 21419 | 10000 | 20000 | 0.832 | 0.849 | 0.834 |
| 203 | 2 | IPC-1 | 40 | 64-22 | 5.2 | 4.5 | 100 | 229.6 | 2296 | 5 | | 362911 | 10000 | 20000 | 0.960 | 0.974 | 0.971 |
| 204 | 5 | IPC-1 | 40 | 64-22 | 5.2 | 4.5 | 100 | 249.8 | 2498.3 | 5 | | 362911 | 10000 | 20000 | 0.947 | 0.966 | 0.962 |
| 205 | 15 | IPC-1 | 40 | 64-22 | 5.2 | 4.5 | 100 | 102.1 | 1020.5 | 5 | | 362911 | 10000 | 20000 | 0.930 | 0.954 | 0.949 |
| 206 | 10 | IPC-1 | 40 | 64-22 | 5.2 | 4.5 | 150 | 232.2 | 1547.9 | 5 | | 59402 | 10000 | 20000 | 0.887 | 0.910 | 0.901 |
| 207 | 12 | IPC-1 | 40 | 64-22 | 5.2 | 4.5 | 150 | 219.5 | 1463.4 | 5 | | 59402 | 10000 | 20000 | 0.914 | 0.932 | 0.925 |
| 208 | 23 | IPC-2 | 40 | 64-22 | 5.2 | 4.5 | 150 | 333.2 | 2221.1 | 5 | | 59402 | 10000 | 20000 | 0.908 | 0.927 | 0.919 |
| 209 | 9 | IPC-1 | 40 | 64-22 | 5.2 | 9.5 | 100 | 144.4 | 1443.6 | 5 | | 264119 | 10000 | 20000 | 0.921 | 0.946 | 0.941 |
| 210 | 4 | IPC-2 | 40 | 64-22 | 5.2 | 9.5 | 100 | 150.1 | 1500.8 | 5 | | 264119 | 10000 | 20000 | 0.920 | 0.945 | 0.940 |
| 211 | 18 | IPC-1 | 40 | 64-22 | 5.2 | 9.5 | 100 | 143.2 | 1431.7 | 5 | | 264119 | 10000 | 20000 | 0.929 | 0.952 | 0.947 |
| 212 | 12 | IPC-1 | 40 | 64-22 | 5.2 | 9.5 | 150 | 215.1 | 1434.2 | 5 | | 43231 | 10000 | 20000 | 0.917 | 0.932 | 0.925 |
| 213 | 13 | IPC-1 | 40 | 64-22 | 5.2 | 9.5 | 150 | 215.1 | 1434.2 | 5 | | 43231 | 10000 | 20000 | 0.880 | 0.901 | 0.891 |
| 214 | 25 | IPC-2 | 40 | 64-22 | 5.2 | 9.5 | 150 | 217.7 | 1451.6 | 5 | | 43231 | 10000 | 20000 | 0.880 | 0.901 | 0.891 |
| 215 | 5 | IPC-1 | 70 | 64-22 | 4.2 | 4.5 | 137.5 | 110.4 | 802.64 | 5 | | 136082 | 10000 | 20000 | 0.883 | 0.915 | 0.906 |
| 216 | 23 | IPC-1 | 70 | 64-22 | 4.2 | 4.5 | 137.5 | 123.7 | 899.79 | 5 | | 136082 | 10000 | 20000 | 0.853 | 0.894 | 0.883 |
| 217 | 13 | IPC-2 | 70 | 64-22 | 4.2 | 4.5 | 137.5 | 118.1 | 858.94 | 5 | | 136082 | 10000 | 20000 | 0.869 | 0.905 | 0.895 |

| | | | | | | | | | | | | | | | | | |
|---|---|---|---|---|---|---|---|---|---|---|---|---|---|---|---|---|---|
| 218 | 11 | IPC-1 | 70 | 64-22 | 4.2 | 4.5 | 200 | 159.7 | 798.26 | 5 | | 79442 | 10000 | 20000 | 0.745 | 0.804 | 0.784 |
| 219 | 29 | IPC-2 | 70 | 64-22 | 4.2 | 4.5 | 200 | 155.7 | 778.39 | 5 | | 79442 | 10000 | 20000 | 0.843 | 0.879 | 0.867 |
| 220 | 20 | IPC-1 | 70 | 64-22 | 4.2 | 4.5 | 200 | 146.0 | 730.13 | 5 | | 79442 | 10000 | 20000 | 0.830 | 0.870 | 0.856 |
| 221 | 15 | IPC-1 | 70 | 64-22 | 4.2 | 9.5 | 137.5 | 87.2 | 634.51 | 5 | | 92534 | 10000 | 20000 | 0.916 | 0.936 | 0.930 |
| 222 | 22 | IPC-1 | 70 | 64-22 | 4.2 | 9.5 | 137.5 | 84.8 | 616.73 | 5 | | 92534 | 10000 | 20000 | 0.853 | 0.889 | 0.878 |
| 223 | 1 | IPC-2 | 70 | 64-22 | 4.2 | 9.5 | 137.5 | 66.5 | 483.89 | 5 | | 10000 | 20000 | | 0.843 | 0.827 | |
| 224 | 4 | IPC-1 | 70 | 64-22 | 5.2 | 4.5 | 200 | 195.0 | 974.77 | 5 | | 145898 | 10000 | 20000 | 0.767 | 0.832 | 0.815 |
| 225 | 24 | IPC-1 | 70 | 64-22 | 5.2 | 4.5 | 200 | 151.5 | 757.71 | 5 | | 145898 | 10000 | 20000 | 0.884 | 0.916 | 0.908 |
| 226 | 19 | IPC-2 | 70 | 64-22 | 5.2 | 4.5 | 200 | 97.0 | 485.07 | 5 | | 145898 | 10000 | 20000 | 0.816 | 0.867 | 0.854 |
| 227 | 14 | IPC-1 | 70 | 64-22 | 5.2 | 9.5 | 137.5 | 80.6 | 586.21 | 5 | | 169942 | 10000 | 20000 | 0.912 | 0.938 | 0.932 |
| 228 | 22 | IPC-2 | 70 | 64-22 | 5.2 | 9.5 | 137.5 | 77.0 | 560.18 | 5 | | 169942 | 10000 | 20000 | 0.885 | 0.919 | 0.910 |
| 229 | 23 | IPC-2 | 70 | 64-22 | 5.2 | 9.5 | 137.5 | 79.4 | 577.1 | 5 | | 169942 | 10000 | 20000 | 0.883 | 0.917 | 0.909 |
| 230 | 8 | IPC-1 | 70 | 64-22 | 5.2 | 9.5 | 200 | 107.8 | 538.99 | 5 | | 99209 | 10000 | 20000 | 0.774 | 0.830 | 0.813 |
| 231 | 19 | IPC-1 | 70 | 64-22 | 5.2 | 9.5 | 200 | 102.0 | 509.96 | 5 | | 99209 | 10000 | 20000 | 0.820 | 0.864 | 0.851 |
| 232 | 17 | IPC-2 | 70 | 64-22 | 5.2 | 9.5 | 200 | 103.5 | 517.69 | 5 | | 99209 | 10000 | 20000 | 0.848 | 0.886 | 0.875 |
| 233 | 28 | IPC-1 | 100 | 64-22 | 4.2 | 4.5 | 387.5 | 70.5 | 181.82 | 5 | | 35592 | 10000 | 20000 | 0.751 | 0.789 | 0.768 |
| 234 | 27 | IPC-1 | 100 | 64-22 | 4.2 | 4.5 | 387.5 | 83.5 | 215.39 | 5 | | 35592 | 10000 | 20000 | 0.741 | 0.781 | 0.759 |
| 235 | 6 | IPC-2 | 100 | 64-22 | 4.2 | 4.5 | 387.5 | 63.5 | 163.8 | 5 | | 35592 | 10000 | 20000 | 0.730 | 0.772 | 0.749 |
| 236 | 13 | IPC-1 | 100 | 64-22 | 4.2 | 9.5 | 312.5 | 40.5 | 129.59 | 5 | | 22483 | 10000 | 20000 | 0.849 | 0.864 | 0.851 |
| 237 | 10 | IPC-2 | 100 | 64-22 | 4.2 | 9.5 | 312.5 | 40.4 | 129.39 | 5 | | 22483 | 10000 | 20000 | 0.745 | 0.772 | 0.749 |
| 238 | 19 | IPC-1 | 100 | 64-22 | 4.2 | 9.5 | 312.5 | 40.7 | 130.2 | 5 | | 22483 | 10000 | 20000 | 0.784 | 0.807 | 0.787 |
| 239 | 3 | IPC-1 | 100 | 64-22 | 4.2 | 9.5 | 387.5 | 50.9 | 131.28 | 5 | | 8940 | 2000 | 4000 | 0.700 | 0.766 | 0.736 |
| 240 | 24 | IPC-1 | 100 | 64-22 | 4.2 | 9.5 | 387.5 | 50.8 | 131.03 | 5 | | 2000 | 4000 | | 0.688 | 0.647 | |
| 241 | 5 | IPC-2 | 100 | 64-22 | 4.2 | 9.5 | 387.5 | 48.3 | 124.7 | 5 | | 8940 | 2000 | 4000 | 0.700 | 0.766 | 0.736 |
| 242 | 16 | IPC-1 | 100 | 64-22 | 5.2 | 4.5 | 312.5 | 43.5 | 139.29 | 5 | | 278516 | 10000 | 20000 | 0.898 | 0.931 | 0.924 |

| | | | | | | | | | | | | | | | | | |
|---|---|---|---|---|---|---|---|---|---|---|---|---|---|---|---|---|---|
| 243 | 11 | IPC-2 | 100 | 64-22 | 5.2 | 4.5 | 312.5 | 33.5 | 107.19 | 5 | | 278516 | 10000 | 20000 | 0.857 | 0.903 | 0.894 |
| 244 | 9 | IPC-2 | 100 | 64-22 | 5.2 | 4.5 | 312.5 | 37.0 | 118.52 | 5 | | 278516 | 10000 | 20000 | 0.858 | 0.904 | 0.894 |
| 245 | 26 | IPC-1 | 100 | 64-22 | 5.2 | 9.5 | 387.5 | 49.0 | 126.41 | 5 | | 27820 | 10000 | 20000 | 0.750 | 0.782 | 0.761 |
| 246 | 3 | IPC-2 | 100 | 64-22 | 5.2 | 9.5 | 387.5 | 37.3 | 96.236 | 5 | | 27820 | 10000 | 20000 | 0.762 | 0.793 | 0.772 |
| 247 | 24 | IPC-2 | 100 | 64-22 | 5.2 | 9.5 | 387.5 | 35.7 | 92.163 | 5 | | 27820 | 10000 | 20000 | 0.747 | 0.780 | 0.758 |
| 248 | 35 | IPC-1 | 40 | 64-22 | 4.2 | 9.5 | 150 | 205.8 | 1371.9 | 0 | 14930 | 21535 | 4000 | 7500 | 0.497 | 0.609 | 0.565 |
| 249 | 43 | IPC-2 | 40 | 64-22 | 4.2 | 9.5 | 150 | 196.5 | 1309.8 | 0 | 28140 | 21535 | 7500 | 15000 | 0.506 | 0.601 | 0.557 |
| 250 | 39 | IPC-1 | 40 | 64-22 | 4.2 | 9.5 | 215 | 262.7 | 1221.8 | 0 | 2820 | 2615 | 1000 | 1500 | 0.504 | 0.650 | 0.615 |
| 251 | 40 | IPC-2 | 40 | 64-22 | 4.2 | 9.5 | 215 | 255.7 | 1189.1 | 0 | 2410 | 2615 | 1000 | 1500 | 0.497 | 0.639 | 0.603 |
| 252 | 40 | IPC-1 | 40 | 64-22 | 5.2 | 4.5 | 100 | 150.2 | 1502 | 0 | 357470 | 338245 | 100000 | 200000 | 0.516 | 0.570 | 0.538 |
| 253 | 42 | IPC-2 | 40 | 64-22 | 5.2 | 4.5 | 100 | 155.6 | 1556 | 0 | 319020 | 338245 | 100000 | 200000 | 0.482 | 0.538 | 0.504 |
| 254 | 41 | IPC-2 | 40 | 64-22 | 5.2 | 4.5 | 215 | 299.6 | 1393.7 | 0 | 4450 | 5380 | 1000 | 2000 | 0.486 | 0.659 | 0.600 |
| 255 | 44 | IPC-2 | 40 | 64-22 | 5.2 | 4.5 | 215 | 310.5 | 1444.1 | 0 | 6310 | 5380 | 200 | 4000 | 0.521 | 0.638 | 0.585 |
| 256 | 38 | IPC-1 | 70 | 64-22 | 4.2 | 4.5 | 137.5 | 88.1 | 640.5 | 0 | 130000 | 145000 | 30000 | 60000 | 0.486 | 0.568 | 0.530 |
| 257 | 45 | IPC-1 | 70 | 64-22 | 4.2 | 4.5 | 137.5 | 99.4 | 723.16 | 0 | 160000 | 145000 | 30000 | 80000 | 0.526 | 0.606 | 0.558 |
| 258 | 44 | IPC-1 | 70 | 64-22 | 4.2 | 9.5 | 280 | 170.3 | 608.25 | 0 | 14260 | 25130 | 3000 | 7500 | 0.476 | 0.615 | 0.547 |
| 259 | 42 | IPC-1 | 70 | 64-22 | 4.2 | 9.5 | 280 | 179.8 | 642.2 | 0 | 36000 | 25130 | 7500 | 15000 | 0.529 | 0.626 | 0.586 |
| 260 | 35 | IPC-1 | 70 | 64-22 | 5.2 | 4.5 | 200 | 117.2 | 585.98 | 0 | 129930 | 139015 | 30000 | 65000 | 0.490 | 0.571 | 0.529 |
| 261 | 36 | IPC-2 | 70 | 64-22 | 5.2 | 4.5 | 200 | 126.8 | 634.16 | 0 | 148100 | 139015 | 50000 | 75000 | 0.511 | 0.566 | 0.545 |
| 262 | 8 | IPC-1 | 70 | 64-22 | 5.2 | 4.5 | 280 | 158.8 | 566.98 | 0 | 55300 | 64000 | 10000 | 25000 | 0.485 | 0.597 | 0.541 |
| 263 | 39 | IPC-1 | 70 | 64-22 | 5.2 | 4.5 | 280 | 167.0 | 596.31 | 0 | 72700 | 64000 | 20000 | 35000 | 0.521 | 0.593 | 0.563 |
| 264 | 31 | IPC-2 | 70 | 64-22 | 5.2 | 9.5 | 137.5 | 66.7 | 485.1 | 0 | 176050 | 167725 | 35000 | 90000 | 0.530 | 0.604 | 0.558 |
| 265 | 32 | IPC-2 | 70 | 64-22 | 5.2 | 9.5 | 137.5 | 60.5 | 440.29 | 0 | 159400 | 167725 | 25000 | 80000 | 0.481 | 0.582 | 0.519 |
| 266 | 42 | IPC-1 | 100 | 64-22 | 4.2 | 4.5 | 387.5 | 63.5 | 163.9 | 0 | 31296 | 34983 | 7500 | 15000 | 0.490 | 0.594 | 0.550 |
| 267 | 16 | IPC-1 | 100 | 64-22 | 4.2 | 4.5 | 387.5 | 65.1 | 168.02 | 0 | 38670 | 34983 | 7500 | 15000 | 0.511 | 0.617 | 0.576 |

| | | | | | | | | | | | | | | | | | |
|---|---|---|---|---|---|---|---|---|---|---|---|---|---|---|---|---|---|
| 268 | 40 | IPC-2 | 100 | 64-22 | 4.2 | 4.5 | 420 | 54.7 | 130.34 | 0 | 23470 | 25610 | 5000 | 12500 | 0.486 | 0.606 | 0.544 |
| 269 | 41 | IPC-1 | 100 | 64-22 | 4.2 | 4.5 | 420 | 55.8 | 132.78 | 0 | 27750 | 25610 | 5000 | 15000 | 0.512 | 0.630 | 0.561 |
| 270 | 48 | IPC-1 | 100 | 64-22 | 4.2 | 9.5 | 312.5 | 48.3 | 154.52 | 0 | 23888 | 26802 | 5000 | 10000 | 0.479 | 0.603 | 0.555 |
| 271 | 46 | IPC-2 | 100 | 64-22 | 4.2 | 9.5 | 312.5 | 33.9 | 108.43 | 0 | 29716 | 26802 | 5000 | 10000 | 0.521 | 0.638 | 0.596 |
| 272 | 58 | IPC-1 | 100 | 64-22 | 4.2 | 9.5 | 420 | 47.0 | 111.99 | 0 | 5773 | 6249 | 1000 | 2000 | 0.484 | 0.668 | 0.611 |
| 273 | 45 | IPC-2 | 100 | 64-22 | 4.2 | 9.5 | 420 | 37.7 | 89.842 | 0 | 6725 | 6249 | 1000 | 3000 | 0.517 | 0.690 | 0.608 |
| 274 | 46 | IPC-2 | 100 | 64-22 | 5.2 | 4.5 | 312.5 | 38.9 | 124.52 | 0 | 278840 | 266425 | 70000 | 120000 | 0.524 | 0.584 | 0.559 |
| 275 | 43 | IPC-2 | 100 | 64-22 | 5.2 | 4.5 | 312.5 | 36.5 | 116.84 | 0 | 254010 | 266425 | 50000 | 100000 | 0.485 | 0.567 | 0.532 |
| 276 | 29 | IPC-2 | 100 | 64-22 | 5.2 | 9.5 | 387.5 | 35.3 | 91 | 0 | 30755 | 27320 | 7500 | 15000 | 0.514 | 0.610 | 0.567 |
| 277 | 30 | IPC-2 | 100 | 64-22 | 5.2 | 9.5 | 387.5 | 36.5 | 94.138 | 0 | 23885 | 27320 | 5000 | 10000 | 0.489 | 0.609 | 0.563 |
| 278 | 33 | IPC-2 | 100 | 64-22 | 5.2 | 9.5 | 420 | 34.7 | 82.714 | 0 | 19271 | 18461 | 5000 | 10000 | 0.510 | 0.614 | 0.568 |
| 279 | 37 | IPC-1 | 100 | 64-22 | 5.2 | 9.5 | 420 | 35.9 | 85.486 | 0 | 17650 | 18461 | 5000 | 9000 | 0.491 | 0.597 | 0.556 |
| 280 | 34 | IPC-2 | 40 | 64-22 | 4.2 | 4.5 | 150 | 293.7 | 1958.3 | 5 | | 25263 | 10000 | 20000 | 0.778 | 0.805 | 0.785 |
| 281 | 36 | IPC-1 | 40 | 64-22 | 4.2 | 4.5 | 150 | 276.5 | 1843.3 | 5 | | 25263 | 10000 | 20000 | 0.900 | 0.912 | 0.903 |
| 282 | 38 | IPC-2 | 40 | 64-22 | 4.2 | 9.5 | 100 | 164.3 | 1643.2 | 5 | | 228333 | 10000 | 20000 | 0.909 | 0.937 | 0.931 |
| 283 | 30 | IPC-2 | 40 | 64-22 | 4.2 | 9.5 | 100 | 151.2 | 1512.4 | 5 | | 228333 | 10000 | 20000 | 0.839 | 0.890 | 0.878 |
| 284 | 36 | IPC-1 | 40 | 64-22 | 4.2 | 9.5 | 215 | 353.6 | 1644.7 | 1 | | 2615 | 600 | 1000 | 0.747 | 0.814 | 0.790 |
| 285 | 37 | IPC-1 | 40 | 64-22 | 4.2 | 9.5 | 215 | 335.3 | 1559.5 | 1 | | 2615 | 600 | 1000 | 0.702 | 0.781 | 0.754 |
| 286 | 6 | IPC-2 | 40 | 64-22 | 5.2 | 4.5 | 150 | 275.1 | 1834.1 | 1 | | 106991 | 10000 | 20000 | 0.804 | 0.854 | 0.840 |
| 287 | 37 | IPC-1 | 40 | 64-22 | 5.2 | 4.5 | 150 | 265.3 | 1768.7 | 1 | | 106991 | 10000 | 20000 | 0.789 | 0.843 | 0.828 |
| 288 | 47 | IPC-1 | 40 | 64-22 | 5.2 | 4.5 | 215 | 479.1 | 2228.2 | 10 | | 5380 | 2500 | | 0.882 | 0.896 | |
| 289 | 3 | IPC-2 | 40 | 64-22 | 5.2 | 4.5 | 215 | 347.1 | 1614.6 | 10 | | 5380 | 1500 | 2500 | 0.872 | 0.898 | 0.887 |
| 290 | 28 | IPC-2 | 70 | 64-22 | 4.2 | 9.5 | 280 | 150.5 | 537.59 | 5 | | 25130 | 10000 | 20000 | 0.745 | 0.775 | 0.752 |
| 291 | 18 | IPC-2 | 70 | 64-22 | 4.2 | 9.5 | 280 | 163.8 | 585.17 | 5 | | 25130 | 10000 | 20000 | 0.726 | 0.758 | 0.734 |
| 292 | 31 | IPC-2 | 70 | 64-22 | 5.2 | 4.5 | 137.5 | 100.0 | 727.25 | 10 | | 272815 | 10000 | 20000 | 0.928 | 0.952 | 0.947 |

| | | | | | | | | | | | | | | | | | |
|---|---|---|---|---|---|---|---|---|---|---|---|---|---|---|---|---|---|
| 293 | 7 | IPC-2 | 70 | 64-22 | 5.2 | 4.5 | 137.5 | 105.9 | 770.11 | 10 | | 272815 | 10000 | 20000 | 0.950 | 0.966 | 0.963 |
| 294 | 29 | IPC-1 | 70 | 64-22 | 5.2 | 4.5 | 280 | 201.2 | 718.57 | 1 | | 64000 | 10000 | 20000 | 0.732 | 0.789 | 0.767 |
| 295 | 38 | IPC-2 | 70 | 64-22 | 5.2 | 4.5 | 280 | 194.2 | 693.53 | 1 | | 64000 | 10000 | 20000 | 0.698 | 0.762 | 0.738 |
| 296 | 38 | IPC-2 | 70 | 64-22 | 5.2 | 9.5 | 200 | 100.6 | 502.87 | 1 | | 106773 | 10000 | 20000 | 0.716 | 0.789 | 0.767 |
| 297 | 28 | IPC-1 | 70 | 64-22 | 5.2 | 9.5 | 200 | 105.8 | 529.16 | 1 | | 106773 | 10000 | 20000 | 0.752 | 0.816 | 0.797 |
| 298 | 43 | IPC-1 | 100 | 64-22 | 4.2 | 4.5 | 312.5 | 58.0 | 185.51 | 1 | | 101233 | 10000 | 20000 | 0.812 | 0.859 | 0.845 |
| 299 | 44 | IPC-2 | 100 | 64-22 | 4.2 | 4.5 | 312.5 | 50.8 | 162.53 | 1 | | 101233 | 10000 | 20000 | 0.682 | 0.762 | 0.738 |
| 300 | 35 | IPC-2 | 100 | 64-22 | 4.2 | 4.5 | 420 | 75.0 | 178.48 | 5 | | 25610 | 10000 | 20000 | 0.762 | 0.791 | 0.770 |
| 301 | 39 | IPC-2 | 100 | 64-22 | 4.2 | 4.5 | 420 | 68.8 | 163.81 | 5 | | 25610 | 10000 | 20000 | 0.634 | 0.678 | 0.646 |
| 302 | 29 | IPC-1 | 100 | 64-22 | 4.2 | 9.5 | 420 | 56.8 | 135.28 | 10 | | 6249 | 2000 | 4000 | 0.670 | 0.728 | 0.693 |
| 303 | 31 | IPC-1 | 100 | 64-22 | 4.2 | 9.5 | 420 | 54.2 | 129.08 | 10 | | 6249 | 2000 | 4000 | 0.680 | 0.737 | 0.702 |
| 304 | 27 | IPC-1 | 100 | 64-22 | 5.2 | 9.5 | 312.5 | 33.0 | 105.56 | 1 | | 70550 | 10000 | 20000 | 0.786 | 0.834 | 0.817 |
| 305 | 35 | IPC-1 | 100 | 64-22 | 5.2 | 9.5 | 312.5 | 32.1 | 102.74 | 1 | | 70550 | 10000 | 20000 | 0.785 | 0.832 | 0.815 |
| 306 | 20 | IPC-1 | 40 | 58-28 | 4.2 | 4.5 | 145 | 191.1 | 1317.6 | 0 | 71250 | 75423 | 20000 | 35000 | 0.495 | 0.573 | 0.540 |
| 307 | 24 | IPC-1 | 40 | 58-28 | 4.2 | 4.5 | 145 | 221.6 | 1528.5 | 0 | 85000 | 75423 | 20000 | 40000 | 0.519 | 0.597 | 0.560 |
| 308 | 19 | IPC-2 | 40 | 58-28 | 4.2 | 4.5 | 145 | 194.6 | 1342 | 0 | 70020 | 75423 | 20000 | 35000 | 0.486 | 0.566 | 0.533 |
| 309 | 4 | IPC-1 | 40 | 58-28 | 4.2 | 9.5 | 170 | 204.9 | 1205.3 | 0 | 30760 | 33393 | 7500 | 15000 | 0.491 | 0.594 | 0.550 |
| 310 | 20 | IPC-1 | 40 | 58-28 | 4.2 | 9.5 | 170 | 179.7 | 1056.9 | 0 | 22610 | 33393 | 5000 | 10000 | 0.478 | 0.600 | 0.552 |
| 311 | 18 | IPC-2 | 40 | 58-28 | 4.2 | 9.5 | 170 | 250.7 | 1474.7 | 0 | 46810 | 33393 | 10000 | 20000 | 0.524 | 0.617 | 0.577 |
| 312 | 5 | IPC-1 | 40 | 58-28 | 5.2 | 4.5 | 170 | 199.9 | 1176 | 0 | 36160 | 43530 | 7500 | 15000 | 0.481 | 0.594 | 0.550 |
| 313 | 7 | IPC-1 | 40 | 58-28 | 5.2 | 4.5 | 170 | 207.8 | 1222.1 | 0 | 53970 | 43530 | 15000 | 25000 | 0.524 | 0.599 | 0.570 |
| 314 | 9 | IPC-1 | 40 | 58-28 | 5.2 | 4.5 | 170 | 205.3 | 1207.4 | 0 | 40460 | 43530 | 10000 | 20000 | 0.497 | 0.592 | 0.549 |
| 315 | 2 | IPC-1 | 40 | 58-28 | 5.2 | 9.5 | 145 | 153.4 | 1058 | 0 | 79000 | 81487 | 20000 | 40000 | 0.498 | 0.579 | 0.540 |
| 316 | 19 | IPC-2 | 40 | 58-28 | 5.2 | 9.5 | 145 | 152.8 | 1054 | 0 | 88900 | 81487 | 20000 | 40000 | 0.514 | 0.596 | 0.558 |
| 317 | 21 | IPC-2 | 40 | 58-28 | 5.2 | 9.5 | 145 | 163.8 | 1129.7 | 0 | 76560 | 81487 | 20000 | 35000 | 0.494 | 0.575 | 0.543 |

| | | | | | | | | | | | | | | | | | |
|---|---|---|---|---|---|---|---|---|---|---|---|---|---|---|---|---|---|
| 318 | 6 | IPC-1 | 70 | 58-28 | 4.2 | 4.5 | 200 | 82.4 | 411.94 | 0 | 38210 | 40860 | 10000 | 15000 | 0.494 | 0.588 | 0.562 |
| 319 | 1 | IPC-2 | 70 | 58-28 | 4.2 | 4.5 | 200 | 72.8 | 364.06 | 0 | 39350 | 40860 | 10000 | 20000 | 0.498 | 0.591 | 0.549 |
| 320 | 11 | IPC-2 | 70 | 58-28 | 4.2 | 4.5 | 200 | 110.7 | 553.27 | 0 | 45020 | 40860 | 10000 | 20000 | 0.514 | 0.608 | 0.567 |
| 321 | 2 | IPC-1 | 70 | 58-28 | 4.2 | 9.5 | 262.5 | 97.2 | 370.27 | 0 | 23760 | 25480 | 5000 | 10000 | 0.494 | 0.612 | 0.566 |
| 322 | 22 | IPC-1 | 70 | 58-28 | 4.2 | 9.5 | 262.5 | 73.0 | 277.93 | 0 | 27760 | 25480 | 5000 | 12000 | 0.521 | 0.635 | 0.582 |
| 323 | 37 | IPC-2 | 70 | 58-28 | 4.2 | 9.5 | 262.5 | 112.1 | 427 | 0 | 24920 | 25480 | 5000 | 12000 | 0.498 | 0.617 | 0.560 |
| 324 | 3 | IPC-1 | 70 | 58-28 | 5.2 | 4.5 | 262.5 | 118.1 | 449.81 | 0 | 54230 | 53827 | 15000 | 25000 | 0.502 | 0.584 | 0.554 |
| 325 | 12 | IPC-1 | 70 | 58-28 | 5.2 | 4.5 | 262.5 | 109.9 | 418.65 | 0 | 58540 | 53827 | 15000 | 25000 | 0.521 | 0.600 | 0.572 |
| 326 | 20 | IPC-2 | 70 | 58-28 | 5.2 | 4.5 | 262.5 | 96.4 | 367.3 | 0 | 48710 | 53827 | 10000 | 20000 | 0.478 | 0.587 | 0.543 |
| 327 | 17 | IPC-1 | 70 | 58-28 | 5.2 | 9.5 | 200 | 41.0 | 204.83 | 0 | 79640 | 80480 | 20000 | 35000 | 0.499 | 0.581 | 0.549 |
| 328 | 4 | IPC-2 | 70 | 58-28 | 5.2 | 9.5 | 200 | 52.6 | 262.77 | 0 | 85659 | 80480 | 20000 | 40000 | 0.519 | 0.598 | 0.561 |
| 329 | 12 | IPC-2 | 70 | 58-28 | 5.2 | 9.5 | 200 | 67.3 | 336.28 | 0 | 76140 | 80480 | 20000 | 35000 | 0.488 | 0.570 | 0.538 |
| 330 | 18 | IPC-1 | 70 | 58-28 | 5.2 | 9.5 | 262.5 | 74.4 | 283.51 | 0 | 25310 | 26833 | 5000 | 12000 | 0.495 | 0.615 | 0.558 |
| 331 | 20 | IPC-1 | 70 | 58-28 | 5.2 | 9.5 | 262.5 | 60.8 | 231.46 | 0 | 30080 | 26833 | 7000 | 15000 | 0.516 | 0.615 | 0.568 |
| 332 | 11 | IPC-2 | 70 | 58-28 | 5.2 | 9.5 | 262.5 | 71.2 | 271.12 | 0 | 25110 | 26833 | 5000 | 12000 | 0.497 | 0.616 | 0.559 |
| 333 | 22 | IPC-1 | 100 | 58-28 | 4.2 | 4.5 | 415 | 29.3 | 70.682 | 0 | 20673 | 23488 | 5000 | 10000 | 0.485 | 0.600 | 0.552 |
| 334 | 3 | IPC-2 | 100 | 58-28 | 4.2 | 4.5 | 415 | 28.8 | 69.44 | 0 | 22550 | 23488 | 5000 | 10000 | 0.498 | 0.612 | 0.566 |
| 335 | 10 | IPC-2 | 100 | 58-28 | 4.2 | 4.5 | 415 | 28.0 | 67.415 | 0 | 27240 | 23488 | 7000 | 12000 | 0.521 | 0.614 | 0.581 |
| 336 | 26 | IPC-1 | 100 | 58-28 | 4.2 | 9.5 | 295 | 19.3 | 65.312 | 0 | 100000 | 89187 | 20000 | 50000 | 0.523 | 0.607 | 0.560 |
| 337 | 16 | IPC-2 | 100 | 58-28 | 4.2 | 9.5 | 295 | 21.1 | 71.434 | 0 | 93430 | 89187 | 20000 | 40000 | 0.504 | 0.591 | 0.553 |
| 338 | 17 | IPC-2 | 100 | 58-28 | 4.2 | 9.5 | 295 | 17.2 | 58.327 | 0 | 74130 | 89187 | 20000 | 35000 | 0.480 | 0.564 | 0.531 |
| 339 | 22 | IPC-1 | 100 | 58-28 | 5.2 | 4.5 | 295 | 15.4 | 52.25 | 0 | 185000 | 182797 | 35000 | 90000 | 0.502 | 0.586 | 0.538 |
| 340 | 16 | IPC-2 | 100 | 58-28 | 5.2 | 4.5 | 295 | 15.1 | 51.297 | 0 | 203390 | 182797 | 50000 | 100000 | 0.524 | 0.588 | 0.555 |
| 341 | 24 | IPC-1 | 100 | 58-28 | 5.2 | 4.5 | 295 | 15.0 | 50.798 | 0 | 160000 | 89187 | 20000 | 35000 | 0.478 | 0.555 | 0.517 |
| 342 | 11 | IPC-1 | 100 | 58-28 | 5.2 | 4.5 | 415 | 24.1 | 57.996 | 0 | 43000 | 182797 | 35000 | 90000 | 0.498 | 0.595 | 0.553 |

| | | | | | | | | | | | | | | | | | |
|---|---|---|---|---|---|---|---|---|---|---|---|---|---|---|---|---|---|
| 343 | 1 | IPC-2 | 100 | 58-28 | 5.2 | 4.5 | 415 | 24.2 | 58.2 | 0 | 38000 | 182797 | 50000 | 100000 | 0.479 | 0.599 | 0.550 |
| 344 | 23 | IPC-1 | 100 | 58-28 | 5.2 | 4.5 | 415 | 25.3 | 60.958 | 0 | 58000 | 182797 | 40000 | 80000 | 0.529 | 0.605 | 0.577 |
| 345 | 15 | IPC-1 | 100 | 58-28 | 5.2 | 9.5 | 415 | 19.4 | 46.753 | 0 | 43000 | 46333 | 10000 | 20000 | 0.503 | 0.599 | 0.557 |
| 346 | 7 | IPC-2 | 100 | 58-28 | 5.2 | 9.5 | 415 | 17.9 | 43.241 | 0 | 47000 | 46333 | 7000 | 15000 | 0.513 | 0.609 | 0.569 |
| 347 | 5 | IPC-2 | 100 | 58-28 | 5.2 | 9.5 | 415 | 14.1 | 34.051 | 0 | 33000 | 46333 | 15000 | 25000 | 0.478 | 0.615 | 0.543 |
| 348 | 41 | IPC-1 | 40 | 58-28 | 4.2 | 4.5 | 170 | 237.2 | 1395 | 5 | | 41000 | 10000 | 20000 | 0.912 | 0.925 | 0.918 |
| 349 | 5 | IPC-2 | 40 | 58-28 | 4.2 | 4.5 | 170 | 251.7 | 1480.7 | 5 | | 41000 | 10000 | 20000 | 0.850 | 0.874 | 0.861 |
| 350 | 7 | IPC-2 | 40 | 58-28 | 4.2 | 4.5 | 170 | 249.6 | 1468.3 | 5 | | 41000 | 5000 | 15000 | 0.860 | 0.882 | 0.870 |
| 351 | 1 | IPC-1 | 40 | 58-28 | 4.2 | 9.5 | 145 | 222.6 | 1534.9 | 5 | | 35661 | 10000 | 20000 | 0.888 | 0.912 | 0.903 |
| 352 | 7 | IPC-2 | 40 | 58-28 | 4.2 | 9.5 | 145 | 176.4 | 1216.7 | 5 | | 35661 | 10000 | 20000 | 0.868 | 0.896 | 0.886 |
| 353 | 3 | IPC-2 | 40 | 58-28 | 4.2 | 9.5 | 145 | 169.1 | 1166.3 | 5 | | 35661 | 10000 | 20000 | 0.877 | 0.904 | 0.894 |
| 354 | 6 | IPC-1 | 40 | 58-28 | 5.2 | 4.5 | 145 | 189.8 | 1308.8 | 5 | | 67569 | 10000 | 20000 | 0.915 | 0.936 | 0.929 |
| 355 | 18 | IPC-1 | 40 | 58-28 | 5.2 | 4.5 | 145 | 183.2 | 1263.3 | 5 | | 67569 | 10000 | 20000 | 0.960 | 0.970 | 0.967 |
| 356 | 15 | IPC-2 | 40 | 58-28 | 5.2 | 4.5 | 145 | 195.6 | 1349.2 | 5 | | 67569 | 10000 | 20000 | 0.930 | 0.947 | 0.941 |
| 357 | 3 | IPC-1 | 40 | 58-28 | 5.2 | 9.5 | 145 | 190.0 | 1310.6 | 5 | | 90784 | 10000 | 20000 | 0.940 | 0.954 | 0.949 |
| 358 | 10 | IPC-2 | 40 | 58-28 | 5.2 | 9.5 | 145 | 173.2 | 1194.6 | 5 | | 90784 | 10000 | 20000 | 0.925 | 0.943 | 0.937 |
| 359 | 29 | IPC-1 | 40 | 58-28 | 5.2 | 9.5 | 145 | 127.9 | 882.32 | 5 | | 90784 | 10000 | 20000 | 0.887 | 0.914 | 0.905 |
| 360 | 8 | IPC-1 | 40 | 58-28 | 5.2 | 9.5 | 170 | 186.9 | 1099.7 | 5 | | 81482 | 10000 | 20000 | 0.879 | 0.898 | 0.888 |
| 361 | 16 | IPC-2 | 40 | 58-28 | 5.2 | 9.5 | 170 | 191.4 | 1126.1 | 5 | | 81482 | 10000 | 20000 | 0.888 | 0.906 | 0.897 |
| 362 | 28 | IPC-2 | 40 | 58-28 | 5.2 | 9.5 | 170 | 179.9 | 1058.1 | 5 | | 81482 | 10000 | 20000 | 0.891 | 0.909 | 0.900 |
| 363 | 8 | IPC-1 | 70 | 58-28 | 4.2 | 4.5 | 262.5 | 115.5 | 440.04 | 5 | | 38598 | 10000 | 20000 | 0.768 | 0.797 | 0.777 |
| 364 | 2 | IPC-2 | 70 | 58-28 | 4.2 | 4.5 | 262.5 | 105.1 | 400.24 | 5 | | 38598 | 10000 | 20000 | 0.800 | 0.825 | 0.807 |
| 365 | 39 | IPC-2 | 70 | 58-28 | 4.2 | 4.5 | 262.5 | 145.5 | 554.11 | 5 | | 38598 | 10000 | 20000 | 0.753 | 0.784 | 0.762 |
| 366 | 8 | IPC-1 | 70 | 58-28 | 4.2 | 9.5 | 200 | 93.3 | 466.41 | 5 | | 26210 | 10000 | 20000 | 0.848 | 0.873 | 0.860 |
| 367 | 5 | IPC-1 | 70 | 58-28 | 4.2 | 9.5 | 200 | 73.6 | 367.77 | 5 | | 26210 | 10000 | 20000 | 0.845 | 0.870 | 0.857 |

| | | | | | | | | | | | | | | | | | |
|---|---|---|---|---|---|---|---|---|---|---|---|---|---|---|---|---|---|
| 368 | 24 | IPC-2 | 70 | 58-28 | 4.2 | 9.5 | 200 | 71.6 | 358.16 | 5 | | 26210 | 10000 | 20000 | 0.832 | 0.860 | 0.846 |
| 369 | 27 | IPC-1 | 70 | 58-28 | 4.2 | 9.5 | 262.5 | 114.7 | 437.09 | 5 | | 39288 | 10000 | 20000 | 0.781 | 0.803 | 0.783 |
| 370 | 21 | IPC-2 | 70 | 58-28 | 4.2 | 9.5 | 262.5 | 108.5 | 413.45 | 5 | | 39288 | 10000 | 20000 | 0.779 | 0.801 | 0.781 |
| 371 | 23 | IPC-2 | 70 | 58-28 | 4.2 | 9.5 | 262.5 | 79.1 | 301.49 | 5 | | 39288 | 10000 | 20000 | 0.729 | 0.755 | 0.731 |
| 372 | 10 | IPC-1 | 70 | 58-28 | 5.2 | 4.5 | 200 | 71.6 | 357.77 | 5 | | 21466 | 10000 | 20000 | 0.931 | 0.948 | 0.942 |
| 373 | 45 | IPC-1 | 70 | 58-28 | 5.2 | 4.5 | 200 | 113.6 | 568.08 | 5 | | 21466 | 10000 | 20000 | 0.905 | 0.927 | 0.919 |
| 374 | 46 | IPC-2 | 70 | 58-28 | 5.2 | 4.5 | 200 | 115.0 | 575.03 | 5 | | 21466 | 10000 | 20000 | 0.881 | 0.909 | 0.900 |
| 375 | 2 | IPC-1 | 70 | 58-28 | 5.2 | 4.5 | 262.5 | 112.8 | 429.67 | 5 | | 82935 | 10000 | 20000 | 0.805 | 0.840 | 0.824 |
| 376 | 13 | IPC-1 | 70 | 58-28 | 5.2 | 4.5 | 262.5 | 116.6 | 444 | 5 | | 82935 | 10000 | 20000 | 0.824 | 0.856 | 0.841 |
| 377 | 44 | IPC-2 | 70 | 58-28 | 5.2 | 4.5 | 262.5 | 79.9 | 304.44 | 5 | | 82935 | 10000 | 20000 | 0.826 | 0.857 | 0.843 |
| 378 | 22 | IPC-1 | 70 | 58-28 | 5.2 | 9.5 | 200 | 44.4 | 221.96 | 5 | | 45315 | 10000 | 20000 | 0.883 | 0.909 | 0.900 |
| 379 | 23 | IPC-1 | 70 | 58-28 | 5.2 | 9.5 | 200 | 55.8 | 278.97 | 5 | | 45315 | 10000 | 20000 | 0.851 | 0.883 | 0.872 |
| 380 | 14 | IPC-2 | 70 | 58-28 | 5.2 | 9.5 | 200 | 70.4 | 351.93 | 5 | | 45315 | 10000 | 20000 | 0.872 | 0.900 | 0.890 |
| 381 | 21 | IPC-1 | 100 | 58-28 | 4.2 | 4.5 | 295 | 22.5 | 76.134 | 5 | | 67926 | 10000 | 20000 | 0.837 | 0.878 | 0.866 |
| 382 | 12 | IPC-2 | 100 | 58-28 | 4.2 | 4.5 | 295 | 30.9 | 104.85 | 5 | | 67926 | 10000 | 20000 | 0.896 | 0.921 | 0.913 |
| 383 | 13 | IPC-2 | 100 | 58-28 | 4.2 | 4.5 | 295 | 27.6 | 93.614 | 5 | | 67926 | 10000 | 20000 | 0.868 | 0.900 | 0.890 |
| 384 | 23 | IPC-1 | 100 | 58-28 | 4.2 | 4.5 | 415 | 32.8 | 78.967 | 5 | | 96110 | 10000 | 20000 | 0.769 | 0.795 | 0.774 |
| 385 | 4 | IPC-2 | 100 | 58-28 | 4.2 | 4.5 | 415 | 29.0 | 69.917 | 5 | | 96110 | 10000 | 20000 | 0.718 | 0.748 | 0.723 |
| 386 | 42 | IPC-2 | 100 | 58-28 | 4.2 | 4.5 | 415 | 37.0 | 89.088 | 5 | | 96110 | 10000 | 20000 | 0.729 | 0.763 | 0.738 |
| 387 | 6 | IPC-1 | 100 | 58-28 | 4.2 | 9.5 | 415 | 33.6 | 80.906 | 5 | | 23484 | 10000 | 20000 | 0.756 | 0.780 | 0.758 |
| 388 | 15 | IPC-2 | 100 | 58-28 | 4.2 | 9.5 | 415 | 29.9 | 71.988 | 5 | | 23484 | 10000 | 20000 | 0.658 | 0.692 | 0.661 |
| 389 | 13 | IPC-1 | 100 | 58-28 | 4.2 | 9.5 | 415 | 31.3 | 75.472 | 5 | | 23484 | 10000 | 20000 | 0.702 | 0.732 | 0.705 |
| 390 | 14 | IPC-1 | 100 | 58-28 | 5.2 | 4.5 | 295 | 24.2 | 82.184 | 5 | | 21415 | 10000 | 20000 | 0.950 | 0.965 | 0.961 |
| 391 | 8 | IPC-2 | 100 | 58-28 | 5.2 | 4.5 | 295 | 24.4 | 82.602 | 5 | | 21415 | 10000 | 20000 | 0.919 | 0.943 | 0.938 |
| 392 | 19 | IPC-2 | 100 | 58-28 | 5.2 | 4.5 | 295 | 25.6 | 86.945 | 5 | | 21415 | 10000 | 20000 | 0.901 | 0.930 | 0.923 |

| | | | | | | | | | | | | | | | | | |
|---|---|---|---|---|---|---|---|---|---|---|---|---|---|---|---|---|---|
| 393 | 17 | IPC-1 | 100 | 58-28 | 5.2 | 4.5 | 415 | 34.7 | 83.513 | 5 | | 183209 | 10000 | 20000 | 0.798 | 0.834 | 0.818 |
| 394 | 21 | IPC-1 | 100 | 58-28 | 5.2 | 4.5 | 415 | 34.9 | 84.041 | 5 | | 183209 | 10000 | 20000 | 0.773 | 0.813 | 0.795 |
| 395 | 4 | IPC-2 | 100 | 58-28 | 5.2 | 4.5 | 415 | 26.2 | 63.205 | 5 | | 183209 | 10000 | 20000 | 0.764 | 0.807 | 0.787 |
| 396 | 1 | IPC-1 | 100 | 58-28 | 5.2 | 9.5 | 295 | 19.8 | 67.126 | 5 | | 44766 | 10000 | 20000 | 0.914 | 0.938 | 0.932 |
| 397 | 6 | IPC-2 | 100 | 58-28 | 5.2 | 9.5 | 295 | 18.8 | 63.861 | 5 | | 44766 | 10000 | 20000 | 0.884 | 0.918 | 0.910 |
| 398 | 9 | IPC-2 | 100 | 58-28 | 5.2 | 9.5 | 295 | 17.6 | 59.507 | 5 | | 44706 | 10000 | 20000 | 0.868 | 0.906 | 0.897 |
| 399 | 27 | IPC-1 | 100 | 58-28 | 5.2 | 9.5 | 415 | 16.6 | 39.906 | 5 | | 167069 | 10000 | 20000 | 0.777 | 0.815 | 0.796 |
| 400 | 26 | IPC-1 | 100 | 58-28 | 5.2 | 9.5 | 415 | 18.1 | 43.541 | 5 | | 167069 | 10000 | 20000 | 0.753 | 0.795 | 0.774 |
| 401 | 13 | IPC-2 | 100 | 58-28 | 5.2 | 9.5 | 415 | 21.1 | 50.798 | 5 | | 167069 | 10000 | 20000 | 0.744 | 0.787 | 0.766 |
| 402 | 32 | IPC-1 | 40 | 58-28 | 4.2 | 4.5 | 170 | 266.6 | 1568.2 | 0 | 34905 | 40822 | 10000 | 20000 | 0.492 | 0.582 | 0.538 |
| 403 | 33 | IPC-1 | 40 | 58-28 | 4.2 | 4.5 | 170 | 240.5 | 1414.6 | 0 | 37436 | 40822 | 10000 | 20000 | 0.512 | 0.600 | 0.575 |
| 404 | 26 | IPC-1 | 40 | 58-28 | 4.2 | 4.5 | 220 | 302.5 | 1375 | 0 | 8940 | 40822 | 10000 | 20000 | 0.508 | 0.644 | 0.593 |
| 405 | 40 | IPC-1 | 40 | 58-28 | 4.2 | 4.5 | 220 | 288.1 | 1309.6 | 0 | 7710 | 36171 | 10000 | 20000 | 0.492 | 0.629 | 0.597 |
| 406 | 28 | IPC-1 | 40 | 58-28 | 4.2 | 9.5 | 145 | 182.6 | 1259.2 | 0 | 62180 | 36171 | 10000 | 15000 | 0.496 | 0.609 | 0.544 |
| 407 | 31 | IPC-1 | 40 | 58-28 | 4.2 | 9.5 | 145 | 180.5 | 1244.8 | 0 | 65950 | 8325 | 2000 | 4000 | 0.502 | 0.592 | 0.552 |
| 408 | 25 | IPC-1 | 40 | 58-28 | 4.2 | 9.5 | 220 | 256.9 | 1167.7 | 0 | 6600 | 8325 | 2000 | 3000 | 0.494 | 0.646 | 0.592 |
| 409 | 30 | IPC-1 | 40 | 58-28 | 4.2 | 9.5 | 220 | 280.5 | 1275 | 0 | 7800 | 64065 | 10000 | 30000 | 0.508 | 0.639 | 0.597 |
| 410 | 43 | IPC-1 | 40 | 58-28 | 5.2 | 4.5 | 145 | 177.0 | 1220.4 | 0 | 98590 | 64065 | 15000 | 30000 | 0.507 | 0.573 | 0.551 |
| 411 | 31 | IPC-1 | 40 | 58-28 | 5.2 | 4.5 | 145 | 171.6 | 1183.2 | 0 | 93100 | 7200 | 1500 | 3000 | 0.496 | 0.562 | 0.540 |
| 412 | 39 | IPC-1 | 40 | 58-28 | 5.2 | 9.5 | 170 | 193.6 | 1138.9 | 0 | 36000 | 7200 | 2000 | 3500 | 0.486 | 0.597 | 0.553 |
| 413 | 30 | IPC-2 | 40 | 58-28 | 5.2 | 9.5 | 170 | 187.0 | 1100 | 0 | 44780 | 95845 | 30000 | 45000 | 0.516 | 0.626 | 0.568 |
| 414 | 34 | IPC-1 | 40 | 58-28 | 5.2 | 9.5 | 220 | 228.0 | 1036.3 | 0 | 7910 | 95845 | 30000 | 45000 | 0.488 | 0.650 | 0.584 |
| 415 | 31 | IPC-1 | 40 | 58-28 | 5.2 | 9.5 | 220 | 225.7 | 1025.8 | 0 | 10620 | 24560 | 7500 | 12000 | 0.513 | 0.654 | 0.605 |
| 416 | 43 | IPC-2 | 70 | 58-28 | 4.2 | 4.5 | 262.5 | 107.6 | 410.06 | 0 | 27630 | 24560 | 5000 | 10000 | 0.512 | 0.605 | 0.575 |
| 417 | 25 | IPC-2 | 70 | 58-28 | 4.2 | 4.5 | 262.5 | 147.1 | 560.27 | 0 | 21490 | 12360 | 4000 | 7000 | 0.488 | 0.604 | 0.557 |

| | | | | | | | | | | | | | | | | | |
|---|---|---|---|---|---|---|---|---|---|---|---|---|---|---|---|---|---|
| 418 | 27 | IPC-2 | 70 | 58-28 | 4.2 | 4.5 | 330 | 143.1 | 433.56 | 0 | 14040 | 12360 | 2000 | 5000 | 0.513 | 0.618 | 0.579 |
| 419 | 28 | IPC-2 | 70 | 58-28 | 4.2 | 4.5 | 330 | 141.7 | 429.53 | 0 | 10680 | 41750 | 10000 | 20000 | 0.485 | 0.638 | 0.569 |
| 420 | 39 | IPC-2 | 70 | 58-28 | 4.2 | 9.5 | 200 | 59.9 | 299.57 | 0 | 39300 | 41750 | 10000 | 20000 | 0.482 | 0.580 | 0.536 |
| 421 | 29 | IPC-2 | 70 | 58-28 | 4.2 | 9.5 | 200 | 80.6 | 403 | 0 | 44200 | 89935 | 15000 | 30000 | 0.517 | 0.610 | 0.569 |
| 422 | 33 | IPC-1 | 70 | 58-28 | 5.2 | 4.5 | 200 | 80.2 | 400.82 | 0 | 72570 | 89935 | 25000 | 50000 | 0.482 | 0.582 | 0.541 |
| 423 | 32 | IPC-2 | 70 | 58-28 | 5.2 | 4.5 | 200 | 93.2 | 466.13 | 0 | 107300 | 29650 | 7500 | 15000 | 0.517 | 0.594 | 0.557 |
| 424 | 42 | IPC-1 | 70 | 58-28 | 5.2 | 4.5 | 330 | 134.8 | 408.55 | 0 | 33160 | 29650 | 5000 | 12000 | 0.514 | 0.613 | 0.571 |
| 425 | 37 | IPC-2 | 70 | 58-28 | 5.2 | 4.5 | 330 | 111.5 | 337.82 | 0 | 26140 | 96535 | 30000 | 50000 | 0.489 | 0.613 | 0.555 |
| 426 | 30 | IPC-1 | 100 | 58-28 | 4.2 | 4.5 | 295 | 18.0 | 61.032 | 0 | 105510 | 96535 | 20000 | 40000 | 0.515 | 0.581 | 0.554 |
| 427 | 31 | IPC-2 | 100 | 58-28 | 4.2 | 4.5 | 295 | 25.1 | 85.158 | 0 | 87560 | 11185 | 2500 | 6000 | 0.487 | 0.576 | 0.536 |
| 428 | 35 | IPC-2 | 100 | 58-28 | 4.2 | 4.5 | 500 | 33.4 | 66.762 | 0 | 12300 | 11185 | 2000 | 4500 | 0.504 | 0.639 | 0.577 |
| 429 | 34 | IPC-2 | 100 | 58-28 | 4.2 | 4.5 | 500 | 33.7 | 67.486 | 0 | 10070 | 26760 | 5000 | 11000 | 0.496 | 0.642 | 0.582 |
| 430 | 9 | IPC-2 | 100 | 58-28 | 4.2 | 9.5 | 415 | 30.0 | 72.248 | 0 | 23500 | 26760 | 7500 | 15000 | 0.486 | 0.606 | 0.553 |
| 431 | 11 | IPC-2 | 100 | 58-28 | 4.2 | 9.5 | 415 | 26.2 | 63.196 | 0 | 30020 | 9255 | 2000 | 4000 | 0.513 | 0.609 | 0.566 |
| 432 | 33 | IPC-1 | 100 | 58-28 | 4.2 | 9.5 | 500 | 31.8 | 63.517 | 0 | 8040 | 9255 | 2500 | 5000 | 0.489 | 0.629 | 0.575 |
| 433 | 32 | IPC-2 | 100 | 58-28 | 4.2 | 9.5 | 500 | 30.8 | 61.622 | 0 | 10470 | 19575 | 5000 | 10000 | 0.511 | 0.637 | 0.587 |
| 434 | 35 | IPC-1 | 100 | 58-28 | 5.2 | 4.5 | 500 | 34.9 | 69.713 | 0 | 21420 | 19575 | 5000 | 9000 | 0.508 | 0.617 | 0.572 |
| 435 | 25 | IPC-1 | 100 | 58-28 | 5.2 | 4.5 | 500 | 23.2 | 46.352 | 0 | 17730 | 167565 | 30000 | 75000 | 0.496 | 0.617 | 0.579 |
| 436 | 32 | IPC-1 | 100 | 58-28 | 5.2 | 9.5 | 295 | 12.3 | 41.738 | 0 | 158740 | 167565 | 45000 | 80000 | 0.487 | 0.577 | 0.528 |
| 437 | 24 | IPC-2 | 100 | 58-28 | 5.2 | 9.5 | 295 | 13.8 | 46.937 | 0 | 176390 | 36171 | 10000 | 20000 | 0.514 | 0.580 | 0.552 |
| 438 | 37 | IPC-2 | 40 | 58-28 | 4.2 | 4.5 | 170 | 224.8 | 1322.2 | 10 | | 36171 | 10000 | 20000 | 0.874 | 0.894 | 0.883 |
| 439 | 38 | IPC-1 | 40 | 58-28 | 4.2 | 4.5 | 170 | 290.7 | 1710.2 | 10 | | 8325 | 2000 | 4000 | 0.884 | 0.902 | 0.892 |
| 440 | 17 | IPC-2 | 40 | 58-28 | 4.2 | 4.5 | 220 | 306.9 | 1395.1 | 1 | | 8325 | 2000 | 4000 | 0.746 | 0.800 | 0.773 |
| 441 | 36 | IPC-1 | 40 | 58-28 | 4.2 | 4.5 | 220 | 308.9 | 1404 | 1 | | 64065 | 10000 | 20000 | 0.745 | 0.795 | 0.769 |
| 442 | 38 | IPC-2 | 40 | 58-28 | 4.2 | 9.5 | 145 | 188.1 | 1297.1 | 1 | | 64065 | 10000 | 20000 | 0.813 | 0.853 | 0.838 |

| | | | | | | | | | | | | | | | | | |
|---|---|---|---|---|---|---|---|---|---|---|---|---|---|---|---|---|---|
| 443 | 12 | IPC-1 | 40 | 58-28 | 4.2 | 9.5 | 145 | 183.7 | 1266.6 | 1 | | 33393 | 10000 | 20000 | 0.754 | 0.806 | 0.786 |
| 444 | 36 | IPC-1 | 40 | 58-28 | 4.2 | 9.5 | 170 | 229.2 | 1348.4 | 5 | | 33393 | 10000 | 20000 | 0.814 | 0.842 | 0.826 |
| 445 | 35 | IPC-2 | 40 | 58-28 | 4.2 | 9.5 | 170 | 230.7 | 1357.2 | 5 | | 7200 | 2000 | 3500 | 0.872 | 0.891 | 0.880 |
| 446 | 10 | IPC-2 | 40 | 58-28 | 4.2 | 9.5 | 220 | 299.4 | 1360.7 | 10 | | 7200 | 2000 | 3500 | 0.848 | 0.878 | 0.865 |
| 447 | 14 | IPC-1 | 40 | 58-28 | 4.2 | 9.5 | 220 | 292.1 | 1327.5 | 10 | | 9265 | 2500 | 5000 | 0.799 | 0.838 | 0.821 |
| 448 | 35 | IPC-1 | 40 | 58-28 | 5.2 | 9.5 | 220 | 236.5 | 1074.8 | 1 | | 9265 | 2500 | 5000 | 0.787 | 0.828 | 0.806 |
| 449 | 25 | IPC-1 | 40 | 58-28 | 5.2 | 9.5 | 220 | 242.0 | 1099.9 | 1 | | 40860 | 10000 | 20000 | 0.740 | 0.790 | 0.764 |
| 450 | 14 | IPC-1 | 70 | 58-28 | 4.2 | 4.5 | 200 | 88.1 | 440.25 | 5 | | 40860 | 10000 | 20000 | 0.875 | 0.896 | 0.886 |
| 451 | 16 | IPC-2 | 70 | 58-28 | 4.2 | 4.5 | 200 | 107.9 | 539.37 | 5 | | 12360 | 3000 | 6000 | 0.832 | 0.860 | 0.846 |
| 452 | 9 | IPC-2 | 70 | 58-28 | 4.2 | 4.5 | 330 | 154.3 | 467.67 | 10 | | 12360 | 3000 | 6000 | 0.728 | 0.782 | 0.756 |
| 453 | 18 | IPC-1 | 70 | 58-28 | 4.2 | 4.5 | 330 | 182.6 | 553.34 | 10 | | 89935 | 10000 | 20000 | 0.715 | 0.772 | 0.744 |
| 454 | 30 | IPC-2 | 70 | 58-28 | 5.2 | 4.5 | 200 | 88.0 | 439.75 | 1 | | 89935 | 10000 | 20000 | 0.835 | 0.875 | 0.862 |
| 455 | 38 | IPC-1 | 70 | 58-28 | 5.2 | 4.5 | 200 | 79.7 | 398.31 | 1 | | 29650 | 10000 | 20000 | 0.780 | 0.833 | 0.816 |
| 456 | 28 | IPC-2 | 70 | 58-28 | 5.2 | 4.5 | 330 | 140.3 | 425.09 | 5 | | 29650 | 10000 | 20000 | 0.768 | 0.800 | 0.780 |
| 457 | 29 | IPC-1 | 70 | 58-28 | 5.2 | 4.5 | 330 | 137.4 | 416.38 | 5 | | 29650 | 10000 | 20000 | 0.741 | 0.776 | 0.754 |
| 458 | 15 | IPC-1 | 100 | 58-28 | 4.2 | 4.5 | 295 | 26.2 | 88.792 | 10 | | 96535 | 10000 | 20000 | 0.896 | 0.922 | 0.914 |
| 459 | 29 | IPC-2 | 100 | 58-28 | 4.2 | 4.5 | 295 | 25.3 | 85.81 | 10 | | 96535 | 10000 | 20000 | 0.836 | 0.876 | 0.864 |
| 460 | 34 | IPC-1 | 100 | 58-28 | 4.2 | 9.5 | 500 | 37.4 | 74.73 | 5 | | 9255 | 2000 | 4500 | 0.605 | 0.694 | 0.647 |
| 461 | 42 | IPC-2 | 100 | 58-28 | 4.2 | 9.5 | 500 | 37.0 | 74.072 | 5 | | 9255 | 2000 | 4000 | 0.654 | 0.731 | 0.696 |
| 462 | 39 | IPC-1 | 100 | 58-28 | 5.2 | 4.5 | 415 | 32.7 | 78.738 | 1 | | 46333 | 10000 | 20000 | 0.713 | 0.765 | 0.742 |
| 463 | 36 | IPC-2 | 100 | 58-28 | 5.2 | 4.5 | 415 | 31.1 | 74.928 | 1 | | 46333 | 10000 | 20000 | 0.706 | 0.760 | 0.736 |
| 464 | 41 | IPC-2 | 100 | 58-28 | 5.2 | 4.5 | 500 | 41.7 | 83.494 | 10 | | 19575 | 10000 | 15000 | 0.668 | 0.697 | 0.680 |
| 465 | 49 | IPC-1 | 100 | 58-28 | 5.2 | 4.5 | 500 | 40.4 | 80.876 | 10 | | 19575 | 10000 | 15000 | 0.718 | 0.743 | 0.728 |
| 466 | 33 | IPC-2 | 100 | 58-28 | 5.2 | 9.5 | 415 | 21.8 | 52.603 | 10 | | 41000 | 10000 | 20000 | 0.751 | 0.794 | 0.773 |
| 467 | 52 | IPC-1 | 100 | 58-28 | 5.2 | 9.5 | 415 | 23.5 | 56.731 | 10 | | 41000 | 10000 | 20000 | 0.769 | 0.808 | 0.789 |

# APPENDIX B

## SUMMARY OF QUALITY CONTROL/QUALITY ASSURANCE RESULTS

Two IPC (IPC-1 and IPC-2) beam fatigue devices were used in this study. It was important to insure that both devices measure statistically identical responses during the experimental testing program. In order to accomplish this goal, statistical ANOVA experiments were designed and implemented to verify this hypothesis.

Table B-1 to B-6 show a summary of results obtained from the comparative studies that were performed between the two IPC beam fatigue machines to insure that there is no statistical difference between the two machines results. The following is a description of the different tables shown in this appendix.

- Table B-1 shows the flexural stiffness of the synthetic beams under different test conditions.
- Table B-2 shows the analysis of variance on the IPC1 and IPC2 data using synthetic beams.
- Because of the significant difference results obtained in the first experiment, it was necessary to re-calibrate the machines and carefully tune them.
- Table B-3 shows the flexural stiffness of the synthetic beams under different test conditions after re-calibration.
- Table B-4 shows the analysis of variance on the IPC1 and IPC2 data using synthetic beams after re-calibration.
- Table B-5 shows the flexural stiffness of the HMA beams under different test conditions.
- Table B-6 shows the analysis of variance on the IPC1 and IPC2 data using HMA beams.

**Table B-1. Stiffness of Synthetic Beams (in psi) for first experiment.**

| Machine Type | Beam Stiffness | | | | | |
|---|---|---|---|---|---|---|
| | Low | | Medium | | High | |
| | Low Strain Level | High Strain Level | Low Strain Level | High Strain Level | Low Strain Level | High Strain Level |
| **IPC 1** | 99946 | 96794 | 166500 | 163808 | 356391 | 350240 |
| | 93030 | 93330 | 168694 | 165120 | 361653 | 358960 |
| Average | 96488.0 | 95062.0 | 167597.0 | 164464.0 | 359022.0 | 354600.0 |
| Standard Deviation | 4890.4 | 2449.4 | 1551.4 | 927.7 | 3720.8 | 6166.0 |
| Coefficient of variation, % | 5.1 | 2.6 | 0.9 | 0.6 | 1.0 | 1.7 |
| **IPC 2** | 99957 | 93709 | 173738 | 166747 | 368045 | 368929 |
| | 102855 | 95107 | 174970 | 169706 | 381828 | 377047 |
| Average | 101406.0 | 94408.0 | 174354.0 | 168226.5 | 374936.5 | 372988.0 |
| Standard Deviation | 2049.2 | 988.5 | 871.2 | 2092.3 | 9746.1 | 5740.3 |
| Coefficient of variation, % | 2.0 | 1.0 | 0.5 | 1.2 | 2.6 | 1.5 |

**Table B-2. Analysis of Variance for the Logarithm Transformed IPC1 and IPC2 Data Using Synthetic Beams.**

| Source | Sum of Squares | DF | Mean Square | F Value | Prob > F |
|---|---|---|---|---|---|
| Model | 1.34 | 4 | 0.34 | 3769.02 | < 0.0001 significant |
| Machine Type | 1.25E-03 | 1 | 1.25E-03 | 14.01 | 0.0014 |
| Beam Type | 1.34 | 2 | 0.67 | 7526.64 | < 0.0001 |
| Strain Level | 7.85E-04 | 1 | 7.85E-04 | 8.8 | 0.0079 |
| Residual | 1.70E-03 | 19 | 8.92E-05 | | |
| Lack of Fit | 6.81E-04 | 7 | 9.73E-05 | 1.15 | 0.395 not significant |
| Pure Error | 1.01E-03 | 12 | 8.45E-05 | | |
| Correlation Total | 1.35 | 23 | | | |
| Std. Dev. | 9.45E-03 | | R-Squared | 0.9987 | |
| Mean | 5.26 | | Adj R-Squared | 0.9985 | |
| C.V. | 0.18 | | Pred R-Squared | 0.998 | |

**Table B-3. Stiffness Results (in psi) of the Repeated Experiment After Re-Calibration Using Synthetic Beams.**

| Machine Type | Beam Stiffness | | | | | |
|---|---|---|---|---|---|---|
| | Low | | Medium | | High | |
| | Low Strain Level | High Strain Level | Low Strain Level | High Strain Level | Low Strain Level | High Strain Level |
| IPC 1 | 99946 | 96794 | 166500 | 163808 | 356391 | 350240 |
| | 93030 | 93330 | 168694 | 165120 | 361653 | 358960 |
| Average | 96488.0 | 95062.0 | 167597.0 | 164464.0 | 359022.0 | 354600.0 |
| Standard Deviation | 4890.4 | 2449.4 | 1551.4 | 927.7 | 3720.8 | 6166.0 |
| Coefficient of variation, % | 5.1 | 2.6 | 0.9 | 0.6 | 1.0 | 1.7 |
| IPC 2 | 99391 | 98190 | 168211 | 164207 | 357373 | 354662 |
| | 101535 | 95032 | 173583 | 163663 | 360103 | 361799 |
| Average | 100463.0 | 96611.0 | 170897.0 | 163935.0 | 358738.0 | 358230.5 |
| Standard Deviation | 1516.0 | 2233.0 | 3798.6 | 384.7 | 1930.4 | 5046.6 |
| Coefficient of variation, % | 1.5 | 2.3 | 2.2 | 0.2 | 0.5 | 1.4 |

**Table B-4. Analysis of Variance for The IPC1 and IPC2 Data After Re-Calibration Using Synthetic Beams.**

| Source | Sum of Squares | DF | Mean Square | F Value | Prob > F |
|---|---|---|---|---|---|
| Model | 2.91E+11 | 4 | 7.28E+10 | 8408.07 | < 0.0001 significant |
| Machine Type | 2.26E+07 | 1 | 2.26E+07 | 2.61 | 0.1227 |
| Beam Type | 2.91E+11 | 2 | 1.46E+11 | 16810.9 | < 0.0001 |
| Strain Level | 6.87E+07 | 1 | 6.87E+07 | 7.94 | 0.011 |
| Residual | 1.65E+08 | 19 | 8.66E+06 | | |
| Lack of Fit | 2.84E+07 | 7 | 4.05E+06 | 0.36 | 0.9102 not significant |
| Pure Error | 1.36E+08 | 12 | 1.13E+07 | | |
| Cor Total | 2.91E+11 | 23 | | | |
| | | | | | |
| Std. Dev. | 2942.26 | | R-Squared | 0.9994 | |
| Mean | 2.07E+05 | | Adj R-Squared | 0.9993 | |

**Table B-5. Stiffness of HMA Beams (in psi).**

| Machine Type | Test Temperature | | | | | |
|---|---|---|---|---|---|---|
| | 40 F | | 70 F | | 100 F | |
| | Low Strain Level | High Strain Level | Low Strain Level | High Strain Level | Low Strain Level | High Strain Level |
| **IPC 1** | 1713850 | 1685934 | 603145 | 647078 | 154210 | 188782 |
| | 1496119 | 1319385 | 637156 | 776303 | 158065 | 156016 |
| Average | 1604984 | 1502660 | 620151 | 711691 | 156138 | 172399 |
| Standard Deviation | 153959 | 259189 | 24049 | 91376 | 2726.03 | 23168.8 |
| Coefficient of variation, % | 9.59 | 17.25 | 3.88 | 12.84 | 1.75 | 13.44 |
| **IPC 2** | 1529680 | 1561575 | 599774 | 718700 | 152757 | 173428 |
| | 1672471 | 1375957 | 800803 | 573901 | 158557 | 155748 |
| Average | 1601076 | 1468766 | 700289 | 646301 | 155657 | 164588 |
| Standard Deviation | 100969 | 131252 | 142149 | 102388 | 4100.69 | 12501.5 |
| Coefficient of variation, % | 6.31 | 8.94 | 20.30 | 15.84 | 2.63 | 7.60 |

**Table B-6. Analysis of Variance betwwen IPC1 and IPC2 using HMA specimens.**

| Source | Sum of Squares | DF | Mean Square | F Value | Prob > F |
|---|---|---|---|---|---|
| Temperature | 8.22556E+12 | 2 | 4.11278E+12 | 443.08 | < 0.0001 significant |
| Strain Level | 261102663 | 1 | 261102663 | 0.03 | 0.869 not significant |
| Machine | 1698938055 | 1 | 1698938055 | 0.18 | 0.674 not significant |
| Error | 1.76364E+11 | 19 | 9282340905 | | |
| Correlation Total | 1.76364E+11 | 23 | | | |
| R-Squared | 0.9790 | | | | |
| Adj R-Squared | 0.9746 | | | | |